VOLUME 83 NO. HY3

JUNE 1957

JOURNAL of the

Hydraulics Division

PROCEEDINGS OF THE

AMERICAN SOCIETY OF CIVIL ENGINEERS

BASIC REQUIREMENTS FOR MANUSCRIPTS

This Journal represents an effort by the Society to deliver information t reader with the greatest possible speed. To this end the material herein none of the usual editing required in more formal publications.

Original papers and discussions of current papers should be submitted t Manager of Technical Publications, ASCE. The final date on which a discu should reach the Society is given as a footnote with each paper. Those wh planning to submit material will expedite the review and publication proce by complying with the following basic requirements:

1. Titles should have a length not exceeding 50 characters and spaces.

2. A 50-word summary should accompany the paper.

3. The manuscript (a ribbon copy and two copies) should be double-sp on one side of 8½-in. by 11-in. paper. Papers that were originally prepared oral presentation must be rewritten into the third person before being subm

4. The author's full name, Society membership grade, and footnote refe stating present employment should appear on the first page of the paper.

5. Mathematics are reproduced directly from the copy that is subm Because of this, it is necessary that capital letters be drawn, in black ink, 3/1 high (with all other symbols and characters in the proportions dictated standard drafting practice) and that no line of mathematics be longer than 6½ Ribbon copies of typed equations may be used but they will be proportion smaller in the printed version.

6. Tables should be typed (ribbon copies) on one side of 8½-in. by 1 paper within a 6½-in. by 10½-in. invisible frame. Small tables should be gro within this frame. Specific reference and explanation should be made in the for each table.

7. Illustrations should be drawn in black ink on one side of 8½-in. by 1 paper within an invisible frame that measures 6½-in. by 10½-in.; the ca should also be included within the frame. Because illustrations will be red to 69% of the original size, the capital letters should be 3/16-in. high. Photog should be submitted as glossy prints in a size that is less than 6½-in. by 10½ Explanations and descriptions should be made within the text for each illustra

8. Papers should average about 12,000 words in length and should b longer than 18,000 words. As an approximation, each full page of typed table, or illustration is the equivalent of 300 words.

Further information concerning the preparation of technical papers is tained in the "Technical Publications Handbook" which can be obtained the Society.

This Journal is published bi-monthly by the American Society of Engineers. Publication office is at 2500 South State Street, Ann Arbor, Mich Editorial and General Offices are at 33 West 39 Street, New York 18, New \$4.00 of a member's dues are applied as a subscription to this Journal. Second mail privileges are authorized at Ann Arbor, Michigan.

HY,PO

Journal of the
HYDRAULICS DIVISION
Proceedings of the American Society of Civil Engineers

CONTENTS

June, 1957

Papers

(Over)

Journal of the
HYDRAULICS DIVISION
Proceedings of the American Society of Civil Engineers

HE EFFICACY OF FLOOR SILLS UNDER DROWNED HYDRAULIC JUMPS

Ahmed Shukry,[1] M. ASCE
(Proc. Paper 1260)

SYNOPSIS

In this paper are presented the results of tests on the hydraulic performnce of various types of floor sills. The study is mainly concerned with lowead river barrages which are generally operated under conditions of rowned jumps. Example of this type of barrages is the Edfina Barrage hich controls the escapage discharges of the Rosetta Branch of the River ile into the sea. A scale model of this barrage was constructed with a fixed ed. The distribution of velocities, for various types and locations of sills, ere recorded by a Pitot-static tube. The efficiency of any sill against bedcour is indicated by the rate of adjustment of the flow to the normal distriution in the downstream channel.

INTRODUCTION

The hydraulic jump which forms within or downstream of an hydraulic tructure may be described as a: (a) perfect jump, (b) repelled jump that kes place downstream of the location of a perfect jump, and (c) drowned mp that occurs upstream of the location of a perfect jump.

On horizontal floors, the type of jump may be predicted from the wellnown formula:

$$Y_2 = \sqrt{\frac{2\,q^2}{g\,Y_1} + \frac{Y_1^2}{4}} - \frac{Y_1}{2} \qquad (1)$$

which Y_1 is the depth of flow before the jump, Y_2 is the conjugate depth of

ote: Discussion open until November 1, 1957. Paper 1260 is part of the copyrighted Journal of the Hydraulics Division of the American Society of Civil Engineers, Vol. 83, No. HY 3, June, 1957.

. Prof. of Irrig., Faculty of Eng., Alexandria Univ., Alexandria, Egypt.

flow after the jump, q is the discharge per unit width and g is the acceleratio of gravity.[2]

A perfect jump is formed when the depth of water in the downstream chan nel is equal to the conjugate depth Y_2. On the other hand, the repelled and th drowned jumps occur, respectively, with a downstream depth smaller or larg er than the conjugate depth Y_2.

The perfect jump is a powerful energy dissipator. However, if it occurs on the unprotected bed, intensive erosive action may take place. In tail- water design it is necessary, therefore, not only to create favourable condi- tions for the occurrence of a perfect jump, but also to ensure that the zone o its erosive effect is well confined within the edge of the solid floor. If the jump is repelled out of the floor edge, its location on the floor should be con trolled by the use of baffle piers, sills or stilling basins.(1, 2, 3) These con- trol works are generally designed so as to secure a perfect jump. As a safe ty measure, some authors recommend a slight submergence of the jump to accommodate for differences between the actual and the assumed hydraulic coefficients which may cause the jump to shift downstream from its estimate position.(4) On the other hand, low-head river barrages are generally oper- ated under conditions of deeply drowned jumps. As energy destroyers, the efficiency of such jumps is very low. To make use of the full energy dissipa tion associated with a perfect jump, the floor-level of the barrage is general raised above the bed-level of the downstream channel. Furthermore, a slop- ing or stepping floor transition is so designed that a perfect jump is secured at all downstream stages.(5) However, such a solution is not always feasible especially in silty streams where high elevations of the floor may hinder the passage of the silt loads.

Models with Movable Beds

Tests on models with movable beds have often been made to investigate the efficiency of anti-scour designs downstream of hydraulic structures. Th model is usually constructed according to Froude's criterion of similarity, whereas the movable bed is generally kept out of scale. In spite of this par- tial distortion in the model, experience indicates that models with movable beds, representing high-head structures, have supplied successful designs o various stilling basins.(2) Perfect hydraulic jumps are apt to form down- stream of these structures and gravitational forces are the most predominat ing of all other involved parameters.

In a low-head river barrage, where a deeply drowned jump is liable to form downstream of the piers, viscous forces may be effectively called into action. This is due to the fact that a considerable part of the excess kinetic energy in water escapes from the head of a drowned jump and wanders throu the low-velocity regions, where it is dissipated partly by erosive action and partly by viscous shear. Accordingly, both Reynolds and Froude parameters may be equally effective. Adding to this combination the non-scaled parame ters which define the bed material, the model results may become uncertain even so far as qualitative similarity is concerned. The geometry of the sco

2. Notation: The letter symbols in this paper are defined where they first a pear in the text and are assembled for convenience of reference in the Appendix.

ole may be described, in this case, by the following general relationship:

$$\frac{a_s}{b_s} = C\,\phi\left[F, R, \left(\frac{a_f}{b_f}, \frac{a'_f}{b'_f}, \ldots\right), \left(\frac{a_m}{b_m}, \frac{a'_m}{b'_m}, \ldots\right)\right] \quad (2)$$

n which $\frac{a_s}{b_s}$ is a ratio describing the geometry of the scour hole, F is the Froude number, R is the Reynolds number, $\left(\frac{a_f}{b_f}, \frac{a'_f}{b'_f}, \ldots\right)$ are length ratios escribing the geometry of the floor, piers, sills . . . etc., $\left(\frac{a_m}{b_m}, \frac{a'_m}{b'_m}, \ldots\right)$ re dimensionless parameters describing the physical and the hydraulic prop-rties of the bed material, C is a constant and ϕ denotes a function.

The erratic results obtained from bed-scour tests on open barrages oper-ted under deeply drowned jumps have been noticed in several instances in Egypt. The scour-protection works in most of the Nile barrages were de-igned according to the results of tests on models with movable beds. In all hese tests, the scales of the models varied between 1 : 100 and 10 : 100. Al-hough the tests were carried out at different dates since 1928, the testing echnique was almost the same. For any barrage, a model representing two r more vents was fixed in a long flume with a glass side. The model was ept well above the floor of the flume so that a bed of movable material might e provided. The downstream water-level was adjusted by means of a sliding lain sill at the lower end of the flume. The results of many tests indicate hat in spite of the fact that the general features and hydraulic conditions of ll the Nile Barrages are much the same, floor-sill locations do not follow ny general rule. Figures 1a through f show longitudinal sections of these arrages and the dates of original construction and reconstruction of each. he various points marked by letters in Figures 1a through f are identified s follows:

Point	Description
A	Upstream emergency stop-log grooves
B	Main grooves fitted with two sliding gates
C	Downstream emergency stop-log grooves
D	Main solid floor
E	Upstream bed-protection works
F	Downstream bed-protection works
G	Baffle sill
H	Lip wall or floor sill

An example which raises questions as to the validity of the results ob-ined from movable-bed tests, under conditions of deeply drowned jumps, re those tests carried out by Butcher and Atkinson(6) on a model of the old sna Barrage, Fig. (1f). From the results of those tests, the authors con-uded that, "Under equal conditions of discharge and downstream level, the odel showed that erosion beyond the end of the solid floor was almost always ost severe when the water was passed over the gates, rather less so when ssed under the bottom gate, and very much less when passed between the tes." As a matter of fact, experience indicates that serious tail-erosion oblems are generally associated with undergate rather than with over-top gulation.

Before the construction of Edfina Barrage, Fig. (1a), earlier bed-scour tests showed that the best location of the floor sill was at the middle of the solid floor. The same tests were repeated later under the same hydraulic conditions, but possibly with different compaction of the non-scaled bed material. The results of these latter tests are shown in Fig. (2). It may be noted that the scour holes for some locations of the sill are deeper than the hole formed with plain floor. Furthermore, the smallest scour pool is obtained when the sill is placed at the edge of the floor. It is believed that the disagreement between the two test results may be due to the fact that qualitative similarity of the model is not feasible. The distorting effects of the bed material are magnified under the two predominating flow parameters. Accordingly, it was decided to perform velocity-distribution tests on a fixed-bed model of the barrage. It is believed that more precise conclusions could be obtained by comparing the relative effects of various sills on the flow distribution.

Determination of Shear Stresses Along the Bed

Laboratory determination of the magnitudes of the shearing stresses along the bed, which may cause bed erosion downstream of a barrage, requires a complete survey of the velocity distribution. The bed of the flume should be fixed in order to eliminate the distorting effects of the bed material. Due to the separation wakes of the piers, the problem should be dealt with in three dimensions. Referring to Fig. (3), and assuming a horizontal bed, the differential equation may be expressed as follows:(7)

$$\frac{d F_x}{dx} \delta x + b \tau_o \delta x + \frac{d}{dx} (\beta \rho Q V_x) \delta x = 0 \qquad (3)$$

in which F_x is the pressure difference, b is the width of the flume, τ_o is the shearing stress along the bed, β is the momentum corrective factor, ρ is the density of water, Q is the rate of discharge and V_x is the forward mean velocity.

The momentum corrective factor at any cross-section is given by the following equation:

$$\beta = \frac{\int_0^Y \int_0^b v_x^2 \, dz \, dy}{V_x^2 \, b \, Y} \qquad (4)$$

in which v_x is the forward velocity at any point and Y is the mean depth of flow in the cross-section.

Assuming hydrostatic distribution of pressures, and re-writing equation (3) in a finite form,

$$\frac{\gamma b}{2} (Y_2^2 - Y_1^2) + b \tau_o \delta x = \rho Q (\beta_1 V_1 - \beta_2 V_2) \qquad (5)$$

ence,

$$\frac{Y_2^2 - Y_1^2}{2} + \frac{\tau_o}{\gamma}\delta x = \frac{Q^2}{g\,b^2}\left(\frac{\beta_1}{Y_1} - \frac{\beta_2}{Y_2}\right)$$

nd

$$\tau_o = \frac{\gamma}{\delta x}\left[\frac{Q^2}{g\,b^2}\cdot\left(\frac{\beta_1}{Y_1} - \frac{\beta_2}{Y_2}\right) - \frac{Y_2^2 - Y_1^2}{2}\right] \qquad (6)$$

For a qualitative analysis of the relative performance of various sills, it s sufficient to investigate their effects on the flow distribution in the vertical lane passing by the centerline of the model. The efficiency of any sill gainst bed-scour is measured by the rate of adjustment of the flow to its ormal distribution in the downstream channel.

The Model Tests and the Results Obtained

Fig. (4a) shows a model representing three vents of the Edfina Barrage hich has 46 vents. The model was constructed of metal to a scale of 1:66.7. ig. (4b) shows the general arrangement of the test facilities. The tail gate hich controlled the water-level downstream of the model, consisted of multi-utterfly vertical ribs which could be rotated by a common header. This de-ign eliminated the retarding effect on the bed velocities which might be aused by the commonly-used plain sill. A calibrated Pitot-static tube was sed to obtain velocity measurements at seven vertical sections downstream f the piers. The corresponding locations of these sections in the prototype re shown in Fig. (1a), sections I through VII. An over-head flushing tank as used to expel any air bubbles in the rubber-tubing connections. Tests ere made without floor sills and with sills of various shapes and locations. ig. (5) shows the types of sills used in tests. Figs. (6), (8) and (11a) show elocity-distribution diagrams for some of the tests. In each diagram, the pper thick arrow represents the maximum forward velocity v_{max} in the ection, and the lower thick arrow represents the bed velocity v_b. The latter elocity was always measured at a height above the flume bed of $\frac{1}{10}$ th the ormal depth of flow. It may be noted that the positive areas in the velocity agrams for any one test are not equal. This may be attributed to the wake ffects of the piers, unsteady flow conditions at the surface, flow vortices riginating at the bed and to the variation in specific gravity of the water due the entrained air.(8)

For each test, the following dimensionless plots were drawn:

$\frac{v_{max}}{V_o}$ and $\frac{v_b}{V_o}$ versus $\frac{L_f}{Y_o}$, where V_o and Y_o are the mean velocity and the ean depth of flow, respectively, when the flow assumes its normal distribu-n in the downstream channel, and L_f is the distance along the floor mea-red from the pier edges. Examples of these plots are given in Figs. (7b),) and (11b). (ii) $\frac{Y}{Y_o}$ and $\frac{y_{v_{max}}}{Y_o}$ versus $\frac{L_f}{Y_o}$, where Y is the mean depth of w at any section and $y_{v_{max}}$ is the height of the filament of maximum veloci- above the bed-level of the flume. Examples of these plots are given in g. (7a).

When the flow assumes its normal distribution in the downstream channel, the general trends of the functions given in (i) and (ii) become horizontal. Accordingly, the plots indicate the relative flow disturbances as well as the effects of the different sills. Since there were no appreciable differences between recorded and hydrostatic pressures at any section, comparisons were not made of pressure distributions.

Discussion of Results

a. The Methods of Passing the Discharge through the Double Sliding Gates of the Vents

These initial tests were carried out to investigate the effect of the method of regulation on the erosive forces. When the discharge is passed under the bottom gate, a huge surface vortex is formed, Fig. (6a). Under a constant discharge and a variable downstream depth of flow, the extension of this vortex beyond the pier edges is nearly constant. However, when the discharge is either passed between the bottom and the top gates, Fig. (6b), or over the top gate, Fig. (6c), the vortex does not appear downstream of the piers. The behavior of the downstream flow for the three methods of regulation is shown in Figs. (7a) and (7b). It may be noted that the erosive action is most severe when the discharge is passed under the bottom gate and very much less when passed either between the gates or over the top gate. It may be also noted that the least erosive action is associated with over-top regulation. These conclusions are in disagreement with those obtained by Butcher and Atkinson from bed-scour tests.(6)

Fig. (7a) shows the test results for undergate regulation associated with a deeply drowned jump. The erratic manner of the flow may be noted from the fluctuation of the path of maximum-velocity sheet. Therefore, in all other tests the discharge was always passed under the bottom gate in order to magnify the effects of the floor sills. The working head h on the barrage, (difference between upstream and downstream water-levels), was kept constant at 6.0 cms. (2.46 inches) and the discharge at 8.3 liters per sec. (131.5 gal. per min.). These hydraulic conditions correspond, respectively, to a hypothetical working head on the prototype of 4.0 ms. (13.12 feet) and to a flood discharge through the three barrage vents of 302 cubic ms. per sec. (106,700 cubic feet per sec.).

b. Location of the Floor Sill

When a solid sill of the type shown in Fig. (5a) is placed between the piers or near the pier edges, a bed vortex of a considerable length is formed, Figs (8a) and (8b). The strong reversed currents in this vortex may thus take place over the movable bed and will then participate in the formation of the scour pool. On the other hand, when the sill is placed far from the pier edge the length of the surface vortex is increased, Fig. (8d). In this case, the development of the normal velocity distribution may be retarded until the flow has discharged over the movable bed, sections I through V, Fig. (8d). Since the shearing forces along the bed increase with abrupt changes in the velocity distribution, the development of the normal distribution of flow on the loose bed may give rise to serious local scour.

It seems reasonable, therefore, that the best location of the sill is indicat

by the smallest sizes of both the surface and the bed vortices. In Edfina Barrage, this condition is satisfied with a sill located at the middle of the solid floor, a distance of 2.5 h from the pier edges, Fig. (8c).

Fig. (9) illustrates the relative disturbances in the bed velocities for various locations of sill on the floor. The disadvantage of the extreme locations of sill may be evidenced from the trends of functions $\frac{v_b}{v_o}$, sections I, II and V.

c. Efficiency of Different Types of Sills

The three types of sills shown in Fig. (5) were tested alternately at sections III and V, which correspond to the middle and the downstream edge of the floor of Edfina Barrage, respectively. Fig. (10) illustrates the relative effects of these sills on the velocity distribution when they are placed at section III. The dentated sill shows slightly better qualities than a solid sill of the same peripheral dimensions. This is true for both positions III and V. The broad sloping sill, which is sometimes recommended, causes larger variations in bed velocities and has no advantage over ordinary types of sills.

d. The Combined Action of Two Floor Sills

In order to ensure safety against bed-scour, some of the River Nile Barrages are fitted with two floor sills placed opposite each other, Figs. (1a), (1d) and (1f). The upstream sill, called the baffle sill, is placed between piers or near pier edges. Its function is to interrupt flow issuing from the gates and to form a jump which dissipates part of the hydraulic energy. The downstream sill, called the lip wall or the floor sill, is intended to deflect the high-velocity current upward from the river bed.

Fig. (11a) shows velocity-distribution diagrams for the baffle sill fixed at the downstream emergency grooves and the floor sill placed alternately at the middle and the edge of the solid floor, sections III and V, respectively. In the first position, a bed vortex occupies the space between the two sills, (upper diagrams in Fig. 11a). The water cushion formed thereby is so effective in energy dissipation that the flow is adjusted to its normal distribution before it leaves the floor edge. In the second position, the size of the bed vortex does not change, (lower diagrams in Fig. 11a), but the sill creates disturbance in the flow over the loose bed. The advantage of a middle-floor sill in stabilizing the flow is clear in Fig. (11b). Functions $\frac{v_{max}}{v_o}$ and $\frac{v_b}{v_o}$, (trends in full lines), become almost parallel upstream of section V, the edge of the solid floor.

GENERAL CONCLUSIONS

The behavior of anti-scour sills below open river barrages, operated under conditions of deeply drowned jumps, may be clearly investigated by means of velocity-measurement tests on models with fixed beds. The results of such tests indicate that the best efficiency of sill is obtained when it is placed neither too close to the downstream edges of piers nor at the edge of the protecting solid floor. This is true whether the sill is used alone or in combination with a baffle sill. It is also true in case of dentated sills. The hydraulic advantage of these latter sills seems, however, to be over-estimated.

APPENDIX. NOTATION

The following letter symbols adopted for use in this paper conform essentially with American Standard Letter Symbols for Hydraulics (ASA-Z10.2-1942) prepared by a Committee of the American Standard Association, with Society participation and approved by the Association in 1942.

$\frac{a}{b}, \frac{a'}{b'}, \ldots$ = hypothetical mathematical ratios describing the geometry or form, with subscripts s, f or m referring to the scour hole, the floor or the bed material, respectively;

b = width of the flume;

C = a constant;

F = the Froude number;

F_x = force component along centerline of the channel;

g = acceleration of gravity;

h = working head on a barrage, the difference between upstream and downstream water-levels;

L = length;

L_f = longitudinal distance along the floor measured from the downstream edges of piers;

Q = rate of discharge;

q = rate of discharge per unit width of channel;

R = the Reynolds number;

V_x = forward mean velocity in a given section;

V_o = mean velocity in the section where the flow attains its normal distribution;

v_x = forward velocity at any point;

v_b = forward velocity near the bed of the flume measured at a depth $0.1\ Y_o$ above the fixed bed;

v_{max} = maximum forward velocity in a vertical section;

Y = mean depth of flow, with subscripts generally denoting the section of measurement;

Y_o = mean depth in the section where the flow attains its normal distribution;

β = momentum corrective factor, with subscripts generally denoting the section of measurement;

γ = specific weight of water;

ρ = density;

τ_o = shearing stress along the flume bed; and

ϕ = a function.

REFERENCES

1. "Engineering for Dams," by W. P. Creager, J. D. Justin and J. Hinds, John Wiley and Sons, Inc., New York, 1947, Vol. I, p.p. 75-79.

2. "Development of Hydraulic Design, Saint Antony Falls Stilling Basin," by Fred W. Blaisedell, Trans. ASCE, Vol. 113, 1948, p.p. 483-561.

3. "Control of Hydraulic Jump by Sills," by J. W. Forster and R. A. Skrinde, Trans. ASCE, Vol. 115, 1950, p.p. 973-1022.

4. "Irrigation and Hydraulic Design," by S. Leliavsky, Chapman & Hall Ltd., London, 1955, Vol. I, p. 292.

5. "Hydraulics of Steady Flow in Open Channels," by S. M. Woodward and C. J. Posey, John Wiley & Sons, Inc., New York, 1941, p.p. 24-37.

6. "The Causes and Prevention of Bed Erosion, with Special Reference to the Protection of Structures Controlling Rivers and Canals," by A. D. D. Butcher and J. D. Atkinson, Minutes of Proc. of the Inst. of Civil Engineers, London, Vol. 235, Session 1932-33, Pt. I, p. 204.

7. "A Generalised Treatment of Varied Flow in Open Channels," by A. Fathy, Faculty of Engineering, Alexandria Univ., 1954.

8. "Modern Types of Movable Weirs," by J. Smentana, Paper 51, Fifteenth International Navigation Congress, Bruxelles, 1935.

FIG.(I) BARRAGES ON THE RIVER NILE (Dim^s in ms.)

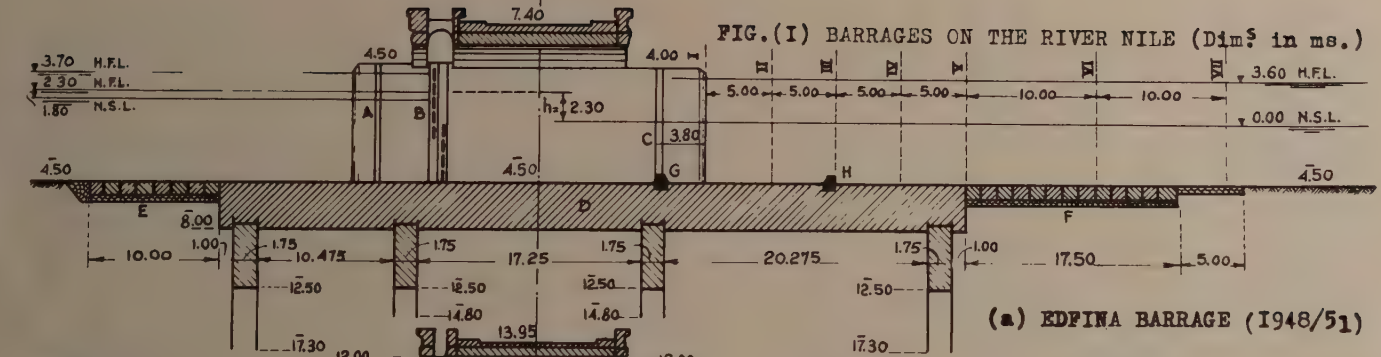

(a) EDFINA BARRAGE (1948/51)

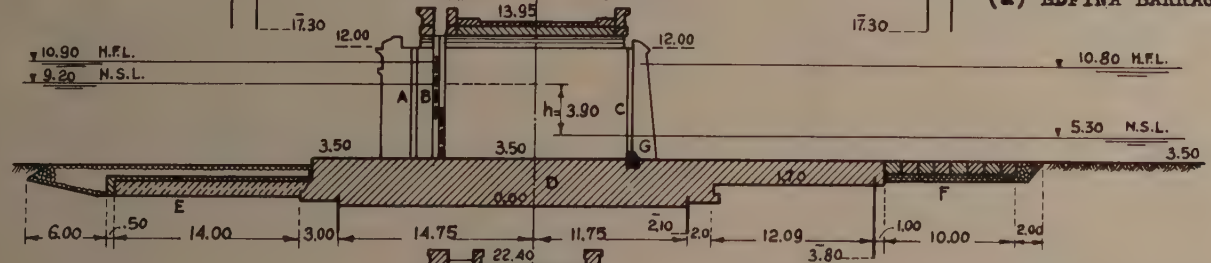

(b) ZIFTA BARRAGE (1901/03 &1953/55)

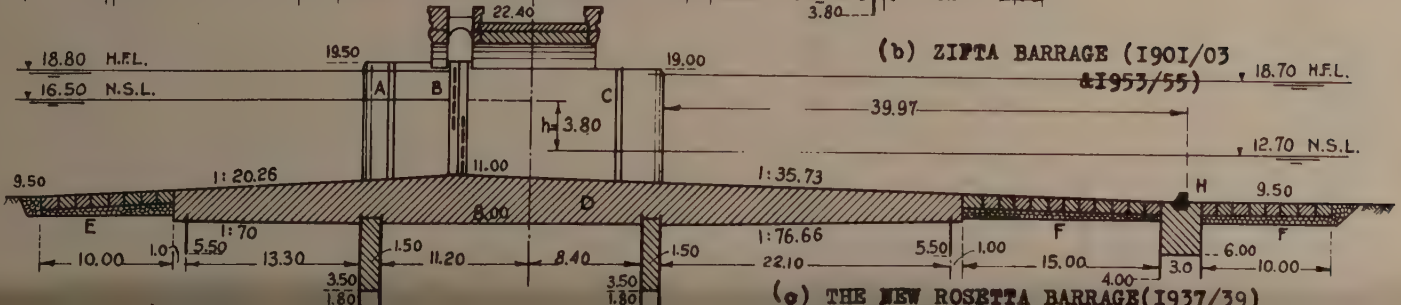

(c) THE NEW ROSETTA BARRAGE(1937/39)

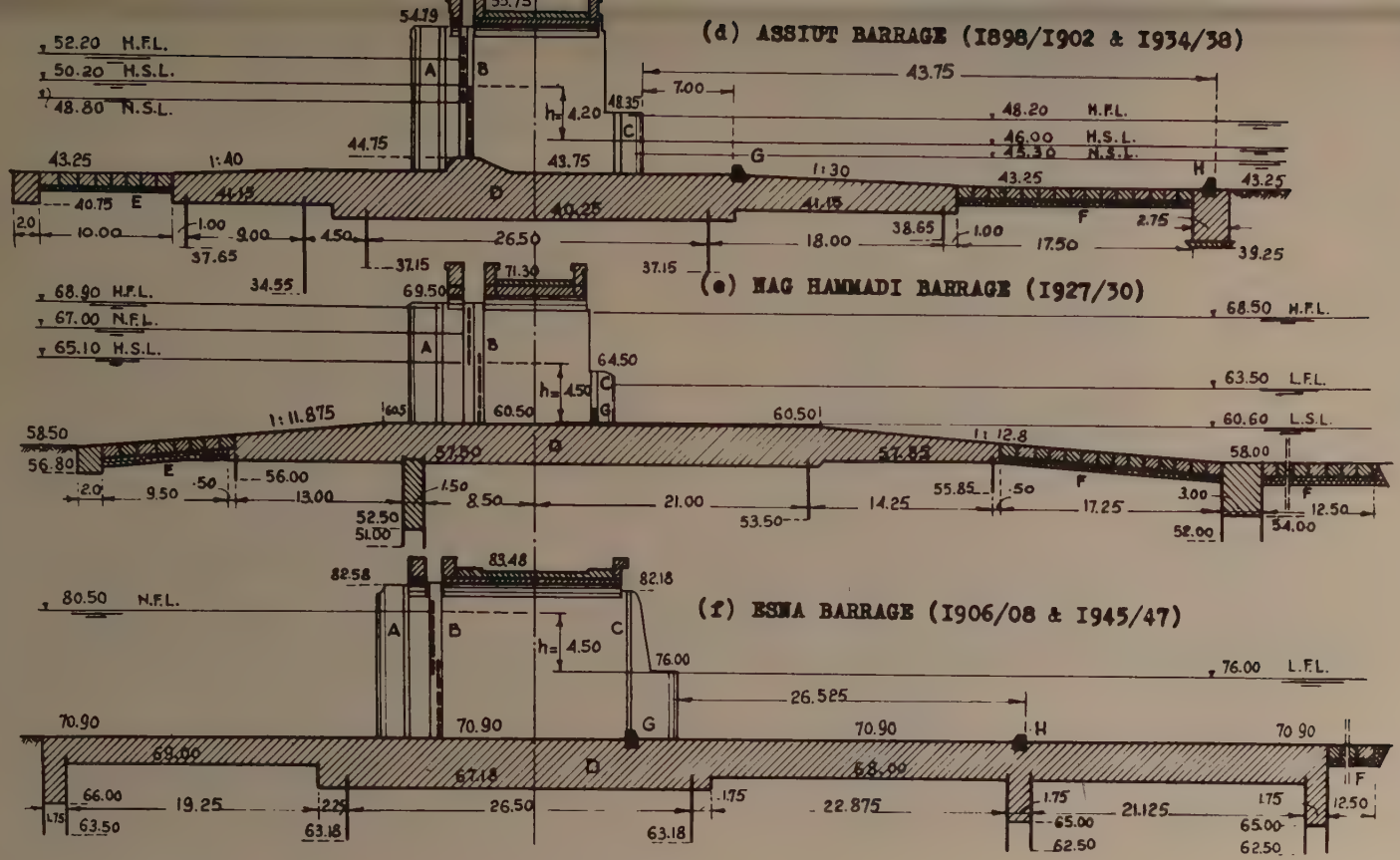
(d) ASSIUT BARRAGE (1898/1902 & 1934/38)
52.20 H.F.L.
50.20 H.S.L.
48.80 N.S.L.
54.19
55.75
A
B
C
D
E
F
G
H
h= 4.20
48.35
7.00
43.75
48.20 H.F.L.
46.00 H.S.L.
45.30 N.S.L.
44.75
43.25
1:40
1:30
40.75
41.15
40.25
38.65
1.00
2.75
2.0
10.00
9.00
4.50
26.50
18.00
17.50
37.65
37.15
34.55
39.25
(e) NAG HAMMADI BARRAGE (1927/30)
68.90 H.F.L.
67.00 N.F.L.
65.10 H.S.L.
69.50
71.30
64.50
h= 4.50
60.50
68.50 H.F.L.
63.50 L.F.L.
60.60 L.S.L.
58.50
56.80
1:11.875
1:12.8
57.30
57.35
58.00
2.0
9.50
.50
56.00
13.00
1.50
8.50
21.00
53.50
14.25
55.85
17.25
3.00
12.50
52.50
51.00
52.00
54.00
(f) ESNA BARRAGE (1906/08 & 1945/47)
80.50 N.F.L.
82.58
83.48
82.18
h= 4.50
76.00
76.00 L.F.L.
26.525
70.90
69.00
67.18
66.00
19.25
2.25
26.50
1.75
22.875
21.125
65.00
62.50
63.50
63.18

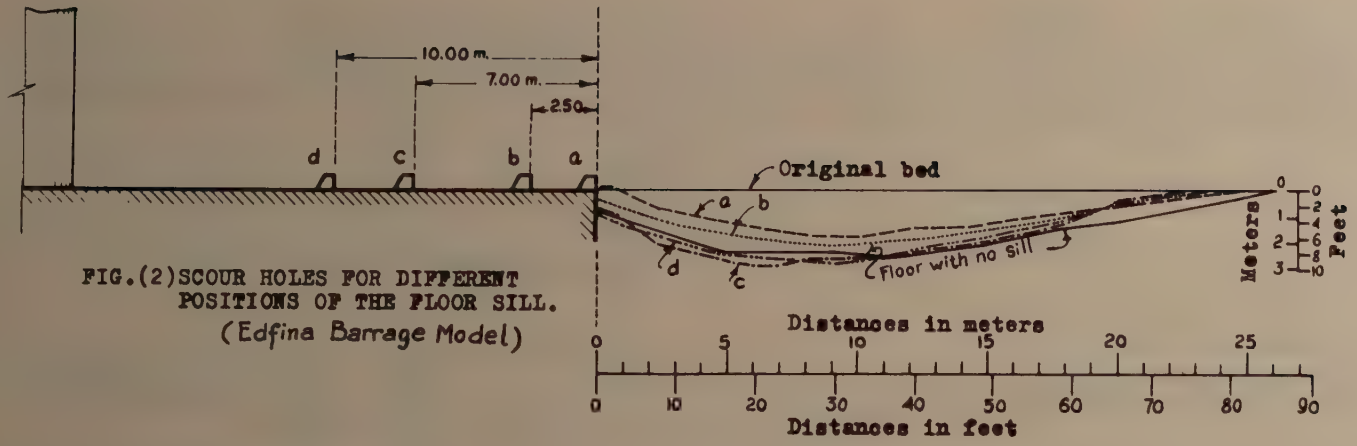

FIG.(2)SCOUR HOLES FOR DIFFERENT POSITIONS OF THE FLOOR SILL.
(Edfina Barrage Model)

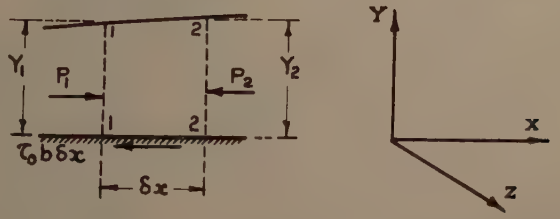

FIG. 3

FIG.(4a) THE MODEL

FIG.(4b) GENERAL ARRANGEMENT OF TEST FACILITIES

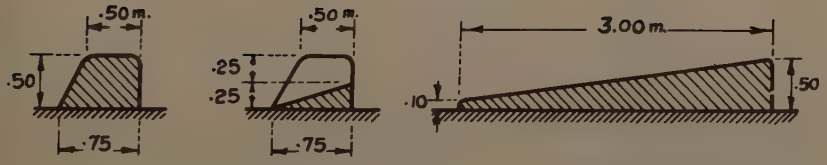

(a) Solid sill (b) Dentated sill (c) Broad sloping sill

FIG.(5) FLOOR SILLS USED IN TESTS

FIG.(6) THE VELOCITY DISTRIBUTIONS IN THE THREE METHODS OF REGULATION.

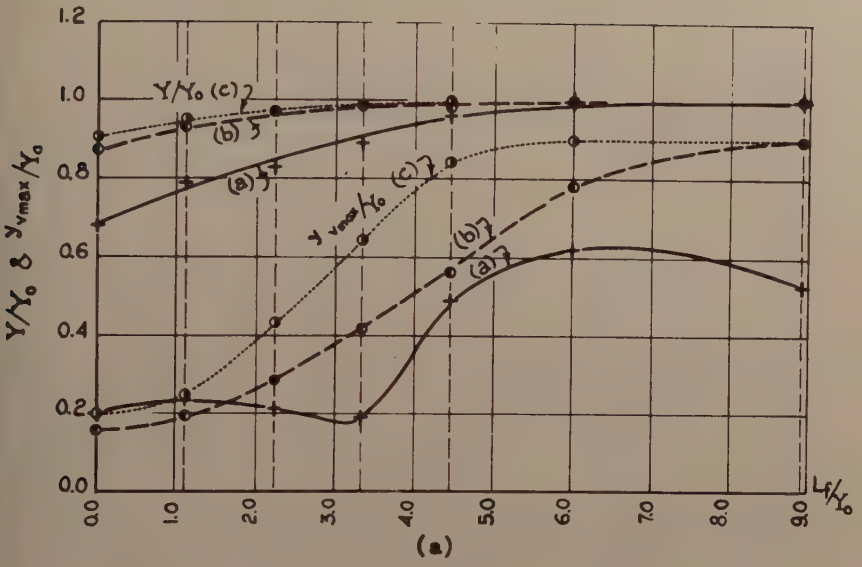

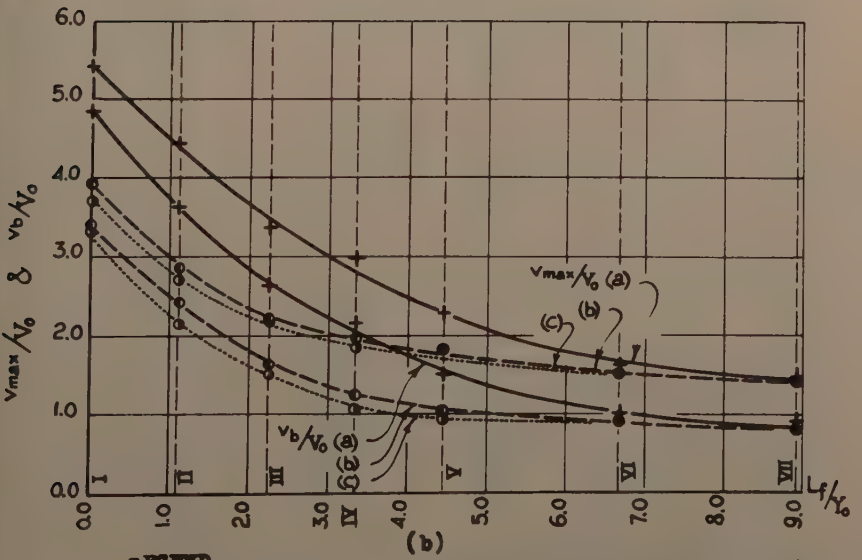

LEGEND

(a) ——+—— Discharge passed under gate
(b) ———●——— Discharge passed between gates
(c) ·····●····· Disch. passed over top gate

FIG.(7) THE BEHAVIOUR OF THE DOWNSTREAM FLOW IN THE THREE METHODS OF REGULATION.

FIG.(8) VELOCITY DISTRIBUTION FOR DIFFERENT POSITIONS OF ONE SOLID SILL.

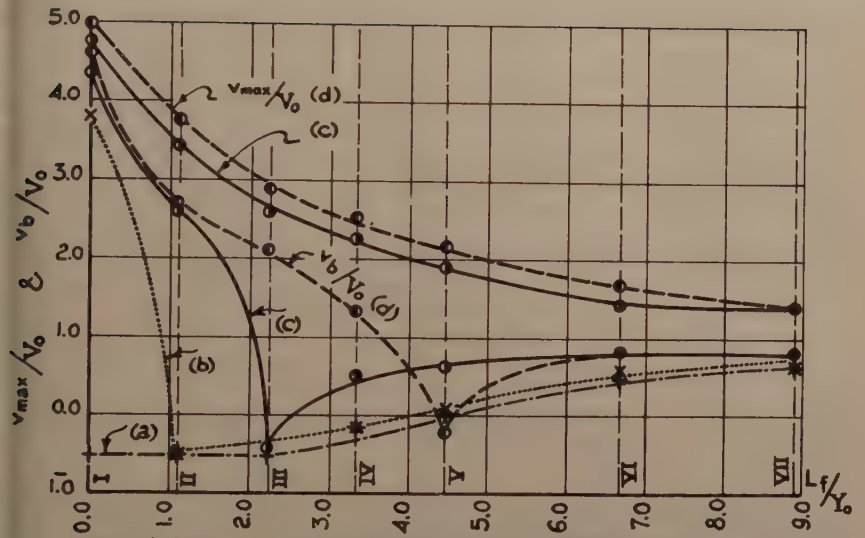

FIG. (9) THE FLOW DISTRIBUTION WITH DIFFERENT POSITIONS OF ONE SOLID SILL.

LEGEND
(a) ——·—+—·—— sill placed at d.s.groove
(b) ·····×····· sill placed at section II
(c) ———o——— sill placed at sectionIII
(d) – – – –o– – – – sill placed at section V

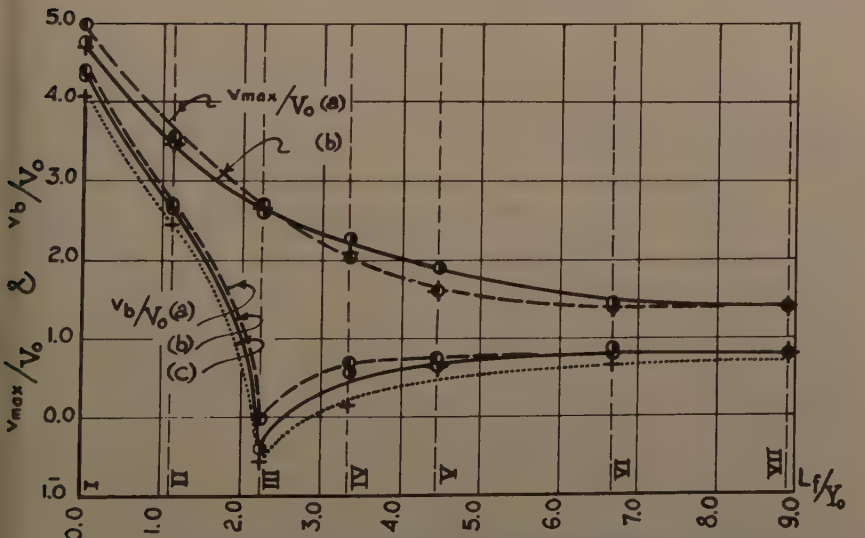

FIG.(10) THE FLOW DISTRIBUTION WITH DIFFERENT SHAPES OF ONE FLOOR SILL PLACED AT SECTION III .

LEGEND
(a) – – –o– – – Dentated sill
(b) ———o——— Solid sill
(c) ·····+····· Broad sloping sill

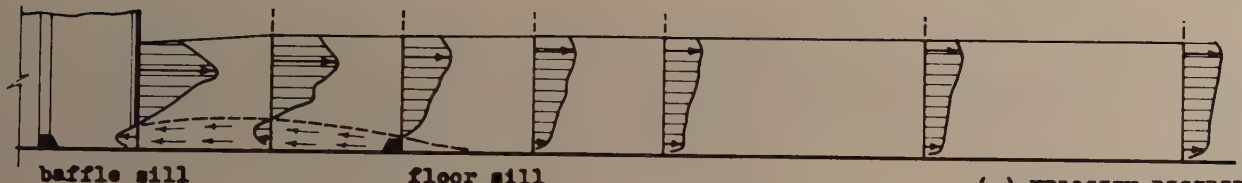

(a) VELOCITY DISTRIBUTION

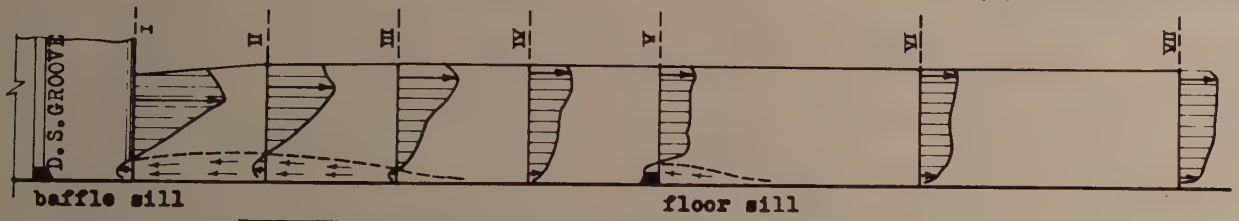

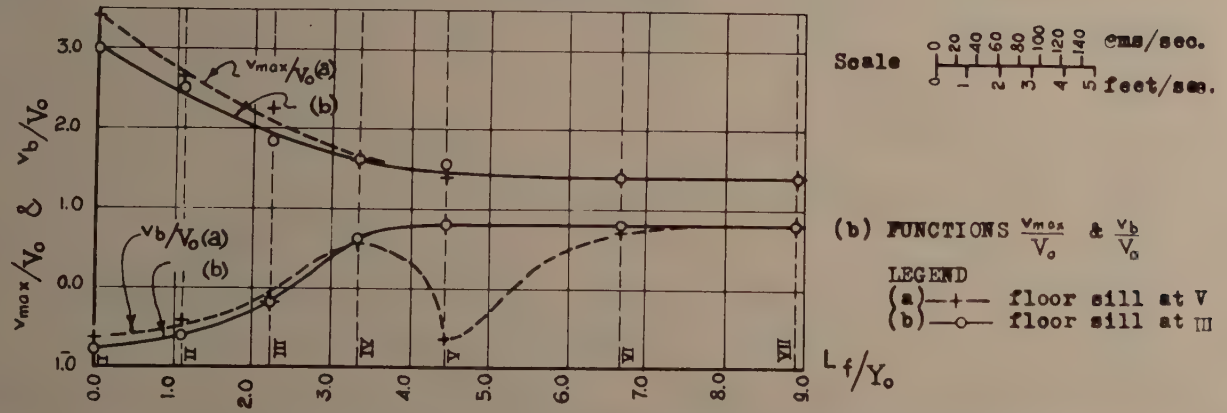

FIG.(II) THE COMBINED EFFECT OF A BAFFLE SILL AND A FLOOR SILL.

Journal of the
HYDRAULICS DIVISION
Proceedings of the American Society of Civil Engineers

LOSSES DUE TO ICE STORAGE IN HEART RIVER, NORTH DAKOTA[1]

H. M. Erskine,[2] M. ASCE
(Proc. Paper 1261)

SYNOPSIS

Winter flows in the lower reaches of the Heart River in western North Dakota have been regulated by the Heart Butte Dam since 1949. Flow records indicate water losses due to storage as ice is relatively low for smaller discharges, particularly if the rate of release is decreased somewhat as the winter progresses; however, the opposite is true for higher flows and increasing rates of release.

During recent years the flow in the lower reaches of the Heart River in western North Dakota has been controlled by the Heart Butte Dam. Winter flows have generally been maintained at a rate considerably higher than prevailed under uncontrolled conditions. Gaging station records at three well-spaced locations between the reservoir and the mouth frequently show a decreasing rate of flow from the upper to the lower stations during the winter months. Storage in the form of ice in the channel probably accounts for nearly all of the decrease in flow at the downstream points.

The Heart River, one of the principal tributaries to the Missouri River, rises about 30 miles east of the western boundary of North Dakota and flows in an easterly direction for about 120 miles to its confluence with the Missouri River near Bismarck, N. Dak. The drainage basin of approximately 3,400 square miles lies between latitudes 46°22' and 47°11'. (See Fig. 1.)

Most of the basin is composed of gently rolling prairie although there are some relatively large areas with quite steep slopes, particularly in regions adjacent to the main stream and its larger tributaries. Altitudes range from about 1,650 feet at the mouth to about 2,800 feet at the divide at the upper end of the basin. Water courses are well defined and have moderate slopes. It is

Note: Discussion open until November 1, 1957. Paper 1261 is part of the copyrighted Journal of the Hydraulics Division of the American Society of Civil Engineers, Vol. 83, No. HY 3, June, 1957.

1. Publication authorized by the Director, U.S. Geological Survey, presented before the Hydraulics Division of the American Society of Civil Engineers, August 22, 23, 1956, at Madison, Wis.

2. Dist. Engr., Geological Survey, U.S. Dept. of the Interior, Bismarck, N. Dak.

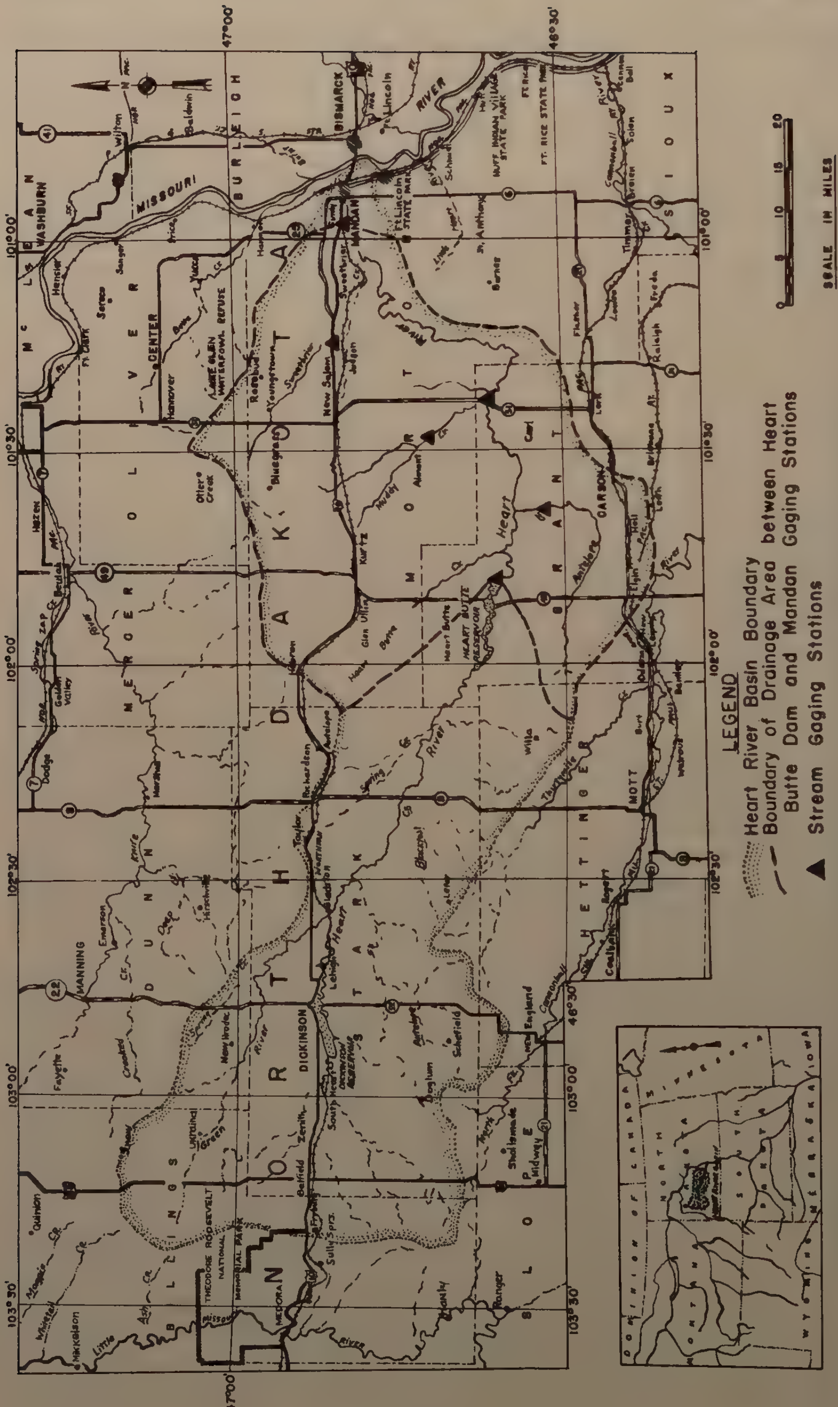

Figure 1.--Heart River Basin, North Dakota

estimated that about one-fifth of the area is under cultivation, principally for the production of small grains. The remainder is range land with a firm cover of native grass.

The soils range from shallow to moderate depth and are largely derived from the weathering of the underlying sandy clays and shales of the Fort Union formation. Exceptions are the bottom lands adjacent to the river and its larger tributaries which are composed of alluvium containing much fine sand and ranging in width from a few hundred feet to about a mile, relatively small areas in the lower part of the basin where some glacial till is found, and scattered sandstone capped buttes near the edges of the basin. Figures 2 to 5 are typical of the terrain along Heart River.

The average annual precipitation for the basin is approximately 16 inches. About three-fourths of this normally occurs during the growing season. During the winter season precipitation, which is nearly always in the form of snow, is usually light. The averages during the winter months range from about half an inch of water content per month during December, January and February, to about three-fourths inch during March. The average

Figure 2.--Gaging Station on Heart River below Heart Butte Dam. February 28, 1956.

Figure 3.--Heart River near Flasher. February 28, 1956.

Figure 4.--Heart River just below the Lark Gaging Station. February 28, 1956.

Figure 5.--Heart River near Carson. June 17, 1956. Note Ice Scars on Cottonwood Trees on Left Bank.

temperatures during these months are approximately 15, 10, 13 and 26°F. respectively. Periods with minimum temperatures of -30°F. or colder usually occur each winter. The average annual temperature is about 41°F.

The average annual runoff for the basin has been about 1-1/4 inch during the past few decades. The volume of runoff is very erratic from year to year and the bulk of it generally occurs during the spring breakup period.

Near the end of 1949 the Heart Butte Dam was completed by the Bureau of Reclamation. This dam is an earth-fill structure located about 104 miles above the mouth. The drainage area above the dam is 1,760 square miles, slightly over one-half of the total area of the basin. It is a multi-purpose project to provide water for irrigation, flood control, low-flow augmentation for stock and other water supplies, waste dilution, and for recreation. The gross capacity of the reservoir is 428,000 acre-feet; however, only 68,700 acre-feet of this is controlled storage held below the crest of the uncontrolle

glory hole type spillway. The releases from the controlled storage are through a gate controlled conduit. The reservoir first filled to above the spillway level in the spring of 1950.

Ice thickness ranging from 2 to 3 feet are normal on the water bodies in this area by midwinter. The volume of ice accumulating on the Heart River in the reach below the Heart Butte Reservoir is of considerable importance particularly to those in the Mandan area where serious flooding sometimes occurs.

The spring breakup on the Heart River traditionally precedes the Missouri River breakup in the Mandan vicinity by about two weeks. Thus in years when there are moderate or high flows during the breakup period, the Heart River ice is prevented from entering the Missouri River by the heavy ice cover on that stream. As a result the Heart River ice accumulates in the channel and on the bottom lands for several miles immediately above its mouth obstructing the flow of the stream and causing flooding over rather large areas. Although levees now protect the city of Mandan against all but extremely severe floods, a large area in the vicinity is subject to fairly frequent flooding and considerable damage. It is apparent that any reduction in the volume of ice forming in the river would reduce the flood hazard in its lower reaches.

Three stream-gaging stations are operated by the U.S. Geological Survey on the Heart River between Heart Butte Dam and Mandan, and one is operated reasonably near the mouth of each of the three principal tributaries to this reach of the river (see Fig. 1). Pertinent data relative to these gaging stations is given in Table 1. The flow records collected at these stations offer an excellent opportunity to evaluate the volume of water that is retained in the river in the form of ice under various winter conditions and for different rates of stream flow.

Table 1. --Gaging stations in lower Heart River basin

Stream and location	Miles above mouth	Datum of Gage above mean sea level	Drainage area in square miles
Heart River below Heart Butte Dam----------	103	1,998.87	1,710
Antelope Creek near Carson-	4	1,974	221
Muddy Creek near Almont---	12	1,864	456
(Intervening Area - ungaged)-	-	-	313
Heart River near Lark --------	62	1,802.83	2,750
Sweetbriar Creek near Judson	16	1,886	157
(Intervening Area - ungaged)	-	-	403
Heart River near Mandan------	14	1,638.70	3,310

Note. --All stations have recording gages, except Antelope Creek near Carson, which has a wire-weight gage.

An examination of the records indicated that portions of the winter periods during the four water years 1953 to 1956 were suitable for use in a study of the losses due to ice formation. The winter records for each of the six gaging stations are given graphically in Figures 6 to 9. U.S. Weather Bureau maximum and minimum daily temperatures and daily precipitation recorded

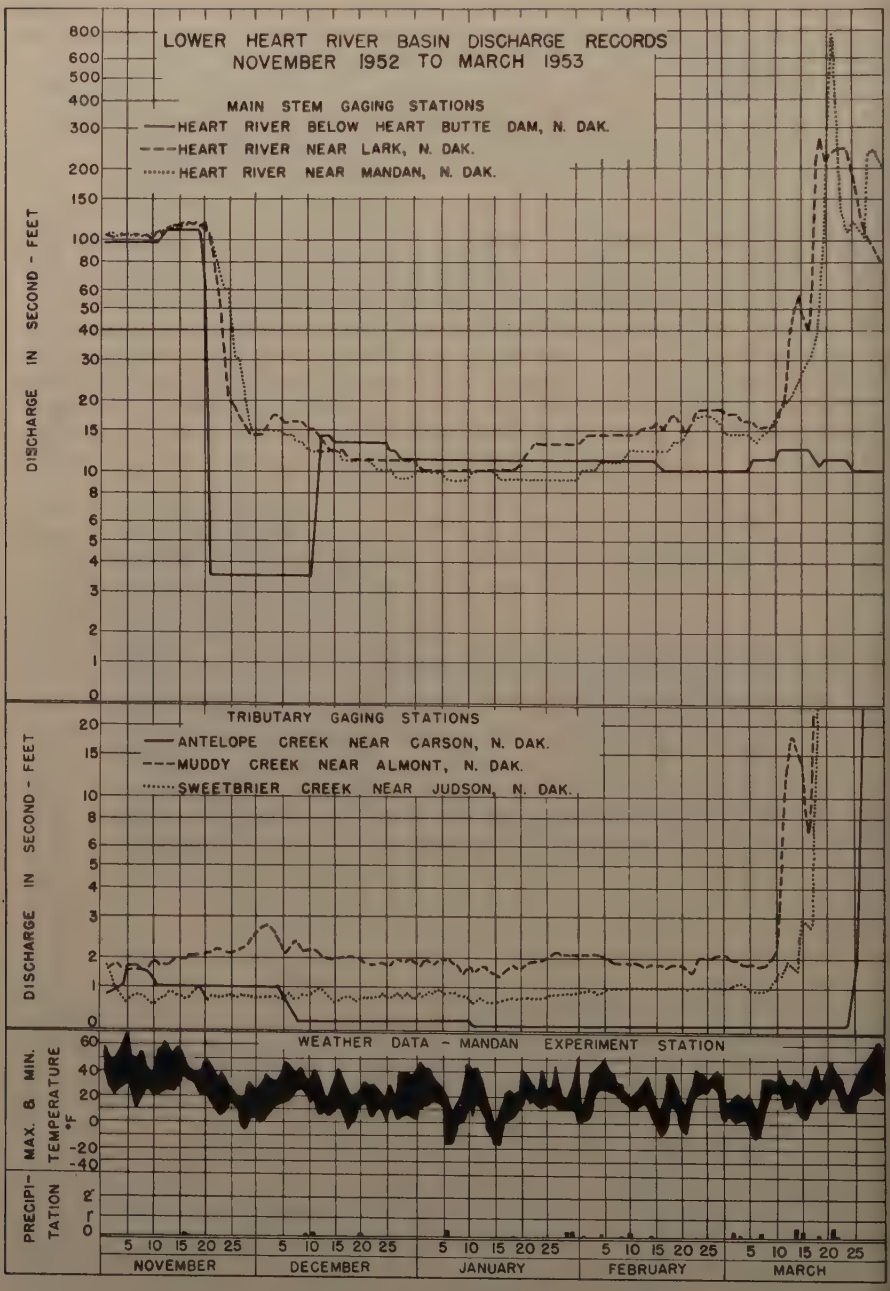
LOWER HEART RIVER BASIN DISCHARGE RECORDS
NOVEMBER 1952 TO MARCH 1953
MAIN STEM GAGING STATIONS
HEART RIVER BELOW HEART BUTTE DAM, N. DAK.
HEART RIVER NEAR LARK, N. DAK.
HEART RIVER NEAR MANDAN, N. DAK.
DISCHARGE IN SECOND - FEET
800
600
500
400
300
200
150
100
80
60
50
40
30
20
15
10
8
6
5
4
3
2
1
0
TRIBUTARY GAGING STATIONS
ANTELOPE CREEK NEAR CARSON, N. DAK.
MUDDY CREEK NEAR ALMONT, N. DAK.
SWEETBRIER CREEK NEAR JUDSON, N. DAK.
DISCHARGE IN SECOND - FEET
20
15
10
8
6
5
4
3
2
1
0
WEATHER DATA - MANDAN EXPERIMENT STATION
MAX. & MIN. TEMPERATURE °F
60
40
20
0
-20
-40
PRECIPITATION
R
T
0
5 10 15 20 25
NOVEMBER
DECEMBER
JANUARY
FEBRUARY
MARCH

FIGURE 6

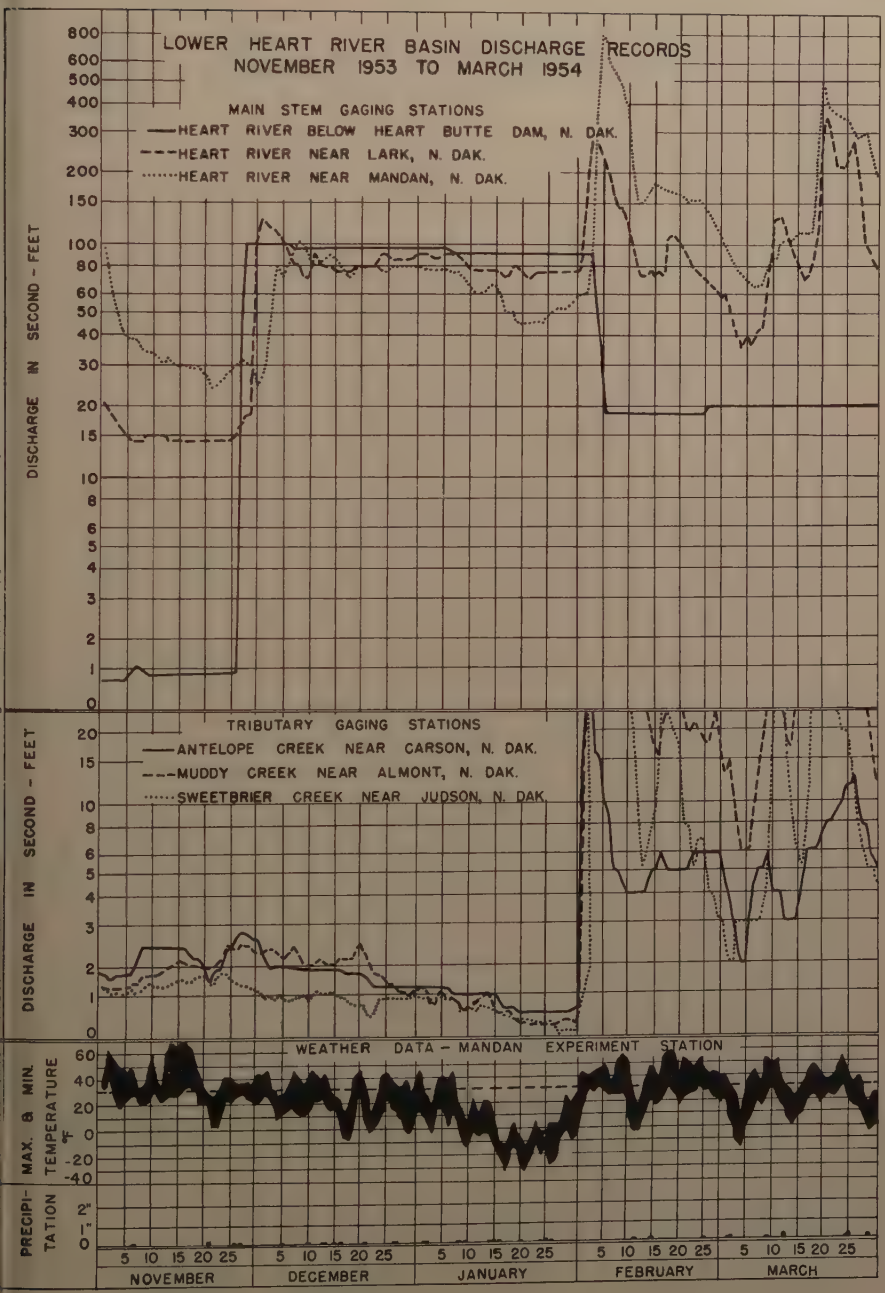
LOWER HEART RIVER BASIN DISCHARGE RECORDS
NOVEMBER 1953 TO MARCH 1954
MAIN STEM GAGING STATIONS
HEART RIVER BELOW HEART BUTTE DAM, N. DAK.
HEART RIVER NEAR LARK, N. DAK.
HEART RIVER NEAR MANDAN, N. DAK.
DISCHARGE IN SECOND - FEET
800
600
500
400
300
200
150
100
80
60
50
40
30
20
15
10
8
6
5
4
3
2
1
0
TRIBUTARY GAGING STATIONS
ANTELOPE CREEK NEAR CARSON, N. DAK.
MUDDY CREEK NEAR ALMONT, N. DAK.
SWEETBRIER CREEK NEAR JUDSON, N. DAK.
DISCHARGE IN SECOND - FEET
20
15
10
8
6
5
4
3
2
1
0
WEATHER DATA - MANDAN EXPERIMENT STATION
MAX. & MIN. TEMPERATURE °F
60
40
20
0
-20
-40
PRECIPITATION
2"
1"
0
5 10 15 20 25
NOVEMBER
DECEMBER
JANUARY
FEBRUARY
MARCH

FIGURE 7

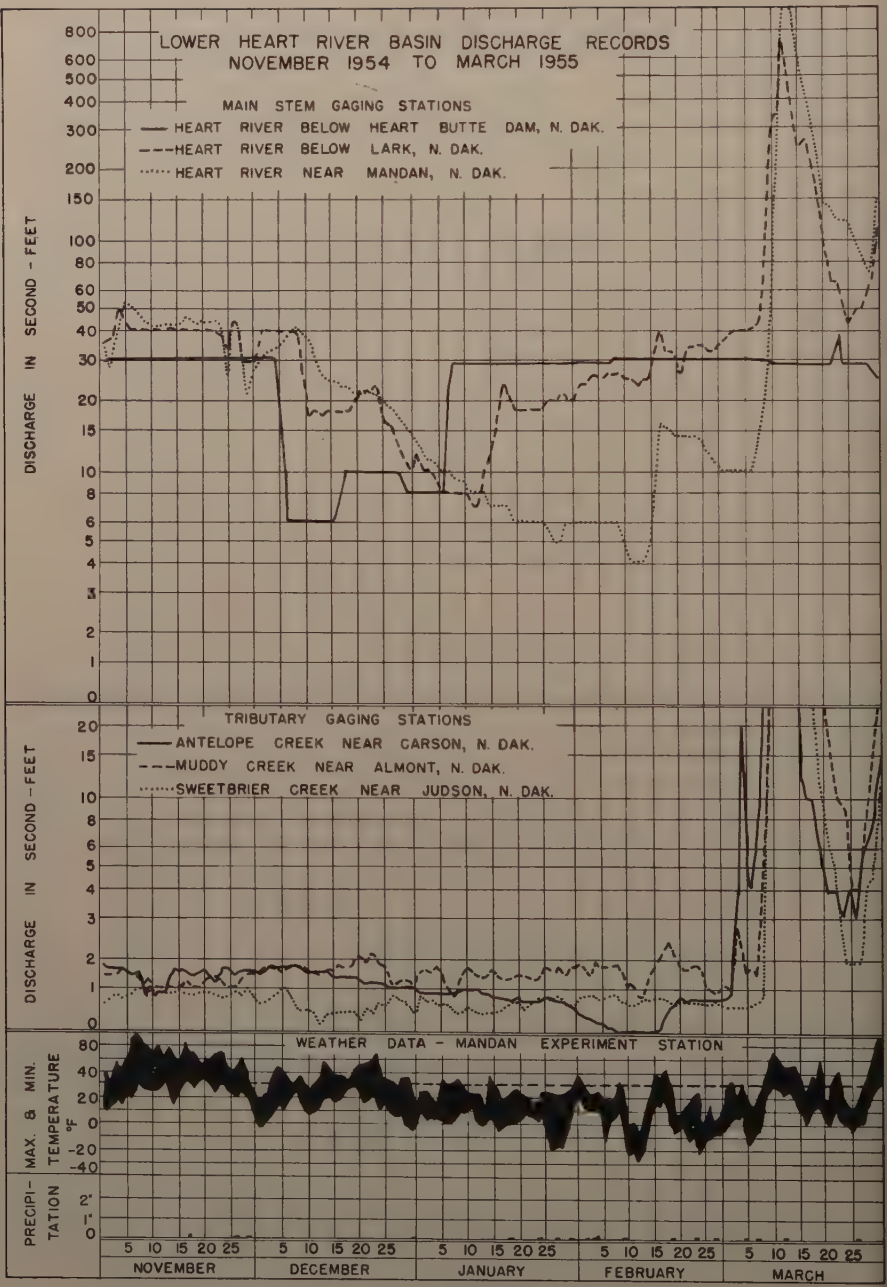
LOWER HEART RIVER BASIN DISCHARGE RECORDS
NOVEMBER 1954 TO MARCH 1955
MAIN STEM GAGING STATIONS
HEART RIVER BELOW HEART BUTTE DAM, N. DAK.
HEART RIVER BELOW LARK, N. DAK.
HEART RIVER NEAR MANDAN, N. DAK.
DISCHARGE IN SECOND-FEET
TRIBUTARY GAGING STATIONS
ANTELOPE CREEK NEAR CARSON, N. DAK.
MUDDY CREEK NEAR ALMONT, N. DAK.
SWEETBRIER CREEK NEAR JUDSON, N. DAK.
WEATHER DATA - MANDAN EXPERIMENT STATION
MAX. & MIN. TEMPERATURE °F
PRECIPITATION
NOVEMBER
DECEMBER
JANUARY
FEBRUARY
MARCH

FIGURE 8

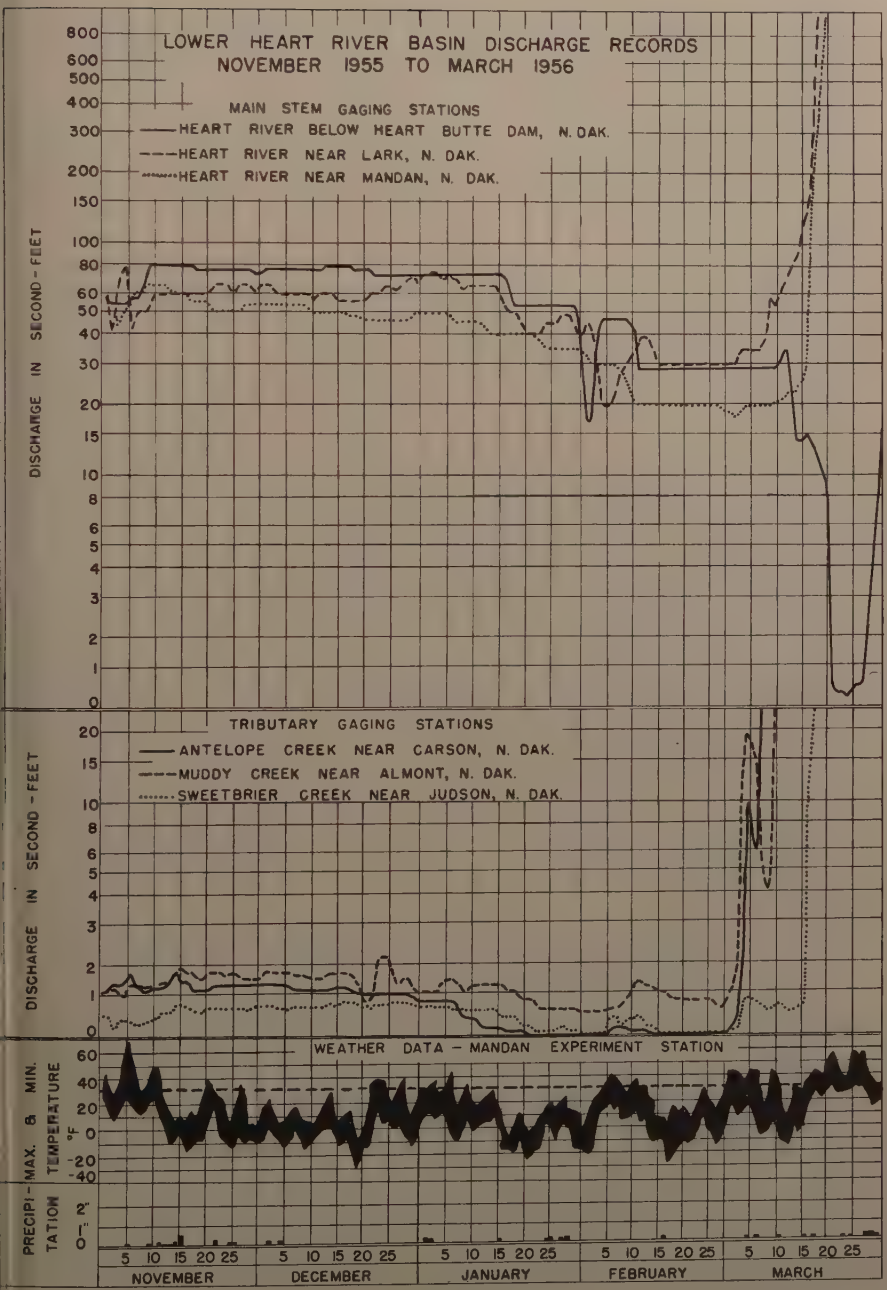
LOWER HEART RIVER BASIN DISCHARGE RECORDS
NOVEMBER 1955 TO MARCH 1956
MAIN STEM GAGING STATIONS
HEART RIVER BELOW HEART BUTTE DAM, N. DAK.
HEART RIVER NEAR LARK, N. DAK.
HEART RIVER NEAR MANDAN, N. DAK.
DISCHARGE IN SECOND-FEET
800
600
500
400
300
200
150
100
80
60
50
40
30
20
15
10
8
6
5
4
3
2
1
0
TRIBUTARY GAGING STATIONS
ANTELOPE CREEK NEAR CARSON, N. DAK.
MUDDY CREEK NEAR ALMONT, N. DAK.
SWEETBRIER CREEK NEAR JUDSON, N. DAK.
DISCHARGE IN SECOND-FEET
20
15
10
8
6
5
4
3
2
1
0
WEATHER DATA - MANDAN EXPERIMENT STATION
MAX. & MIN. TEMPERATURE °F
60
40
20
0
-20
-40
PRECIPITATION
2"
0
5 10 15 20 25
NOVEMBER
DECEMBER
JANUARY
FEBRUARY
MARCH

FIGURE 9

at the Mandan Experiment Station are also shown for each year.

The periods selected for study begin as soon as possible after the freezing weather started at a time of fairly steady releases from the reservoir and with base flow conditions prevailing on the tributaries. The periods were ended just prior to the first sign of surface water inflow from snow melt as indicated by the hydrographs for the tributaries provided reasonably steady flow from the reservoir prevailed for several days subsequent to the ending date. This procedure eliminated making adjustments for changes in channel storage and snow-melt runoff inflow which could not be adequately evaluated with the data available.

December 16 to March 10 was chosen as the study period for the 1953 water year. Figure 6 shows that the reservoir outflow was quite low ranging from 13 cfs (cubic feet per second) at the beginning to 10 cfs near the end of the period. Tributary inflow was reasonably constant. The winter was mild with no extremely cold periods and each month several degrees above normal.

December 6 to January 31 was selected as the study period for the 1954 water year. Figure 7 shows the reservoir release was steady at 100 cfs at the beginning of the period and decreased rather gradually to 90 cfs at the end. Tributary inflow declined steadily during the period. The period was rather short due to snow-melt inflow developing on February 1. The average December temperature was several degrees above normal but the January average was about the same amount below normal.

The period of study for the 1955 water year extended from November 27 to March 2. Figure 8 shows the reservoir release was steady at 31 cfs until December 5 when it was reduced to from 6 to 10 cfs for about 30 days then increased to from 29 to 31 cfs where it was held the remainder of the winter. Tributary inflow had a generally declining tendency during the period. Average temperatures were within a few degrees of normal during each month.

Particularly noteworthy during this period is the hydrograph for the Heart River near Mandan following the increase in release from the reservoir on January 7. It will be noted that the flow at Mandan shows no response to the increase in flow from the reservoir until 40 days later and then the increase in flow is less than half of the increment at the dam. Apparently all but a very small portion of the increase in the release was absorbed in storage in the form of ice.

November 11 to February 29 was used as the study period for the 1956 water year. The data for this period are shown in Figure 9. Release from the reservoir was reasonably steady, varying from 73 to 79 cfs, until January 16 when it was reduced to 54 cfs for about 12 days, then fluctuated down and then up moderately until February 11 when it was held steady at 29 cfs for the remainder of the period. This was a cold and prolonged winter with the average temperature several degrees below normal every month although there were no periods of unusually intense cold.

Of particular significance on the hydrograph is the position of the Lark graph with respect to the Heart Butte Dam graph during the latter half of February. This was the first time during this winter period that the flow at the lower station exceeded that at the upper. Apparently this happened because the reduction in release at the reservoir allowed the water to drop away from the ice cover or at least reduced the under pressure on the ice cover so that there was no further freezing of the flowing water.

The runoff in acre-feet for each gaging station for each month or partial month during the periods of study are Tabulated in Table 2. An estimate of

ERSKINE

RUNOFF IN ACRE-FEET

PERIOD	Heart River below Heart Butte Dam	Antelope Creek near Carson	Muddy Creek near Almont	Intervening Area (Estimated)	TOTAL	Heart River near Lark	GAIN OR LOSS Heart Butte Dam to Lark	Heart River near Lark	Sweetbriar Creek near Judson	Intervening Area (Estimated)	TOTAL	Heart River near Mandan	GAIN OR LOSS Lark to Mandan	GAIN OR LOSS Heart Butte Dam to Mandan
Dec. 16-31, 1952	394	25	64	22	505	354	-151	354	20	25	399	326	-73	-224
January, 1953	676	64	119	46	905	674	-231	674	39	50	763	573	-190	-421
February	585	151	103	64	903	849	-54	849	48	61	958	708	-250	-304
March 1-10	209	41	36	19	305	315	10	315	18	23	356	280	-76	-66
TOTAL	1,864	281	322	151	2,618	2,192	-426	2,192	125	159	2,476	1,887	-589	-1,015
Dec. 6-31, 1953	4,950	80	94	44	5,168	4,200	-968	4,200	45	58	4,303	4,230	-73	-1,041
January 1954	4,640	50	34	21	4,745	4,820	75	4,820	31	40	4,891	3,680	-1,211	-1,136
TOTAL	9,590	130	128	65	9,913	9,020	-893	9,020	76	98	9,194	7,910	-1,284	-2,177
Nov. 27-30, 1954	246	12	11	6	275	261	14	261	7	9	277	236	-41	-27
December	795	85	101	49	1,030	1,480	450	1,480	32	41	1,553	816	-737	-287
January 1955	1,520	50	90	35	1,695	871	-824	871	37	47	955	239	-716	-1,540
February	1,690	19	91	28	1,828	1,590	-238	1,590	41	52	1,683	252	-1,431	-1,669
March 1-2	123	4	4	2	133	147	14	147	2	3	152	40	-112	-126
TOTAL	4,374	170	297	120	4,961	4,349	-612	4,349	119	152	4,620	1,583	-3,037	-3,649
Nov. 11-30, 1955	3,040	56	64	30	3,190	2,440	-750	2,440	27	35	2,502	2,180	-322	-1,072
December	4,640	69	95	41	4,845	3,730	-1,115	3,730	44	56	3,830	3,030	-800	-1,915
January 1956	3,930	16	60	19	4,025	3,460	-565	3,460	24	31	3,515	2,530	-985	-1,550
February	1,880	2	46	12	1,940	1,790	-150	1,790	5	6	1,801	1,310	-491	-641
TOTAL	13,490	143	265	102	14,000	11,420	-2,580	11,420	100	128	11,648	9,050	-2,598	-5,178

the inflow from the ungaged tributary area in the reach from Heart Butte Dam to the Lark gage, and from the Lark to the Mandan gage was made. This inflow is believed to be extremely small during the winter months and has been estimated on the assumption that the runoff rate per square mile from the ungaged area was about one-half of the rate from the gaged tributaries.

The total flow entering each reach is computed and compared with the flow at the gaging station at the lower end of the reach for each month or partial month and for each complete period. The indicated gain or loss for each reach and the total gain or loss between Heart Butte Dam and Mandan is listed in Table 2.

Efforts were made to develop relationships between the indicated water losses and some of the other variables but no satisfactory relationship was found.

Figure 10 has been prepared to illustrate the indicated losses in the reach from Heart Butte Dam to Mandan. The mean temperature at the Mandan Experiment Station and the mean discharge at Heart Butte Dam has been shown with the plotting of the indicated water loss for each month or partial month.

The plotting for 1952-53 indicates a relatively small accumulation of ice, with the water loss for the 85-day period totaling 1,015 acre-feet. The average temperature was about 8 degrees above normal. The rate of release from the reservoir was quite low at the beginning of the period and was decreased slightly at intervals during the period. A comparison with the graphs for other years indicates that this combination of conditions was very favorable for minimizing ice formation.

The 1953-54 graph shows a much more rapid accumulation of ice during December than in the previous year. The average temperature was several degrees higher and the rate of release from the reservoir nearly eight times as great. Although the average temperature during January was several degress below normal, the rate of loss did not increase, probably because of a small decrease in rate of release from the reservoir. In a period of 56 days, the indicated loss amounted to 2,177 acre-feet.

The 1954-55 period began with a very low loss during December when the release rate was quite low and the average temperatures about 10°F. above normal. The rate of loss increased sharply during January and even more during February. The average temperature was a few degrees above normal during January and a few degrees below during February. The average discharge at the reservoir was increased during each of these months. The indicated loss during this period of 96 days totaled 3,649 acre-feet.

The winter of 1955-56 began early with the reservoir release rate at 80 cfs. The average temperatures ranged from about 10°F. below normal in November to about 4°F. below during February. Indicated water loss rose sharply during November and December when the discharge rate was maintained quite steady. The rate of loss decreased moderately during January and considerably during February. The average rate of release from the reservoir was being decreased considerably during these months. A total loss of 5,178 acre-feet is indicated for this 110-day period.

Conclusions drawn from Figure 10 are complicated by differences in temperature and other factors. However, we might say that generally the rate of loss is relatively low for the smaller discharges, particularly if the rate of release is decreased somewhat as the winter progresses. Higher losses are usually indicated for higher rates of release as is to be expected of a stream of this type which widens rapidly as the discharge increases in the range of

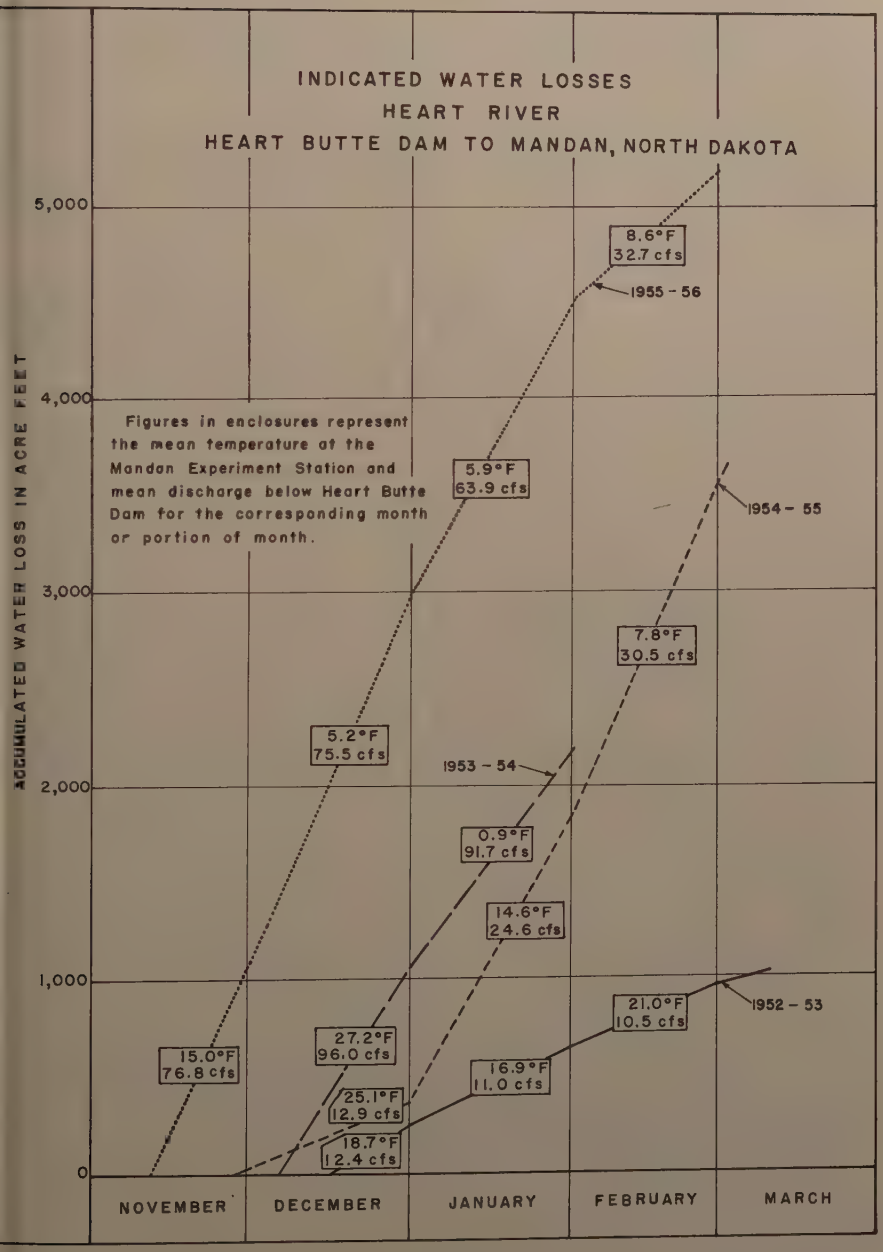
INDICATED WATER LOSSES
HEART RIVER
HEART BUTTE DAM TO MANDAN, NORTH DAKOTA
ACCUMULATED WATER LOSS IN ACRE FEET
5,000
4,000
3,000
2,000
1,000
0
Figures in enclosures represent the mean temperature at the Mandan Experiment Station and mean discharge below Heart Butte Dam for the corresponding month or portion of month.
8.6°F 32.7 cfs
1955 - 56
5.9°F 63.9 cfs
1954 - 55
7.8°F 30.5 cfs
5.2°F 75.5 cfs
1953 - 54
0.9°F 91.7 cfs
14.6°F 24.6 cfs
21.0°F 10.5 cfs
1952 - 53
15.0°F 76.8 cfs
27.2°F 96.0 cfs
16.9°F 11.0 cfs
25.1°F 12.9 cfs
18.7°F 12.4 cfs
NOVEMBER
DECEMBER
JANUARY
FEBRUARY
MARCH

FIGURE 10

flow being considered. Decreases in the rate of flow during a given period tend to decrease the rate of loss in all ranges of flow experienced. Increases in the rate of release add substantially to the rate of loss probably owing to water breaking through the existing ice cover and flowing on top where it is readily frozen.

The question arises whether all the indicated losses shown by this study are caused by the water going into storage in the form of ice. Possibly some flow is lost from the channel by seepage into the ground. There are no diversions during the winter months and the only consumptive use is a very minor amount for stock watering.

September 25 to November 18, 1952 was selected for study of possible seepage losses. During this period there was no appreciable precipitation for several weeks, the reservoir release was quite steady for several days prior to the beginning and the ending of the period, base flow conditions prevailed on the tributaries, evaporation losses were low and there was no loss due to transpiration, there were no known diversions for irrigation or other purposes, and there were no complications due to freezing.

The stream flow and weather records from August to December 1952 are shown on Figure 11. The reservoir release was steady at 76 cfs at the beginning of the study period and was steady at 110 cfs for several days prior to the end of the period. The release was reduced to about 25 to 30 cfs for several days on two occasions during October. Tributary inflow increased slightly during the period.

The data for the study period are in Table 3. The method of computation used was the same as in the winter water loss studies (Table 2) except that an evaporation adjustment has been included. This adjustment was computed using an average river width of 75 feet and evaporation depths of 0.8 inch, 2.0 inches and 0.5 inch respectively for the portions of September, October, and November included in the study period. Inflow from the ungaged intervening areas was computed on the same basis as it was for the winter periods

The tabulation for the total period shows a 99 acre-feet loss in the Heart Butte Dam to Lark reach but a 697 acre-feet gain in the Lark to Mandan reach. The net total for entire reach from Heart Butte Dam to Mandan indicates a gain of 598 acre-feet, approximately 6 percent of the Mandan flow. During the period, November 1-18, when the flow at all stations was almost constant it is noted that the gain at Mandan was 60 acre-feet, less than 2 percent of the Mandan flow. The reason for this indicated gain cannot be positively stated; however, it is probable that it results from seepage inflow from the alluvium forming the valley fill in the lower portion of the basin.

This study indicates that probably none of the indicated water losses during the winter months are due to seepage from the river. On the contrary, it appears that the losses ascribable to ice storage may actually be greater than indicated in Table 2 because seepage inflow is disregarded.

It appears proper to conclude that the losses due to ice storage are at least as great as indicated by the computations. These ice losses are, of course, temporary as far as total runoff is concerned because they are recovered during the breakup period.

On February 28, 1956, the writer examined the Heart River at a number of sites in an effort to obtain field data upon which to base estimates of the volume of ice in the river channel. Most of the rural roads were blocked by drifted snow but the river was examined at four highway crossings in the reach being studied. The ice thickness was measured near each bridge and

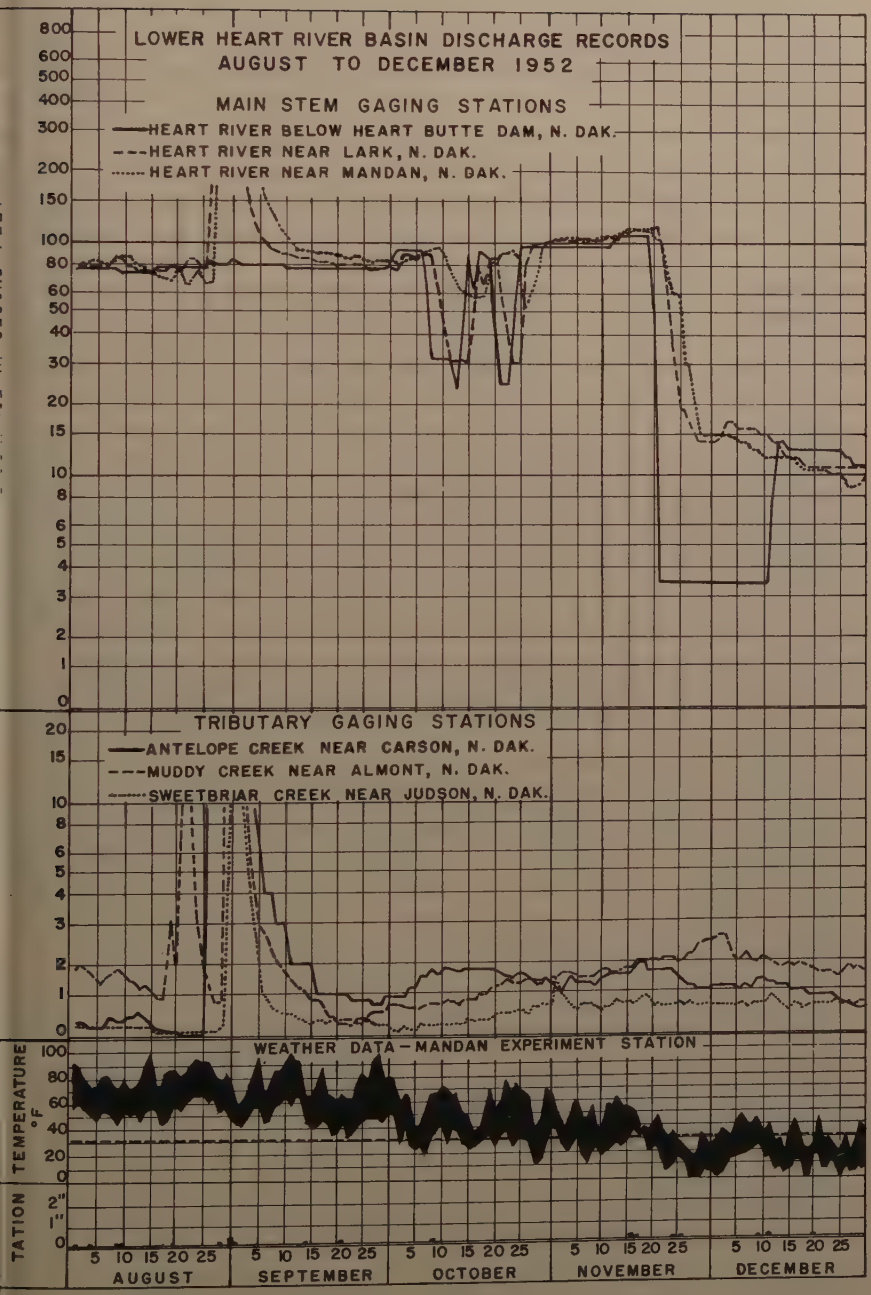
LOWER HEART RIVER BASIN DISCHARGE RECORDS
AUGUST TO DECEMBER 1952
MAIN STEM GAGING STATIONS
HEART RIVER BELOW HEART BUTTE DAM, N. DAK.
HEART RIVER NEAR LARK, N. DAK.
HEART RIVER NEAR MANDAN, N. DAK.
800
600
500
400
300
200
150
100
80
60
50
40
30
20
15
10
8
6
5
4
3
2
1
0
TRIBUTARY GAGING STATIONS
ANTELOPE CREEK NEAR CARSON, N. DAK.
MUDDY CREEK NEAR ALMONT, N. DAK.
SWEETBRIAR CREEK NEAR JUDSON, N. DAK.
20
15
10
8
6
5
4
3
2
1
0
WEATHER DATA - MANDAN EXPERIMENT STATION
TEMPERATURE °F
100
80
60
40
20
0
TATION
2"
1"
0
5 10 15 20 25
AUGUST
5 10 15 20 25
SEPTEMBER
5 10 15 20 25
OCTOBER
5 10 15 20 25
NOVEMBER
5 10 15 20 25
DECEMBER

FIGURE 11

Table 3. --Summary of runoff lower Heart River basin September 25 to November 18, 1952

Gaging Station or Other Source	Runoff in Acre-Feet			
	Sept. 25-30	Oct. 1-30	Nov. 1-18	Totals
Heart River below Heart Butte Dam	925	4,230	3,610	8,765
Antelope Creek near Carson	9	95	51	155
Muddy Creek near Almont	5	60	58	123
Intervening Area	4	39	25	68
Evaporation	-18	-43	-11	-72
Total	925	4,381	3,733	9,039
Heart River near Lark	920	4,200	3,820	8,940
GAIN OR LOSS - Heart Butte Dam to Lark	-5	-181	87	-99
Heart River near Lark	920	4,200	3,820	8,940
Sweetbriar Creek near Judson	3	20	26	49
Intervening Area	5	26	34	65
Evaporation	-21	-51	-13	-85
Total	907	4,195	3,867	8,969
Heart River near Mandan	986	4,840	3,840	9,666
GAIN OR LOSS - Lark to Mandan	79	645	-27	697
GAIN OR LOSS - Heart Butte Dam to Mandan	74	464	60	598

he width of the ice cover was estimated by pacing at a number of sections vithin several hundred feet above and below each bridge. The ice thicknesses neasured ranged from 2.4 to 2.9 feet and the stream widths ranged from 55 o 110 feet with most width measurements in a range from 90 to 100 feet. On he basis of these samples an average ice thickness of 2.6 feet and average vidth of 90 feet was assumed for the total reach. The ice was found to begin bout 2 miles below Heart Butte Dam. A computation of the ice volume in the each between the dam and Mandan based on this information indicates an ice olume of 2,500 acre-feet. The computations based on the streamflow records ndicate that the volume at this time was about 5,100 acre-feet, or practically wice as much.

It is believed that the discrepancy between these two figures is largely due o the samples of ice thickness not being representative of the overall reach. process known locally as glaciation is believed responsible for this situa-ion. During this process, water breaks through the ice from underneath or nters from the sides, flows over the ice and freezes upon it, thus causing bnormal thickness. Hydrographers working on this river as well as others n the general area, sometimes encounter ice thickness of from 4 to 6 feet hen searching for sections for making current-meter measurements. It is ot uncommon to find that water flows from holes cut in the ice in connection ith current-meter measurements or gage readings, indicating that the water s flowing under appreciable pressure and would rise above the ice surface hen cracks or other openings permit. Ranchers occasionally report cutting hrough 5 and 6 feet of ice to obtain water for stock. Where this glaciation rocess has been operative, it is probable that the width of the ice is sub-tantially greater than indicated by the samples used in the computation. The idth sampling did not take into account the ice that forms in the mouths of he numerous small tributaries as the ice formation on the main stream orces backwater into these areas.

These circumstances lead to the conclusion that a volume of ice storage omputed from a few samples of ice thickness and width is likely to be un-eliable, and that the volume of ice storage should be determined by water oss studies.

Journal of the
HYDRAULICS DIVISION
Proceedings of the American Society of Civil Engineers

ATTENUATION OF SOLITARY WAVES ON A SMOOTH BED

Yoshiaki Iwasa[1]
(Proc. Paper 1262)

SUMMARY

The hydraulic characteristics of solitary waves have been considered in a receding paper.(1) In this paper, further development of the study of solitary waves is treated. Especially considered is the mathematical analysis of the attenuation process of solitary waves. The theoretical results are compared to experimental data of Russell and Ippen.

It should be also noticed that the total kinetic energy minus the potential energy is twice the amount of the kinetic energy of the vertical motion, as Starr(2) has already verified.

I. INTRODUCTION

Theoretical and experimental researches on the solitary wave, defined as a single elevation of water surface above the still water level moving with constant celerity without change of form, may be found in many fruitful references.(3,4)

Although the purpose of the study on this problem was originally based on the mathematical interest, regardless of the phenomenon's actual existence, it is well known that a close analogy exists between the hydraulic characteristics of a solitary wave and those of an incoming water wave in surfs near coasts. Therefore, there has recently been a renewed interest in obtaining the complete characteristics of solitary waves in order to apply them to the problems of coastal engineering.(4,5)

The previously published papers(1,6) were concerned with the hydraulic configuration of open channel flows with appreciable vertical acceleration. It was shown that the solution of a second order approximation of translation

Note: Discussion open until November 1, 1957. Paper 1262 is part of the copyrighted Journal of the Hydraulics Division of the American Society of Civil Engineers, Vol. 83, No. HY 3, June, 1957.

[1] Asst. Prof. of Hydraulics, Dept. of Civ. Eng., Faculty of Eng., Kyoto Univ., Kyoto, Japan, visiting fellow, Hydrodynamics Lab., Massachusetts Inst. of Technology, Cambridge, Mass.

wave flow was expressed in terms of Jacobi's elliptic function including the solitary wave as one of the limiting cases, which also revealed some fundamental hydraulic characteristics of the solitary wave.

In this paper, further development of the study of solitary waves will be presented. Especially considered is the attenuation process of solitary wave by viscous shear within the laminar boundary layer between the main potential flow under a passing solitary wave and a smooth horizontal channel bed. The mathematics of the attenuation problem was first treated by G. H. Keulegan[7] in 1948, based on the small amplitude theory of wave motion. In 1953, J. W. Daily and S. C. Stephan[4] published an empirical formula for the attenuation, a result of much experimental data, and in 1955 and 1956 A. T. Ippen and G. Kulin[8,9] published results of further experiments and presented a new approximate attenuation formula based on the Blasius' formula of coefficient of friction experimentally verified by their experiment.

The finite amplitude theory of solitary waves is here considered in the treatment of viscous damping in the laminar boundary layer. It should be noticed, therefore, that the total kinetic energy is larger than the potential energy by twice the amount of the kinetic energy of the vertical motion, as V. P. Starr[2] first verified in 1947. Assuming that the flow within the laminar boundary layer under a solitary wave is also translatory, as is the main flow outside of the boundary layer, and the velocity distribution is given by some suitable formulas, the viscous damping of a solitary wave may be evaluated by using the usual concept that the rate of energy loss of the wave is equivalent to the rate of dissipation of energy in the laminar boundary layer.

II. HYDRAULIC CHARACTERISTICS OF SOLITARY WAVES

As described in the previous section, some hydraulic characteristics of solitary waves are now derived, considering translation wave flow with appreciable acceleration in the vertical motion. In this section hydraulic characteristics of solitary waves are presented for the convenience of discussion in a later section. But it should be prerequisitely noticed that in the theory discussed the velocity distribution in the horizontal direction is assumed to be truly translatory.

The solitary wave profile is given as the Rayleigh's type

$$\eta = a_o \operatorname{sech}^2 \left[\frac{1}{2y_o} \sqrt{\frac{3a_o}{y_o + a_o}} \cdot (x - Ct) \right], \qquad (1$$

where η = elevation of wave profile above still water level, a_o = amplitude, y_o = still water depth, x = horizontal distance along the wave measured from the wave crest, t = time, and C = wave celerity expressed by $\sqrt{g(y_o + a_o)}$ from consideration of the law of continuity.

After transforming the coordinate system into the moving one,

$$x - Ct \rightarrow x$$

Putting $y_o >> a_o$, the expression of Boussinesq and of Keulegan for solitary waves is obtained.

The horizontal velocity in the main flow is given by considering the law of continuity,

$$u_0 = C\frac{\eta}{y_0+\eta} \quad , \tag{2}$$

and the vertical velocity is given by using the usual hydrodynamic concept of stream line,(1)

$$v_0 = \sqrt{3}\,C\left(\frac{a_0}{y_0}\right)^{\frac{1}{2}}\left(1+\frac{a_0}{y_0}\right)^{\frac{1}{2}}\left[\left(\frac{\eta}{y_0}\right)\left(1+\frac{\eta}{y_0}\right)^{-2}\left(1-\frac{\eta}{y_0}\right)^{\frac{1}{2}}\left(\frac{y}{y_0}\right)\right] \quad , \tag{3}$$

where y = vertical distance from the channel bottom.

The volume of the solitary wave per unit width is obtained by integrating η from negative infinity to positive infinity.

$$V_0 = \frac{4}{\sqrt{3}}\,y_0^2\left(\frac{a_0}{y_0}\right)^{\frac{1}{2}}\left(1+\frac{a_0}{y_0}\right)^{\frac{1}{2}} \quad . \tag{4}$$

Now, consider the energy of solitary waves: in the small amplitude theory of wave motion, the energy is half potential and half kinetic. This forms the basic idea of the study on attenuation by Keulegan(7) as well as Ippen.(8) In 1947, Starr(2) first integrated the energy integral for the periodic gravity wave and applied it to the problem of solitary waves. His results explain that the kinetic energy is larger than the potential energy by twice the amount of kinetic energy of the vertical motion. But it is rather difficult to discuss quantitatively the hydraulic characteristics of solitary waves in Starr's derivation. The same conclusions as Starr's have been obtained by using the theoretical results of reference(6) and are as follows.

The potential energy is given by

$$E_P = \frac{1}{2}\rho g\int_{-\infty}^{+\infty}\eta^2\,dx \quad ,$$

where ρ = density of fluid, and g = acceleration of gravity. Substituting η, expressed by Eq. (1), and integrating

$$E_P = \frac{4}{3\sqrt{3}}\,\rho g y_0^3\left(\frac{a_0}{y_0}\right)^{\frac{3}{2}}\left(1+\frac{a_0}{y_0}\right)^{\frac{1}{2}} \quad . \tag{5}$$

The kinetic energy of the horizontal motion is

$$E_{KU_0} = \frac{1}{2}\rho\int_{-\infty}^{+\infty}u_0^2(y_0+\eta)\,dx \quad .$$

The integration yields

$$E_{KU_0} = \frac{2}{\sqrt{3}} \rho g y_0^3 \left[\left(\frac{a_0}{y_0}\right)^{\frac{1}{2}} \left(1 + \frac{a_0}{y_0}\right)^{\frac{3}{2}} - \frac{1}{2}\left(1 + \frac{a_0}{y_0}\right) \log_e \frac{1 + \sqrt{\frac{\frac{a_0}{y_0}}{1 + \frac{a_0}{y_0}}}}{1 - \sqrt{\frac{\frac{a_0}{y_0}}{1 + \frac{a_0}{y_0}}}} \right] \tag{6}$$

The kinetic energy of the vertical motion is given by

$$E_{KV_0} = \frac{1}{2} \rho \int_{-\infty}^{+\infty} v_0^2 (y_0 + \eta)\, dx .$$

Again integration yields

$$E_{KV_0} = \frac{2}{\sqrt{3}} \rho g y_0^3 \left[\frac{1}{3} \left(\frac{a_0}{y_0}\right)^{\frac{1}{2}} \left(1 + \frac{a_0}{y_0}\right)^{\frac{1}{2}} \left(3 + \frac{a_0}{y_0}\right) - \frac{1}{2}\left(1 + \frac{a_0}{y_0}\right) \log_e \left| \frac{1 + \sqrt{\frac{\frac{a_0}{y_0}}{1 + \frac{a_0}{y_0}}}}{1 - \sqrt{\frac{\frac{a_0}{y_0}}{1 + \frac{a_0}{y_0}}}} \right| \right] \tag{7}$$

The total energy of a solitary wave per unit width is expressed by the sum of Eqs. (5), (6), and (7), that is,

$$E = \frac{4}{\sqrt{3}} \rho g y_0^3 \left[\left(\frac{a_0}{y_0}\right)^{\frac{1}{2}} \left(1 + \frac{a_0}{y_0}\right)^{\frac{3}{2}} - \frac{1}{2}\left(1 + \frac{a_0}{y_0}\right) \log_e \left| \frac{1 + \sqrt{\frac{\frac{a_0}{y_0}}{1 + \frac{a_0}{y_0}}}}{1 - \sqrt{\frac{\frac{a_0}{y_0}}{1 + \frac{a_0}{y_0}}}} \right| \right] . \tag{8}$$

The above equation is the total energy of the finite amplitude wave. When the wave amplitude is very small compared with the original water depth, $y_0 >> a_0$, Eq. (8) becomes

$$E = \frac{8}{3\sqrt{3}} \rho g y_0^{\frac{3}{2}} a_0^{\frac{1}{2}} . \tag{9}$$

Eq. (9) is the same as Keulegan's expression, and it follows that the potential energy is equal to the kinetic energy in the small amplitude theory. Denoting E_k as the total kinetic energy, the following relation between the kinetic and potential energies is obtained:

$$E_K - E_P = 2E_{Ku_0} \cdot \tag{10}$$

This relation shows that the kinetic energy in the finite amplitude theory is larger than the potential energy, and the difference between them is twice the amount of the kinetic energy of the vertical motion, as Starr first derived in his gravitational wave theory. Figure 1 shows the relation between the dimensionless energy, expressed as $E' = E/\rho g y_0^3$, and the relative amplitude, a_0/y_0.

The rate of energy dissipation when the solitary wave passes through the channel is given by differentiating Eq. (8) with respect to the time, that is,

$$\frac{dE}{dt} = -\frac{2}{\sqrt{3}} \rho g^{\frac{3}{2}} y_0^{\frac{5}{2}} \left[4\left(\frac{a_0}{y_0}\right)^{\frac{1}{2}} \left(1 + \frac{a_0}{y_0}\right) - \left(1 + \frac{a_0}{y_0}\right)^{\frac{1}{2}} \log_e \left| \frac{1 + \sqrt{\frac{\frac{a_0}{y_0}}{1 + \frac{a_0}{y_0}}}}{1 - \sqrt{\frac{\frac{a_0}{y_0}}{1 - \frac{a_0}{y_0}}}} \right| \right] \frac{d\left(\frac{a_0}{y_0}\right)}{d\left(\frac{s}{y_0}\right)} , \tag{11}$$

where s = travel distance of a wave.

The above relation is one of the fundamental equations in evaluating the damping process of solitary waves in the laminar as well as turbulent boundary layer.

III. RATE OF ENERGY DISSIPATION IN THE LAMINAR BOUNDARY LAYER

The rate of dissipation of energy per unit volume, Φ, in the two-dimensional laminar boundary layer is given by

$$\Phi = \mu \left[2\left(\frac{\partial u}{\partial x}\right)^2 + 2\left(\frac{\partial v}{\partial y}\right)^2 + \left(\frac{\partial v}{\partial x} + \frac{\partial u}{\partial y}\right)^2 \right] , \tag{12}$$

where u and v = horizontal and vertical velocities in the boundary layer, and μ = dynamic viscosity of the fluid. It is sufficient to consider that the gradient of horizontal velocity in the y-direction is very large compared with other terms, thus the principal part of the above equation becomes

$$\Phi = \mu \left(\frac{\partial u}{\partial y}\right)^2 . \tag{13}$$

Damping of a solitary wave on a smooth channel bed is usually considered to be due to the viscous shear expressed by the above equation. If the velocity distribution in the laminar boundary layer is determined from the original Navier-Stokes equations of motion, the rate of energy dissipation can be obtained by integrating from the channel bottom to the thickness of the boundary layer, and from negative infinity to positive infinity. It is, however, very difficult to integrate the original hydrodynamic equations. Although Keulegan

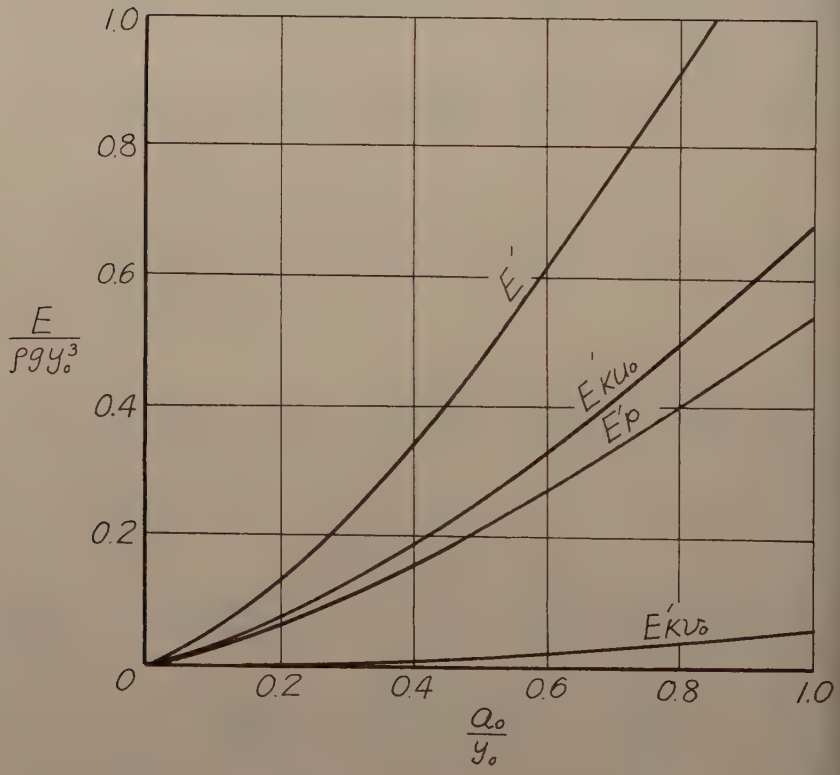

Fig. 1 Relation between energy and relative amplitude

did, his theory implies the assumption that the thickness of the boundary ayer extends to infinity, while the flow is actually confined. Under some appropriate conditions, the original dynamic equations become linear, and a rigorous solution is obtained, but the expression is so complicated, by being composed of a Fourier series, as to be impractical. This difficulty is mainly due to the finite thickness of the boundary layer.

Ippen, Kulin, and Raza[8] first measured the velocity distribution in the aminar boundary layer by an electrical differential gauge, reported in 1955, nd their results show that the velocity distribution in the boundary layer can e assumed to be linear or parabolic as in the steady regime. In this paper, he distribution of velocity is also assumed to be given by the Couette Linear) and parabolic types of flow. Thus, by integrating the above equation, he rate of energy dissipation per unit width is given by,

for Couette flow:

$$\frac{dE}{dt} = \mu \int_{-\infty}^{+\infty} \frac{U_0^2}{\delta}\, dx \,, \tag{14}$$

for parabolic flow:

$$\frac{dE}{dt} = 2\mu \int_{-\infty}^{+\infty} \frac{U_0^2}{\delta}\, dx \,, \tag{15}$$

where δ = thickness of boundary layer. It is, therefore, necessary to evaluate the process of development of a boundary layer under a passing solitary wave.

As the thickness of the boundary layer may be considered to be rather thin compared with the main potential flow, except near and at negative infinity, it is assumed that the flow is unconfined. Hence, the development process of the boundary layer is simply given by the following equation (10):

$$\left(\frac{u^*}{U_0}\right)^2 = \frac{\partial \theta}{\partial x} + \frac{1}{U_0}\frac{\partial U_0}{\partial x}(2\theta + \delta^*) + \frac{1}{U_0^2}\frac{\partial}{\partial t}(U_0 \cdot \delta^*) \,. \tag{16}$$

where u* = frictional velocity, and θ and δ^* = momentum and displacement thickness defined by

$$\theta = \int_0^{\delta} \left(\frac{u}{U_0} - \frac{u^2}{U_0^2}\right) dy \quad , \qquad \delta^* = \int_0^{\delta} \left(1 - \frac{u}{U_0}\right) dy \,.$$

ransforming the coordinate system into the moving one with constant elerity

$$\left(\frac{u^*}{u_0}\right)^2 = \frac{d\theta}{dx} - \frac{c}{u_0}\frac{d\delta^*}{dx} + \frac{1}{u_0}\frac{du_0}{dx}\left(2\theta + \delta^* - \frac{c}{u_0}\delta^*\right) . \qquad (17)$$

Assuming that the velocity distribution in the boundary layer is given by Couette and parabolic types of flow, the momentum and displacement thicknesses become, respectively,

for Couette flow:

$$\theta = \frac{\delta}{6} , \qquad \delta^* = \frac{\delta}{2} ,$$

for parabolic flow:

$$\theta = \frac{2\delta}{15} , \qquad \delta^* = \frac{\delta}{3}$$

Hence, the following boundary layer equations, substituting the above values into Eq. (17), are obtained, respectively,

$$\frac{d\delta^2}{dx} + \frac{2}{u_0}\frac{3c - 5u_0}{3c - u_0}\frac{du_0}{dx}\delta^2 = -\frac{12\nu}{3c - u_0} , \qquad (18a)$$

$$\frac{d\delta^2}{dx} + \frac{2}{u_0}\frac{5c - 9u_0}{5c - 2u_0}\frac{du_0}{dx}\delta^2 = -\frac{30\nu}{5c - 2u_0} , \qquad (18b)$$

Transforming the independent variable from x to η and introducing the dimensionless parameters $\eta = a_0\sigma$, $\delta = a_0 i$, and $a_0 = y_0\lambda_0$, Eqs. (18a) and (18b) become

$$\frac{di^2}{d\sigma} + \frac{2}{\sigma}\frac{(3 - 2\lambda_0\sigma)}{(1+\lambda_0\sigma)(3+2\lambda_0\sigma)} i^2 = \pm\frac{12}{\sqrt{3}\,R_c}\lambda_0^{-\frac{5}{2}}\frac{(1+\lambda_0\sigma)}{\sigma\sqrt{1-\sigma}\,(3+2\lambda_0\sigma)} , \qquad (19a)$$

and

$$\frac{di^2}{d\sigma} + \frac{2}{\sigma}\frac{(5 - 4\lambda_0\sigma)}{(1+\lambda_0\sigma)(5+3\lambda_0\sigma)} i^2 = \pm\frac{30}{\sqrt{3}\,R_c}\lambda_0^{-\frac{5}{2}}\frac{(1+\lambda_0\sigma)}{\sigma\sqrt{1-\sigma}\,(5+3\lambda_0\sigma)} . \qquad (19b)$$

where R_c = Reynolds number of celerity, determined by the given flow condition expressed by $g^{1/2}y_0^{3/2}/\nu$, the upper positive sign means the equation for the positive direction from the origin to the infinity, and the lower negative sign, the equation for the negative direction. As it is still difficult to solve the above equation, the following equation, as the first approximation for small values of λ_0, can be assumed for parabolic flow:

$$\frac{di^2}{d\sigma} + \frac{2}{\sigma} i^2 = \pm \frac{6}{\sqrt{3}\,R_c} \lambda_0^{-\frac{5}{2}} \frac{1}{\sigma\sqrt{1-\sigma}} \quad . \tag{20}$$

lthough this equation has a singular point at $\sigma = 0$, the solution for the approximate equation under the boundary conditions $i_1 = 0$ at $\sigma = 0$ for the ositive direction and $i_2 = i_1$ at $\sigma = 1$ for the negative one becomes

$$\begin{cases} \sigma^2 i_1^2 = \dfrac{8}{\sqrt{3}\cdot R_c} \lambda_0^{-\frac{5}{2}} \left[1 - \left(1 + \dfrac{\sigma}{2}\right)\sqrt{1-\sigma}\right] , \\ \sigma^2 i_2^2 = \dfrac{8}{\sqrt{3}\,R_c} \lambda_0^{-\frac{5}{2}} \left[1 + \left(1 + \dfrac{\sigma}{2}\right)\sqrt{1-\sigma}\right] , \end{cases} \tag{21}$$

here subscripts 1 and 2 show the values in the positive and negative directions, respectively. This is the approximation equation for the development f laminar boundary layer under a passing solitary wave. Figure 2 shows an

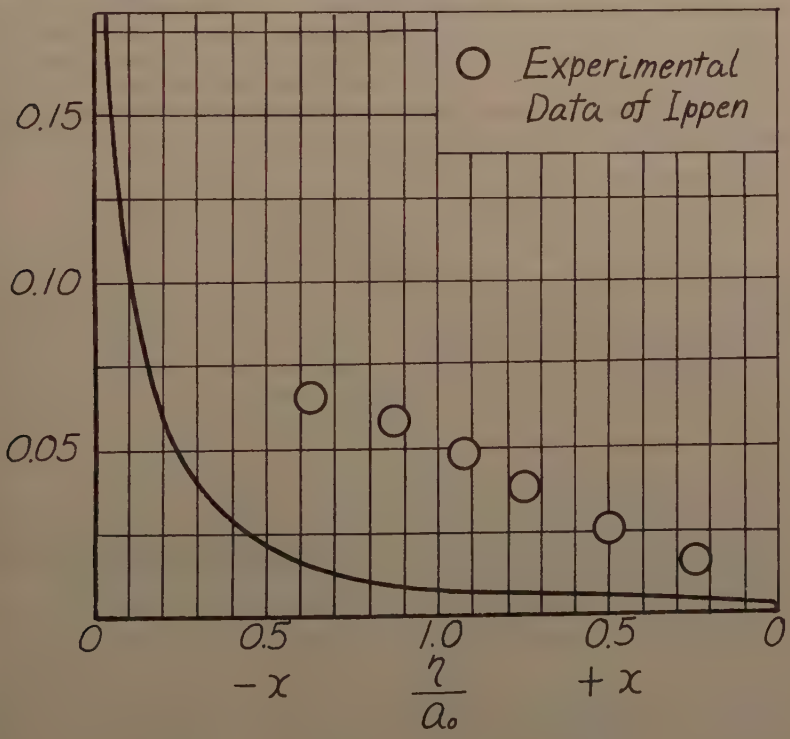

Fig. 2 Development of the boundary layer

example of the development process of the boundary layer. The above equation implies that at negative infinity the thickness of the boundary layer becomes infinite although the actual flow is confined. Hence, Eqs. (21) may be applied to the present problem from positive infinity to the point at where the thickness of the boundary layer is equal to the water depth. This point is calculated by the following relation, with sufficient accuracy, for parabolic flow:

$$\sigma_c \approx \frac{4}{\sqrt[4]{27}} R_c^{-\frac{1}{2}} \cdot \lambda_0^{-\frac{1}{4}} .$$

In the same way, the critical point for the case of Couette flow is given by:

$$\sigma_c \approx \frac{4\sqrt{2}}{\sqrt[4]{27}} R_c^{-\frac{1}{2}} \cdot \lambda_0^{-\frac{1}{4}} .$$

From this point to negative infinity, the thickness of the boundary layer will be considered to be equal to the water depth, that is, the fully developed laminar regime will be attained. Although the behavior of the development process in the boundary layer at the negative branch in the present analysis seems very doubtful, its actual behavior cannot be confirmed.

Applying Eqs. (21) to this problem, the thickness of the boundary layer under the crest of a solitary wave is given by,

for parabolic flow:

$$\delta^2_{x=0} = \frac{8}{\sqrt{3}\, R_c} y_0^{\frac{5}{2}} a_0^{-\frac{1}{2}} ,$$

for Couette flow:

$$\delta^2_{x=0} = \frac{16}{3\sqrt{3}\, R_c} y_0^{\frac{5}{2}} a_0^{-\frac{1}{2}} .$$

The theoretical thickness of the above expressions are very small, and about one-fifth of the experimental results presented by Ippen, Kulin and Raza. More detailed experiments will be needed to clarify the development process of the laminar boundary layer.

Therefore, the expression of the rate of energy dissipation in the laminar boundary layer for parabolic flow from Eqs. (2), (15) and (21) is

$$\frac{dE}{dt} = 2\mu \int_{-\infty}^{-|x|_{\sigma=\sigma_c}} \frac{u_0^2}{y_0+\eta}\, dx + 2\mu \int_{-|x|_{\sigma=\sigma_c}}^{0} \frac{u_0^2}{\delta_2}\, dx + 2\mu \int_0^{+\infty} \frac{u_0^2}{\delta_1}\, dx$$

$$= 2\mu \int_{-\infty}^{+\infty} u_0^2 \left[\frac{1}{\delta_1} + \frac{1}{\delta_2}\right] dx - 2\mu \int_{-\infty}^{-|x|_{\sigma=\sigma_c}} u_0^2 \left[\frac{1}{\delta_2} - \frac{1}{y_0+\eta}\right] dx$$

$$= \frac{2^{\frac{1}{2}}}{3^{\frac{1}{4}}} \mu g y_o R_c^{\frac{1}{2}} \lambda_o^{\frac{7}{4}} (1+\lambda_o)^{\frac{3}{2}} \left[\int_0^1 \frac{\sigma\sqrt{2+\sigma\sqrt{3+\sigma}}}{\sqrt{3+\sigma}\sqrt{1-\sigma}(1+\lambda_o\sigma)^2} d\sigma \right.$$

$$\left. - \int_0^\sigma \frac{\sigma\, d\sigma}{\sqrt{1-\sigma}(1+\lambda_o\sigma)^2} \left\{ \frac{1}{2} \frac{\sigma}{\sqrt{1+\left(1+\frac{\sigma}{2}\right)\sqrt{1-\sigma}}} - \frac{2^{\frac{1}{2}}}{3^{\frac{1}{4}} R_c^{\frac{1}{2}} \lambda_o^{\frac{1}{4}}} \frac{1}{(1+\lambda_o\sigma)} \right\} \right]. \qquad (22)$$

For the case of Couette flow, the following relation of the rate of energy dissipation is derived in a similar manner:

$$\frac{dE}{dt} = \frac{3^{\frac{1}{4}}}{2} \mu g y_o R_c^{\frac{1}{2}} \lambda_o^{\frac{7}{4}} (1+\lambda_o)^{\frac{3}{2}} \left[\int_0^1 \frac{\sigma\sqrt{2+\sigma\sqrt{3+\sigma}}}{\sqrt{3+\sigma}\sqrt{1-\sigma}(1+\lambda_o\sigma)^2} d\sigma \right.$$

$$\left. - \int_0^{\sigma_c} \frac{\sigma\, d\sigma}{\sqrt{1-\sigma}(1+\lambda_o\sigma)^2} \left\{ \frac{1}{2} \frac{\sigma}{\sqrt{1+\left(1+\frac{\sigma}{2}\right)\sqrt{1-\sigma}}} - \frac{2}{3^{\frac{1}{4}} R_c^{\frac{1}{2}} \lambda_o^{\frac{1}{4}}} \frac{1}{(1+\lambda_o\sigma)} \right\} \right]. \qquad (23)$$

These above two relations are also fundamental equations in evaluating the process of viscous damping in the laminar boundary layer under a passing solitary wave.

IV. ATTENUATION FOR A SMOOTH BED

As already shown in the previous section, the basic principle of attenuation of solitary waves is that the rate of energy dissipation in the laminar boundary layer under a passing solitary wave must be equal to the rate of energy loss manifested in the amplitude decrease of the wave. For the present case of parabolic flow, the following relation, from Eqs. (11) and (22) is obtained:

$$\lambda_o^{-\frac{5}{4}} (1-\lambda_o)^{-\frac{3}{2}} \left[1 - 1.6667\lambda_o - 0.1333\lambda_o^2 - \cdots \right] d\lambda_o$$

$$- \left[\int_0^1 \frac{\sigma\sqrt{2+\sigma\sqrt{3+\sigma}}}{\sqrt{3+\sigma}\sqrt{1-\sigma}(1+\lambda_o\sigma)^2} d\sigma - \int_0^{\sigma_c} \frac{1}{2} \frac{\sigma^2 d\sigma}{\sqrt{1-\sigma}(1+\lambda_o\sigma)^2} \left\{ \frac{1}{\sqrt{1+\left(1+\frac{\sigma}{2}\right)\sqrt{1-\sigma}}} \right. \right. \qquad (24)$$

$$\left. \left. - \frac{2^{\frac{3}{2}}}{3^{\frac{1}{4}} R_c^{\frac{1}{2}} \lambda_o^{\frac{1}{4}}} \frac{1}{\sigma(1+\lambda\sigma)} \right\} \right] \cdot \frac{3^{\frac{1}{4}}}{2^{\frac{3}{2}}} R_c^{-\frac{1}{2}} d\left(\frac{\delta}{y_o}\right) = 0 .$$

Integrating the above equation under the boundary condition of $(a_o/y_o) = (a_i/y_o)$ at $s = 0$ yields,

$$\lambda_o^{-\frac{1}{4}} \left[1 - 0.8062\lambda_o - 2.0027\lambda_o^2 - \cdots \right] - \lambda_i^{-\frac{1}{4}} \left[1 - 0.8062\lambda_i \right.$$

$$\left. - 2.0027\lambda_i^2 - \cdots \right] = 0.1499 R_c^{-\frac{1}{2}} \left(\frac{\delta}{y_o}\right) . \qquad (25)$$

where $\lambda_i = a_i/y_o$.

This is the two-dimensional attenuation formula based on distance traversed. If the channel is of limited width, however, some factor to include the frictional effect along the side walls must be added. If $(1 + 2y_o/B)$ is used as a first approximation, which is only correct for very low waves, the following relation for the rectangular channels is obtained:

$$\lambda_o^{-\frac{1}{4}}\left[1-0.8062\lambda_o-2.0027\lambda_o^2-\cdots\right]-\lambda_i^{-\frac{1}{4}}\left[1-0.8062\lambda_i -2.0027\lambda_i^2-\cdots\right]=0.1499\,R_c^{-\frac{1}{2}}\left(1+\frac{2y_o}{B}\right)\left(\frac{\Delta}{y_o}\right) . \tag{26}$$

In the same way, for the case of Couette flow, the attenuation equation is

$$\lambda_o^{-\frac{1}{4}}\left[1-0.8062\lambda_o-2.0027\lambda_o^2-\cdots\right]-\lambda_i^{-\frac{1}{4}}\left[1-0.8062\lambda_i -2.0027\lambda_i^2-\cdots\right]=0.0918\,R_c^{-\frac{1}{2}}\left(1+\frac{2y_o}{B}\right)\left(\frac{\Delta}{y_o}\right) . \tag{27}$$

V. DISCUSSION ON THE ANALYTICAL RESULTS

To verify the above theoretical approach, classical experimental data of Russell as well as recent data of Ippen will be considered. In Figure 3, these experimental data are plotted with the parametric notation λ_i. In Russell's data, the temperature is assumed by Keulegan to be 15.8°C, and in Ippen's data the kinematic viscosity is assumed to be 1×10^{-5} ft^2/sec. Although the experimental data are very scattered, the value of K'

$$K' = (\lambda_i^{-\frac{1}{4}} - \lambda_o^{-\frac{1}{4}}) \Big/ R_c^{-\frac{1}{2}}\left(1-\frac{2y_o}{B}\right)\left(\frac{\Delta}{y_o}\right)$$

seems to increase as the ratio of λ_i to λ_o increases. K' is not constant, but a variable of the amplitude as well as, rigorously speaking, the Reynolds number of celerity in this theory. It is constant for the small amplitude theory, that is, 1/12 for Keulegan's expression, and 1/14 for Ippen's expression. Curves of K' versus λ_i/λ_o expressed by parametric values of λ_i are also shown in the same figure. The dotted lines show the relation of the attenuation equation when Couette flow is assumed. Comparing these curves, it seems that Eq. (26), which represents the attenuation equation of a solitary wave in the laminar boundary layer by assuming parabolic distribution of velocity, is considered to be fair. More approximately, Ippen's expression based on the Blasius' formula of the coefficient of friction seems better than Keulegan's equation.

Although this approach to attenuation implies some physical assumptions which will influence the development process of the boundary layer to a

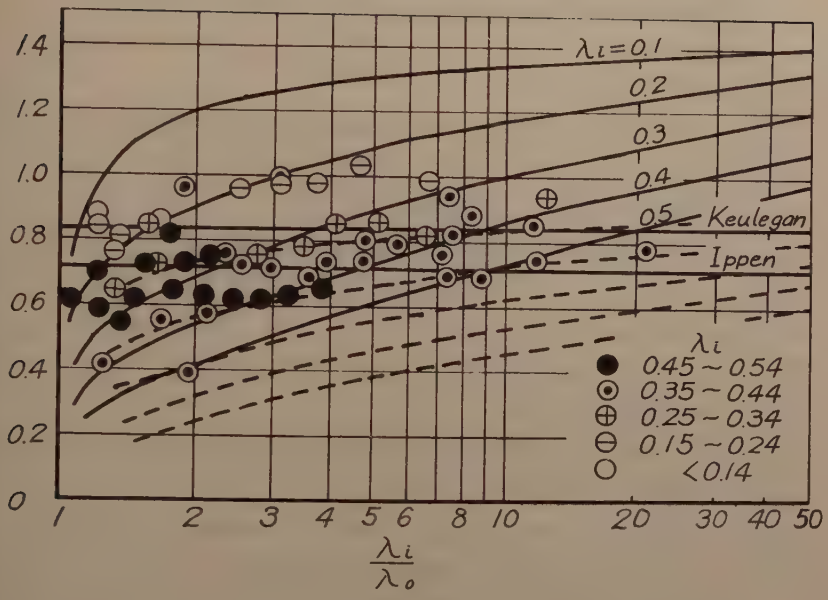

Fig. 3 Relation between K' and λ_i/λ_o

onsiderable extent, it cannot be ascertained whether these assumptions are orrect or not, because the experimental technique is still too primitive to btain detailed behavior in the boundary layer. After establishment of urther progress in experimental technique, a discussion of these assumptions will become helpful.

ACKNOWLEDGMENTS

The author wishes to express his grateful appreciations to Professor T. shihara, Director of the Hydraulic Laboratory of Kyoto University, for his onsiderable instruction; to Professor A. T. Ippen, Director of the Hydrodynamics Laboratory of the Massachusetts Institute of Technology for his ordial guidance and suggestions during the author's stay at MIT; and also hanks are due to Mr. J. G. Housley for his earnest help in preparing this aper.

LIST OF SYMBOLS

a : solitary wave height above still water level

B : channel width

C : wave celerity

$--_c$: subscript "c", referring to critical condition except Rc

E : wave energy per unit width

Ek : kinetic energy per unit width

Eku : kinetic energy of horizontal motion per unit width

Ekv : kinetic energy of vertical motion per unit width

Ep : potential energy per unit width

E' : dimensionless energy of wave expressed E/ gy_o^3

g : acceleration of gravity

$--_i$: subscript "i", referring to initial wave in attenuation theory

K' : damping coefficient in attenuation

$--_o$: subscript "o", referring to main flow condition

Rc : Reynolds number of celerity expressed by

s : horizontal distance of wave travel

t : time

u : horizontal particle velocity

v : vertical particle velocity

$\forall$: wave volume per unit width

x : horizontal distance along wave measured from wave crest

y : vertical distance from channel bottom

$--_1$: subscript "1", referring to values in positive direction of x

$--_2$: subscript "2", referring to values in negative direction of x

δ : thickness of boundary layer

δ^* : displacement thickness

η : surface elevation measured from still water level

θ : momentum thickness

i : dimensionless thickness of boundary layer expressed by δ / a_o

λ : dimensionless wave height expressed by a_o/y_o

μ : dynamic viscosity

ν : kinematic viscosity

ρ : density

η : dimensionless surface elevation expressed by η / a_0

β : rate of dissipation of energy by viscous shear per unit volume

REFERENCES

1. Iwasa, Y., "Analytical Considerations on Cnoidal and Solitary Waves," Memoirs of the Fac. of Eng., Kyoto Univ., Vol. XVII, No. IV, Oct., 1955.
2. Starr, V. P., "Momentum and Energy Integrals for Gravity Waves of Finite Height," Jour. of Marine Research, Vol. VI, No. 3, 1947.
3. Lamb, H., Hydrodynamics, New York, Dover, 1932.
4. Daily, J. W. and Stephan, S. C., "The Solitary Wave," Proc. Third Conq. on Coastal Eng., 1953.
5. Munk, W. H., "The Solitary Wave Theory and Its Application to Surf Problem," Annals of the New York Acad. of Sci., Vol. 51, Art. 3, 1949.
6. Iwasa, Y., "Hydraulic Characteristics of Solitary Waves," presented Japan Soc. Civ. Eng., Annual Conv., May, 1956.
7. Keulegan, G. H., "Gradual Damping of Solitary Waves," Jour. of Res. Nat. Bur. Stand., RP 1895, Vol. 40, 1948.
8. Ippen, A. I., Kulin, G. and Raza, "Damping Characteristics of the Solitary Wave," MIT Hydrodynamics Laboratory Tech. Rep., No. 16, Apr. 1955.
9. Ippen, A. T. and Kulin, G., "The Effect of Boundary Resistance on Solitary Waves," in press, La Houille Blanche, 1956.
10. Goldstein, S., Modern Developments in Fluid Dynamics, Oxford, 1938.

Journal of the
HYDRAULICS DIVISION
Proceedings of the American Society of Civil Engineers

THE ROLE OF SEDIMENTATION IN WATERSHEDS

Fred H. Larson,[1] M. ASCE, and G. Robert Hall[2]
(Proc. Paper 1263)

SYNOPSIS

Federal participation in watershed programs depends upon the premise that benefits must exceed the costs of any proposal. A large part of the benefits are usually due to the reduction of flood water and sediment damages. Since program proposals may have widely divergent effects upon sediment and flood water damages, it is necessary that separate appraisal systems be set up for flood water damages and for sedimentation damages.

This paper outlines the approach to sediment problems being made by the Department of Agriculture. A method is outlined to inventory the damages due to sedimentation and the benefits related to the reductions in these damages attributable to watershed programs.

Authority for the installation of watershed works of improvement by the Department of Agriculture has come in three stages. These are the Flood Control Act of 1936 and appropriations for "pilot watersheds" approved in 1953. The third, and the latest, legislative authority for this type of work is Public Law 566, the Watershed Protection and Flood Prevention Act of 1954, as amended in 1956.

There are 11 watersheds authorized for treatment under the Flood Control Act and 58 authorized as pilot watershed projects.

The basic procedure used in developing these projects is also being used in developing plans for watersheds under Public Law 566. This law states that it is the "policy of the Congress that the Federal Government should cooperate with local public agencies to prevent erosion, flood water and sediment damage and further the conservation, development, utilization and disposal of water."

Note: Discussion open until November 1, 1957. Paper 1263 is part of the copyrighted Journal of the Hydraulics Division of the American Society of Civil Engineers, Vol. 83, No. HY 3, June, 1957.

[1] Head, Eng. and Watershed Planning Unit, Soil Conservation Service, Upper Darby, Pa.
[2] Geologist, Eng. and Watershed Planning Unit, Soil Conservation Service, Upper Darby, Pa.

In the language of the Act, erosion, floodwater and sediment damage are on an equal footing. This is a significant reflection of the change in emphasis that has developed in watershed and flood control programs during the past generation. Prior to World War II, concept of flood control seldom went beyond the protection of specific localities against inundation.

In the watershed studies made by the U. S. Department of Agriculture, sediment has been considered an integral part of the problem on the grounds that it is deposited largely by flood flows or during flood-producing storms. Sediment damages are not integrated with water damages, sediment benefits are computed independently.

The water conservation program of the Department of Agriculture emphasizes the proper use of every acre. The widespread practice of strip-cropping, contour cultivation, terracing and other soil and water conservation measures by landowners and operators reduce sedimentation. This effect is related to but not solely a function of the hydraulics of flow.

Benefits from watershed treatment must be related to damages. This type and extent of the treatments proposed are predicated upon the benefits. Therefore, watershed projects usually start with a resource inventory, including a sediment damage survey. When damages are tabulated, the nature and scope of the proposed plans are indicated. The anticipated costs and benefits of alternate plans are then determined.

Perhaps the clearest way to present the Department of Agriculture's approach to sediment problems in watershed planning is to outline the procedures used in developing this phase of the watershed plan.

The investigation consists of four phases:

1. Determination of damage from sediment.
2. Determination of sediment sources and yields.
3. Developing the plan of treatment.
4. Benefit computations.

In the sediment damage surveys it may or may not be important to go further into the type of damaging sediment than mere bulk properties would indicate. In many watersheds damages may be related to type of sediment, which in turn may be related to a source. This may isolate an area where control should be specified.

Bottomland Damage Survey

The bottomland damage survey is the starting place. Over the years it has developed into a rather standard procedure. A classification of the bottomland is made. This classification is usually by "damage reaches." A damage reach may be an area of high sediment damage or it may be based on a hydraulic function, related cultural features or other considerations remote from sediment damages. Since the sediment damage study must be coordinated with other studies, it has been found more efficient to coordinate these studies from the beginning rather than interrelate them at a later date.

Once the "reaches" have been selected, the geologist, by a random sampling method, selects the locations of the valley cross sections. These may not be the hydrologic cross sections.

The bottomland damage survey is a field job. The geologist proceeds from valley wall to valley wall, recording the length along the section and

the percent of damage or benefit of each separate occurrence. The standard form (Fig. 1) provides for five types of damage to the land and an estimate of the percent of damage caused by each separate occurrence. Overwash, swamping, streambank erosion, floodplain scour and valley trenching are the types of damage enumerated.

Overwash

Infertile overwash is the deposition of relatively infertile sediment upon an old soil. It may take place on alluvial or colluvial soils and may take various forms, such as overbank splays, fans, or vertical deposits. Sterile sand or gravel commonly cause the damage, but silts and clays derived from subsoil are harmful in some areas, especially when deposited on heavy soils.

It is possible to have a soil improved by the deposition of more fertile overwash, or by changing the texture. For instance, a silty deposit may improve a very sandy soil. These areas are appraised and the benefit weighted against the damage on other areas to obtain an estimate of overwash damage in the watershed.

Swamping

Swamping is any impairment of drainage of bottomland or colluvial soils by sediment deposit. It may be caused by filling of stream channels with the products of erosion, which raises the watertable on the bottomlands, or formation of natural levees by sediment deposits which prevent proper surface drainage. Deposits of clay upon bottomland soils cause "puddling," reduce permeability and prevent internal drainage.

In some cases a benefit, rather than a damage, may be found, such as when sand is deposited on very heavy textured soils.

Streambank Erosion

Streambank erosion is the recession of the bank of a stream. This recession of the bank is usually accompanied by a replacement of material on the opposite side of the stream.

In estimating damage, a comparison is made between the production of the replaced material and the uneroded area. Interviews with farmers, tree growth, and photogrammetric evidence help estimate recovery and the time involved.

The "net" cross sectional area of material removed is recorded. Under fairly typical conditions the eroding bank may be six feet high, tapering to the six foot depth over a length of 30 feet. In that case, for example, the cross sectional area recorded would be 90 square feet, although the gross volume transported by the process would exceed that amount.

Floodplain Scour

Scour includes localized scour channels on the floodplain, sheet removal of large areas of soil from the bottomland, and erosion of terrace soils by flood flows.

Since evidence of scour damage is often eliminated by farm operations, it is difficult to express this damage on a historic basis. Landowners observations are an invaluable guide to this decision.

STREAM AND VALLEY SEDIMENTATION SURVEY
Range _____
_____ River Survey

From Station (1) to Station													Total or Average
Overwash	Distance												
	Percentage Damage (2)												
	Average Depth (3)												
	X-sectional Area (4)												
Swamping	Distance												
	Percentage Damage												
	Average Depth												
	X-sectional Area												
Streambank Erosion	Distance												
	Percentage Damage												
	Average Depth												
	X-sectional Area												
Floodplain Scour	Distance												
	Percentage Damage												
	Average Depth												
	X-sectional Area												
Valley Trenching	Distance												
	Percentage Damage												
	Average Depth												
	X-sectional Area												
Land Use (5)	Original												
	Present												

(1) All measurements from left side of valley, looking downstream, unless otherwise noted.
(2) To nearest 10 percent
(3) In feet and tenths
(4) In square feet
(5) By crop

FIGURE 1

Often it is found that the amount of scour determined by the survey is typical of the year-to-year occurrence. In this case the damage is assumed to be the average annual damage.

Valley Trenching

Valley trenching is the term used to describe a gully on the bottomlands. It may be caused by a concentration of overbank flows. This in turn causes an eroding channel or a side tributary that partly or entirely abandons its channel and erodes a new passageway along or across bottomland to the main stream.

Valley trenches are often transitory. Again, landowners observations are valuable as a guide to their history and rate of growth.

The percent of damage caused by these occurrences is a determination the field man must make on each damaged area. His criteria for the damage estimates are developed with experienced soil and crop specialists in the area. These specialists help him determine, for instance, how much a six-inch deposit of sand will affect production from a particular bottomland soil. The combined judgments are based on pot studies (where yield comparisons are made between the sediment and unaffected bottomland soils), plot yield studies (where the yield from an affected plot is compared with yield from an unaffected plot often in the same field), and chemical analysis.

Table 1 is an example of the guide developed to aid the field men in their determinations.

Unfortunately, a great many of our watersheds offer few opportunities to compare affected areas with unaffected areas. Surprisingly few unaffected bottomland areas exist today.

In summarizing data for the bottomlands, the lineal distance of damage is totaled and the "weighted average" of the damage is computed for each range. The several ranges for each reach are then summarized. In short, an "average" range for each reach is developed.

The next step is to expand the damage to the reach of bottomland in question. If bottomland area is available from aerial photographs, the average range length is divided into the area to obtain a valley length factor. If acreage is not available the mileage of stream valley in each reach is measured from the best maps available.

The acres affected by each occurrence are then computed by the formula:

$$a = 0.121\ b\ c$$

where
- a = acres affected
- b = av. lineal distance on each range, in feet
- c = mileage of valley in this reach

When this process is completed we have developed an inventory of the bottomland. It shows the area affected to date by these different types of damage and the amount of damage, percentage-wise.

This inventory summarizes conditions as they exist on the bottomlands in the watershed. It is a total occurrence to date of the area and extent of the damage, or benefit, caused by sediment and erosion on the bottomlands.

Due to the widely variable land use histories and physiographic conditions found in the watersheds, no single method has been found for converting the total damage to an average annual basis.

Table 1

Soils Laboratory Analysis of Recent Sediment and Old Soils From Chigley Sandy Creek Valley Washita River Watershed, Oklahoma 1/

Sample No.	pH	Available Phosphorous	Available Potash	Percent Organic Matter	Percent Sand	Silt	Clay
(1) Sediment	8.2 (basic)	0 (low)	162 (med.)	1.74 (med)	79	21	0
(2) Sediment	8.5 (basic)	0 (low)	162 (med.)	1.34 (med.)	85.5	12	2.5
(1) Old Soil	6.6 (s. acid)	10 (med.)	202 (high)	2.3 (high)	33.5	39.5	27
(2) Old Soil	7.1 (neutral)	204 (high)	244 (high)	2.5 (high)	35	28	37

Table 2

Percentages of Damage to Valley Lands as Related to Depth and Texture, Chigley Sandy Creek Valley, Washita River Watershed, Oklahoma. 1/

Depth Increment	Type of Sediment	Percent Damage
4-8 inches	Fine and coarse sand and silt	20
4-8 inches or 8-12 inches	Medium and coarse sand	40
	Fine and coarse sand	40
12-24 inches	Coarse sand	60
12-24 inches	Coarse sand and gravel	90

1/ Marshall, R. L. - Sedimentation Damages and Sediment Contribution Rates in Chigley Sandy Creek Drainage Area, Washita River Basin, Oklahoma, a part of a flood control work plan (unpublished). USDA-SCS, Ft. Worth, Texas.

In the case of erosion damage we are fortunate in universally available aerial photographs. Many of the watersheds have been photographed two or more times, with a time lapse of 8 to 12 years between coverages. In areas with two sets of photos, it is possible to measure the changes in channel alignment that occurred between the flights and thus obtain reasonably accurate measurement of the amount of streambank erosion that occurred. This readily gives an average annual rate. Where only one flight is available the rate can be determined by ground measurements to the cutting edge of the bank from carefully identified points on the photos, and on the ground. It might be pertinent to mention that the line measured on the ground is a straight line between two identifiable points, one left and one right of the channel. This permits an exact rectification of the photographic scale on this line.

Photographic measurements are used only to determine the average annual rate of occurrence. This is compared with the "gross" area affected as determined in the valley land damage study, primarily for the purpose of relating the "gross volume" of sediment produced, as determined by the bottomland damage survey, to an average annual volume of sediment produced from this source.

There is usually a degree of natural recovery on areas of bottomland damages. In monetary evaluation, the geologist provides the economist with data on the total area damaged and the loss in productivity. The estimate of the portion of the damage that could be expected to recover were it no longer subjected to flooding or deposition is also given. The economist can evaluate the annual loss in income from the damaged area based on the present damage. The loss in value of production from the non-recoverable portion of the sediment damage will continue after the installation of a program. The reduction of deposition as a result of the program is applied to the recoverable portion to determine the benefits from the reduction of sediment damage accruing to the program.

Other Sediment Damages

A number of sediment damages are appraised in addition to bottomland damages. Not all of these exist in any one watershed, however, their importance must be considered in any watershed survey.

Reservoir Sedimentation

This damage is the loss of storage capacity by sedimentation of water supply, power, recreational, desilting, flood control and other reservoirs.

The first step in evaluating reservoir sedimentation damage is the compilation of a list of reservoirs in the watershed, by physiographic provinces or problem areas, including data on capacity, size of drainage area, use, date of construction, and cost of construction. In some cases, water supply reservoirs, alternate water sources and associated costs of development are determined.

The second step is to determine the capacity loss and from this the damage caused by sediment.

The damage computations may be based on either of the following:

1. Damage to present structures.

2. Cost of restoration of capacity (dredging).
3. Estimated cost of alternate source development.

In the case of water supply reservoirs, the city or industrial engineers in charge of the facility can usually supply all of these answers except the rate of sedimentation.

Sediment damage to power reservoirs is complicated. Not only the amount of sediment, but the location of this sediment in the reservoir area is important. Therefore, quite detailed studies, in cooperation with the power company, are usually necessary.

A great many power reservoirs have lost all reserve storage and are now operating on run-of-the river flow. Sand and other coarse material may then move across the silted reservoir, through the intake canals, and into the turbines and other equipment.

This type of damage is evaluated as the cost of replacement parts, labor, loss of power and other costs directly connected with repairing the damage caused by the sediment. On the other hand, some power companies find it cheaper to prevent the damage rather than to repair it. They usually develop some method of dredging the sand from the intake canal and prevent its reaching the turbines. In this case the annual cost of dredging represents the damage.

Damage to Transportation Facilities

Sediment deposits damage highways and railways by collecting in ditches and culverts and upon the roadways, and by filling and constricting channels beneath bridges. These sediment deposits must be removed to keep the highway and railways functioning properly.

In surveying this type of damage the cost of sediment removal is usually obtained from the maintenance division of the highway department. In addition to this cost of sediment removal, associated damages are quite high in some localities. By causing a malfunction in the drainage system of the roadway, damage from frost action is increased enormously. The stability of fills and shoulders is often destroyed and the diverted runoff may remove fill, road gravel and, in some cases, entire sections of highway surface.

Highways are usually classified as to type of construction; sometimes the fact that they are state, county or township roads indicates the general type of construction and expedites the analysis of highway department records. In most areas the damage is obtained from the records of the highway departments. The data consist of the length of road and price level as well as:

1. Annual cost of removing sediment from ditches, culverts, and road surfaces.
2. Annual cost of channel dredging to protect bridges and highways.
3. Annual cost of repairing washouts due to plugged culverts and ditches.

Field and laboratory studies are sometimes necessary to identify the type and origin of this sediment. For instance, winter sanding is a particularly important distinction to make. As a general rule, visual inspection of a number of damage points will enable the geologist to determine the source of damaging sediments.

In many watersheds, for instance, road ditch sediments are fine materials originating from sheet erosion; while plugging the culverts will be bed

aterial of purely local origin from the streambed adjacent to the culvert. his type of breakdown is very important in developing a program to allevi- te the damage or in predicting the benefits expected to accrue to the overall atershed plan.

In some watersheds, harbor or canal dredging is necessary to provide or rotect transportation facilities. In these cases, the annual cost of dredging s considered to be the annual damage, but those costs incurred due to water- ned sediments must be segregated from costs due to industrial waste, lit- ral drift, etc.

rainage Ditch Sedimentations

Drainage ditches, irrigation ditches, and floodways are vulnerable to edimentation. As they fill with sediment they lose their effectiveness. To etermine the damage, usually it is only necessary to determine the costs of ean-out over the years and convert this cost to an average annual cost on e price level used for the report.

creased Flood Stages

When channels become clogged by sediment, flood crests for the same scharges are constantly forced to higher levels and floodwater damage in- reases.

Since river gages are located in stable reaches, this occurrence is not ually discernible from the gaging records of a stream. The reliable ethod of determining this aggradation is by comparing new surveys with evious cross section or channel profiles. Unfortunately, very few of ese older surveys are available and in the case of old highway or railway rveys are open to question due to construction activities. Where such cords are available, the damage due to the increased stage or frequency computed.

diment Damage to Property

After most floods, deposits of sediment are found on streets and in homes, tories, sewers, wells, and other places where they cause damage. The st of removing this sediment is considered the damage.

It is necessary to obtain records for a period of years for cities, indus- es and farms. These figures can then be reduced to an average annual mage during this period. In this regard, the problem of cleaning up after lood, regardless of the amount of sediment deposited, is always present. e costs identified as sediment damages are the cost associated with the ysical effort to remove a mass of material, as distinguished from washing wn and scrubbing up always required after a flood. We call the "shoveling " a sediment damage and the "scrubbing down" a floodwater damage.

Determination of Sediment Sources

Since the Department's watershed projects encompass sediment damage as ll as floodwater damage, it is encumbent upon the people developing the ogram to consider sediment sources, sediment entrainment and sediment nsport. These parameters of the sediment problem are usually expressed the sediment yield at the damage point in question.

Some or all of the following types of erosion may be important: sheet erosion, shallow gullies, deep gullies, valley trenches, streambank erosion, floodplain scour, roadside erosion, gravel pits, mine waste, industrial waste and construction activities.

There are several different methods of computing the amount of sediment produced by sheet erosion. They were primarily developed to determine the amount of soil lost from the field (erosion) and consequently they do not express sediment yield without due consideration being given to the processes of entrainment and transport.

Measurements of soil loss from experimental plots on different soils, slopes, and with different climatic conditions and rainfall patterns under different kinds and combinations of land use were summarized by the Soil Conservation Service.[3]

Measurements were available from nineteen research stations and covered periods of from 5 to 15 years.

From the study and evaluation of these data, it was determined that the rate of sheet erosion is related to a number of major factors, and that certain relationships exist between these factors. An empirical formula was developed:

$$E = F \times S^{1.35} \times L^{0.36} \times P^{1.75} \times C$$

where
- E is the probable soil loss in tons per acre per year.
- F is a soil factor, based upon the erodibility of the soil and other physical factors.
- S is the steepness of slope in percent.
- P is the rainfall. The amount used is the maximum 30-minute rainfall expected in the locality from a 2-year frequency basis.[4]
- C is a cropping factor which may be the product of several factors related to the use of the land.

These formulas have been found usable to estimate the amount of sheet erosion.

The amount of sediment originating from gully erosion is determined by field surveys, the procedure being similar to the methods used for measuring streambank erosion.

Sediment production rates for mine wastes, construction activities, roads gravel pits and related sources are problems commonly encountered but with no common solution. Many roads and skid trails can be cross sectioned and the volume of erosion to date determined. If the history of that stretch of road is known and the extent of the cut involved in construction is determined, the gross amount of erosion, to date, can be determined. Average annual amounts can then be estimated.

Areas involved in housing developments, super highways, airports, strip mining and other activities are given independent consideration. The amoun of sediment produced is usually estimated by the geologist, in consultation with the others on the planning party, as well as the engineers in charge of the development. Many of these sources are, here-today-gone-tomorrow

3. G. W. Musgrave - The Quantitative Evaluation of Factors in Water Erosion, Journal of Soil and Water Conservation, July 1949.
4. See U.S.D.A. Misc. Pub. No. 204.

fairs, that have little influence upon a long range watershed program. On e other hand, many areas are being converted from agricultural to urban se and the effect of this conversion upon sediment production, as well as ydraulic characteristics of the watershed, must be recognized.

Sediment Source - Damage Relationship

The total sediment yield from the various types of erosion, on an annual asis, are converted to percentages of total sediment. The relative impor- nce of each type of erosion can then be determined for specific damages. These figures apply only to the sediment as a whole within the watershed. he relative importance of the various sediment sources in the case of rticular types of sediment damage will vary either way from these mean lues. Some types of sediment damage are caused largely by one type of diment. The location of the damage point, whether in the headwaters or the mouth of the river, influence the relative importance of its sediment urce. Some types of sediment, after erosion, are redeposited a short dis- nce from their original source. Some types of erosion, such as floodplain our, may not occur in headwater areas. It is therefore necessary to de- lop for each type of sediment damage and for each damage area, the rela- ve importance of the various sediment sources. The measured relative urce areas are used as a guide. These data are most usable when con- rted to percentages of damaging sediment and tabulated in the following rm:

SEDIMENT SOURCES IN PERCENT "X" WATERSHED

	Sheet Erosion	Gully Erosion	Stream-bank Erosion	Flood-plain Scour	Road-side Erosion	Total	Av. Annual Dollar Damage
tershed "X"	65	5	10	5	15	100	
erwash	50	5	30	10	5	100	31,100
amping	40	5	40	10	5	100	15,300
ghway culverts	20	20	40	10	10	100	21.700
ghway ditches	40	10	-	-	50	100	63,000
rm Ponds	90	5	-	-	5	100	1,600
servoir #1	75	10	-	-	15		900

Developing the Program

The tabulation of sediment sources by percent is a useful device, not only show the relation of the sources to the damage but also in computing the ects of the program. By referring to the above table, the effect of any osion reduction in terms of benefit are evident.

For example, 50 percent of the overwash damage, amounting to $15,550 r year, is due to sheet erosion. Assuming that sheet erosion can be re- ced by 60 percent, the benefit from reduction of overwash damage would $9,330 or $31,100 x .50 x .60 = $9,330.

In developing a watershed program, a great many factors affect the final lection of the practices and measures to be recommended. In general, the ms to be included in the plan are those items which offer the most benefit

with the least cost. It is quite obvious that the results of the damage survey and the effects of the independent and interdependent measures that are proposed for inclusion in the plan must be presented in such a manner as to facilitate alternate appraisals.

The effect of the land use changes can be predicted through the recomputation of soil losses - with the land treatment measures installed, using the soil loss formula previously discussed.

The effect of structural measures on sediment production can also be predicted.

The sum of these effects provides a basis for predicting the reduction of sediment damages.

Sedimentation Considerations in Detail Designs

Following the acceptance of the watershed plan by the local people and its approval by the Government, detailed designs for all of the works of improvement are made.

The sediment storage requirements in floodwater detention reservoirs are computed for each individual reservoir and the data are usually summarized on a form similar to Figure 2.

The estimated sediment yield used in the design of a particular floodwater retarding structure is based on watershed conditions above the structure. These computations, for a 50-year period, are based upon conditions at the time of the inspection, adjusted for the amount and effectiveness of land treatment and other measures to be applied in the watershed.

The trap efficiency of the reservoir is estimated by the use of envelope curves based on capacity-inflow ratio.[5] The total capacity (sediment pool plus retarding pool) to emergency spillway level of the reservoir is used in determining the capacity-watershed or capacity-inflow ratio.

The weight of the sediment in the reservoir is estimated from volume-weight determinations made on sediments in farm ponds or other reservoirs within the area. In computing the volume of sediment in dry pools and in the floodwater retarding area, ultimate compaction of the aeriated deposit is assumed. Compaction of volume of sediments below the normal pool level is based on ultimate compaction under submerged conditions.

The distribution of sediment in the reservoir is dependent on the nature of the sediment, the topography and shape of the reservoir, nature of the sediment, the topography and shape of the reservoir, nature of approach channel above it, and the time required to empty the retarding pool. Allocation of capacity for sediment accumulation in the reservoir is made in two general locations, the lower of which is termed the sediment pool (below the normal pool level) and the higher of which is termed the retarding pool. The volume of sediment estimated to occur in the sediment pool may fix the elevation of the crest of the principal spillway.

The problem of bed load transport, both as related to floodwater detention structures and other installations deserve mention. Where total sediment transport rates are high, bed material accounts for a minor part of the total load and, while in no case is it ignored, it is realistically given minor consideration.

5. Trap Efficiency of Reservoirs, G. M. Brune, Transactions A.G.U., Vol. 3 No. 3, 1953.

Site No. _____ Location _____ Watershed Area: Acres: _____ Square Miles _____

SOURCE				TOTAL (Acre Feet)	DELIVERY RATE (Percent)	AVERAGE ANNUAL VOLUME OF SEDIMENT DELIVERED TO SITE (Acre Feet)
1. SHEET EROSION CULTIVATED LAND	ACRES	SOIL LOSS * (Tons Per Acre)	TOTAL		(Circle % Used)	
CLASS I						
CLASS II						
CLASS III						
CLASS IV						
OTHER						
IDLE LAND						
PASTURE						
WOODS						
		SUB-TOTAL			20 40 60 80 100	
2. CHANNEL EROSION						
GULLIES					20 40 60 80 100	
STREAMBANK					20 40 60 80 100	
3. FLOODPLAIN SCOUR					20 40 60 80 100	
4. OTHER (ROADS, ETC.)					20 40 60 80 100	

Computed By: _____

Date: _____

* Average for various conditions: See work sheet for details. TOTAL: _____

DEPOSITION

AVERAGE ANNUAL VOLUME OF SEDIMENT DELIVERED TO SITE FROM ALL SOURCES (ACRE FEET)	TRAP EFFICIENCY (PERCENT)	AVERAGE ANNUAL DEPOSITION (ACRE FEET)

STORAGE REQUIRED

AVERAGE ANNUAL DEPOSITION	RATIO WEIGHT OF SOIL / WEIGHT OF SEDIMENT	VOLUME STORAGE / YEAR	STORAGE LIFE YEARS	TOTAL STORAGE REQUIRED	ALLOCATION	
					SEDIMENT POOL	OTHER

Fig. 2

In the watersheds, such as the mountainous forest and pasture areas of the Northeast, where total transport is low, bed material transport may account for most of the sediment damage and consequently warrants close consideration. A number of formulas of the Du Boys type have been, and are being used, as well as the procedure developed by Dr. Hans Einstein.[6]

Unfortunately, these calculations, while requiring a rather high order of precise mathematics, give an index of magnitude rather than a precise estimate. This is not a deterrent in planning activities since most of the damages caused by bed material (such as channel filling, bridge and culvert plugging, etc.) involve a physical effort for their relief. These damages are usually expressed in the cost of removing the material. Consequently, the benefit is expressed as a percent reduction in damages.

Design problems are more difficult since they often involve a volumetric estimate.

Since none of the existing bed load formulas are precise when applied to untested conditions, the procedure most generally followed is to compute the bed load transport by two or three formulas,[7] and from these computations select, by judgment, the most conservative result to use in design of the work of improvement.

6. The Bed Load Function for Sediment Transportation in Open Channel Flows, H. A. Einstein, U.S.D.A. Technical Bulletin No. 1026, September 1950.
7. Engineering Hydraulics, page 795, edited by Hunter Rouse, 1949.

Journal of the
HYDRAULICS DIVISION
Proceedings of the American Society of Civil Engineers

STILLING BASIN EXPERIENCES OF THE CORPS OF ENGINEERS[a]

R. H. Berryhill,[1] A.M. ASCE
(Proc. Paper 1264)

SYNOPSIS

The Corps of Engineers has designed and built more than 150 reservoir ojects during the past twenty-five years. Most of these projects have been ilt since the Congress passed the Flood Control Act of 1936. Some of the periences of the Corps of Engineers in the design, operation and mainte-nce of the stilling basins below the spillways and outlet works of these pro-cts are described herein. Also described are several model and prototype rrelations and some conclusions which may be drawn from the experiences scribed. This paper is one of a series of four papers assigned to a task rce of the Design Committee of the Hydraulics Division on the general sub-rt "Energy Dissipators for Spillways and Outlet Works."

INTRODUCTION

A number of different types of stilling devices have been used for the safe ndling of flows released from the many spillways and outlet works built by Corps of Engineers. For spillways, the stilling devices used include nventional horizontal stilling basins with and without baffle piers, end sills l end sill controls, as well as sloping and stepped stilling basins, two-level sins, and bucket-type basins. Under the classification of bucket-type still-basins, the following types have been used: roller buckets, deflector kets, and high deflector buckets with or without subdams downstream. Many navigation and power dams under the jurisdiction of the Corps of gineers, with "run-of-the-river" flows, have experienced major spillway

e: Discussion open until November 1, 1957. Paper 1264 is part of the copyrighted Journal of the Hydraulics Division of the American Society of Civil Engineers, Vol. 83, No. HY 3, June, 1957.

Presented at American Society of Civil Engineers Annual Meeting, Pittsburgh, Pa., October 18, 1956.

Civ. Engr., Southwestern Div., Corps of Engrs., U. S. Dept. of the Army, Dallas, Texas.

releases which have provided good tests of the adequacy of the stilling basin design. Notable among these is the Bonneville Dam spillway, which passed 1,000,000 cu. ft. per sec. during the flood of 1948. Of the reservoir projects with flood control storage, however (and these comprise the majority) there are few spillways which have experienced large flow releases. This is of course brought about primarily by the fact that the flood control storage provided will often contain the entire flood of record on this type of project, and only rare floods will produce major spillway discharges. Since the average Corps of Engineers reservoir project has been in operation less than 15 years, a number of years may elapse before many of these projects experience large spillway flows.

Discharges from the outlet works at most Corps of Engineers reservoir projects are of course frequent. At several projects where the stilling basin is common to both spillway and outlet works, flows released from the outlet works have been more critical for design of the stilling basin than have the flows from the spillway. Energy dissipating devices that have been used for outlet works include most of the types used for spillways as enumerated above, and in addition include deflector or splitter blocks.

Discussed in the following pages are some of the stilling basins and other stilling devices which may be of interest either because of certain flow experiences, model-prototype comparisons, or difficulties encountered during operation. For grouping purposes, the first section involves a discussion of stilling devices below spillways where the discharges from the spillways are of primary interest or importance. The second section deals with stilling devices below spillways where the discharges from sluices located within the spillway weir section are of primary interest. Finally, stilling devices below certain tunnels and conduits are discussed, followed by conclusions which may be drawn from some of the experiences described.

Spillway Stilling Devices

McNary Dam (Washington and Oregon)

At this navigation and power project, the floow flows of the Columbia Rive are passed through a 1,310-ft.-long concrete gravity ogee spillway containing twenty-two 50-ft. by 50-ft. gates separated by 10-ft.-wide spillway piers. The stilling basin is the conventional hydraulic jump type and is designed to pass 2,200,000 cu. ft. per sec. at pool El. 356.5. As shown in Fig. 1, the apron is set at El. 228.0 and is 270 ft. long, with two rows of baffle piers and an end sill. The structure is unusual in that the maximum head on the spillway crest is 65.5 ft., resulting in a discharge into the stilling basin of 1,680 cu. ft. per sec. per ft. of basin width, or 100,000 cu. ft. per sec. for each gat bay.

Extensive use was made of hydraulic models in the development of this project. The spillway models included a 1:100 scale general model, a 1:36 scale sectional spillway model and a 1:10 scale single gate bay model. The apron length selected was equivalent to $3.2D_2$, where D_2 is the maximum conjugate depth after the hydraulic jump. The apron elevation was set so tha the maximum tailwater depth of 75.5 ft. was equal to $0.90D_2$ because of the anticipated effect of the baffle piers. It should be noted that the Froude Number ($V_1/\sqrt{gD_1}$) at design discharge is only 3.3, where V_1 and D_1 are the velocity and depth, respectively, upstream from the hydraulic jump.

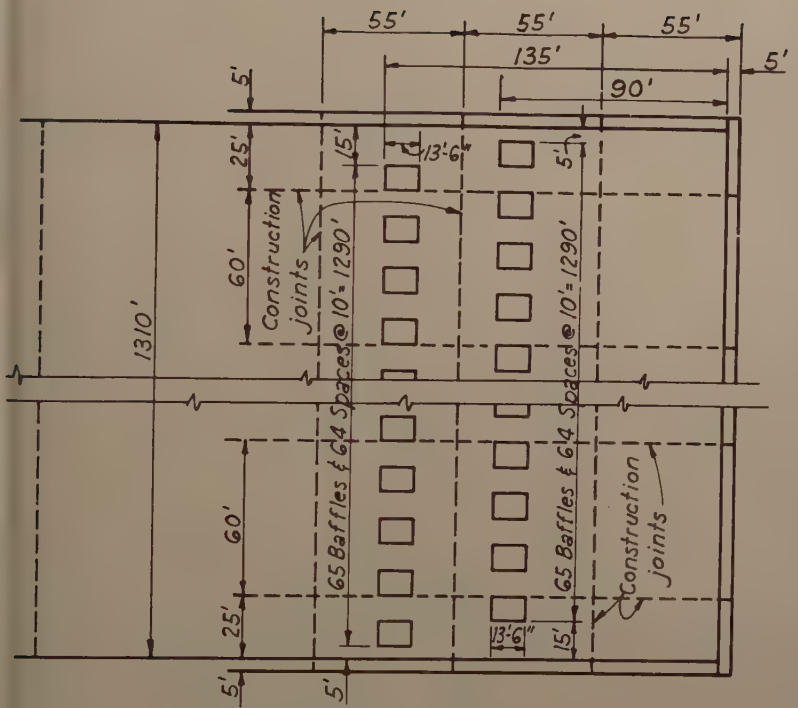

PLAN OF SPILLWAY

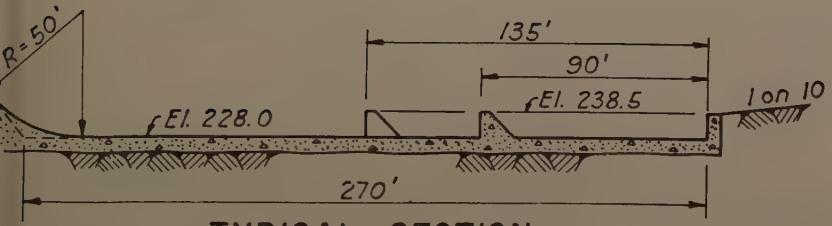

TYPICAL SECTION

Fig. 1. Stilling Basin Dimensions, McNary Dam.

The reservoir pool was raised in December 1953, upon completion of mos of the project features. Prototype operation tests were made in June and Jul 1955 with normal pool elevations of 335 and 340 and with spillway Bays 15, 1 and 17, numbering from the north bank, discharging together and with Bay 16 discharging alone. The purposes of the tests were to determine the magnitude of the pressures on the spillway crest, gate piers and baffle piers by means of piezometers installed in Bay 16, and to determine the conformity between performance of the spillway models and the prototype. The pressures obtained for the crest, gate slots and piers will not be discussed here, except to state that very good correlation with the models was obtained in nearly all instances.

The baffle pier pressures obtained from the prototype tests are shown in Fig. 2. It is noted that piezometer B-1 is located in the middle of the upstream face and B-2 is located at the downstream end of the one-ft. radius along the south side of the baffle. The opposite side of the baffle coincided with the centerline of Bay 16. A third piezometer, located in the top of the baffle, was apparently clogged during the test period. The tailwater elevatio was approximately 269.5 for all tests made with reservoir pool at elevation 335. With pool elevation 340, tailwater elevation was approximately 268.5 fo all conditions except for bays 15, 16 and 17 operating together with gate open ings of 1, 3, 5 and 10 feet, when tailwater elevation was 264.

The low pressures shown for piezometer B-2 indicate that some pitting a erosion of the sides of the baffles may be expected in the future. However, the flow conditions during the test period are not considered normal. Since normal spillway operation at McNary Dam is accomplished by nearly uniform gate settings for all the bays, the larger gate settings would only be used dur ing periods of large river flows and higher tailwater elevations. For exampl full gate openings would normally be accompanied by a tailwater level about 20 to 21 ft. higher than that used in the tests. The operation of a single gate at a large opening will occasionally be required for short periods of time when a load rejection at the powerhouse necessitates an immediate release from the spillway. Based on the above considerations, it is apparent that the pressure conditions shown in Fig. 2 are not as critical as the data seem to indicate.

No comparable information on baffle pier pressures in the models was available. However, pressures near the cavitation range were noted in the model for large flows of short duration.

An indication of the hydraulic losses incurred from reservoir pool to the upstream row of baffles is given by the graph for piezometer B-1 in Fig. 2. Total losses with full gate openings varied from 6.9 ft. for pool El. 340 to 10.9 ft. for pool El. 335, while as percentages of the total available head the losses were 6.5 and 10.7, respectively. It is hoped that additional test readings in the future will either verify these values or narrow the range of results.

The observed stilling basin action was satisfactory, although as might be expected, the large concentrations of flow in the test bay created extremely rough and turbulent flow conditions. With pool elevation 340 and free flow in Bay 16, the hydraulic jump remained in the stilling basin with tailwater 16 f (28%) lower than the minimum tailwater required for a jump as determined the 1:36-scale sectional model. Apparently the side inflow which could not b duplicated in the sectional model was sufficient to partially stabilize the jum in the prototype test bay.

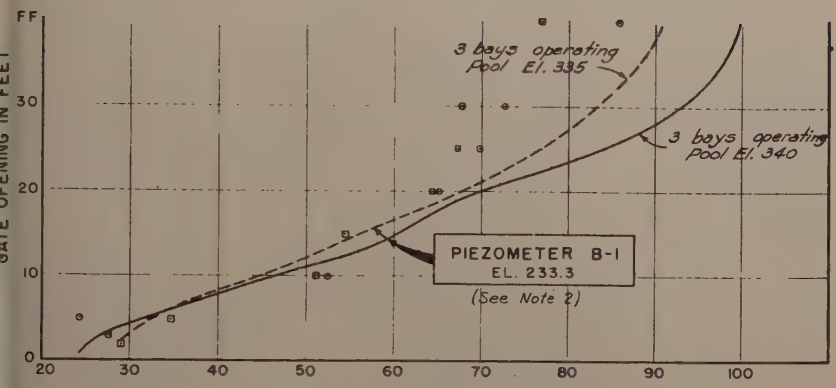

PIEZOMETER PRESSURE IN FEET OF WATER

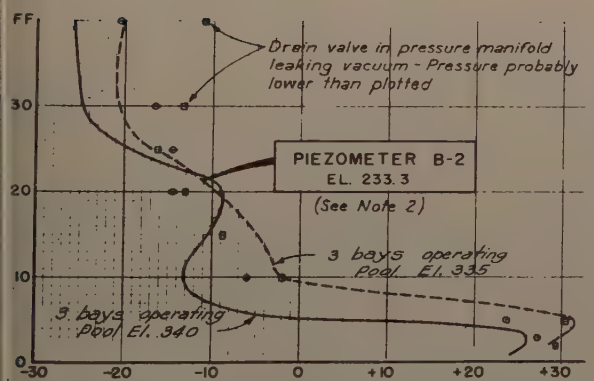

PIEZOMETER PRESSURE IN FEET OF WATER

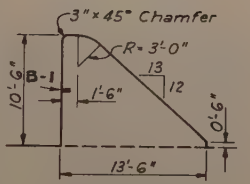

ELEVATION

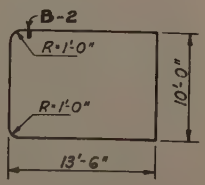

PLAN

BAFFLE DETAIL

NOTES:

1. No model data available for comparison of prototype data for Piezometers B-1 and B-2.
2. ○ Indicates prototype data for single bay operation (adj. bays closed) @ pool El. 340 for Piez. B-1 and B-2.
   □ Indicates prototype single bay data @ pool El. 335.

Fig. 2. Baffle Pier Pressures, McNary Dam.

Fig. 3 shows the turbulent jump action which occurred during passage of the June 1956 flood with flows of 735,000 to 787,000 cu. ft. per sec. As nearly as can be determined by the author from comparison of photographs, the prototype stilling action was as predicted by the models.

It should be noted that the basin length at McNary Dam was made somewhat shorter and the maximum end sill velocities allowed were somewhat higher than would be considered desirable at some locations, because of the very hard durable basaltic rock which lies below the McNary end sill.

It is interesting to note that the downstream portion of the stilling basin training wall is only 7 ft. high beyond a point 105 ft. downstream from the P. of the spillway bucket curve. The wall was made low in order to provide better escape conditions at certain flows for the Columbia River Salmon migrating upstream. No harmful effects were noted as a result of this feature in the general model or in the prototype with the 1956 flood flows. Possibly the low Froude Number accounts for this performance.

Bonneville Dam (Washington and Oregon)

This navigation and power project was completed in 1937. During the ensuing twenty years, the large daily flows and annual flood flows of the Columbia River have subjected the stilling basin baffle piers to extremely heavy pounding for prolonged periods of time, resulting in gradual erosion of the concrete over large areas of the baffle piers and floor. It is estimated that about 1,000,000,000 acre-ft. of water have passed over the spillway to date (1956). Details of the erosion and the repairs made have been described elsewhere.[1, 2] However, several features are of particular interest and are mentioned briefly here.

Nine baffle piers were repaired in 1947 with 9-in. radius on each leading edge and a 2.5-ft. radius connecting top and back slope. This design was developed as a result of model tests conducted in 1941 in a vacuum tank at Carnegie Institute of Technology. During the period 1947 to 1954, these "Carnegie" baffle piers sustained considerably less general wear than the original type of baffle pier without rounded edges, as shown in Fig. 4. In the first of these baffle piers to be reshaped in 1947, deep erosion was later found in areas where unsatisfactory bond had been obtained between the new and old concrete. The change in design had been effected by removing the outer 6 in. of concrete on all exposed faces. During the recent (1954) repairs a minimum of 12 in. thick concrete was provided and anchored with No. 8 hooked reinforcing bars grouted 2 ft. into the original concrete.

One baffle pier in the upstream row was repaired in 1947 with a 3/8-in.-thick steel armor plate all around, anchored with bolts spaced on 12 in. centers. All of the armor plate had been ripped off and the sides were deeply pitted when inspected in 1954.

During the great Columbia River flood of 1948, the stilling basin was subjected to a severe test. For a one-day duration, the peak river flow was 1,000,000 cu. ft. per sec., whereas the design discharge is 1,600,000 cu. ft. per sec. Stilling action was very turbulent, as is shown in Fig. 5. Eye

1. Symposium on Cavitation, "Experiences of the Corps of Engineers," by John C. Harrold, Transactions, A.S.C.E., Vol. 112, 1947, p. 35.
2. "Bonneville Dam Spillway Erosion Repaired," by Donald H. Basgen, Engineering News Record, Apr. 21, 1955.

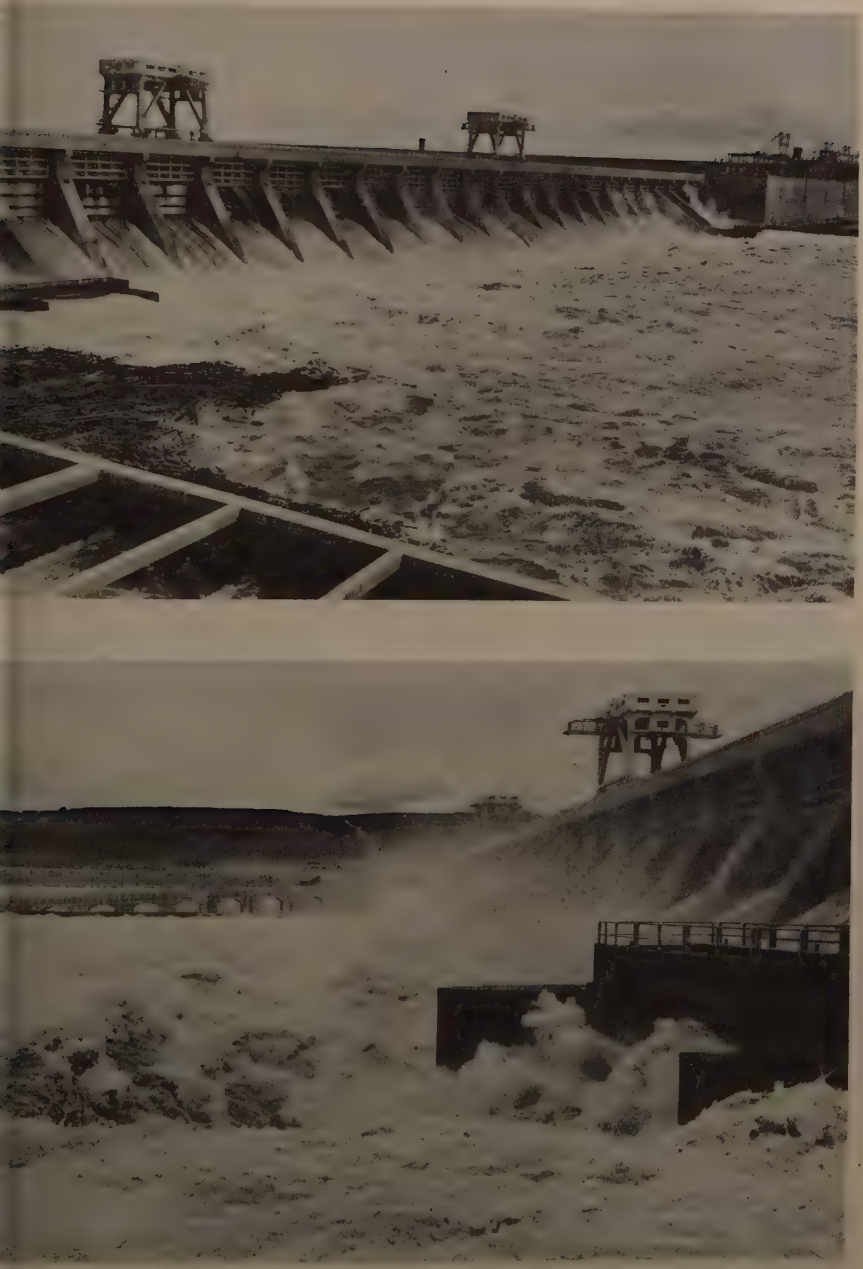

Fig. 3. McNary Dam Stilling Basin During 1956 Flood Flows, (a) 735,000 cu. ft. per sec., (b) 787,000 cu. ft. per sec.

Fig. 4. Erosion of "Carnegie-Type" Baffles Constructed in 1947, Bonneville Dam.

Fig. 5. Stilling Action with 971,000 cu. ft. per sec., Bonneville Dam.

witnesses reported large, almost instantaneous surges near the spillway abutments in the order of 25 to 30 feet vertically. The total flow remained over 900,000 cu. ft. per sec. for 18 days duration.

Recent observations of flows in the south half of the stilling basin, where the downstream row of baffle piers has been filled in solid to form a sill, indicate more turbulent surface conditions than the original basin. Model studies had indicated that the new design basin with solid end sill on the baffle deck would deflect the flow upward, producing more turbulence on the surface but providing a large, slow-moving eddy in an upstream direction on the bottom of the river bed downstream from the lower apron.

Center Hill Dam (Tennessee)

The spillway at this project is a high concrete gravity ogee weir with roller bucket type stilling basin. The basin is 470 ft. wide and is divided into three levels of 7-ft. increments, vertically. Radius of the bucket is 50 ft. and maximum head available from pool to bucket invert is 233 ft. At the lip of the bucket, the angle of tangent with the horizontal is 45 degrees. Design discharge is 458,000 cu. ft. per sec. and the unit discharge is approximately 973 cu. ft. per sec. per ft. width of basin.

Construction work was suspended from March 1943 to January 1946 because of the war effort, and during this time the flow of the Caney Fork River was diverted through the low spillway monoliths and the sluices. A large quantity of rock was spilled in the bucket during construction of a rock fill cofferdam adjacent to the spillway. This rock was not removed and the violent eddies set up by sluice flows during the diversion period resulted in the formation of several large oval-shaped cavities in the bucket. The abrasive action apparently continued over a period of eight years until 1951, when the damage was discovered. The maximum spillway discharge during this period was 41,000 cu. ft. per sec. At this flow, waves about 3 ft. high were caused by the jets from the sluices breaking through the tailwater. A release of 40,000 cu. ft. per sec. was maintained for 8 days. Normal spillway releases since completion of the dam occur about 10 days a year at a rate of about 5,000 cu. ft. per sec.

No difficulty has been experienced with spray action from the bucket during operation of the powerhouse located to the left of the spillway or the switchyard located just downstream, although the stilling action of the bucket is somewhat more violent than a conventional hydraulic jump type basin. The greatest amount of spray occurred with sluice discharges during the diversion period. Since the powerhouse was placed in operation, there have been no releases through the sluices.

It was found that flow releases should be evenly distributed across the spillway, since the back roller that is formed immediately below the bucket will tend to deposit fill against the downstream lip of the bucket. With one section of the lip left low, unbalanced releases may easily cause gravel to be deposited in the bucket. A level bucket would be preferable in this regard.

The Wolf Creek and Dale Hollow projects, located nearby, have similar spillways and roller bucket basins. Since Wolf Creek Dam was completed in 1950, the maximum flow release has been about 40,000 cu. ft. per sec. Continuous releases have been made for 60 days averaging about 22,000 cu. ft. per sec. Since closure of the Dale Hollow Dam in 1943, the largest release has been only 10,200 cu. ft. per sec. No erosion has been apparent at either of these projects.

aldhill Dam (North Dakota)

At this project, the 140-ft. long ogee spillway section is joined to a chute f 15% slope, slightly flaring in plan, and a level apron 70 ft. long and with are in plan of 1 in 6, averaging about 155 ft. wide, complete with two rows f baffle piers and an end sill. Maximum head available from pool to apron s 51 ft., and the design discharge is 43,100 cu. ft. per sec.

A flood of record proportions occurred in April 1950, before completion of onstruction, which required placing the spillway in emergency operation. ince much more than normal storage space was available, the maximum re- ease was maintained at 3,150 cu. ft. per sec. Comparisons between model nd prototype at this flow indicated good agreement. In both, the hydraulic mp began and ended on the chute section, and the flow was distributed fairly niformly across the width of the basin.

For discharges above 10,000 cu. ft. per sec., the model indicated that the mp would begin on the chute and end on the level stilling basin floor. Down- ream depths for this type of flow in the model were fairly consistent with ose obtained from empirical relationships developed by Carl E. Kindsvater, . ASCE[3] for flow in a straight chute and basin. Larger prototype flows than e 1950 releases would be desirable for comparison, but cannot readily be btained because such flows would cause flooding conditions in communities ownstream from the dam.

onchas Dam (New Mexico)

This project was completed in 1939. The spillway consists of a concrete ravity ogee weir 340 ft. wide and 178 ft. high from crest to toe. The basin onsists of a horizontal apron 134 ft. long with one row of 8-ft. high baffle ers and a 12-ft. high end sill. The basin length is unusually short for a roject of this size, and is equivalent to about $2.3D_2$, where D_2 is the maxi- um conjugate depth after the hydraulic jump. In addition, the ends of the aining walls are tapered back 1.1:1 from the end sill. Spillway design dis- arge is 182,000 cu. ft. per sec. Model tests were made of the hydraulic mp action prior to construction.

In 1944, the basin was dewatered for inspection. Total releases up to that me had amounted to two million acre-ft., of which 700,000 acre-ft. were om spillway releases during 1941 and 1942, and the remainder from sluice leases. Inspection revealed that most of the basin was in good condition. ehind the baffle pier attached to the training wall on either side, however, e floor was eroded to a depth of 9 to 12 inches in the area bounded by the ffle pier, training wall and end sill. The wear also extended into the train- g wall and downstream face of baffle pier as much as 6 in. This wear was used by eddies which formed in the "dead" spots behind the two end baffle ers. In later basins, the end baffle piers have been placed a short distance ay from the training walls in order to prevent such eddy action. In addi- n to the above, erosion on the level apron downstream from two of the gulating sluices varied from a depth of 3 in. near the baffle piers to virtual- none at the spillway toe. Repairs consisted of replacing the concrete be- nd each of the end baffles.

Downstream from the end sill, the exit channel side slopes are protected

[3] "The Hydraulic Jump in Sloping Channels," by Carl E. Kindsvater, Transactions, A.S.C.E., Vol. 109, 1944, pp. 1107-1154.

by a 10-ft. blanket of sand and gravel covered with a 3-ft. layer of derrick stone on slopes of 1 1/2:1. Substantial displacement of the derrick stone occurred after the 1941 and 1942 flood releases and subsequently. Causes of the failure were thought to be slippage of the over-burden along the surface of the shale and sandstone, influenced by saturation of the overburden, undercutting of the revetment toe by the violent eddies from the stilling basin, and vibration of the revetment which had been noticed earlier during spillway releases.

Observation of the prototype spillway flows up to 38,000 cu. ft. per sec. indicated that the hydraulic jump was completely submerged, whereas model tests had indicated that a free jump should occur for flows less than 75,000 cu. ft. per sec. for all anticipated tailwater conditions. Since the prototype tailwater elevations were within the expected limits, although near the maximum anticipated, the reasons for this discrepancy between prototype and model flow action are not known.

As noted elsewhere,[4] degradation of the streambed downstream from this project is recognizable for a distance of more than 40 miles. The streambed near the dam has lowered a maximum of 10 ft. to rock outcrops.

Folsom Dam (California)

The spillway for this project is a high concrete gravity ogee weir topped with five 42-ft. wide by 50-ft. high "operating" tainter gates and three similar "emergency" tainter gates, 42-ft. wide by 55-ft. high. The service stilling basin below the five operating gates consists of an 8:1 ramp, 175 ft. long joined to a level apron, 147 ft. long. A 15-ft.-high vertical end sill is also provided. The height of the weir crest above the level apron is 303 ft. Below the emergency gates, a high level bucket is provided. Design discharge for the service stilling basin is 200,000 cu. ft. per sec., although all structures were designed to be safe against failure during the spillway design flood of 567,000 cu. ft. per sec. Since the service basin is 242 ft. wide, the design unit discharge is 826 cu. ft. per sec. per ft. of width. The stilling basin designs were evolved in conjunction with a series of model tests. A level stilling basin was chosen for the service basin instead of a flip-bucket because of increased safety to the adjoining powerhouse and because maintenance costs would be reduced, with less eroded material entering the tailrace area.

During the flood of December 1955, a flow of 64,000 cu. ft. per sec. was released from the five service gates, providing a unit discharge of 264 cu. ft. per sec. per ft. of width. The pool level was 36.7 ft. above the spillway crest and 340 ft. above the level apron. Tailwater was 63 ft. above the level apron. As predicted by the model, stilling action was less than complete, and moderately high velocity flow continued downstream from the end sill for a considerable distance, as shown in Fig. 6. In the model, a simulated discharge of 110,000 cu. ft. per sec. resulted in bottom velocities of 16 ft. per sec. immediately downstream from the basin end sill. However, with a scour hole simulated in the exit channel in this area, the model indicated bottom velocities of only 12 ft. per sec. and upstream in direction.

4. "Sediment Studies at Conchas Reservoir in New Mexico." by D. C. Bondurant, Transactions, A.S.C.E., Vol. 116, 1951, p. 1288.

Fig. 6. Flow Conditions in Exit Channel, Folsom Dam.

Arkabutla Dam (Mississippi)

This project has a 300-ft. long uncontrolled concrete chute spillway with ogee weir and 3:1 chute slope. Design discharge is 89,000 cu. ft. per sec. The stilling basin as developed from model tests in 1940 is 95 ft. long, with level apron, two rows of baffle piers, and an end sill. In 1953, the spillway went into operation for the first time, with a maximum discharge of 7,100 cu. ft. per sec. Measurements were made of the spillway discharge and water surface elevations along the chute. Stilling action was observed to be satisfactory and well-distributed across the basin.

It was noted that tailwater for the 1953 flow was 16 ft. higher than that used for the model tests. After inquiring, it was found that the outlet channel was not constructed to the bottom grade and width as used in the model study. The channel had been excavated to a bottom grade varying from 5 ft. higher at the lower end to 13 ft. higher at the upper end than the bottom grade used for the determination of the tailwater data for the model tests. Also, the spillway exit channel was densely grown up with vegetation, resulting in a roughness coefficient "n" in Manning's formula of 0.070 during the 1953 flood.

Lock and Dam No. 1, Mississippi River (Minnesota)

The ogee, Ambursen type fixed crest spillway at this navigation project is 574 ft. long and has a level concrete apron approximately 80 ft. long at an elevation 30 ft. below the spillway crest. The concrete apron is too high for a hydraulic jump except for higher flows. In 1952, the maximum flood of record occurred and a discharge of 69,200 cu. ft. per sec. passed over the spillway. The hydraulic jump apparently formed near the downstream edge of the apron. Tailwater depth at this time was 21 ft. Excessive scour occurred below the apron, and a hydraulic model study was made to determine the most feasible method of modifying the apron. As a result, a baffle wall was constructed with 2-ft. by 2-ft. openings which would move the hydraulic jump well up on the apron. The baffle wall was placed about 30 ft. downstream from the toe of the weir. Action of the basin with a discharge of 21,500 cu. ft. per sec. is shown in Fig. 7.

There are 26 navigation dams on the Upper Mississippi River. At many of these projects, the spillway structures are founded on pile structures in the sand bed of the river. In the usual case, the low concrete sill is followed by a concrete stilling basin about 50 ft. long containing two rows of baffles, an end sill and approximately 50 ft. of derrick stone below the end sill. In a few instances, this stone has been undermined by erosion of sand and gravel located further downstream. The usual cause of this loss has been concentrated flow when some of the spillway gates were bulkheaded for extended period of time. Remedial works usually require that a timber mattress be constructed, floated into position, sunk, and the entire mattress covered with a one-ft. layer of one-man stone. This work has been relatively permanent. The gate operation schedule on a number of these projects founded on piling is so arranged that the maximum velocity over the end sill does not exceed about 5.5 ft. per sec., as determined from model tests with erodible beds.

Demopolis Lock and Dam (Alabama)

This navigation project was completed in November 1955. A flood occurred in April 1955, when the dam was essentially complete except for several

Fig. 7. Effect of Baffle Wall Added to Basin at Lock & Dam No. 1, Mississippi River.

cofferdam cells which were still in place. The maximum discharge was 85,000 cu. ft. per sec., with pool at elevation 79.6 and tailwater at 74.0, or a net head of 5.6 ft. In the model, the most critical stilling basin conditions were obtained with a flow of 80,000 cu. ft. per sec. and a net head of 5.9 ft. The observed performance of the prototype appeared the same as the model. No erosion was reported.

The stilling basin is a roller type, with two sections. One section is 585 ft. long and has a 27.5 ft. level apron set at El. 19.0, surmounted by a 4.4 ft.-high sloping end sill. The other section is 895 ft. long and has a 29-ft. level apron set at El. 45.0, with a 3-ft.-high sloping end sill. Spillway crest is at El. 73.0.

Old Hickory Dam (Tennessee)

This is a low-head power and navigation project with normal lift of 60 ft. A bucket-type energy dissipator, with bucket radius of 34 ft., was provided in order to deflect low to medium spillway flows upward and away from the streambed. At high flows, the spillway will be submerged and the overflow will ride the upper layers of the tailwater. This project is still under construction. However, diversion flows up to 34,000 cu. ft. per sec. have been passed through 4 of the 45 ft. wide gate bays, creating more turbulent stilling action than will be experienced after the project is completed, since tailwater was appreciably lower than normal during this period. Stilling action appeared turbulent but satisfactory.

Spillway Stilling Devices with Sluice Flows

Bull Shoals Dam (Arkansas)

This dam is a straight, concrete gravity structure 284 ft. high, with an overflow spillway located in the central portion of the valley. Flow over the spillway is controlled by 17 tainter gates, 40-ft. wide by 28-ft. high. Release of floodwaters when the reservoir pool is below spillway crest is accomplished by 16 sluices, 4-ft. wide by 9-ft. high, controlled by hydraulic slide gates. As shown in Fig. 8(a), the stilling basin was constructed with a stepped apron 808-ft. wide and 203.3-ft. long, with elevations varying from 437.2 to 446.5, and a 4-ft.-high end sill. The apron had a 1.0 ft.-high step located 35.3 ft. downstream from the toe of the dam, a 1.5 ft.-high step located 47.3 ft. downstream from the toe and 2.5 ft.-high steps located 71.8 and 98.8 ft. downstream from the toe. Each step was shaped as a quadrant of an ellipse, with semi-minor axis equal to the height of the step and semi-major axis of twice this amount. This design is similar to the basin at Cherokee Dam (TVA) and was adopted after model tests were made in 1944-45. The alternative design was a more costly basin with horizontal apron at El. 435 equipped with two rows of baffle piers and end sill. Stilling action for sluice flows was a controlling factor in the basin design. The dam was completed in 1951.

After approximately 2,600,000 acre-feet of water had been released through the sluices, extensive damage was noticed near several of the sluice outlet portals. The basin was unwatered in October 1952 and a careful investigation made. Erosion, varying from a depth of less than 2 feet to a maximum of 3.5 feet had occurred in the 5-foot thick concrete slab below the outle

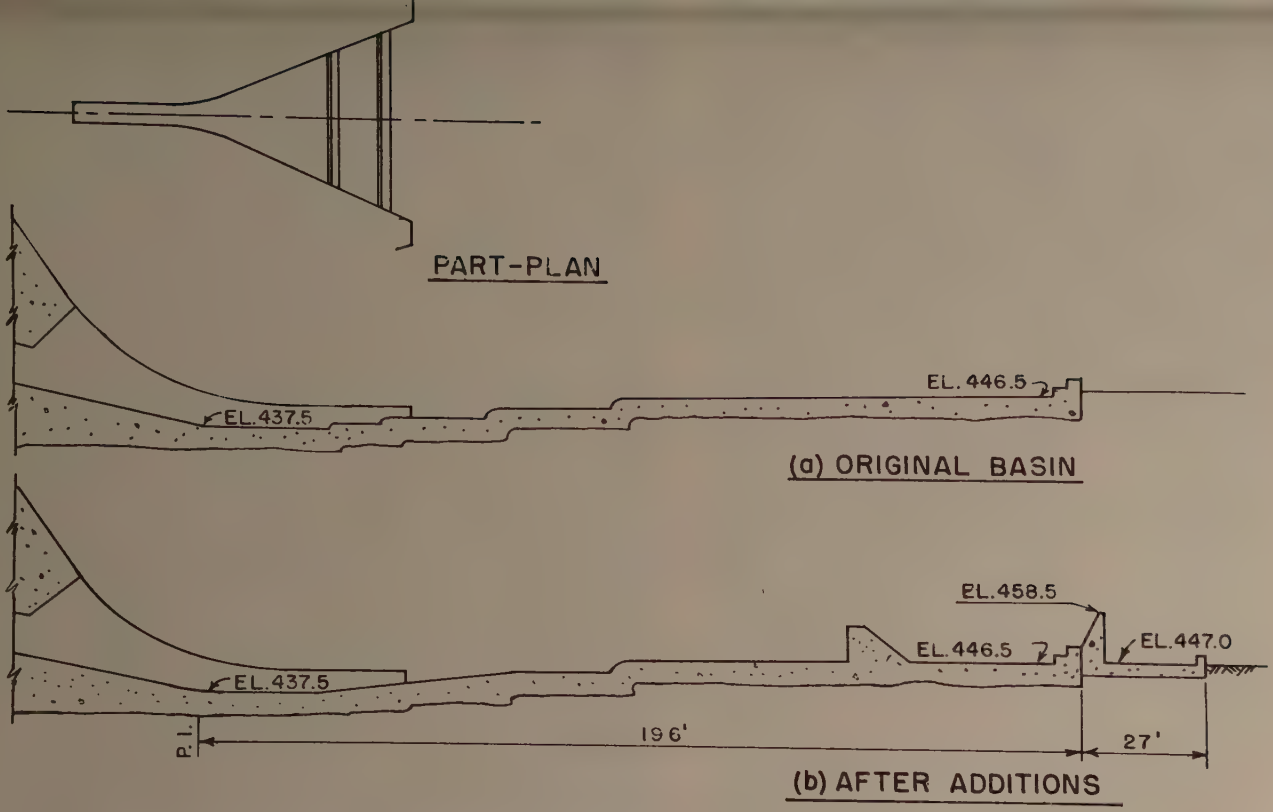

Fig. 8. Bull Shoals Stilling Basin Dimensions, (a) Original Basin, (b) After Additions.

portals of twelve of the sixteen sluices. Typical of the four or five most severely eroded areas was monolith 22, shown in Fig. 9(a). The severe erosion on top of the first step appeared to be the result of cavitation. Once started, it seemed probable that the erosion process may have been accelerated by dislodged concrete and broken reinforcing steel. However, neither the surface character of the eroded holes nor the stone and steel indicated that abrasion was the primary cause. There was clear evidence of impact abrasion or sandblast effect on the faces of the second and third steps downstream.

An excellent example of the erosion of the first step in its early stages was afforded by monolith 35, shown in Fig. 9(b). The sluice in this monolith had passed only about 5,000 acre-feet of flow, as compared to 420,000 acre-feet for the sluice in monolith 22 described above.

Temporary repairs were made in the damaged areas while awaiting the results of prototype pressure cell tests, new model tests and new analyses leading to a permanent solution. The damaged steps were cut back and replaced with smooth, upward sloping slabs. The slabs replaced the two upstream steps at all conduit outlets except two. At the outlet in Monolith 21, adjacent to the left training wall, all four steps were replaced. At Monolith 23, where the sluice had not been in operation, the undamaged steps were retained for testing purposes.

Electrical pressure cells were installed in the stilling basin in conjunction with the repair work described above. At the top of the first step in Monolith 23, three cells were installed along the sluice centerline at distances of 2.67, 3.67 and 4.67 ft., respectively, from the upstream end of the step. Reservoir pool El. during the prototype tests was 638.4 and tailwater just downstream from the end sill was at El. 452. Conduit discharge was approximately 3,300 cu. ft. per sec. at full gate opening and 1,300 cu. ft. per sec. at half gate opening, with corresponding velocities of about 92 and 82 ft. per sec. respectively. At the half gate opening, instantaneous pressure readings in the cavitation range (-35.8 ft. of water) were obtained at the pressure cell furthest upstream. The average pressure reading for this cell at half gate was +3.0 and the maximum was +24.3 ft. of water. At full gate opening, the three cells were rendered inoperative. The conclusion derived from the results of these tests was that the damage had resulted from cavitation.

It is interesting to note that the 1944-45 model tests, using piezometers connected to a manometer bank, gave a fair prediction of the average prototype pressure (+6.5 ft. versus the +3.0 ft. reading quoted above). Of course the piezometers could not reflect the transient pressures encountered.

Observation of the prototype flow from the conduit in Monolith 23 with tailwater completely repelled because of a partial cofferdam indicated that the spread of the jet was complete over the width between the flared guide walls before it reached the end of the guide walls and was almost complete at the location of the first step. At the latter location, the jet was slightly thicker in the center than on either side, and compared closely with the cross sections and longitudinal profile of the unsubmerged jet as measured in the 1944-45 model tests.

Observations of the prototype stilling basin performance with sluice discharges and with ramps installed in lieu of the first two steps indicated that tailwater elevations below approximately elevation 459 were insufficient to create a hydraulic jump and consequently the conduit jet extended beyond the basin end sill with considerable energy for some distance downstream. The

Fig. 9. Erosion at Bull Shoals Dam, (a) Eroded Step of Monolith 22, (b) Pitting at Top of First Step of Monolith 35.

deficiency in tailwater was verified in the model, and an analytical study also indicated that a tailwater elevation of 460 to 464 would be required for an adequate hydraulic jump. In order to increase the effective tailwater depth for sluice flows, the final design for the stilling basin additions incorporated a 12-ft. high end sill, as shown in Fig. 8(b). The upstream face of the end sill was provided with a 1:2 slope in order to increase the lateral spread of individual conduit flows over the sill. Since a relatively large drop-down occurs over the high end sill, a 24-ft.-long secondary basin with 2-ft.-high sill was added. One row of 8-ft. high baffles, 7.5 ft. wide spaced 8.5 ft. apart, was added to the main basin to improve stilling action for large spillway flows. The elliptical step furthest downstream was left intact, as shown in the figure. Repairs were completed early in 1955.

The concrete mix for the original basin contained manufactured sand and about 4 1/2 bags of cement per cu. yd. For the basin revisions, the mix utilized natural sand, 5 1/2 bags of cement per cu. yd., 1 1/2 in. maximum size aggregate, and a water-cement ratio of 0.41 to 0.45.

From soundings made of the exit channel in the first 100 feet downstream from end sill in 1948 and again in 1953, erosion in the order of 2 to 5 feet was found in a number of locations in the moderately hard limestone.

Nimrod Dam (Arkansas)

This project was completed in 1942. The spillway is composed of a concrete gravity ogee weir with a conventional hydraulic jump type stilling basin consisting of a level apron 88 ft. wide and 198 ft. long, surmounted by a single row of 6-ft. high stepped baffle piers and a 4-ft. high stepped end sill. Seven sluices, 6-ft. wide by 7.5-ft. high are provided in the base of the spillway and discharge into the basin. The sluice inverts intersect the level apron at a slope of 4:1. In plan, the flaring sidewalls of the sluice outlets intersect the spillway bucket. The sluices are separated into groups of 2, 3 and 2 by two longitudinal dividing walls, 14-ft. high, extending through the basin to the end sill.

The action of the dividing walls is particularly striking under some conditions of operation. As shown in Fig. 10, three distinct water levels are evident within the basin. In this photograph, the three center sluices were operating with a net head of 51 ft. The walls function to prevent the formation of large eddies within the basin, thereby allowing maximum spreading of the sluice flows. In addition, the amount of gravel carried into the basin is held to a minimum. Stilling basin action is satisfactory, although with two end sluices operating alone, there is a noticeable concentration of high-velocity flow for a considerable distance downstream from the basin.

The basin was dewatered and inspected in 1952 after almost 9,000,000 acre-ft. of water had been released through the sluices. Rough concrete was found at the outlet of the third sluice, with maximum erosion depth of 5 in. Reinforcing steel was not exposed, however. Erosion depths of 4 in. were encountered at the outlets of the two adjacent sluices. There was practically no erosion at the end sluices. Since there was no relationship between the quantities of flow released and the erosion, and in fact the maximum erosion had occurred at the sluice which had discharged the least, it was concluded that the characteristics of the various concrete pours in the basin were the primary factors contributing to the amount of erosion encountered. The baffle piers were in good condition, with only slight erosion on the upstream faces

Fig. 10. Effect of Dividing Walls at Nimrod Dam.

the baffle piers located in the center of the basin. No repairs were made to the stilling basin, but another inspection will be made in the next few years as a precaution.

Norfork Dam (Arkansas)

This project has a concrete gravity ogee spillway with conventional horizontal-type stilling basin 568 ft. wide by 185 ft. long. Two rows of 8-ft.-high baffles and a 6-ft.-high end sill are provided. Eleven sluices, each 4-ft. wide by 6-ft. high, are evenly spaced across the base of the spillway. The average head for sluice releases is about 170 ft.

An inspection of the Norfork stilling basin in 1945 has been described elsewhere.[5] It was noted that approximately 2,000,000 acre-ft. of water had passed through the stilling basin at that time, mostly from sluice releases, and that some of the baffle piers had been damaged quite severely. The damage was attributed to erosion by recirculated debris which had not been cleaned out of the basin when the project was completed in 1944. That this was the case was confirmed in 1953, when the stilling basin was again inspected. An additional 2,000,000 acre-ft. of water had passed through the sluices since the previous inspection. Comparison of conditions in the basin in 1953 with photographs taken in 1945 indicated a very small amount of additional wear had occurred in the 8-year period. The additional wear was noticed in slight rounding of the upstream edges of the baffle piers. Several rough, shallow cup-shaped eroded spots were found on the apron upstream from the baffles near the right side of the basin. No repairs to the baffles or the apron were considered necessary.

Fort Gibson Dam (Oklahoma)

This project was completed in 1950, except for the powerhouse. The spillway consists of a concrete gravity ogee weir controlled by 30 tainter gates, 40-ft. wide by 35-ft. high, separated by 10-ft.-wide piers. Total width of spillway is 1,490 ft. Ten sluices, each 5.67-ft. wide by 7-ft. high, are located in the base of the spillway, along the center line of each of ten successive spillway monoliths. The inverts of the sluices are horizontal at their outlets through the spillway weir, and are located about 16 ft. above the stilling basin apron. The sluice outlets are the "jet deflector" type, with a tetrahedral concrete block 3-ft. high located within the exit portal. Maximum reservoir pool El. is 582.1, spillway crest El. is 547, basin floor El. is 477 to 485, and maximum tailwater El. is 551. The stilling basin as model tested and constructed for the spillway design flood of 919,000 cu. ft. per sec. is a roller-type basin composed of a 60-ft. long apron and a 6-ft. high stepped end sill. Below the sluices, however, the model indicated that a somewhat longer apron would be desirable in order to obtain adequate stilling action and uniform spreading of the sluice flow before passing over the end sill. Accordingly, the basin was made 20 ft. longer in the section downstream from the sluices, with dividing walls separating this portion of the basin from the remainder.

The stilling basin was unwatered for inspection in 1953. The basin was found to be in good condition except in the area occupied by the ten sluices. The apron below several of the sluices was eroded to a depth of 3 to 4 in. in spots. The end sill steps were eroded a like amount in several locations.

5. Transactions, ASCE, Vol. 112, 1947, p. 101.

Below the end sluice on the left, eroded depths up to 8 in. were found in the apron, with reinforcing steel exposed in some spots. Most of the latter erosion was in the center third of the apron and from about 15 to 35 ft. from the basin dividing wall. In addition, the steps on the end sill directly in line with this sluice were eroded to a maximum depth of 6 in.

The basin in the section of greatest wear had been subjected to a discharge of more than 100,000 cu. ft. per sec. in 1949 while being used for diversion during the construction of the dam. At that time, a construction bridge with steel I-beam legs was fastened to anchor bolts embedded in the stilling basin apron. A barge belonging to the contractor broke loose during the peak of the 1949 flood and swept out one span of the bridge. At the time of unwatering for the next step of construction, it was noted that large boulders had lodged around the legs of the construction bridge and by continual movement had scoured a large, deep area near one of the legs. After the construction period described, each of the sluices had released about 2,000,000 acre-ft. of water by the time of the inspection in 1953.

Most of the erosion is believed to have been started by the action of eddies transporting gravel and boulders during the diversion stage. Subsequently, sluice flows deepened the eroded areas. The fan-shaped pattern of discharge from several of the sluices was visible in the eroded basin floor below, but erosion in such instances was only to a depth of about 1/4-in. Since the usual head on the sluices was about 55 ft., and the outlet deflectors spread the flow in fan-shaped patterns into tailwater depths of about 5 to 10 ft. in the stilling basin, the concrete mortar was evidently not resistant to water action.

It was noted that grout placed three inches deep in anchor bolt recesses for the construction bridge had washed out.

Pine Flat Dam (California)

Two levels of sluices are provided through the high gravity spillway weir at this project. The upper level of sluices discharges onto the downstream weir face and flip bucket basin, whereas the lower tier of sluices discharges through "deflector type" sluice outlets located in the downstream face, underneath the lip of the spillway flip bucket. Photographs of flow releases through the sluices indicate satisfactory spreading of the flows. It is understood that some repairs were necessary in eroded portions of several of the tetrahedral jet deflectors in the lower tier of sluices. It is also understood that the sluices have operated with maximum heads in the order of 280 ft.

Outlet Works Stilling Devices

Hucky Peak Dam (Idaho)

This project was completed in 1955. The outlet works consists of an intake structure, a 23-ft. diameter steel-lined tunnel, and an unusual gate-controlled manifold at the downstream end of the tunnel with a design capacity of 30,000 cu. ft. per sec. As shown in Fig. 11, outflow is regulated by six 8.25-ft. by 10-ft. hydraulic slide gates discharging freely into the atmosphere. One 30-in. diameter hollow jet valve is provided for close adjustment of the outflow. Tunnel flows are directed by six individual flip buckets into an unlined stilling pool, excavated in the rock and overburden of the river channel. Since the top of flood control pool El. is 3060 and the floors of the gate

passages are at El. 2827, heads up to 233 ft. and velocities up to 122 ft. per sec. are attained with small gate openings. Model tests were made of the manifold and stilling area because of the high heads and unusual nature of the facilities provided.

In May and June of 1955, the reservoir was filled to a maximum El. of 3059 by lowering Arrowrock Reservoir upstream, resulting in heads up to 232 feet at the slide gates. Irrigation releases up to 5,000 cu. ft. per sec. were made through one or two gates on a rotational basis at openings ranging from 5 to 8 ft. during the reservoir filling operation and until July 14, except for the period June 28 to July 4, when three gates were operated at 3 feet. Releases up to 5,000 cu. ft. per sec. were made through five gates at openings of 2 ft. until July 26. It was then apparent that this 13-day period of operation had resulted in erosion of the concrete invert and walls downstream from the gates, so releases for the following five days or until July 31 were made from gate No. 1 (upstream) at 8 ft. opening. Thereafter, all releases were made from gate No. 3 which had been out of service previously.

The observed flow conditions during this period indicated satisfactory dispersal and stilling action of the jets. As shown in Fig. 12, the action of the flip buckets provided a spectacular view.

The outlets were inspected on July 7, 1955, at which time some minor erosion, not over 1 in. deep, was noted on the walls downstream from the stoplog slots. This was believed to have been caused by cavitation induced by flow past small vertical "ridges" of concrete that protruded only 1/8 to 3/16 in. from the walls at the trailing edge of the 12-in. taper at the downstream end of the stoplog slots. Additional, more extensive erosion was noted on the left wall near the floor downstream from gate No. 1. The wall was eroded to a depth of 6 to 8 in., and extended to a height of 2 ft. above the floor for a distance of 3 ft. downstream from the gate frame. Some pitting was also noted in the gate frames and seals nearby.

The outlets were inspected again on August 4, when it was found that operation with 2-ft. gate openings had caused extensive erosion of the level concrete floor and flip buckets downstream from the gates, as shown for gate No. 1 in Fig. 13. Fig. 13(a) shows that the eroded areas extended in symmetrical patterns from the downstream edge of the gate frames. Maximum depth of erosion was 40 in.

As a result of these inspections, it was concluded that erosion was not caused at gate openings of about 3.5 ft. and larger. At small gate openings, cavitation pressures are apparently produced by penetration of the downward jetting flow from each gate slot into the normal horizontal sluice flow, with rebound on the invert and resultant low-pressure areas, similar to the jet rebound effects noted elsewhere.[4] For larger gate openings, the jets apparently cannot penetrate the greater depths of horizontal sluice flow with sufficient force to produce pressures in the cavitation range. It should be noted that the gate lip was of standard design with 45 degree bevel to the lowest tip of the gate, located at the downstream edge of the gate slot.

Apparently, the jet action from the gate slots was a result of a 4 in. offset at the downstream edge of each slot, since similar erosion has not occurred at other projects with comparably high heads where there are no such offsets.

The eroded concrete was a 4-bag mix with 3-in. maximum size aggregate.

4. Boulder Canyon Project Final Reports, Bureau of Reclamation, Part VI, Bulletin 1, "Model Studies of Spillways," 1938, pp. 163-182.

Fig. 11. Details of Stilling Devices at Lucky Peak Dam.

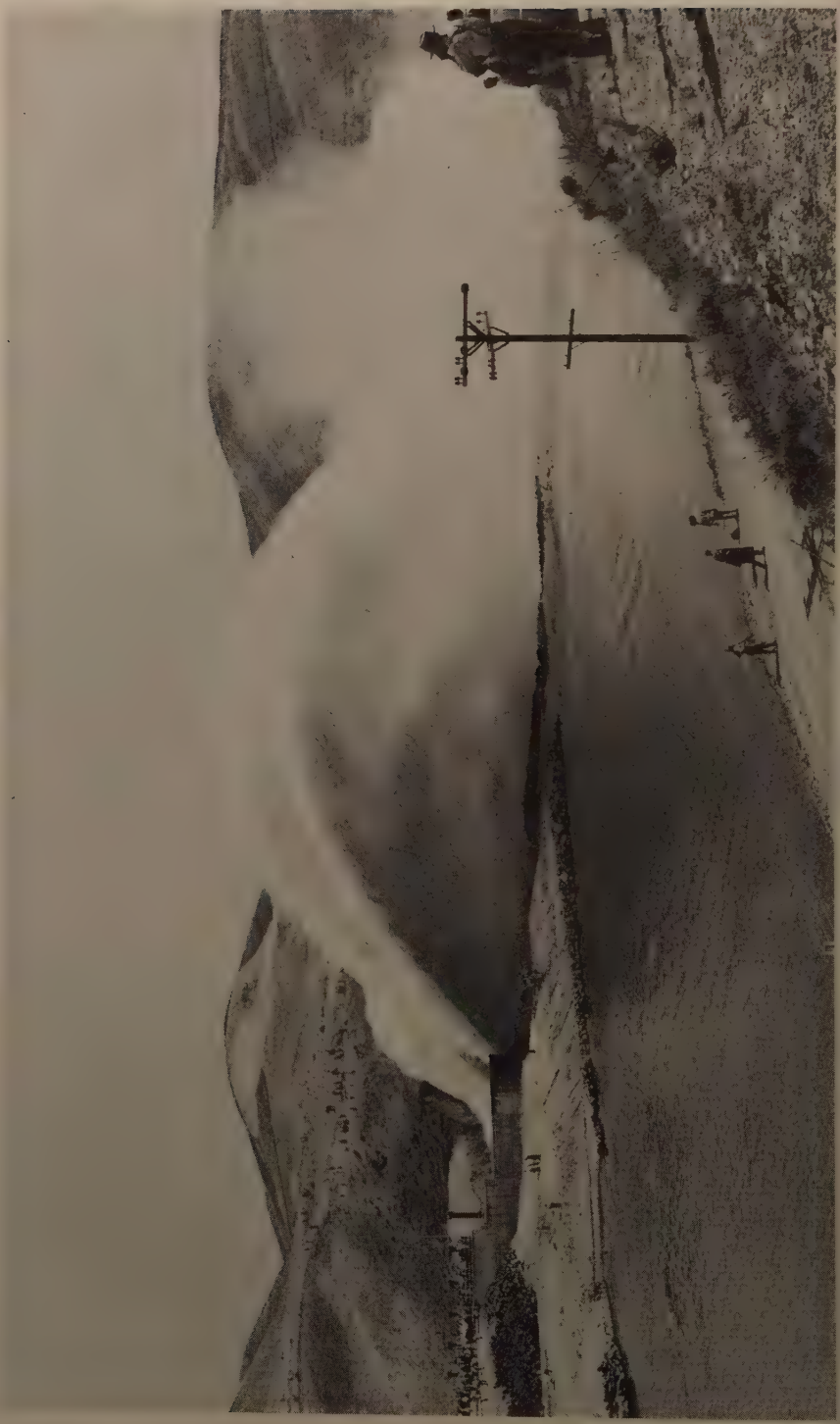

A 12-in. strip of concrete located adjacent to the downstream edge of each of the gate frames, composed of a 6.25-bag mix with 3/4-in. maximum aggregate had practically no erosion.

Repairs to the outlets consisted of installing 3/4-in.-thick steel plate liners on the floors and walls of the outlet channels. At gate No. 1, the lining extends to the end of the flip bucket whereas on the other gates it extends only to the ends of the piers. Piezometer taps were placed in the floor and left wall at gate No. 1, so that prototype pressure data could be obtained.

Two hydraulic models of the outlets were tested during the design stage, one a comprehensive model of the manifold, flip buckets and a portion of the river channel downstream, to a scale of 1:28.75, and the other a 1:16 scale model of the main conduit and one branch lateral, including gate slots and flared walls downstream. Although cavitation-producing pressures were noted with the 1:16 scale model in the vicinity of the gate slots with larger gate openings (but not at full opening) positive pressures were recorded for gate openings below 7 ft. The model did indicate the tendency of the gate at part opening to deflect the flow downward and outward into the gate slots.

Prototype pressure tests were made in July 1956, utilizing the piezometers placed in the floor and left wall below gate No. 1 during the repair period. Two longitudinal rows of 5 piezometers each had been placed in the floor at distances downstream from the face of the gate seal of 5, 6.5, 9, 11, and 14.5 ft., respectively. Row A was placed 6 in. to the left of the gate centerline. Row B was placed from 24 to 30 inches to the right of the centerline, in the area where the erosion pattern had originated. Some of the test results are shown below:

AVERAGE PIEZOMETRIC PRESSURES IN FLOOR BELOW GATE NO. 1

Dist. D/S fr Gate Seal, ft	Average Piezometric Pressure in Ft of Water									
	1-Ft. Gate Opening		2-Ft. Gate Opening		3-Ft. Gate Opening		4-Ft. Gate Opening		5-Ft. Gate Opening	
	Row A	Row B	Row A	Row B	Row A	Row B	Row A	Row B	Row A	Row B
5	/2.9	-9.0	/3.4	-8.0	/7.5	/2.4	/14.3	/9.2	/21.7	/17.7
6.5	-1.0	-6.1	-1.2	-8.4	/1.3	-1.0	/6.1	/3.1	/11.2	/10.1
9	/4.7	-7.9	/3.1	-5.3	-0.1	-0.3	/2.6	-0.5	/6.0	/3.2
11	/6.1	/2.6	/5.0	-1.5	/1.7	/1.8	/3.6	/1.5	/6.0	/4.0
14.5	/4.9	/1.8	/0.70	/3.3	/1.6	/2.1	/2.7	-1.0	/4.7	/0.4

As expected, pressures were lowest at 1- and 2-ft. gate openings, and at these critical gate openings the pressures for the upstream piezometers in Row B were substantially lower than the corresponding piezometers in Row A.

One piezometer was located in the left sidewall 1.5 ft. above the floor and 1 ft.-8 in. downstream from the face of gate seal. The pressures obtained at this piezometer corresponded closely to those obtained with the first two piezometers of Row A.

In the author's opinion, these data serve to verify the earlier supposition that the concrete erosion was caused by fluctuating pressures in the cavitation range induced by high-velocity jets originating in the gate slots.

Denison Dam (Texas and Oklahoma)

The outlet works at this project consists of three 20-ft.-diameter circular conduits which discharge into an upper stilling basin terminated by an ogee

Fig. 13b. Erosion at Lucky Peak Dam. Eroded Area in Flip Bucket.

weir, and thence into a lower stilling basin. Spreading of the flow from the conduits into the upper basin is aided by divisional piers approximately 80 ft. long. The two-level stilling basin was adopted in order that the basin and outlet channel might be founded on a thin layer of Goodland limestone, rather than on the Walnut marly clay and Trinity sand below. Model tests were made of the adopted design in 1939 and 1940.

As shown in Fig. 14, the upper basin is 335 ft. long and a maximum of 172 ft. wide, and has two rows of 10-ft.-high baffle piers. The up-stream row of baffle piers lies 209 ft. from the outlet portal. At the end of this basin the weir crest rises 19.5 ft. above the floor. Design flow is 66,750 cu. ft. per sec.

The lower basin is approximately 20 ft. below the upper, and extends 140 ft. downstream from the intermediate weir. Width of the basin is constant at 172 ft. Two rows of 8-ft. high baffle piers and a 7-ft. end sill are provided in this basin.

In 1947, prototype pressure and air-demand tests of the conduits were made. The maximum release was 60,000 cu. ft. per sec., or 90% of design flow. As shown in Fig. 15, the hydraulic jump action was satisfactory but very turbulent. Observation of the high-velocity flow (about 65 ft. per sec.) emerging from the outlet portals indicated that the upstream row of baffle piers was absorbing large impact forces, since the hydraulic jump began forming quite near the baffle piers. Good mixing action was observed within the hydraulic jump. Occasional surges overtopped the 44-ft. high walls of the upper basin, but small quantities of water were involved and no damage was done. Flows over the intermediate weir, although rough, were surprisingly uniform considering the turbulence of the jump in the upper basin. Stilling action in the lower basin may also be described as quite turbulent. Downstream from the end sill, strong currents continued for some distance. Projecting river banks about 2,000 feet downstream suffered some damage through undercutting and sloughing. The model had indicated bottom velocities of 16 to 18 ft. per sec. below the end sill for this discharge.

For the condition of unbalanced flow into the upper basin from one or two conduits, the baffle piers and stilling basin weir are subjected to severe impact.

As closely as can be determined, the model tests had predicted the prototype performance of this stilling basin in every respect. The 1940 model test report states that the hydraulic jump was held in the upper basin by the baffle piers, and that to overcome this condition would have required excessively high sidewalls. Also, the report states that flow in the exit channel beyond the end sill had relatively high bottom velocities of 13-16 ft. per sec. for both small and large discharges. Since the ability of the limestone to withstand the sustained velocities was questioned in the report, about 50 ft. of concrete paving had been provided below the prototype end sill to improve this condition.

The upper and lower basins were inspected in 1948, after 4 years of operation and 8,500,000 acre-ft. of water releases. The upper basin was in excellent condition and no evidences of pitting or cavitation was evident. There were a few chipped spots at random locations on the baffle piers, which were believed to have been caused by large steel rollers from a broken roller chain on one of the Broome gates. Although the rollers were made of hard steel alloy, they were rounded into near-spherical shapes when recovered.

The lower basin was not dewatered but was inspected by a professional

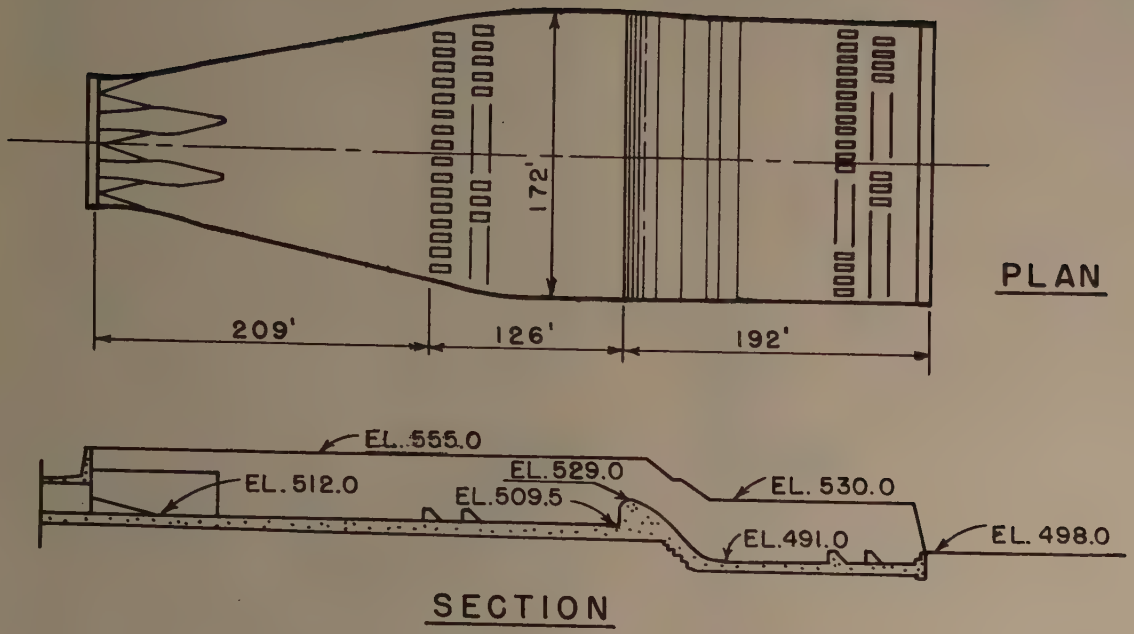

Fig. 14. Stilling Basin Dimensions, Denison Dam Conduits.

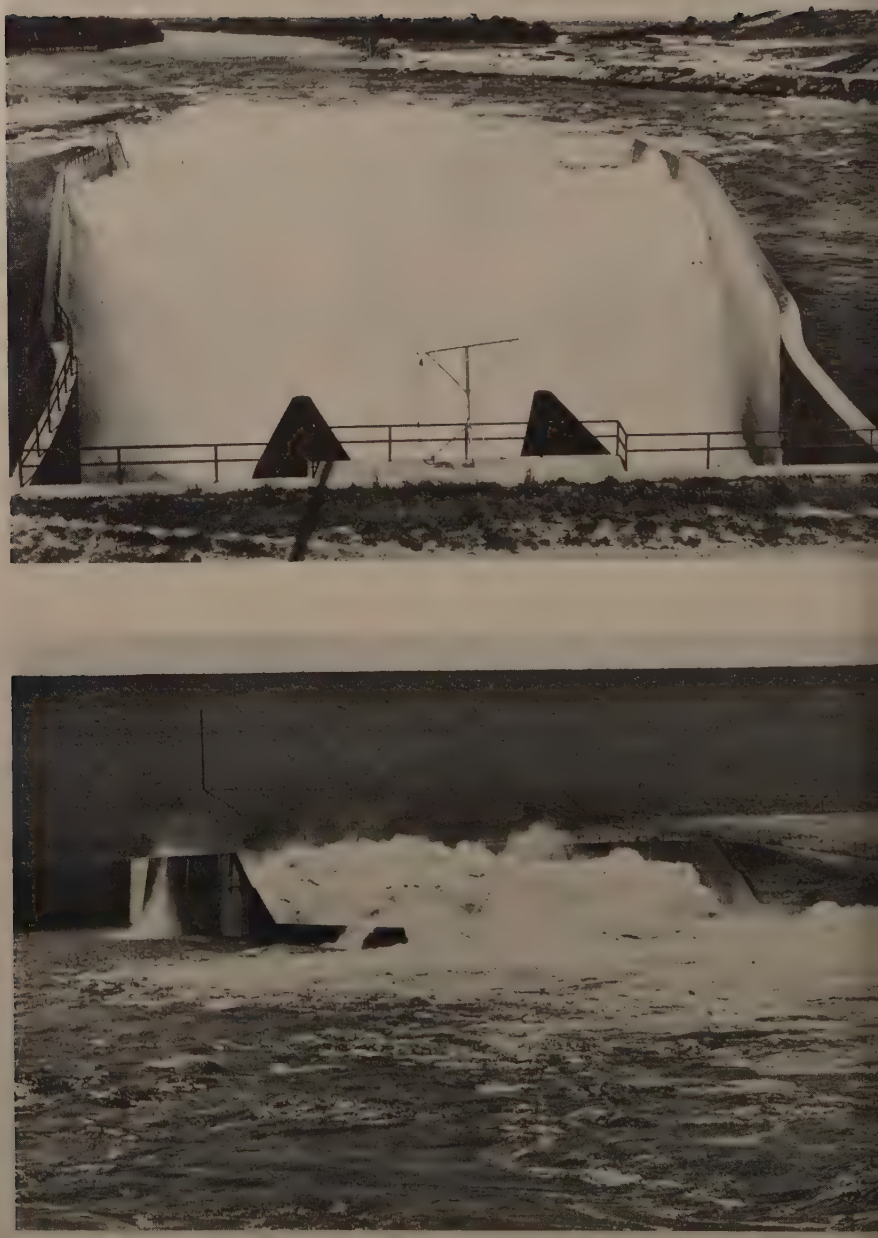

Fig. 15. Stilling Action at Denison Dam with 90% of Design Discharge (a) Upper Basin, (b) Lower Basin.

ver and by engineers using the diving gear. The basin was found to be in od condition and the only notable evidence of wear was found on the floor the downstream edges of the end baffle piers, where a small amount of pit- ng was noted. A considerable number of large rocks were found between e baffle piers and the end sill. The diver reported one rock to be in the der of 8 to 10 feet long and 3 to 4 feet thick.

The limestone exit channel was carefully inspected but no signs of wear ere noted from the sustained high velocities referred to above.

In the Red River channel downstream from the limestone ledge at the out- t works, degradation of the alluvial bed has been progressive over the years nce construction of the dam was initiated in 1939. The effect on tailwater evations at the outlet works in the 15-year period 1939 to 1954 has been a wering of 1.5 ft. at 40,000 cu. ft. per sec., 4.5 ft. at 20,000 cu. ft. per sec., d 6.5 ft. at 5,000 cu. ft. per sec. Little additional degradation is expected the future, since minimum flow releases from the power plant have been served to have only about one ft. of slope in the five miles downstream to e river control section.

anopolis Dam (Missouri)

This project was completed in 1948. The outlet works consists of a tunnel ft. in diameter and a horizontal jump type stilling basin with two rows of ft.-high baffle piers and a 4-ft.-high end sill. From the tunnel portal, the dewalls flare in plan at 3:1 until a basin width of 52 ft. is reached at the lo- tion of the downstream row of baffle piers, and then extend parallel for the maining distance to the end of the basin. At the location of the upstream w of baffle piers, the stilling basin is 40 ft. wide. The length of sloping ron downstream from the portal is 42 ft., whereas the horizontal portion of e apron extends for a distance of 78 feet. Capacity of the outlet works at l reservoir pool is 5,700 cu. ft. per sec., but normal maximum releases e limited to about 3,000 cu. ft. per sec.

A progressive scour problem existed in the outlet channel below the basin. small channel was eroded through the 18-inch rock paving, and some ero- on of the banks had occurred by 1952. In order to stabilize the outlet chan- , the 18 in. depth of grouted rock paving (on 6 in. of gravel) was repaired a distance of 200 ft. downstream from the basin, and a concrete cut-off ll, 8 ft. deep by 3 ft. wide, was placed 100 ft. downstream from the basin. Field observations indicate that a hydraulic jump will occur for discharges to the normal maximum of 3,000 cu. ft. per sec., but for a flow of 5,500 cu. per sec. photographs indicated considerable spray action from the impact tunnel discharges on the upstream row of baffle piers. The result was in- mplete stilling action and considerable turbulence in the outlet channel. er inspection revealed that the sides of the upstream row of baffle piers, well as the floor immediately adjacent, were pitted to a depth of 1 to 2 in. e evidence as shown in photographs clearly indicates that the pitting was result of cavitation. A rough check indicates that tailwater depth was ut 0.7 of the hydraulic jump depth, D_2, at a discharge of 5,500 cu. ft. per .

skingum Reservoirs (Ohio)

During the 1940 flood in the Muskingum River Basin, observations and s were made at the outlet tunnels and conduits for Atwood, Bolivar,

Leesville, Mohawk and Wills Creek Dams. These projects, with the exceptio of the latter, have conventional hydraulic jump stilling basins with level apro two rows of baffle piers and end sill. The Wills Creek basin has one row of baffle piers and no end sill. Because of limitations on the channel capacities downstream, it was not feasible to open all gates at these projects so as to observe hydraulic action under conditions approaching maximum capacity of the outlet works. However, flows of 16 to 71 percent of maximum capacity were observed. In each case, the hydraulic jump was well within the basin, with good energy dissipation and well-distributed, acceptably low velocities over the end sill. Photographs taken of the stilling action at Bolivar and Mohawk Dams were compared with similar photographs of hydraulic model tests conducted in 1935. In each case, the prototype performance was equal or better than that anticipated as a result of the model tests.

DISCUSSION AND CONCLUSIONS

The performance record of the stilling devices at Corps of Engineers reservoir projects has been good. Stilling action has been equal or better than anticipated during the design and model testing stage, except in the few instances described above. Some erosion of the energy dissipating structure has been experienced at several projects, and these instances have been discussed in this paper because of their interest and the possibility that others may apply the results to the prevention of similar erosion on future projects. However, most of the structures have withstood the erosive forces of high-velocity flow releases with little or no damage.

Of the stilling basins below spillways at Corps of Engineers projects whic have experienced large discharges, probably the most severely tested of the group has been the Bonneville Dam basin, with an experienced discharge with in 62 percent of design discharge and with about one billion acre-ft. of total flow during past years. Stilling action has been adequate to date, but recent modifications to the stilling basin will improve the basin performance.

Stilling basins below outlet works have been tested near design discharge more frequently. Model-prototype conformity has been good.

It is interesting to note that the causes of the erosion experienced include in the author's opinion, the following: Apron not long enough for complete stilling action, apron not deep enough for the formation of a fully effective hydraulic jump, structural shapes within the stilling basin which created areas of cavitation action, abnormal conditions brought about by diversion of river flows during construction, inadequate stilling action brought about by other, unforeseeable factors and misconceptions which were prevalent in hy draulic design procedures at the time the project was designed, including in some cases model testing procedures, inability of the concrete to resist the erosive forces of the water action in cases where "adequate" stilling action was provided by the basin design, and combinations of the above.

No damages were reported from inadequate structural design. Many of these types of structures are probably somewhat overdesigned as compensation for some of the unknown forces which may be inherent or developed in t structures. Exceptions to this statement may be instances such as the deter mination of the centrifugal forces developed in bucket curves where the forc

involved are larger than has been generally realized, as noted by D. B. Gumenski, M. ASCE.[6]

In the author's opinion the experiences presented in this paper lead to the conclusion as suggested by Gumenski that the hydraulic design of these structures is the most important single phase in their development. Although the engineer responsible for the hydraulic design of a project receives from model tests important and at times indispensable help, particularly when no adequate means of analysis exists (and in any case the model aids in verifying the adequacy of the design), the primary responsibility for acceptance of a particular design must rest with the hydraulic designer. He must determine what actual conditions may develop in the prototype which cannot be foreseen by model tests.

Baffle piers at Corps of Engineers projects have withstood erosion quite well in most instances. Whereas the erosion of the baffle piers at Bonneville Dam was understandably severe, as described above, and erosion to a lesser extent occurred in the first few years at Norfork Dam and several other projects where gravel deposits were left adjacent to or in the basin upon completion of construction, baffle piers of many projects have had little or no erosion. An example of the latter is Denison Dam, where the baffle piers are subjected to heavy impact forces and yet have had very little erosion to date after passing 15 million acre-ft. of flow.

For standard hydraulic jump type basins composed of a level apron, two rows of baffle piers and end sill, an apron length measured from the P.I. of the spillway bucket curve to the lower end of the end sill equal to $3D_2$ appears to provide adequate stilling action for most of the projects studied, insofar as the limited prototype information at or near design flows indicates. Exceptions to this criterion were the McNary Dam basin with low Froude Number, and basins on especially erodible foundations, where a somewhat longer length was considered desirable.

It has been found desirable to unwater many of the stilling basins periodically for inspection. Substantial quantities of rock and gravel have been removed during some of these inspections.

In some recent instances, conventional hydraulic jump type stilling basins with baffle piers and end sill have been designed for full energy dissipation for the greatest flood of record or a somewhat larger flood, while not allowing the hydraulic jump to sweep out of the basin for the spillway design flood. A high end sill aids in confining the jump to the basin for this condition. In terms of the spillway design flood, the resulting basin dimensions can often be reduced to provide a basin length of $2\ 1/2\ D_2$ and apron floor set high enough that the tailwater depth equals about $0.8D_2$.

With regard to the height of basin training walls for hydraulic jump type basins, experience with hydraulic models (and a few prototype experiences such as at McNary Dam) indicates that some overtopping of the walls, say about 5 feet for the spillway design flood, is not harmful to the stilling action. If the basin were closely confined by an earthen dam, this reduction would not be made.

Present practice of the Corps of Engineers provides for superior quality concrete in critical areas of hydraulic structures. Where velocities exceed 50 ft. per sec. frequently or for prolonged periods of time, the water-cement

---

[6] "Design of Side Walls in Chutes and Spillways," by D. B. Gumenski, Transactions, A.S.C.E., Vol. 119, 1944, p. 355-372.

ratio is held to a maximum of 5 gallons per bag, slump at about 2 inches, and maximum size of aggregate at 1 1/2 inches.

ACKNOWLEDGMENTS

Much of the credit for the information assembled in this paper is due the various district and division offices of the Corps of Engineers concerned for their assistance in obtaining the necessary date.

Journal of the
HYDRAULICS DIVISION
Proceedings of the American Society of Civil Engineers

RECIRCULATION OF COOLING WATER IN RIVERS AND CANALS

Geza L. Bata[1]
(Proc. Paper 1265)

SYNOPSIS

The recirculation of water after it has been used as a coolant in thermo-ectric plants and returned to the river or canal from which it was original-drawn is of great importance to the economy of operation of such plants. mong the many factors that affect the amount of recirculation, the most im-rtant ones are the channel depth and discharge, the distance between intake d outlet of the flow diverted for cooling, the degree of heating of the divert-water, and the relative amount of diversion. The effects of these factors ve been singled out for an extensive analytical and experimental study, the sults of which, together with design criteria derived therefrom, are esented in this paper.

I. INTRODUCTION

A part of the water that has served as a coolant in a steam plant and been urned to the river or canal of origin often finds its way back to the intake the form of an overlying wedge-like layer, from which it is once again en (together with new water) through the cooling system. The amount of irculation of heated water, which directly affects the efficiency of opera-n of a plant and often lowers its maximum capacity, depends on the geome-of the intake, the design of the outlet, the distance between the intake and outlet, the discharge and mean depth of the original flow in the river or al, the relative amount of diversion, and the degree of heating of the di-ted water. The complexity of the recirculation problem necessitates the aration of these factors into groups, the effects of which can be studied arately and then compounded subsequently.

e: Discussion open until November 1, 1957. Paper 1265 is part of the copyrighted Journal of the Hydraulics Division of the American Society of Civil Engineers, Vol. 83, No. HY 3, June, 1957.

Research Asst., Iowa Inst. of Hydr. Research, State Univ. of Iowa, Iowa City, Iowa; on leave from the Inst. of Hydr. Eng., Belgrade, Yugoslavia.

In the present investigation, the last four factors were chosen for careful analytical and experimental study, because they form an organic unit of predominant importance in the determination of recirculation. To eliminate the effects of any particularity of the design of the intake and outlet, the simplest forms were used for these structures: for two-dimensional flow the intake was a bottom slot extending all the way across the concrete channel used to simulate a canal in the laboratory; for three-dimensional flow the intake was a rectangular side opening with its bottom flush with that of the channel; in most cases the outlet extended all the way across the channel and discharged the heated water in such a way that downstream from the outlet the temperature was essentially uniform. In the few available field tests, the temperature distribution changed continuously.(10)

As will be seen from the body of the paper, the amount of recirculation is directly and simply related to the areas occupied by the warm water and the cool water, respectively, at the intake—i.e., to the position of the common interface of the warm and cool layers. If the intake and outlet conditions are essentially the same as those prevailing in the experiments, the problem of recirculation reduces to the problem of determination of the form of the warm wedge, and the results presented herein can be directly used either for prediction of recirculation or for selection of the distance between the intake and the outlet. However, the question then arises: how useful would the results be for other designs at the outlet and the inlet?

The amount of recirculation for any particular geometrical design of the intake depends chiefly on the amount of diversion, the degree of heating, and the location of the interface at the intake—the last of which, for a first approximation, does not depend on the particular intake form used. Thus the method for determination of the form of the warm wedge presented herein is directly useful for the investigation of the effect of the intake design. As to the outlet, its design can be expected to affect the form of the warm wedge only through its effect on the local position of the interface, the equations governing the form of the warm wedge being the same for all outlet designs.

Thus the determination of the form of the warm wedge not only provides a means of predicting the amount of recirculation for intake and the outlet conditions similar to those prevailing in the experiments, but also plays a definite and specific role in the determination of the effects of intake and outlet designs on the amount of recirculation. In short, the method for the determination of the warm wedge presented herein occupies a central position in the solution of the recirculation problem.

Before proceeding, the notion of river or canal, to which the present paper applies, must be understood in the sense that the Froude numbers are not too small—in particular not less than those of the numerous experiments cited herein and of the other field tests to which reference is made. Otherwise the waterway behaves like a lake and the intake conditions change completely, as analyzed theoretically by Craya(1) and experimentally by Gariel.

II. ANALYSIS

The flow in the canal can be divided (see Fig. 1) into three zones: that upstream from the intake, that between the intake and the outlet, and that downstream from the outlet. In the first zone the warm wedge is stagnant and the fluid in it has no mean velocity. For the particular outlet used in the

xperiments, the third zone is unimportant, because thorough mixing at the utlet destroys downstream stratification. However, the case of stratifica-ion in zone three is included in the analysis. The determination of the form f the warm wedge—which will be the chief concern of the analysis, because his form is intimately related to the amount of recirculation—is complicated y the relative uncertainty of the interfacial shear and the apparent lack of tarting points for the determination of the interface. It will be shown in the ollowing sections that the critical depth (yet to be defined) of the lower layer ccurs at the intake and the outlet, thus providing the starting points needed or the upstream and the middle zones, respectively. With a somewhat ration-l evaluation of the interfacial shear, the one-dimensional equations of motion or the two layers then permit the determination of the interface. Thus the ollowing seemingly unrelated sections are individually necessary and all to-ether sufficient for this determination, and must not be mistaken for discon-ected considerations presented without a central theme.

. Equations of Motion

The flow in both the upper (warm) and lower (cool) layers will be in gener-l non-uniform. If the vertical component of the velocity is neglected and on-the mean velocities in the respective layers are considered, the equations motion are

$$g\frac{dh_1}{dx}+g\frac{dh_2}{dx}+u_1\frac{du_1}{dx}+g(S_{1e}-S_o)=0 \qquad (1)$$

r the upper layer and

$$(1-\frac{\Delta\rho}{\rho})g\frac{dh_1}{dx}+g\frac{dh_2}{dx}+u_2\frac{du_2}{dx}+g(S_{2e}-S_o)=0 \qquad (2)$$

r the lower layer. In these equations, which were given by Schijf and hönfeld,[5] x is the distance measured from a fixed point to any variable int on the interface in the downstream direction, h_1 and h_2 are the depths the warm and cool layers, u_1 and u_2 are the corresponding mean velocities ositive in the downstream direction), ρ and $\rho+\Delta\rho$ represent the densities the upper and lower fluid, respectively, and g is the gravitational accelera-on. S_0 is the slope of the canal bottom; the energy slopes, S_{1e} and S_{2e}, are fined by

$$S_{1e}=\frac{\tau_i}{\rho g h_1} \qquad S_{2e}=\frac{\tau_o-\tau_i}{\rho g h_2} \qquad (3)$$

which the shear stresses, τ_o at the bottom and τ_i at the interface, are ven by

$$\tau_i=f_i\frac{\rho}{8}|u_1-u_2|(u_1-u_2) \qquad \tau_o=f\frac{\rho}{8}|u_2|u_2 \qquad (4)$$

It should be understood throughout this analysis that the density differences

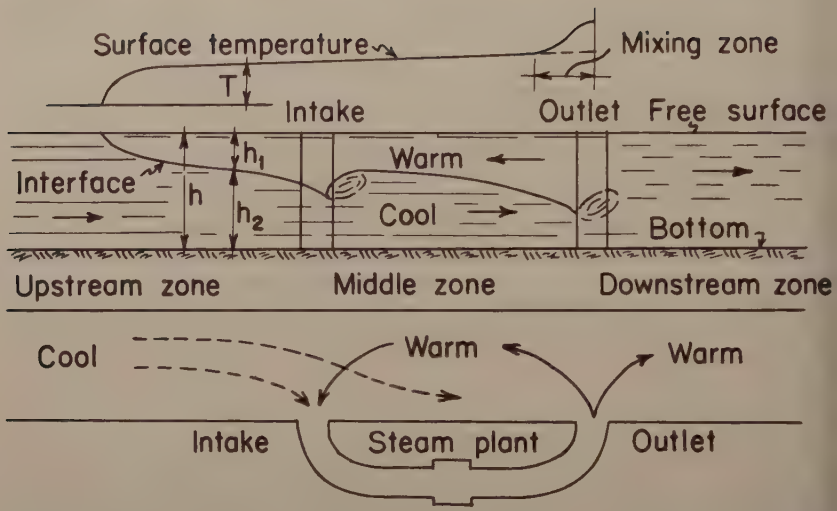

Fig. 1 The Cool and Warm Layers near the Intake and the Outlet of a Steam Plant

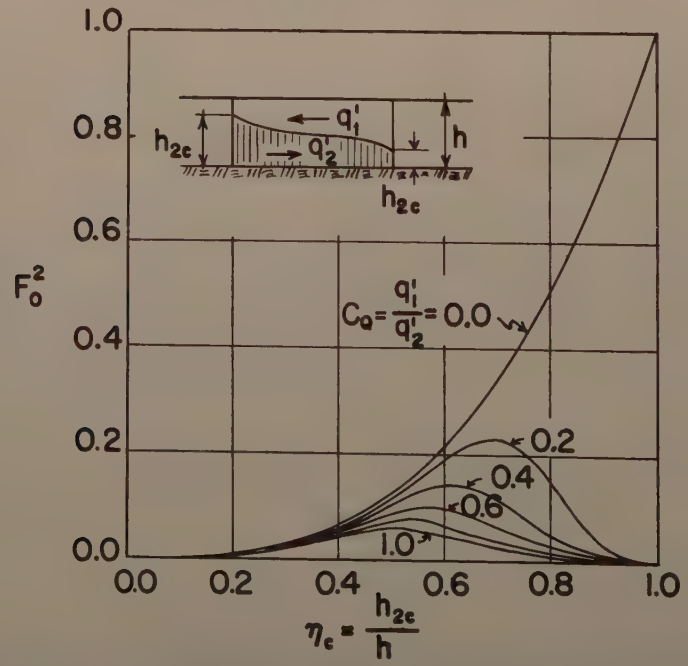

Fig. 2 The Critical Depths for Different Discharge Ratios in the Two Layers

considered will be so low ($\Delta\rho/\rho < 0.003$) that the variations in the free-surface elevation (i.e., in the total depth h) will be negligible in comparison with the variations of the position of the interface. In other words, one may put $h = h_1 + h_2 = \text{const.}$

By subtracting Eqs. (1) and (2), and utilizing the equation of continuity and Eqs. (3) and (4),[9] one can reduce the differential equation for the position of the interface to the dimensionless form

$$\frac{-\frac{1}{F_o^2}\eta^3(1-\eta)^3 - (\eta-1)^3 + C_Q^2\eta^3}{\alpha(1-\eta+C_Q\eta)^2 + (1-\eta)^3}\,d\eta = \frac{f}{8}\,d\left(\frac{x}{h}\right) \tag{5}$$

in which $\eta = h_2/h$, $\alpha = f_i/f$, $C_Q = q_1/q_2$, and

$$F_o = \frac{u_o}{\sqrt{\frac{\Delta\rho}{\rho}gh}} \tag{6}$$

the latter being the densimetric Froude number (after Keulegan[2]), based on the approaching canal flow (u_0 denotes the velocity of the undisturbed flow).

Integration of Eq. (5) can be performed after the proper end conditions for the different zones have been determined. It will be more convenient to calculate the distances x from the downstream end section upwards. Then the sign of x has to be changed in Eq. (5).

. The Critical Depths

In connection with the determination of the form of the warm wedge, the critical depth is defined to be that for which the tangent to the interface is normal to the bottom of the channel—i.e.,

$$\frac{d(x/h)}{d\eta} = 0 \tag{7}$$

From Eq. (5) it follows directly (the subscript c indicating the critical condition) that

$$\frac{1}{F_o^2} = \frac{C_Q^2}{(1-\eta_c)^3} + \frac{1}{\eta_c^3} \tag{8}$$

which was obtained already by Stommel and Farmer[3] in a different way. In the physically real range of $0 < \eta_c < 1$, and for $C_Q \neq 0$, represented in Fig. 2, there are two critical depths for a given Froude number F_O: a lower and a higher one, between which, in accordance with Eq. (5), the interface rises in the upstream direction. If the value of $(F_O)_{max}$ is exceeded, no increase in the elevation of the interface in the upstream direction can take place. For $Q = 0$, which corresponds to a stagnant upper layer, the critical depth is given by its usual definition:

$$\eta_c = \frac{h_{2c}}{h} = \sqrt[3]{\frac{q_2^2}{\frac{\Delta\rho}{\rho} g h^3}} = F_o^{2/3} \tag{9}$$

In computing the critical depths, the total depth h was assumed to be constant. In practice h is always known, because the canal is designed for a certain depth of homogeneous fluid. Otherwise (if the value of h were not given), there would be an infinite set of paris of solutions for Eq. (8) as proved by Benton.(4)

As will be shown in the next article, of the two critical depths the lower one will be established immediately upstream from the outlet as that which corresponds to the end of the stratified flow. Upstream from the outlet the depth of the lower layer is increasing, but it never can exceed the upper critical value.

C. Conditions at the Outlet

In the zone downstream from the outlet the stratification ceases to exist, due to the thorough mixing produced by the form of outlet used in the experiments and a homogeneous fluid of density ρ^x flows farther downstream. Tentatively one may assume that the middle zone has to end with the critical depth or with supercritical flow—in other words, that the conditions downstream from the outlet do not have any influence on the middle zone. This can be justified by finding the downstream depth at the outlet, which would correspond to the critical depth upstream from the outlet.

As indicated in Fig. 3, single primes and double primes denote the quantities upstream and downstream from the outlet, respectively. This notation will be used henceforth unless otherwise stated. By applying the momentum principle to the lower layer, as done by Yih,(6) one has

$$\rho_2 q_2'^2 + h_2' h_1' \rho_1 g + \frac{1}{2}\rho_2 g h_2'^2 + \frac{1}{2}(h_1' + h_1'')(h_2'' - h_2')\rho_1 g = \frac{\rho^x q_2''^2}{h_2''} + h_2'' h_1'' \rho^x g + \frac{1}{2}\rho^x g h_2''^2 \tag{10}$$

Here $q_2' = q_2''$, because the discharge in the cool layer does not change across the outlet. For the upper layer one has to assume that the returned warm water while flowing through the lateral canal has no momentum in the x-direction, and that both discharges q_1' and q_1'' are directed outward from the "control area." Therefore, the impulse-momentum equation for the upper fluid will be

$$\rho_1 \frac{q_1'^2}{h_1'} + \frac{1}{2}\rho_1 g h_1'^2 = \rho^x \frac{q_1''^2}{h_1''} + \frac{1}{2}\rho^x g h_1'^2 \tag{11}$$

Downstream from the outlet one may assume without appreciable error a uniform velocity distribution, and by considering that $h_1' + h_2' = h_1'' + h_2'' = h$ = constant, one obtains

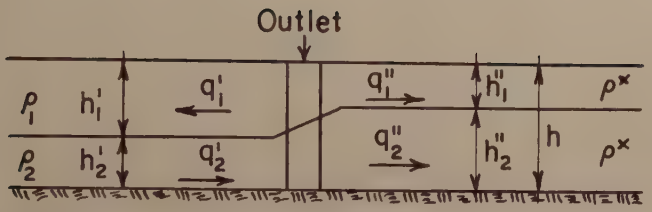

Fig. 3 Transition at the Outlet

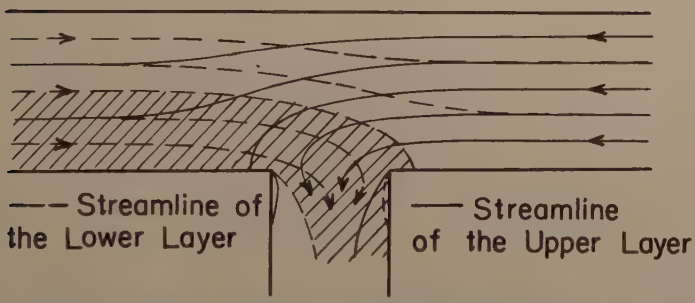

Fig. 4 Flow Pattern near the Intake

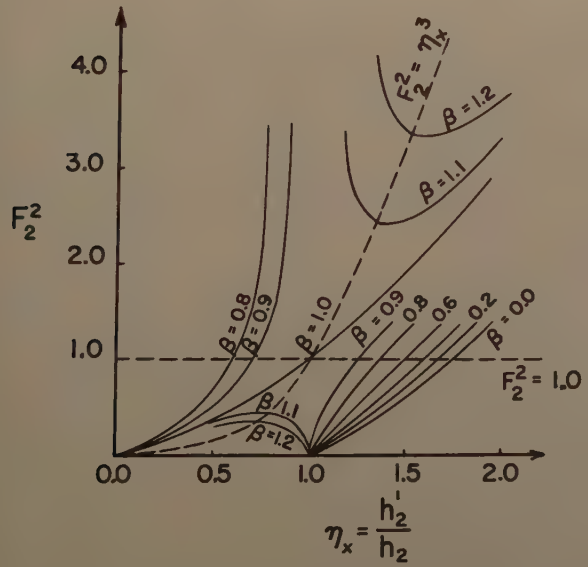

Fig. 5 Conjugate Depths in Cases of Enlargement ($\beta < 1$) and Contraction ($\beta > 1$) of the Channel Width
– After Jaeger –

$$\frac{h_2''}{h} = \frac{q_2''}{q_1'' + q_2''} \qquad (12$$

Equations (10) and (11) specify h_2'/h as a function of q_2''/q_1'' and q_1'/q_2'. In other words, for every value of the upstream parameter q_1'/q_2', which represents the ratio of the discharges in the middle zone, there exists a certain ratio of the downstream discharges q_2''/q_1'' (or a definite value for h_2'/h) for which the depths immediately upstream and downstream from the outlet are conjugate. If the actual ratio of q_2''/q_1'' would be greater (or the actual value of h_2'/h would be less) than indicated by the conjugate state, the conditions downstream from the outlet would influence the middle zone by submerging it.

The upstream parameter q_1'/q_2' can vary between the limits $0 < q_1'/q_2' <$ where the value of 1 corresponds to 100% diversion and is more conducive to submergence than the value of zero. The simultaneous solution of Eqs. (10) and (11) then gives[9] for the conjugate state

$$\frac{h_2'}{h} \approx 0.1; \qquad \frac{q_1''}{q_1'' + q_2''} \approx 0.001 \qquad (13$$

These conditions practically never appear in practice, and as a consequence at the downstream end of the middle zone the critical depth will be established.

The case in which the two layers of densities ρ_1 and ρ_2 are still present downstream from the outlet—as is often true in field conditions—can be treated in a completely similar manner, by solving simultaneously the momentum equations of the upper and lower layers. Due to the fact that the three densities ρ_1, ρ_x, and ρ_2 are very close to unity, the result obtained will be practically identical with Eq. (13). In other words, at the downstream end of the middle zone the critical depth is also established for the case that the stratification downstream from the outlet is not destroyed, thus again giving the necessary starting point for the calculation at the outlet.

D. Conditions at the Intake

In the neighborhood of the side intake used, the flow in both layers can be considered as a potential flow in a manifold efflux,[12] at least at elevations far from the interface. In the lower layer the flow is approaching from the upstream direction, whereas in the upper layer the direction of the approach is opposite to it (Fig. 4). At the mouth of the intake there are correspondingly two stagnation points, and the separation from the walls of the lateral can is on opposite sides for the two layers. Near the stagnation points the velocities are rather low and the pressure in the stagnant layer is increased by the velocity head, whereas in the moving layer the pressure does not change very much from the initial value. The created pressure difference will result in a tendency for the lower fluid to rise near the downstream corner of the intake and an opposite tendency for the upper fluid to sink near the upstream corner. This will cause a secondary helicoidal motion near the intake entrance, with the consequence of mixing in the lateral. The "penetration zone" will be

greater at the downstream corner, because the velocity of approach of the cold layer is always greater.

If the transition at the intake is treated as a sudden enlargement (as indicated by the shaded area in Fig. 4), an analysis(9) similar to that of Jaeger for a homogeneous fluid(11) gives

$$F_2^2 = \frac{\eta_x(\eta_x^2 - 1)}{2(\eta_x - \beta)} \tag{14}$$

In this equation $\eta_x = h_2'/h_2$ denotes the ratio of the two conjugate depths, h_2' being the depth downstream from the intake, the quantity

$$F_2 = \frac{u_2}{\sqrt{\frac{\Delta\rho}{\rho} g h_2}} = \sqrt{\frac{q_2^2}{\frac{\Delta\rho}{\rho} g h_2^3}} \tag{15}$$

is the local densimetric Froude number, and the parameter β denotes the ratio of the discharges in the lower layer: $\beta = q_2'/q_2$.

Another approach for the transition at the intake would be that applied for the neighborhood of the outlet, where the whole width of the canal was included in the calculation and the four discharges (upstream and downstream, for each layer) were different. The application of the momentum principle(9) would then result again in Eq. (14) with the only difference that now the parameter β is replaced by β^2.

It seems that the sudden-enlargement method is more convenient for application to the side-intake conditions, whereas the discharge-variation method (second approach) applies more conveniently to a bottom-slot intake which extends across the whole width of the main canal. At the outlet the warm water is returned to the canal in a jet-like form, which assures that the discharges are distributed more or less along the whole width of the canal, so that the second approach is more appropriate.

The analysis and graphical representation of Eq. (14) were given by Jaeger(11) and the graph is reproduced in Fig. 5. If the upstream conditions are given, together with the parameter β, which actually represents the diversion ratio, the other conjugate depth can be determined from this figure. Assuming critical conditions upstream from the intake ($F_2 = 1$) and taking an average $\beta = 0.5$, the downstream conjugate depth would then be around 50% higher than the critical depth upstream from the intake. This oftentimes will be impossible, because the depths in the middle zone are limited—i.e., they have to be less than the "upper critical depth," given by Eq. (8) and in Fig. 2. The transition then occurs in such a way that a supercritical flow of the lower layer is established downstream from the intake, followed by a jump (Fig. 1). Figure 2 indicates that the jump will be in close proximity to the intake.

In brief, the depth of the lower layer immediately upstream from the intake has to be critical, and this gives the starting point for the calculation of the upstream zone.

. Form of the Warm Wedge

From the earlier analysis it follows that the flow conditions in all three

zones are independent, and hence the form of the warm wedge can be determined in each of them separately. Since it is known that the critical depth is established at the ends of the upstream and middle zones, from these points on the calculation can be performed by using Eq. (5).

For the upstream zone the upper layer is stagnant ($C_Q = 0$). Substituting the value of Eq. (9) into Eq. (5) for x = 0 (x is measured upstream from the intake) and integrating, one has

$$f\frac{x}{h} = \frac{2}{F_o^2}(\eta^4 - F_o^{8/3}) + \frac{1}{F_o^2}\frac{8}{3}\alpha(\eta^3 - F_o^{6/3}) + \\ + \frac{4\alpha(1+\alpha)}{F_o^2}(\eta^2 - F_o^{4/3}) + \frac{8}{F_o^2}[\alpha(1+\alpha)^2 - F_o^2](\eta - F_o^{2/3}) - \\ - \frac{8\alpha}{F_o^2}[(1+\alpha)^3 - F_o^2][\ln(1+\alpha-F_o^{2/3}) - \ln(1+\alpha-\eta)] \qquad (16)$$

It was assumed that the resistance coefficients and the Froude number do not change along the warm wedge. By putting $\eta = h_2/h = 1$, the total length L of the warm wedge in the upstream zone is obtained (Fig. 6). (The experimental points in this and the next figures are the results of the experiments discussed in greater detail in Section III.)

The other extreme case is $C_Q = 1$, which corresponds to 100% diversion, the discharges in the two layers then being equal. Integration of Eq. (5) for this case gives

$$f\left(\frac{x}{h}\right)_A^B = \left\{\frac{2}{F_o^2}\eta^4 + \frac{8\alpha}{F_o^2}\eta + 8\left(1+\frac{\alpha}{F_o^2}\right)\ln\left[1+\frac{1}{\alpha}(1-\eta)^3\right] - \right. \qquad (17)$$
$$- \frac{8}{\alpha^{1/3}}\left(1+\frac{\alpha}{F_o^2}\right)\left[\frac{1}{2}\ln\frac{\alpha^{2/3} - \alpha^{1/3}(1-\eta) + (1-\eta)^2}{(\alpha^{1/3}+1-\eta)^2} + \sqrt{3}\tan^{-1}\frac{2(1-\eta)-\alpha^{1/3}}{\alpha^{1/3}\sqrt{3}}\right] +$$
$$\left. + \frac{8}{3\alpha^{2/3}}\left(1+\frac{\alpha}{F_o^2}+\frac{\alpha^2}{F_o^2}\right)\left[\frac{1}{2}\ln\frac{(\alpha^{1/3}+1-\eta)^2}{\alpha^{2/3} - \alpha^{1/3}(1-\eta)+(1-\eta)^2} + \sqrt{3}\tan^{-1}\frac{2(1-\eta)-\alpha^{1/3}}{\alpha^{1/3}\sqrt{3}}\right]\right\}_A^B$$

where the letters A and B denote symbolically the lower and upper limits. Equation (17) is represented graphically in Fig. 7 for a common experimental value of 0.150 for F_O'—the Froude number of the middle zone. For $0 < C_Q < 1$ the general solution is more complicated, and the best way of carrying out the calculation is by numerical integration of Eq. (5).

The length of the warm wedge in the middle zone is given in Fig. 7. There is a certain adjustment which has to be made in connection with the length of the warm wedge in the middle zone. In the downstream neighborhood of the intake where the expansion takes place (Fig. 4), the discharge q_2' per unit width in the lower layer is larger than farther downstream. Therefore, the ratio $C_Q = q_1'/q_2'$ is smaller. With decreasing C_Q the slope of the interface according to Eq. (5) tends to flatten, so that the upward curvature of the interface (Fig. 7) disappears. The expansion zone is approximately 1 to 2 times B where B is the width of the canal. The total length of the warm wedge is therefore increased approximately by this amount. If the initial ratio of C_Q is close to zero, the expansion is negligible and the flattening effect can be neglected.

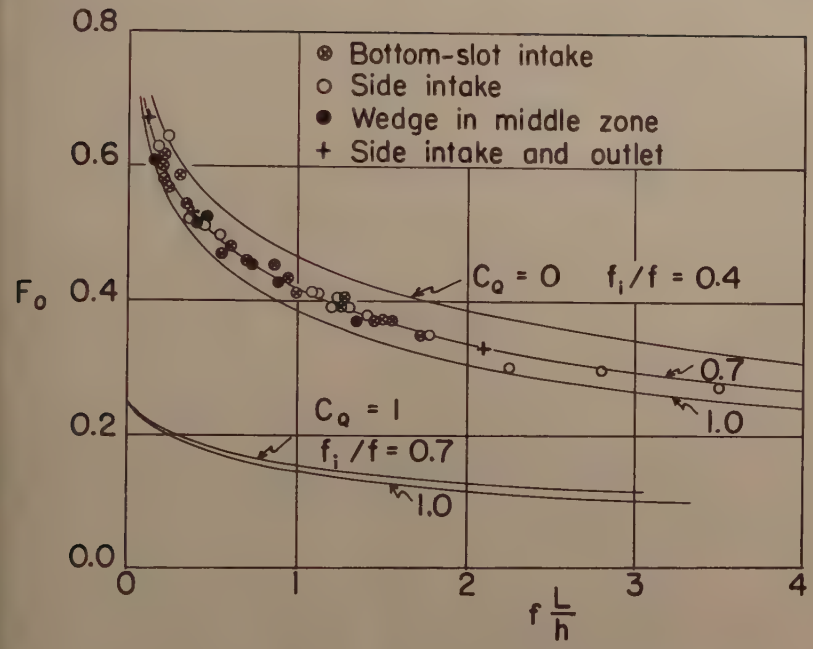

Fig.6 Length of the Warm Wedge

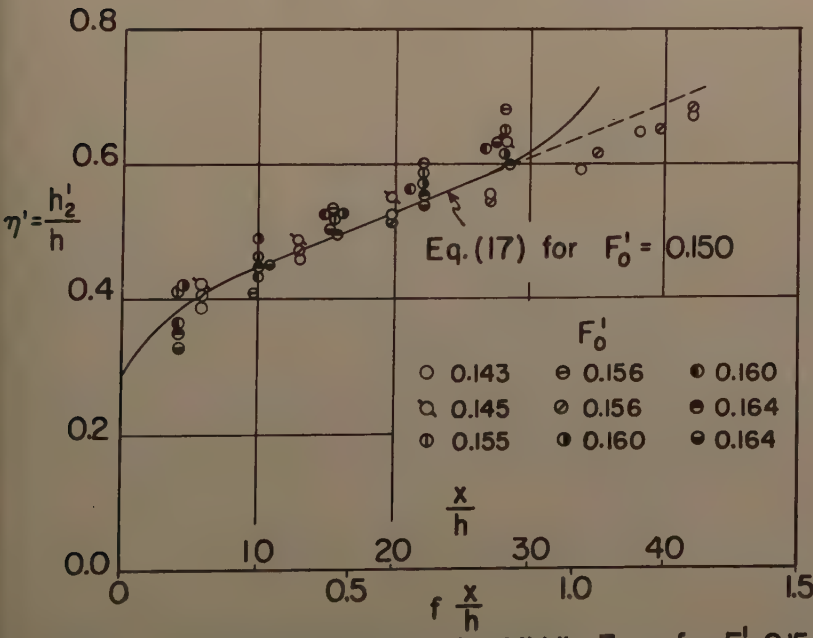

g.7 Shape of the Warm Wedge in the Middle Zone for $F_o' = 0.15$

One of the principal quantities required in the numerical evaluations is the resistance coefficient for turbulent flow at the interface, f_i, or its ratio to the bottom resistance $\alpha = f_i/f$, which will be treated in more detail in the next article. In accordance with the experimental evidence(8) f_i varies along the warm wedge from $f_i = 0$ near the critical end section to $f_i/f = 1$ at its upstream leading edge. This is especially true for the upstream zone with stagnant upper layer, whereas in the middle zone the opposite flow in the two layers soon imposes the final value of the resistance at the interface.

To account for the aforementioned change of f_i/f along the interface one may assume that the actual shape of the warm wedge can be obtained by taking different values of $\alpha = f_i/f$ along the wedge and combining the different segments into one curve. For $F_O = 0.447$ ($F_O^2 = 0.20$), which is the mean value for the experiments, the relative shape of the warm wedge for the upstream zone is obtained this way(8) and it is represented in Fig. 8. Although the procedure is somewhat arbitrary, the curve obtained for the shape of the wedge is closer to actuality than the curves for constant interfacial shear.

As the calculations show, the effect of the Froude number on the relative shape of the wedge is small and can be neglected in a first approximation.

It may be mentioned that for $f = 0$ and $C_Q = 0$ Eq. (5) gives the form of the intrusive saline wedge in an estuary, for which, by a procedure similar to that of the warm wedge,(8) the relative shape is given by

$$\frac{x}{L} = 1 - \frac{\left(\frac{1}{5F_o^2} - 2\right) + 4\frac{h_1}{h} - 2\left(\frac{h_1}{h}\right)^2 - \frac{1}{F_o^2}\left(\frac{h_1}{h}\right)^4 + \frac{4}{5F_o^2}\left(\frac{h_1}{h}\right)^5}{\frac{1}{5F_o^2} - 2 + 3F_o^{2/3} - \frac{6}{5}F_o^{4/3}} \qquad (18$$

Equation (18) is represented graphically (Fig. 9) for two different values of F_O, together with Keulegan's experimental data.(2) One sees that the agreement is very good.

Resistance in Established Stratified Turbulent Flow

For the cases of flow between fixed plates (Fig. 10, No. 1), stratified flow (No. 2) and free-surface flow (No. 3) the hydraulic radius, R, has the values of $h_2/2$, $H/2$, and h_2, respectively, where H is the height of the extrapolated velocity profile (with $h_2 < H < 2\,h_2$). The resistance coefficient, f, does not vary much for the three cases.

It is convenient to assume (arbitrarily) for all stratified-flow cases (No. 1 the same hydraulic radius: $R = h_2$. However, to take care of the variations of the hydraulic radius, then the resistance coefficient (denoted by f*) must be assumed to be variable. The energy gradient for turbulent flow can thus be expressed by

$$S = \frac{f}{4H/2}\frac{u_2^2}{2g} = \frac{f^*}{4h_2}\frac{u_2^2}{2g} \qquad (19$$

One can further conceive that the variable resistance coefficient, f*, is composed of a constant resistance, f, on the bottom, and a variable resistance, f_i

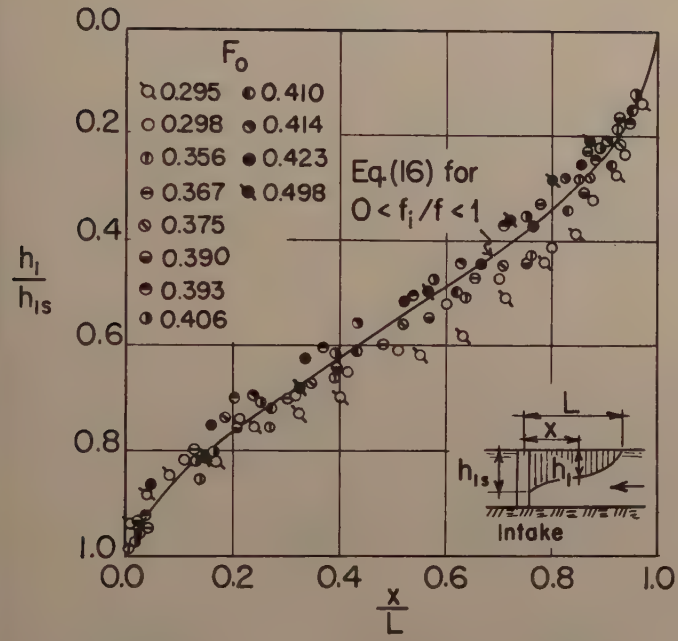

Fig.8 Relative Shape of the Warm Wedge for $C_Q = 0$

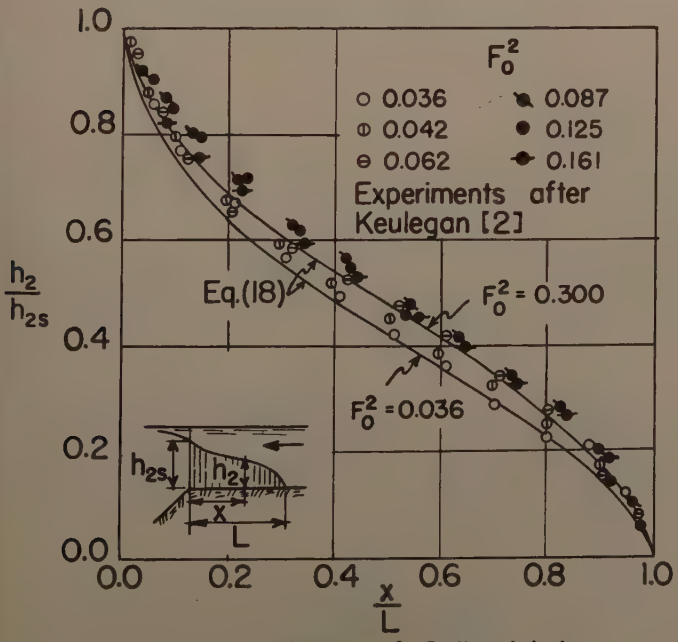

Fig.9 Relative Shape of Saline Wedge

at the interface—i.e., $f^* = f + f_i$—and then from Eq. (19) it follows that

$$\alpha = \frac{f_i}{f} = \frac{2h_2}{H} - 1 \tag{20}$$

In order to obtain a solution for H/h_2 one can express the shear stresses for the upper and lower fluids and equate them. In the upper layer the interfacial shear will remain the same if one substracts or adds a constant velocity to the velocity profile. The interfacial shear is, therefore, the same in cases (a) and (b) in Fig. 11 and is given by

$$\tau_i = \frac{f_1}{8} \rho u_i^2 \tag{21}$$

where f_1 is the resistance coefficient at the interface for the upper fluid and u_i is the velocity at the interface. The former will be discussed in more detail at the end of this section and in the section on design criteria.

For the lower fluid one has by geometric considerations (Fig. 10)

$$\frac{\tau_i}{\tau_o} = 2 - \frac{H}{h_2} \tag{22}$$

Equation (21) divided by

$$\tau_o = \gamma S \frac{h_2}{2} = \frac{f''/2}{8} \rho u_2^2 \tag{23}$$

and equated to Eq. (22) gives

$$2 - \frac{H}{h_2} = 2 \frac{f_1}{f''} \left(\frac{u_i}{u_2}\right)^2 = 2 \frac{f_1}{f} \frac{H}{2h_2} \left(\frac{u_i}{u_{max}}\right)^2 \left(\frac{u_{max}}{u_2}\right)^2 \tag{24}$$

where u_{max} is the maximum velocity in the lower layer.

From the logarithmic velocity distribution of the extrapolated velocity profile the values of u_i/u_{max} and u_2/u_{max} can be obtained,(8) which after substitution in Eq. (24) give

$$2 - \frac{H}{h_2} = \frac{f_1}{f} \frac{H}{h_2} \left[\frac{1 - 2.5A \ln\left(\frac{H}{h_2} - 1\right)}{1 - 2.5A - 2.5A\left(\frac{H}{h_2} - 1\right) \ln\left(\frac{H}{h_2} - 1\right)} \right]^2 \tag{25}$$

where

$$A = \frac{\sqrt{\frac{f}{8}}}{1 + 2.5\sqrt{\frac{f}{8}}}$$

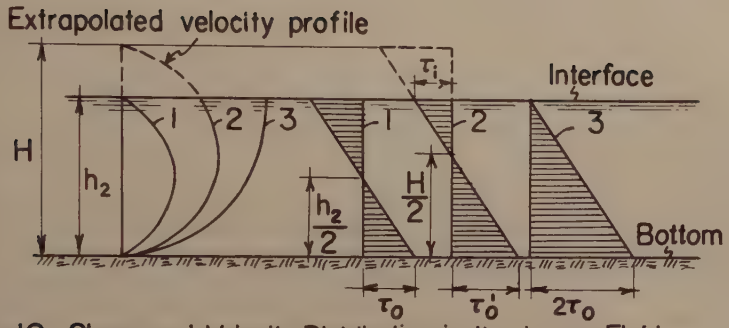

Fig.10 Shear and Velocity Distribution in the Lower Fluid

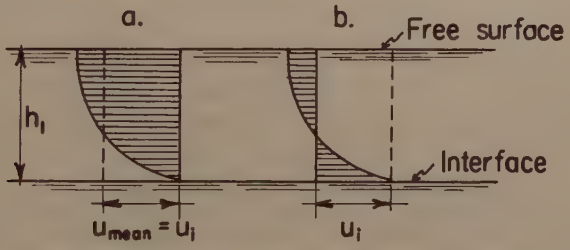

Fig.11 Velocity Distribution in the Upper Fluid

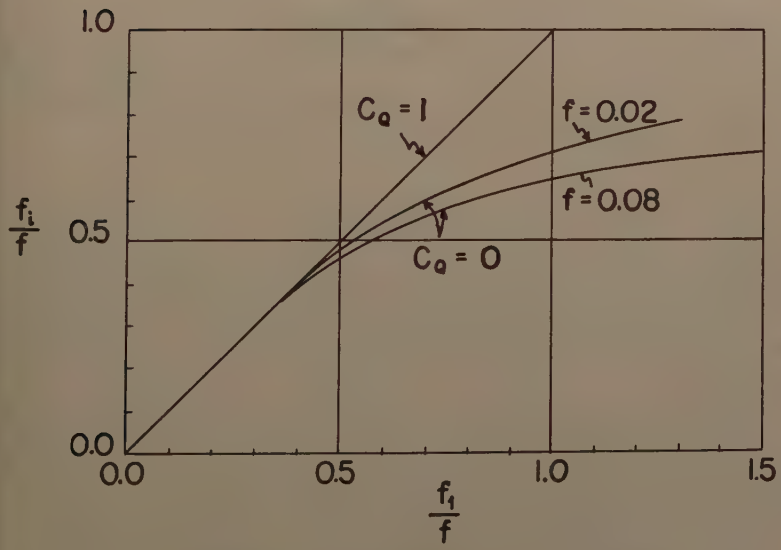

Fig.12 Resistance Coefficient at the Interface in Turbulent Flow

Equation (25) together with Eq. (20) gives the solution for the interfacial resistance which is plotted in a graph in Fig. 12. A slight variation can be observed with the absolute value of f. Equation (25) is valid for stagnant upper layer. In case the two layers are moving in the opposite directions, the velocity distribution is approximately the same as if the interface were replaced by a fixed wall, which is represented in Fig. 12 by a direct-correlation straight line between the interfacial resistance coefficient f_i and that of the upper fluid, f_1.

The problem now lies in the determination of the coefficient f_1—i.e., what resistance is acting on the upper fluid, which is moving on the lower one. Without precise measurements of the velocity distribution in the upper fluid this question can not be answered. Because further evidence is not available, it is here assumed that for the experimental conditions in the laboratory flume the interface was smooth. Falling droplets indicated that there is much greater disturbance near the zero-velocity line than at the interface itself. One could therefore assume the formula for smooth surfaces for calculating f_1 at the interface, whereas for the bottom resistance, f, both smooth and rough surfaces can come into consideration. Knowing the ratio f_1/f one can determine with the aid of Fig. 12 the interfacial resistance coefficient sought—i.e., f_i/f. It is characteristic that even for $f_1/f = 1$ one obtains $f_i/f<1$, which indicates that there is a finite velocity at the interface. Theoretically the interface will be brought to rest only if $f_1/f \to \infty$.

It is here briefly mentioned that by an analysis similar to that of turbulent flow, the variable resistance coefficient in laminar flow can be obtained,(8) and it is given by

$$f^* = 384 \frac{3+N}{3+4N} \frac{1}{R} \tag{26}$$

in which R represents the Reynolds number of the lower fluid (calculated with 4 h_2 for the characteristic hydraulic radius), and the quantity

$$N = \frac{h_1 \mu_2}{h_2 \mu_1} \tag{27}$$

denotes a parameter (μ with the corresponding indices represents the dynamic viscosity). If the discharges are low (especially in the laboratory), laminar flow may occur in the middle zone.

F. Recirculation

As defined in previous works,(7) the recirculation is that percentage of the returned warm water which enters the intake and by which the average temperature of the intake water is raised. The same amount of cool water necessarily by-passes the intake and continues to flow farther downstream. The recirculation can be expressed as

$$r = \frac{T_i - T_2}{T_1 - T_2} \tag{28}$$

here T_i is the temperature of the intake, T_1 is that of the upper fluid, and T_2 is that of the lower fluid.

Limiting Condition for No Recirculation

The intake entrance will not act as a constriction, because the flow through he intake is regulated by the gates at the end of the lateral canal and not by he intake entrance. The drop in elevation of both the free surface and the nterface at the entrance of the lateral will, therefore, be negligible, and one an suppose that the amount of recirculation will be proportional to the area f the intake occupied by the warm layer at that place. This assumption was lready made in[7], where a different approach was followed.

For the expulsion of the warm wedge from the upstream zone, according o Eq. (16), it is required that $F_O \geqq 1$. However, for no recirculation it is ecessary that the depth of the lower fluid downstream from the intake be al- o equal to the total depth. This is the case when the distance between the in- ke and outlet is just equal to the length of the warm wedge in the middle ne. The limiting condition for no recirculation, therefore, is given by Eq. 6) and represented in Fig. 6 for $C_Q = 0$ with fL/h corresponding to the dis- nce between the intake and outlet. From the related Froude number, F_O', e necessary discharge in the middle zone can be calculated; in other words, e maximum diversion for no recirculation can be determined.

For the expulsion of the warm wedge even from the middle zone it is cessary that $F_O' \geqq 1$.

It is interesting to notice that for 100% diversion the condition of no re- rculation would be practically impossible, because in that situation there ould be no flow in the middle zone, the interface would be horizontal, and e warm water would reach the intake no matter how far it might be from e outlet. Of course, for great distances the heat loss through evaporation d radiation would change the analysis.

The Amount of Recirculation

If the upstream and downstream depths at the intake are not equal, the ost reasonable assumption is that the amount of recirculation will be pro- rtional to their mean value, because gravitational effects are small for the nge of temperature differences usually encountered except for very small versions. The upstream depth is the critical depth for a stagnant upper yer, defined by Eq. (9). The downstream depth, t, is governed by the jump ig. 13), and it is less than the elevation of the calculated interface would dicate at the same place. The amount of recirculation can therefore be cal- lated by

$$r = \frac{1}{h}\left[\frac{1}{2}(h - h_{2c}) + \frac{1}{2}(h - t)\right] = \frac{1}{2}\left(1 - \frac{h_{2c}}{h}\right) + \frac{1}{2}\left(1 - \frac{t}{h}\right) \qquad (29)$$

s difficult to estimate how much t is less than h_2' in Fig. 13. A straight- e variation of the t-line between the upper and lower critical depths, sug- sted by the fact that the middle portion of the interface and also its flat- ed end portion are fairly straight, gives for $C_Q = 1$

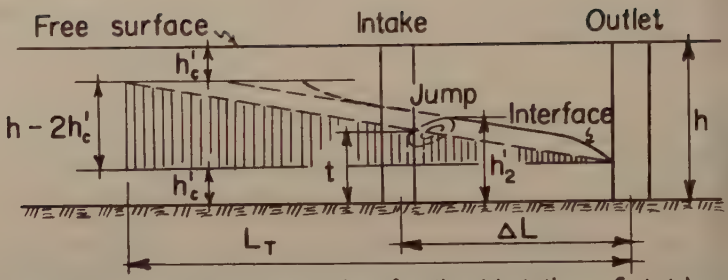

Fig.13 Assumption of a Straight Line for the Variation of t-Line

$$\frac{t-h_c'}{h-2h_c'} = \frac{\eta_t'-\eta_c'}{1-2\eta_c'} = \frac{\Delta L}{L_T} \qquad (30$$

in which ΔL denotes the distance between the intake and outlet and $L_T = \lambda L$ i the length of the t-line, where λ is an empirical coefficient, having a value o 1.28 for $C_Q = 1$ on the basis of experimental data.(9)

Introducing into Eqs. (29) and (30) the value of the critical depth, given by Eq. (9)—which holds approximately for the middle zone, too, for low values o F_O'—the amount of recirculation is obtained in the form

$$r = \frac{1}{2}(1-F_o^{2/3}) + \frac{1}{2}(1-F_o'^{2/3}) - \frac{1}{2}\left(f\frac{\Delta L}{h}\right)\left(\frac{h}{fL_T}\right)(1-2F_o'^{2/3}) \qquad (31$$

From Eq. (17) the parameter $f L_T/h$ is a function of F_O' and C_Q, so that the recirculation is

$$r = \varphi\left(F_o, F_o', f\frac{\Delta L}{h}, C_Q\right) \qquad (32$$

where the functional form is given by the previous equations. Equation (32) states that the recirculation is dependent upon the Froude numbers of the up stream and middle zones (corresponding to the two depths at the intake), the relative distance between the intake and outlet, $f\,\Delta L/h$, and the ratio C_Q of the discharges in the two layers of the middle zone.

The validity of Eq. (31) or Eq. (32) is subject to two limitations. First, i the upstream Froude number F_O is greater than 1, the first term on the rig side of Eq. (31) would be negative, and from Eq. (9) the upstream depth at th intake would turn out to be higher than the total depth, which has no physical significance. The validity of Eq. (31) is therefore limited to $F_O \leqq 1$. For F increasing above 1 but F_O' = const, the downstream depth would remain con stant, and the upstream zone would tend to push the wedge away from the up stream edge of the intake, by keeping its own depth also constant and equal t h. As a result the recirculation decreases only slowly with increasing F_O. Second, there is a lower limit of F_O, below which Eq. (31) does not hold. Equation (31) was derived from Eq. (29), so the second and third terms on it right side represent together the influence of the downstream depth at the

ntake. When the sum of these two terms becomes equal to the first one, the ecirculation becomes

$$r = 1 - F_o^{2/3} \tag{33}$$

nd the upstream and downstream depths at the intake are equal. The elevaon of the interface at the intake is then mostly governed by the upstream epth with some influence of the downstream jump, and the recirculation ould follow Eq. (33), instead of Eq. (31), with values somewhat below it.

Equations (31) and (33) are represented in Fig. 16, together with the limitg Froude number, $(F_O')_{lim}$, for which the length of the warm wedge is just qual to the distance between the intake and outlet. Because there is no reirculation for this case, $(F_O')_{lim}$ = constant coincides with the abscissa—e., with r = 0.

It is interesting to note that the diversion ratio, defined as $D = Q_i/Q_c$, here the indices i and c refer to the discharges at the intake and in the canal, oes not explicitly influence the recirculation. Generally speaking, for a cerin value of diversion, and for the other conditions remaining constant, one un have different values of recirculation. For example, for the limiting contion of no recirculation, by varying the discharges in the canal and intake in e manner that their difference remains always the same, all four parameirs in Eq. (32) remain constant, but the diversion ratio changes. Only if the scharge in the canal or of the plant is assumed to be constant will the diverion ratio influence the Froude number F_O' in the middle zone directly. The le of the diversion ratio as a parameter is then justified.

III. EXPERIMENTAL VERIFICATION

Experiments, for purpose of verifying and supplementing the foregoing alysis, were conducted in a concrete flume 132 ft. long, 5 ft. wide, and 15 in. ep. The lighter fluid was obtained by heating the water with steam. In out the half of the 72 runs[8] the intake was a regulated bottom slot across e whole width of the flume, whereas in the other half[9] it was represented a rectangular 15-inch-wide side canal; it remained at a fixed place for all periments. In one series the outlet was represented also by a 15-inch recngular side canal, with its axis at 90° to the axis of the main canal. Paralexperiments were carried out with a discharge distributor as an outlet by lich the warm water was distributed uniformly across the whole width. Beuse of its mobility and because no principal difference was found between e two arrangements for the shortest distance (between the intake and outlet) vestigated, the discharge distributor was used exclusively thereafter. From e distributor the water fell into a system of stilling screens at the free rface.

The velocities in the canal were too low to be measured by the instruments ailable. Only the points of zero velocity were obtained by injecting dye, the ange of the velocity direction being rather sharply marked. The tempera-e measurements, on the other hand, were very thorough and precise. ermocouples on a movable carriage were arranged on two verticals at ery 0.5-in. height. Moreover, with movable thermocouples every point uld be reached. A 48-channel indicating potentiometer enabled both great

accuracy (0.1°F) and rapidity in reading to be attained. A representative experiment is given in Fig. 14 and the results will be discussed in the following articles.

A. Form of the Warm Wedge

The temperature measurements indicate that there is a diffusion zone near the interface or dividing streamline. Because the two fluids have quite similar characteristics, the heat is probably diffused at the same rate in both fluids so that the middle of the diffusion zone can be considered as a good first approximation for the interface. In the upstream zone the measured points of zero velocity coincide with the upper temperature limit, as suggested by Fig. 11. In the middle zone, on the other hand, the zero-velocity line has been found to coincide with the interface, according to Section II E.

The measurements indicate that there is a slight decrease in the temperature of the upper layer in the upstream direction, with a sharp change at the leading edge (Fig. 1). The densimetric Froude number accordingly varies slightly along the wedge, which had little effect on the form of the wedge, as found in the analysis. The recirculation, however, has to be calculated with T_1 at the intake in Eq. (28), in order to obtain the accurate discharges in the middle zone. This temperature decrease, which is related to the mechanism of the diffusion process between the two layers, and which can be observed as a salinity decrease in the saline-wedge intrusion, has to be further investigated.

In order to compare the analysis with the experiments one has to determine the interfacial shear. The ratio f_i/f is a function of the Reynolds number based on u_2 and $4h_2$, which in the upstream zone varied from 15,000 to 70,000 and in the middle zone from 4,300 to 35,000. For the longer wedges the Reynolds numbers are closer to the lower values, and for that range it was found by separate measurements in the flume that the resistance coefficient on the bottom is $f \approx 0.03$. According to Fig. 12 the ratio f_i/f depends on f_1/f, where for f_1 it was proposed to take the value for smooth surfaces which in this case is $f_1 \approx 0.025$. With these values $f_i/f = 0.66$ for $C_Q = 0$ and $f_i/f = 0.8$ for $C_Q = 1$. For the available field measurements on the Chicago Sanitary and Shipping Canal(10,8) with Reynolds numbers from 3 to 5 million one has $f_1/f = 0.010/0.014 = 0.70$ and from Fig. 12 $f_i/f = 0.60$.

With the foregoing data the total length for $C_Q = 0$ can be calculated, because it will be well represented by an average or mean value of the interfacial shear. In the calculations of the relative shape of the warm wedge, on the other hand, it is necessary to take care of the variations of the interfacial shear along the wedge, as explained in Section II E. Figures 6 and 8 show that the agreement between the analysis and the experiments for $C_Q = 0$ is very good.

The form of the warm wedge in the middle zone (for $C_Q = 1$) can be verified only for portion of the length of the interface, because the total length is almost never achieved in the experiments. In order to group the experimental points by the application of Eq. (17), data with approximately the same Froude number, F_o', have to be chosen. The data in Fig. 7, for different discharge and temperature values, give good agreement with the theoretical curve.

The data for the transition sections at the intake and outlet verify that the critical depth is established at both places. The critical depths at the intake taken at a distance 3/2 h from the intake—are represented on Fig. 15, and th

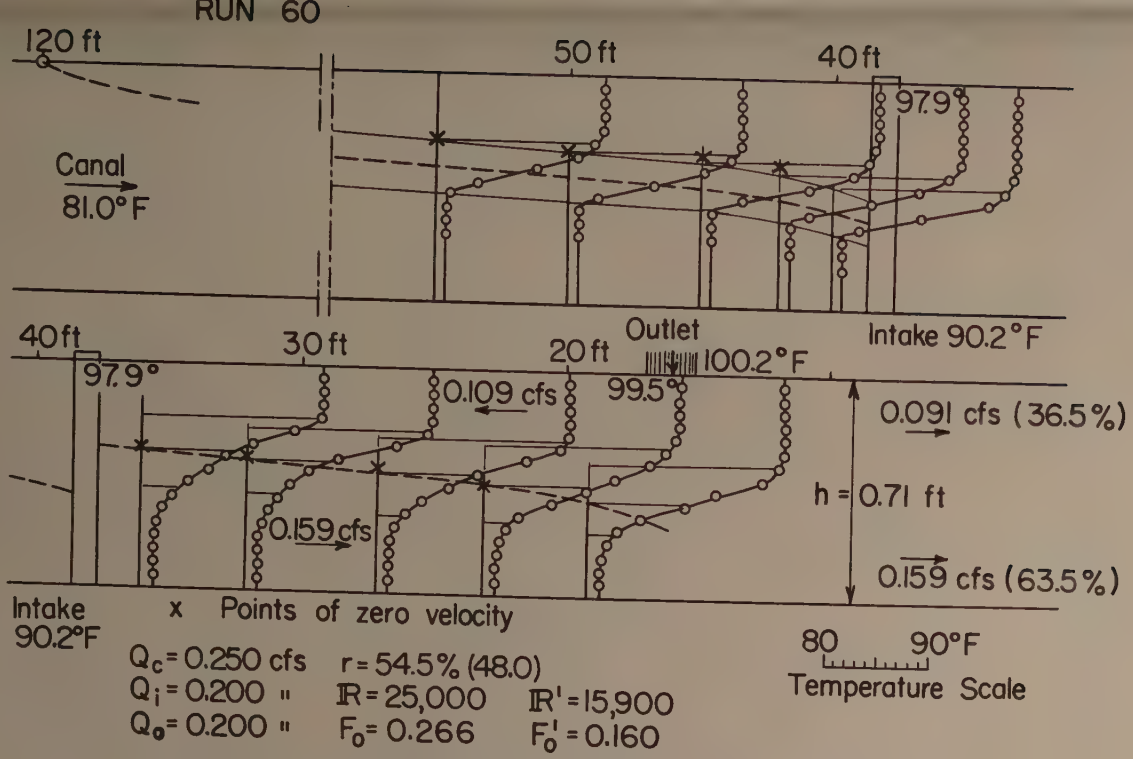

Fig.14 Temperature Distribution in the Laboratory Flume (Width 5 ft)

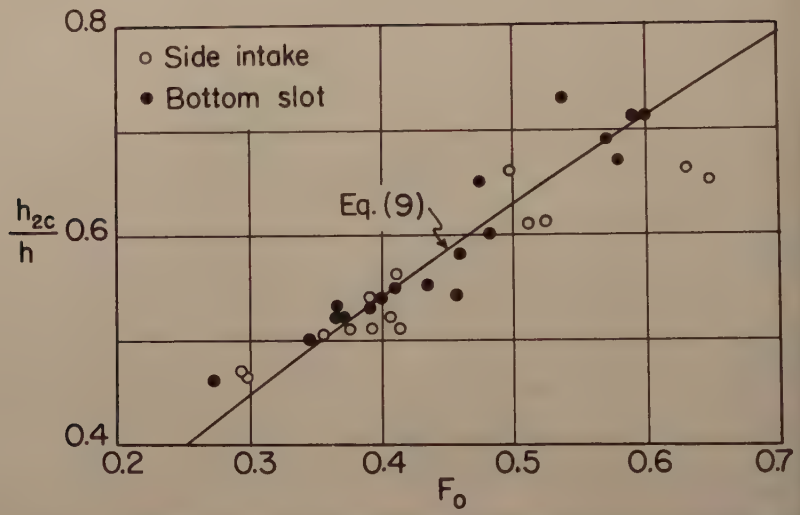

Fig. 15 Critical Depth Immediately Upstream from the Intake

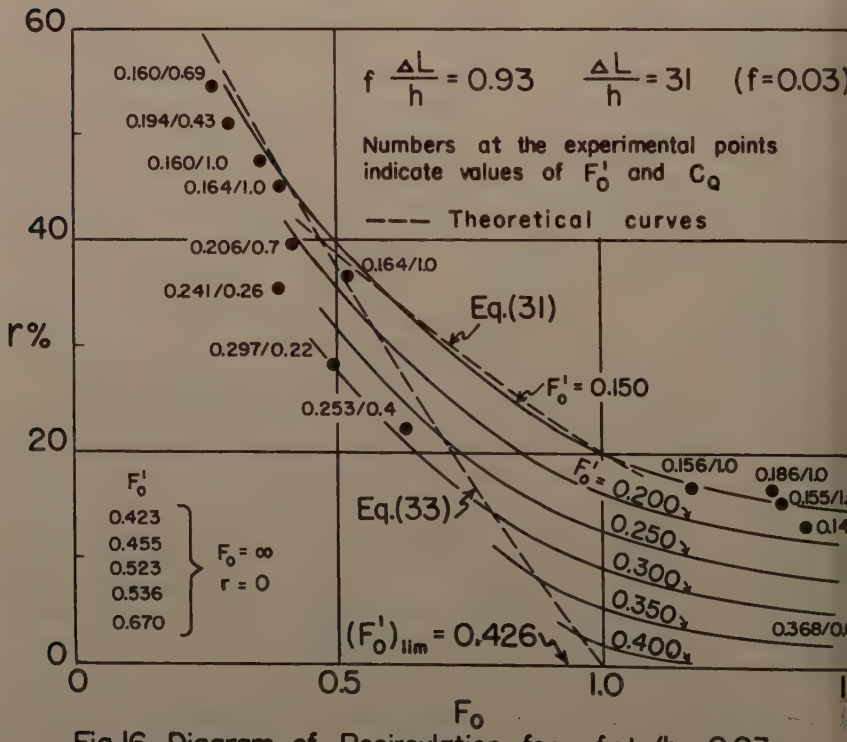

Fig. 16 Diagram of Recirculation for $f\Delta L/h = 0.93$

ow satisfactory agreement with Eq. (9) for both the bottom slot and the side ake. The critical depths at the outlet section can be obtained only by ex- polation, because the measurements at the outlet itself are impossible due the great fluctuations in the mixing zone. These depths, although following . (9), are not represented on Fig. 15.

Finally the qualitative picture of the potential flow was verified in the ex- riments by dyeing the streamlines. The effect of the spiral motion in form- two pools of cool and warm water at the two corners of the intake can be ry definitely seen in the field measurements.(8)

Recirculation

The experiments were performed for three different distances between the ake and outlet, from which the data for $f\Delta L/h = 0.93$ are presented in Fig. Diagrams of recirculation for values 0.372 and 1.36 of $f\Delta L/h$ are avail- e in (9). The experimental data follow the theoretical curves fairly well. e limiting value of F_O' for no recirculation agrees especially well with the oretical value. If the length of the warm wedge is less than the distance ween the intake and outlet, a slowly moving eddy is formed in the upper er, from the leading edge of the warm wedge to the intake. This eddy, vever, does not affect the recirculation, which remains zero.

In order to check if the experimental data for the three distances between intake and outlet are consistent with Eq. (31), from the four parameters Eq. (32) F_O, F_O', and C_Q will be chosen constant and only $f\Delta L/h$ will be variable. With $F_O = 1$ (for which the first term in Eq. (31) vanishes), = 1 and $F_O' = 0.150$ (which is the best defined by the experimental points), (31) is plotted in Fig. 17, together with the experimental data. The agree- nt is very good, so this graph enables one to plot the recirculation curve $F_O' = 0.150$ according to Eq. (31), and for any distance between the intake outlet on the basis of both theoretical and experimental support. The s F_O' = const in Fig. 16, between Eq. (31) for $C_Q = 1$ and $F_O' = 0.150$ on one hand, and the abscissa r = 0 on the other hand can be obtained by in- polation, a greater accuracy being unwarranted due to the changes in C_Q m 1 to 0.

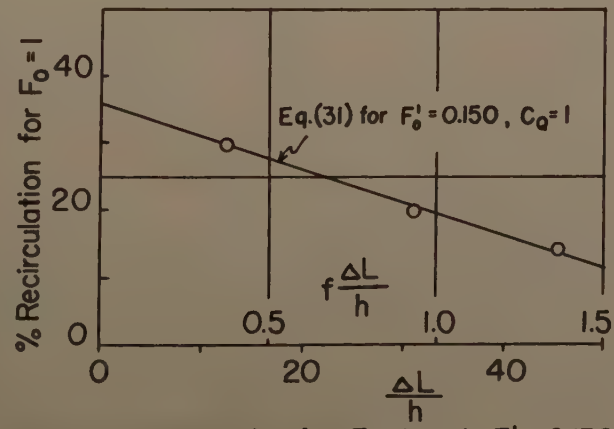

Fig.17 Values of Recirculation for $F_o = 1$ and $F_o' = 0.150$

The amount of recirculation in case of the two-dimensional bottom slot i much less, compared to the three-dimensional side intake[8] and even for 100% diversion (which in this case seems to be the dominant parameter) it only about 10%, regardless of the distance between the intake and outlet. T is because the slot is covered by a layer of cool water, and the warm water can be drawn down only through the action of occasional vortices.

The effect of the intake and outlet forms on the recirculation will now be discussed. Although this problem was not thoroughly investigated, some us ful suggestions, nevertheless, can be made. In one experiment the upper a lower halves of the intake entrance were blocked, successively, and in another one the width of the intake canal was about half of that normally used. The recirculation did not change more than 2 or 3% in all these cases. Thu for the range of the temperature difference and the diversion ratio prevaili in these tests, the intake form for rivers seems to have little effect on the recirculation. In this connection, the reader may be referred to work by Craya.[1]

At the outlet there is an intensive mixing between the warm water and th by-passing cool water, which results in a temperature drop between the re turned hot water and the upper layer of the middle zone. This temperature drop—or, better, the percentage of the plant discharge which mixes with th cool water passing by the outlet, as proposed by Laursen and Hubbard[7]—i a measure of the intensity of the mixing, and it is different for various for of the outlet. From Fig. 1, in which a typical temperature variation of the free surface—i.e., of the upper layer—is given, one sees that the mixing zo extends only to a very short distance from the outlet. If the calculation of Froude number, F_O', is based on the temperature outside of the mixing zo the effect of the outlet form is excluded. This was done in all experiments because the study of the influence of the outlet form requires a separate analysis.

From a series of experiments,[9] in which the cross section and the for of the outlet are varied, one can conclude that if the warm water is returne to the river in a more jet-like form (i.e., with smaller cross-sectional are of the outlet) and directed toward the bottom, the mixing process is more i tensive and the recirculation is less. The amount of recirculation—the oth conditions being unchanged—varied in a range of more than 100% for the di ferent forms. Screens are very undesirable near the outlet section, and th should be moved upstream in the outlet canal. As a general rule the cond tions for decrease in recirculation require a violent introduction of the wa water in the main canal, which is opposite to conditions required for navig tion. The best outlet form is best determined by specific model studies.

IV. DESIGN CRITERIA

The river section with greatest velocity will generally be chosen if seve places for the plant site are available, even with the regulation of the secti considered coming into consideration. With fixed plant discharge and with best outlet form known, the problem is then usually to select the most eco- nomical distance between the intake and outlet.

The safest design would require such a distance that no recirculation would take place even for the lowest discharges in the river. If the minim discharge in the river is greater than the plant discharge, the Froude num

' for the middle zone can be calculated and from Fig. 6 (for $C_Q = 0$) the io f Δ L/h, and so the distance ΔL between the intake and outlet, can be ectly determined. If the Froude number F_O' turns out to be greater than he warm wedge is expelled even from the middle zone and all warm water ws downstream from the outlet. On the other hand, if the minimum river charge is equal to or even less than the plant discharge, recirculation can- be avoided. The question is then how far upstream from the outlet should intake be located from the standpoint of over-all economy.

Several values for ΔL should be chosen and for each a diagram of recircu- ion as a function of the river discharge determined with the aid of Fig. 17, explained in Sections II F and III B (see Fig. 16). From the hydrological a one can determine the number of days on which recirculation would ur. The amount of recirculation per degree and per day is related to the ompanying loss in power production, and an economic study will then show t distance between the intake and outlet represents the optimum.

If recirculation is allowed to occur, the calculation has to proceed by trial error, because in the field the temperature difference between the intake outlet is constant rather than that between the canal and outlet. Also it assumed in the analysis that the shear at the interface will be the same or a smooth surface, which gave satisfactory results in the laboratory ex- iments. Under field conditions this assumption may not be valid and the istance at the interface may be greater, with the final effect that the slope he interface will be steeper. This, would, however, decrease the recircu- on, so that the actual conditions in the field can only be safer than indicat- by the calculation and the laboratory experiments.

V. CONCLUSIONS

On the basis of the good agreement between the analytical and experimental ults presented in the foregoing pages, the following conclusions concerning recirculation of cooling water at a steam plant may be drawn:

The three zones of flow under consideration—upstream from the intake, veen the intake and outlet, and downstream from the outlet—are not in- nced by one another, and the critical depths are established at the end ions of the upstream and middle zones. The length and the shape of the m wedge in each of the first two zones can be determined by applying the ations of non-uniform flow to the two layers of warm and cool water, and onsidering that in the middle zone the elevation of the interface cannot eed the upper critical depth.

n the three-dimensional case with side intake and outlet, the amount of rculation is directly and simply governed in magnitude by the depths im- iately upstream and downstream from the side intake; these in turn are tions of the Froude numbers of the upstream and middle zones, the rela- distance between the intake and outlet, and the discharge ratio of the two rs in the middle zone. The functional dependence of the amount of recir- tion on the four parameters has been determined analytically. The condi- of no recirculation requires that the distance between the intake and outlet qual to the length of the warm wedge. Oftentimes, however, this distance ld be very great, and it is more economical to allow a certain amount of rculation during the low-water stage in the river.

The amount of recirculation for the two-dimensional case of a bottom-slot

intake, determined only experimentally, is much less than that for a side in take, because the slot is covered by a layer of cool water which is only occa sionally penetrated by warm water through vortex action.

ACKNOWLEDGMENTS

Both the analytical and the experimental phases of the foregoing investig tion were conducted under the supervision of Dr. Chia-Shun Yih, Research Engineer of the Iowa Institute of Hydraulic Research. The experiments wer carried out in a flume which had been built with funds contributed by the Co monwealth Edison Company of Chicago, and a 48-channel potentiometer was placed at the writer's disposal by that firm. The project was partially sup- ported by the Office of Ordnance Research, Department of the Army, under Contract DA-11-022-ORD-1729 with the Iowa Institute.

REFERENCES

1. Craya, A., "Recherches théoriques sur l'écoulement de couches super- posées de fluides de densités différentes," La Houille Blanche, No. 1, Jan.-Feb. 1949.
2. Keulegan, G. H., "Sixth progress report on model laws for density cur- rents. Effectiveness of salt barriers in rivers," National Bureau of Standards, No. 1700, June 1952.
3. Stommel, H. and Farmer, H. G., "Control of salinity in an estuary by a transition," Sears Found. Journ. Marine Research, vol. 12, No. 1, 1953.
4. Benton, S. G., "The occurrence of critical flow and hydraulic jumps in multi-layered system," The Johns Hopkins Univ. Dept. Civ. Eng., Tech. Rep. No. 1, Feb. 1953.
5. Schijf, J. B., and Schonfeld, J. C., "Theoretical consideration on the mo tion of salt and fresh water," Minnesota International Hydraulics Conve tion, Sept. 1953, Minneapolis.
6. Yih, C. S., and Guha, C. R., "Hydraulic jump in a fluid system of two layers," Tellus, Vol. 7, No. 3, 1955, Stockholm.
7. Laursen, E. and Hubbard, P. G., "Report on model study of Crawford Station Steam Plant," Internal report of Iowa Institute of Hydraulic Re- search, March 11, 1955.
8. Bata, G., "An investigation of recirculation in stratified flows," M. S. Thesis, State University of Iowa, August 1956.
9. Bata, G., "Recirculation of cooling water discharged from thermo-elec plants," Internal report of Iowa Institute of Hydraulic Research, August 1956.
10. Temperature records in the main canal, in the vicinity of Crawford Sta tion, by the Sanitary District of Chicago, July 1953, Internal Report.
11. Jaeger, Ch., Technische Hydraulik, Basel, 1949.
12. McNown, S. J. and Hsu, E. Y., "Application of the conformal mapping t divided flow," Proc. Midwest Conf. on Fluid Dyn., 1950, Ann Arbor, Michigan.

NOTATION

Except as otherwise noted, the subscript 0 refers to conditions of undisturbed flow; subscript 1, to overlying warm layer; subscript 2, to underlying cool layer; subscript c, to critical state; subscript i, to interface. A single prime (') indicates zone between intake and outlet; a double prime ('), zone beyond outlet.

C_Q = q_1/q_2

f = resistance coefficient

F = Froude number

g = acceleration of gravity

h = depth of flow

L = length of penetrating wedge

q = rate of flow per unit width

r = recirculation

R = Reynolds number

S_e = energy slope

S_O = bed slope

T = temperature

u = mean velocity

x = distance in downstream direction

α = f_i/f

β = q_2'/q_2

η = h_2/h

η_x = h_2'/h_2

ρ = mass density

τ = intensity of shear

τ_O = intensity of bed shear

Journal of the
HYDRAULICS DIVISION
Proceedings of the American Society of Civil Engineers

A STUDY OF BUCKET-TYPE ENERGY DISSIPATOR CHARACTERISTICS

M. B. McPherson,[1] A.M. ASCE, and M. H. Karr,[2] J.M. ASCE
(Proc. Paper 1266)

SUMMARY

Throughout this study the discharge was distributed uniformly over the hannel width, obviating inclusion of the effects of spillway piers, unequal rest gate settings, slotted buckets, or laterally flared spillways or chutes. bucket exit angle of 45° was used throughout, having been found by others be most effective, under a variety of service conditions. A 45° exit angle as been recommended for high head dams.(1)

Both a (1 on 1) and a (1 on 2) entrance slope were intensively investigated. both instances the discharge, entrance head, tailwater depth and bucket adii were varied over a wide range of magnitude and of performance.

General performance characteristics have been delineated. Required ucket radii for the various service conditions are specified. Energy dissiation effectiveness is demonstrated in a comparison with tailwater requirements for a hydraulic jump in a horizontal channel. Information directly useful in approximating spray wall heights is given. A sample preliminary esign calculation directly utilizes the material presented.

Definition of Terms

Referring to Figure 1, h_1 is the total available head relative to the bucket vert, measured as close as practicable to the bucket roller; h_b is the depth the bucket above the bucket invert, h_s is the average surge peak depth lative to the elevation of the bucket invert, and h_2 is the tailwater depth lative to the bucket invert. The bucket radius is designated as R, and q is e discharge in cfs./foot width.

te: Discussion open until November 1, 1957. Paper 1266 is part of the copyrighted Journal of the Hydraulics Division of the American Society of Civil Engineers, Vol. 83, No. HY 3, June, 1957.

Associate Prof. of Civ. Eng., Lehigh Univ., Bethlehem, Pa. (Member, Task Force for Stilling Basins and Energy Dissipators for Spillways and Outlet Works).

Instructor, Civ. Eng., Lehigh Univ., Bethlehem, Pa.

Basis for Using Bucket Invert as Datum for h_2 and h_s

Regions of high velocity downstream from the bucket tend to be concentrated near the surface in this type of stilling basin. The energy dissipation downstream from the bucket, resulting primarily from the expansion of the live stream in the surge, can be regarded as a surface phenomenon for the most part.

Included in Figure 2 are some of the findings from a recent model study(2) drawn to scale. With three original floor configurations, one solid and two movable, and with two stabilized scour patterns, the surface profile was unchanged for the same pool level at (a) and tailwater control level at (e). Other tests on the same model with a long horizontal movable floor at the elevation of the lip, and recent tests with a long solid horizontal floor at the same level as the bucket invert, produced the same surface profiles using the same h_1 and h_2, shown at (d), as before. Although the tests were limited to a specific q, h_1 and h_2, they offer some proof that the phenomenon is indeed concentrated at the surface. Nevertheless, the expanding surge scoured the movable floor.

In the aforementioned model tests, it was found that with a movable floor at the level of the bucket lip, some bed material was thrown into the bucket roller (making several circulatory trips before being expelled). However, when the movable floor was arranged at or near the level of the bucket invert (for a horizontal distance at least as far as the surge peak), there was negligible bed movement near the bucket. Until conclusive evidence to the contrary is obtained, it is recommended that the channel floor immediately downstream from a bucket be set at the elevation of the bucket invert, in general.

Assuming that the above results were reasonably typical, all tests in the current study were conducted with a horizontal floor at the same elevation as the bucket invert.

In a model study recently reported,(3) in which a movable bed was employed, it was found that the point of maximum scour moved slightly downstream with increasing discharge, but the location of the scour hole was unaffected by the elevation of the channel floor. More important, the water surface profile was unaffected by the elevation of the channel floor. The movable bed was set at the elevation of the lip, at the bucket invert, and below the bucket invert. However, the range of tailwater for these particular tests was apparently somewhat limited.

Basic Parameters

The surge height, h_s, is principally dependent upon h_2 and h_b. If h_2 is very large the surge will be "drowned," as will h_b. If h_2 is quite small, the surge will form a free trajectory (herein called a "free-jet") and the bucket roller will be swept out leaving only a live stream in the bucket—typical performance for a "flip bucket."

The flow momentum as it leaves the bucket (or enters the surge) includes a velocity which is a function of $(h_1 - h_b)$.

For the overall phenomenon in question, with effects of boundary friction and surface tension considered negligible,

$$h_b = \phi\,(q, h_1, h_2, R, g).$$

e of the several combinations of dimensionless parameters which satisfy above equation is,

$$\frac{h_b}{h_1} = \phi'\left(\frac{q}{\sqrt{g}\, h_1^{3/2}}, \frac{h_2}{h_1}, \frac{R}{h_1}\right).$$

like manner, h_s can be included, rather than h_b, with

$$h_s = \phi''(q, h_1, h_2, R, g),$$

which one of the several combinations of dimensionless parameters isfying this equation is

$$\frac{h_s}{h_1} = \phi'''\left(\frac{q}{\sqrt{g}\, h_1^{3/2}}, \frac{h_2}{h_1}, \frac{R}{h_1}\right).$$

will be shown later, specific service conditions are independent of the gnitude of R/h_1 (used later as h_1/R for convenience), and for these ditions

$$\frac{h_b}{h_1} = f\left(\frac{q}{\sqrt{g}\, h_1^{3/2}}, \frac{h_2}{h_1}\right)$$

$$\frac{h_s}{h_1} = f'\left(\frac{q}{\sqrt{g}\, h_1^{3/2}}, \frac{h_2}{h_1}\right).$$

parameter which includes the discharge can be equated to a Froude num- but in design computations it is more directly usable as it stands.

Characteristics of A (1 on 1) Entrance Slope (45° Exit)

ertinent results obtained with a (1 on 1) entrance slope are given in ure 3. As h_b is progressively reduced, the flow leaving the bucket even- ly springs free in the manner of a "flip bucket." The value of h_b/h_1 re this occurred was not affected by the magnitude of h_1/R, in any of the s performed throughout the study. This service condition is designated e-jet." An upper limit for a "free-jet" of $h_b = 0.2\, h_2$ was selected, as vn. This limit is not necessarily the exact point at which a "free-jet" rred, but for the data obtainable below this limit the jet was always free, above this limit a roller was always obtained. For the lowest points ed below the $h_b = 0.2\, h_2$ line, h_b equals the depth of the live stream in ucket. Below approximately $h_b = 0.2\, h_2$, a very small decrease in h_2 lted in an abrupt change to a "free-jet."

bove the "free-jet" range, with large values of h_1/R, a "pulsating surge" obtained for some or all runs of a constant $\frac{q}{\sqrt{g}\, h_1^{3/2}}$ series. A "pulsat- urge" is a pronounced vertical, unsteady motion of the surge, and pro- s an accentuated fluctuating condition where the surge strikes the floor.

Inasmuch as a "pulsating surge" would undoubtedly be much more aggressive from the standpoint of scour, operation under this condition would seldom be desirable.

The only obviously erratic data obtained were those for a "pulsating surge." Ignoring all data for which a "pulsating surge" was obtained, the remaining data (for h_b greater than 0.2 h_2), representing good roller action and a normal surge, were plotted in Figure 3. The trends indicated by these remaining data were well defined, and the scatter of points could in no way be attributed to either a variation in R or h_1/R. Referring to Table 1, note that most of the series represent a large range of all variables.

Any scatter of the data points can be attributed to three factors:

1. The parameter $\frac{q}{\sqrt{g}\ h_1^{3/2}}$ was not of exactly the same magnitude for all series (Table 1). (However, in Figure 3, points lying to the left of a curve are generally for a $\frac{q}{\sqrt{g}\ h_1^{3/2}}$ value less than that indicated for the curve and points lying to the right of the curve are for a greater parameter value).
2. h_b fluctuates somewhat making precise measurements of h_b difficult (particularly in low range of h_b/h_1).
3. Evaluation of d_1 was not perfect because of the supercritical flow in the upstream channel, and the velocity V_1 was obtained indirectly from a measurement of d_1.

In Table 1 it may be noted that in some instances a complete range of all variables was not accomplished. The lowest value investigated of $h_1/R = 2$ is not necessarily a minimum. Lesser values, however, are of little practical utility.

In the last column of Table 1 are shown the ranges of h_1/R for which good roller action can be obtained. The upper limits should be regarded as marginal, inasmuch as a "pulsating surge" was obtained for an occasional run in a test series for the higher h_1/R limits.

The ranges of h_1/R given in the last column of Table 1 are recommended for design. The curves appearing in Figure 3 are closely representative of the data for good roller action and are recommended for design. (Only about half of the data taken appears in Figure 3, the remainder being for test runs with a "pulsating surge").

Characteristics of A (1 on 2) Entrance Slope (45° Exit)

In Figure 6 are plotted all data points for which good roller action was obtained. The curves of Figure 3 for a (1 on 1) entrance are reproduced in Figure 6, and appear to be reasonable approximations of the (1 on 2) data. As with the (1 on 1) entrance, the scatter of points could in no way be correlated with either the variation in R or h_1/R and can probably be attributed to the same factors as given for the (1 on 1) entrance, above.

Ranges of test variables, given in Table 2, are adequate but not as broad as those investigated for the (1 on 1) entrance.

A "pulsating surge" did not occur in any of the tests with a (1 on 2) entrance. Instead, for higher values of h_1/R, a long, high surface jump was

rmed originating upstream from the P.C. of the bucket and extending well ownstream from the bucket lip. The bucket did not appear to contribute to e jump roller action, since the latter was merely a standing jump originat- g far up in a sloping channel. The maximum h_1/R given in the last column Table 2 is for good roller action, but with a sloping channel type of jump pending. The sloping channel jump data are not shown in Figure 6; if the ints were plotted, they would lie to the left of the curves.

Note that the upper limits for h_1/R cited in the right column of Table 2 are r good roller action. Higher values of h_1/R will not produce either the ad- rse operation of a "pulsating surge," or bucket roller action, but merely a oping channel type of jump described in the preceding paragraph.

The "free-jet" upper limit of $h_b = 0.2\ h_2$ is the same as for a (1 on 1) en- ance slope.

Effect of Entrance Slope

Tests were performed on a model of the spillway shown in Figure 2, having (10 on 7) approach and a 45° exit.(2) With $\frac{q}{\sqrt{g}\ h_1^{3/2}} = 0.055$ (design head d q), and $h_1/R = 3.4$, a good fit with the curves of Figure 3 was obtained. ually consistent were the data from the original model tests. For these ta h_1 was taken as the difference between headwater pool waterlevel and e bucket invert, inasmuch as the original model tests had proven that the ss of head due to friction over the spillway was relatively small.

Special tests were performed on a modified model of a chute spillway(4) ving a chute slope of 0.104, terminating in a free-trajectory vertical curve iich becomes tangent to the bucket at an angle of 33° with the horizontal. aterally flared side walls in the vicinity of the vertical curve of the model re replaced by parallel walls for the special tests). These tests were for following parameter values:

$\frac{q}{\sqrt{g}\ h_1^{3/2}}$	$\frac{h_1}{R}$
0.038	4.2
0.058	4.9
0.070	5.5

ller action was fairly good up to an h_b/h_1 of about 0.4, above which a jump s formed upstream from the bucket, originating in the trajectory curve or he chute and extending downstream from the bucket lip. The data (for $h_2 \gtrsim 0.4$) was reasonably consistent with the curves of Figure 3 despite complex approach conditions. Since the head loss in the chute was ap- ciable, h_1 was measured just upstream of the vertical trajectory curve.

Broadly interpreting the somewhat limited investigation of entrance slopes cribed, the curves of Figure 3 should provide a reasonable anticipation of formance for approach slopes from (1 on 2) to (10 on 7), provided that R is not too large.

With an approach slope of (1 on 1), the bucket roller becomes "crowded" at

h_1/R values higher than those recommended and the surge becomes unsteady and pulsates. With small slopes, such as (1 on 2), the relatively longer bucket roller is drowned at higher h_1/R values and the bucket roller and surge merge into a single jump apparently indifferent to the presence of the bucket. In both cases the bucket is too small, relative to the depth of the entering live stream, to govern or control the action of the surge.

Energy Dissipation Characteristics

For a non-submerged hydraulic jump in a horizontal channel, a convenient appraisal of entrance conditions is obtained using a Froude number, such as

$\underline{F_1} = \frac{V_1}{\sqrt{g\ D_1}}$, where V_1 and D_1 are the velocity and depth at the entrance to the jump, with $h_1 = D_1 + V_1^2/2g$. Since h_1 is measured from the same datum for both the bucket dissipator (bucket invert) and a hydraulic jump in a horizontal channel, it may be shown that

$$\frac{q}{\sqrt{g}\ h_1^{3/2}} = \frac{\underline{F_1}}{(1+\underline{F_1}^2/2)^{3/2}} = \frac{\underline{F_1}}{(h_1/D_1)^{3/2}} \qquad (1)$$

from which it may be seen that a given value of $\frac{q}{\sqrt{g}\ h_1^{3/2}}$ is equivalent to a specific value of $\underline{F_1}$. Equivalent values of $\underline{F_1}$ for this study are tabulated in Figure 5.

For a standing hydraulic jump in a rectangular, horizontal channel

$$\frac{D_2}{D_1} = \frac{1}{2}\left[\sqrt{1 + 8\underline{F_1}^2} - 1\right] = \frac{h_2}{D_1} \qquad (2$$

Equation (2) is graphed in Figure 5. The test points plotted in Figure 5 were obtained by taking values of h_2/h_1 from Figure 3 at the intersections of the curve for a given equivalent Froude number with the lines for $h_b = 0.2\ h_2$, $0.4\ h_2$, $0.6\ h_2$ and $0.8\ h_2$, and by combining these curve values of h_2/h_1 with values of h_1/D_1 calculated from Equation (1) for the same $\underline{F_1}$: $h_2/h_1 \cdot h_1/D_1 = h_2/D_1$.

For $h_b = 0.2\ h_2$ (the approximate borderline for "free-jet" conditions), the bucket dissipator is in close competition with a jump on a horizontal apron. For $h_b = 0.4\ h_2$ and $\underline{F_1}$ as high as about 16, the bucket dissipator has tailwater requirements which are fairly close to those for a jump on a horizontal floor. Referring again to Figure 3, note that the tailwater requirements for the given upper limit for a "free-jet" ($h_b = 0.2\ h_2$) are not much less than for $h_b = 0.4\ h_2$. Therefore, when a "free-jet" condition must be avoided (for example proximity of electrical equipment), it is recommended that $h_b = 0.4\ h_2$ be used as a limit in design, assuring roller action and efficient energy dissipation.

Inasmuch as the data for a (1 on 2) entrance slope closely approximated the curves of Figure 3, for a (1 on 1) entrance, and since the data from the special test with a (10 on 7) entrance were also in agreement, the h_2/D_1 curves of

re 5 should be nominally representative of this wide range of entrance
es. This is correct, of course, only for true roller action, without either
ulsating surge" or a submerged jump (i.e., provided h_1/R is not beyond
recommended maximums).

Surge Heights

pproximate surge-height characteristics are given in Figure 4 for a (1 on
ntrance slope and in Figure 7 for a (1 on 2) entrance slope. This informa-
should be helpful in setting top elevations of spray or training walls. An
mpt was made to measure an average of typical h_s for all runs, but this
difficult because of the spray and unsteadiness inherent in the surge. The
es are for the same runs as those plotted in Figures 3 and 6, and are an
age fit to the data. Hence they must be regarded as approximate and not
ssarily conservative.
ote that the curves of Figures 4 and 7 differ. Corresponding values of
$_1$ for the (1 on 2) approach slope are less than those for the (1 on 1) slope.
the (10 on 7) slope they were greater than for the (1 on 1) slope).
he only variable which is definitely influenced by the entrance slope is
eak height of the surge, h_s. Comparing Figures 3 and 6, no obvious in-
ce on h_b or h_2 is apparent, and therefore the tailwater requirements for
gy dissipation are virtually identical. Apparently the surge trajectory is
ened as the approach slope is lowered, and vice versa, without materially
ting any of the other variables. The upper limit of a "free-jet" is desig-
d in Figures 4 and 7 as approximately $h_b = 0.15\ h_s$.
he horizontal distance downstream from the bucket lip to the peak of the
e was measured for all runs, but analysis of the data is inconclusive at
ime.
nis study did not include the determination of the distance downstream
the bucket necessary for expansion of the surge. It is no doubt obvious
he surge travels a much greater distance as a "free-jet" than with
et roller action. Maximum scour occurs in the vicinity of the terminus
e surge trajectory, and the channel can be raised beyond this area without
ding the surge (see Figure 2). Appraisal of the horizontal distance to the
hole is needed to complete the study.

Illustration of the Use of Study Data for Design

Table 3 are presented a hypothetical spillway profile and a tailwater
g curve. The accompanying calculations are preliminary since h_1 is the
head without any correction for the spillway head loss. For the first
the tailwater is found to be too low to provide roller action, with a "free-
ndicated for all rates of flow:

	Values of h_2/h_1	
3/2	Available from "(1) First Trial", via "(a) Tailwater Curve", of Table 3:	From Figure 3, approximate minimum to avoid a "free-jet":
48	0.267	0.34
42	0.263	0.32
36	0.259	0.30
25	0.237	0.25
10	0.166	0.17

(Also shown is the fact that the tailwater would likewise be insufficient to hold a jump on a horizontal apron. In either case, an end sill could be employed to raise h_2).

In the second trial, in which the bucket invert is lowered 7-feet, roller a tion is assured at all rates of flow. The lowest value of h_b/h_2 happens to be 0.4, the recommended safe minimum for good roller action. The calculated points are plotted in (c), a reproduction of part of Figure 3.

The approach slope happens to be (10 on 7), and for $\frac{q}{\sqrt{g}\ h_1^{3/2}} = 0.04$ a value of $h_1/R = 5$ is selected since in Table 1, for the lesser approach slope of (1 on 1), a value of 6 would provide only marginally satisfactory perform ance. The approximate appraisal of h_s was obtained using Figure 4.

Various design combinations of q, h_1 and h_2 will yield unique trends whe plotted on Figure 3; the given sample is but one such combination. A sampl computation for a high head has not been included because effects resulting from air-entrainment would be unknown factors.

RECOMMENDATIONS AND CONCLUSIONS

Results of a study limited to a 45° exit angle and a uniform distribution discharge over the channel width have been presented.

Recommendations for design:

a) A thickness of bucket lip less than R/10 was used in this study. For most applications this thickness is adequate to accommodate reinforcing.

b) It is recommended (on the basis of limited information) that the downstream channel be excavated to the elevation of the bucket invert, at least in the region adjacent to the bucket lip.

c) The curves of Figure 3 (reproduced in Figure 6) should be usable for approach slopes from (1 on 2) to (10 on 7). The curves are representative of good roller action up to specified maximum values of h_1/R. "Free-jet" performance can be expected whenever h_b is less than 0.2 h_2, in general. The maximum values of h_1/R recommended in Table indicate probable commencement of a "pulsating surge," whereas in Table 2 the maximums delineate the termination of bucket roller acti and commencement of a sloping channel type jump apparently uninfluenced by the presence of the bucket. The magnitude of these upper limits of h_1/R were almost identical, but there is no way to tell wheth a "pulsating surge" would or would not occur at these same limits fo an intermediate approach slope.

d) The absence of any influence on good roller action due to the size of t bucket radius has been demonstrated. An examination of Figures 3 a 5 will show that a wide range of service conditions has been studied. The wide coverage of test variables listed in Tables 1 and 2 sustain t direct value of the results in design.

e) Within the restrictions of a 45° exit angle and a uniformly distributed discharge only one major item remains to be investigated: the horizo tal distance from the lip of the bucket to the scour hole (or the

termination of the surge expansion). This item is of importance only in guaranteeing an adequately large basin. The horizontal natural channel requirement in Figure 2 (which is to scale) is only about 2.4 h_2; a horizontal apron in place of the bucket in this instance would be much longer.(5)

The required natural channel length could best be investigated using a vable bed model. With the presentation of this study, if sufficient interest xhibited by the profession in this particular item, the sponsors of the cur- t study are agreeable to a future cooperative extension of the program.

ACKNOWLEDGMENTS

This study was conducted by the hydraulic division of Fritz Engineering oratory, Lehigh University. Professor W. J. Eney is Director of the oratory and Head of the Department of Civil Engineering. The initial se of this study (to run #125) was sponsored by the Department, and was for graduate credit by the junior author.

The more recent and major phase of this study (runs #126-457 and ials) was sponsored by Gannett, Fleming, Corddry and Carpenter, Inc., neers, of 600 N. Second St., Harrisburg, Penna.,* as a contribution to the ession, primarily to the designer.

The authors sincerely hope that more basic studies will be made in the re, providing design information to the profession through the cooperative rts of consulting firms and universities. Without the unselfish participa- of the sponsor only a fraction of this study would have been completed. he technical advice and encouragement given by the sponsoring firm ugh Mr. W. H. Corddry, Mr. J. A. Romano and their hydraulic staff, are efully acknowledged.

REFERENCES

Hydraulic Design, Spillways"—Engineering Manual, Civil Works Construc- on (Preliminary), Part CXVI—Chapter 3, p. 41, Department of the Army, ffice of the Chief of Engineers, March, 1953.

Movable Bed Model Study of Greensboro, N. C. Dam—Reedy Fork Creek roject," for William C. Olsen and Associates, (design by Justin and ourtney), by M. B. McPherson and H. S. Strausser, April, 1955.

Hydraulic Model Tests on Flood Spillway of Sakuma Dam," by Atsuya kada and Takeshi Ishibashi, Central Research Institute, Electric Power dustry, Japan, June 1, 1956.

to 100 Scale Model Study (and design) of Chute Spillway, Penn Forest m," for the Bethlehem Authority, by M. B. McPherson and H. S. rausser, August 15, 1955.

Progress Report II, Research Study on Stilling Basins, Energy Dissipa- rs, and Associated Appurtenances," Hydraulic Lab. Report No. Hyd.— 9, U. S. Bureau of Reclamation, Denver, June 1, 1955.

oductions of original data may be obtained by writing to the sponsors, ntion of Mr. Romano.

TABLE 1

RANGES OF VARIABLES INVESTIGATED - (1 ON 1) ENTRANCE AND 45° EXIT

Range of $\frac{q}{\sqrt{g}\ h_1^{3/2}}$	Range of h_1, feet	Range of q, cfs./ft.	Range of h_2, feet	Radii, R used, feet	Test Range of h_1/R	Range of for Good Roller Ac
0.089 -0.091	2.7 - 2.8	2.3	1.1 - 2.2	0.30 0.35 0.60 1.20	2.3 - 9.1	2 - 5
0.058 -0.061	2.5 - 4.1	1.3 - 3.0	0.9 - 2.3	0.30 0.35 0.60 1.20	2.1 - 8.3	2 - 6
0.039 -0.043	2.4 - 3.5	0.8 - 1.5	0.7 - 2.1	0.30 0.35 0.60 1.20	2.0 - 11.2	2 - 6
0.025 -0.029	2.3 - 7.2	0.5 - 2.9	0.6 - 3.8	0.30 0.35 0.60 1.20	1.9 - 11.4	3 - 6
0.012 -0.013	3.4 - 6.2	0.5 - 1.1	0.6 - 2.2	0.30 0.60 1.20	2.9 - 11.6	3 - 8
0.010 -0.011	4.1 - 7.7	0.5 - 1.3	0.6 - 3.7	0.60 1.20	6.4 - 7.2	? - 6 - 7
0.005	7.2	0.5	0.7 - 3.0	1.20	6.0	? - 6 - 1

TABLE 2

RANGES OF VARIABLES INVESTIGATED - (1 ON 2) ENTRANCE AND 45° EXIT

nge of $\frac{q}{h_1\ 3/2}$	Range of h_1, feet	Range of q, cfs./ft.	Range of h_2, feet	Radii, R used, feet	Test Range of h_1/R	Range of h_1/R for Good Roller Action
).085).092	2.8 - 2.9	2.3 - 2.4	1.1 - 2.0	0.3 0.4 0.6 1.2	2.3 - 9.7	2 - 5
).059).060	2.6 - 2.7	1.4 - 1.5	0.9 - 2.0	0.3 0.4 0.6 1.2	2.2 - 8.9	2 - 6
).040 .042	2.4 - 2.5	0.9	0.8 - 2.0	0.3 0.4 0.6 1.2	2.0 - 8.4	2 - 6
..025 .027	2.4	0.5	0.6 - 2.0	0.3 0.4 0.6 1.2	2.0 - 8.0	3 - 6
..013	2.3	0.3	0.4 - 1.9	1.2	1.9	? - 2

TABLE 3

SAMPLE COMPUTATIONS—PRELIMINARY DESIGN

(a) Tailwater Curve

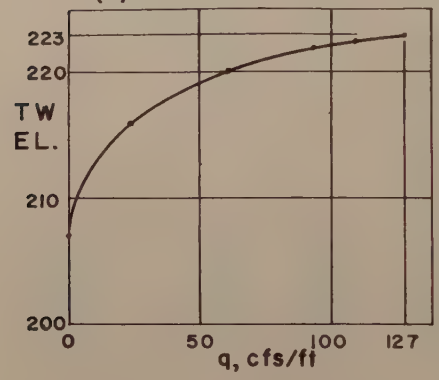

(b) Spillway Profile

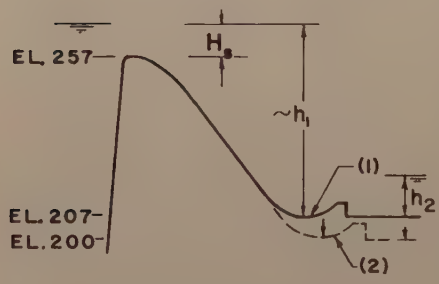

(c) From Figure 3

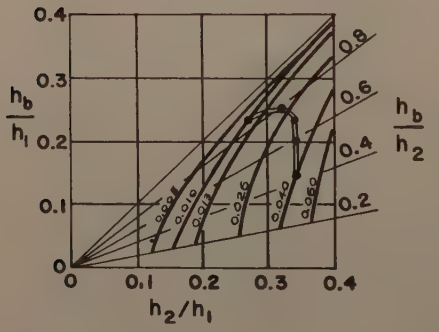

(1) FIRST TRIAL:

H_s ft	$\sim h_1$ ft	q	$\frac{q}{\sqrt{g}\ h_1^{3/2}}$	h_2 ft	h_2/h_1
10	60	127	0.048	16.0	0.267
9	59	108	0.042	15.5	0.263
8	58	91	0.036	15.0	0.259
6	56	59	0.025	13.3	0.237
3	53	21	0.010	8.8	0.166

Referring to Fig. 3, the above values of h_2/h_1 are all to the left of the $\frac{q}{\sqrt{g}\ h_1^{3/2}}$ curves. Therefore, free-jet action for all rates of flow. (At maximum q, TW is insufficient to obtain a hydraulic jump in a horz. channel; $F_1 = 7.5$, $h_1/D_1 = 29.1$, $h_2/D_1 = 7.8$ but $h_2/D_1 = 10$ is needed - Fig. 5)

(2) SECOND TRIAL:
(Try lowering bucket 7')

H_s ft	$\sim h_1$ ft	q	$\frac{q}{\sqrt{g}\ h_1^{3/2}}$	h_2 ft	h_2/h_1
10	67	127	0.041	23.0	0.343
9	66	108	0.036	22.5	0.341
8	65	91	0.031	22.0	0.339
6	63	59	0.021	20.3	0.323
3	60	21	0.008	15.8	0.263

The results are plotted in (c). Maximum q near $h_b = 0.4h_2$ and equivalent $F_1 = 8.2$. Referring to Fig. 5, h_2/D_1 for bucket same as for hydraulic jump with horiz. floor.

With $h_1/R = 5$, $R = 13.4'$

From Fig. 4 maximum h_s/h_1 is approx. = 0.47. Therefore, $h_{s_{max}} \cong 31.5'$.

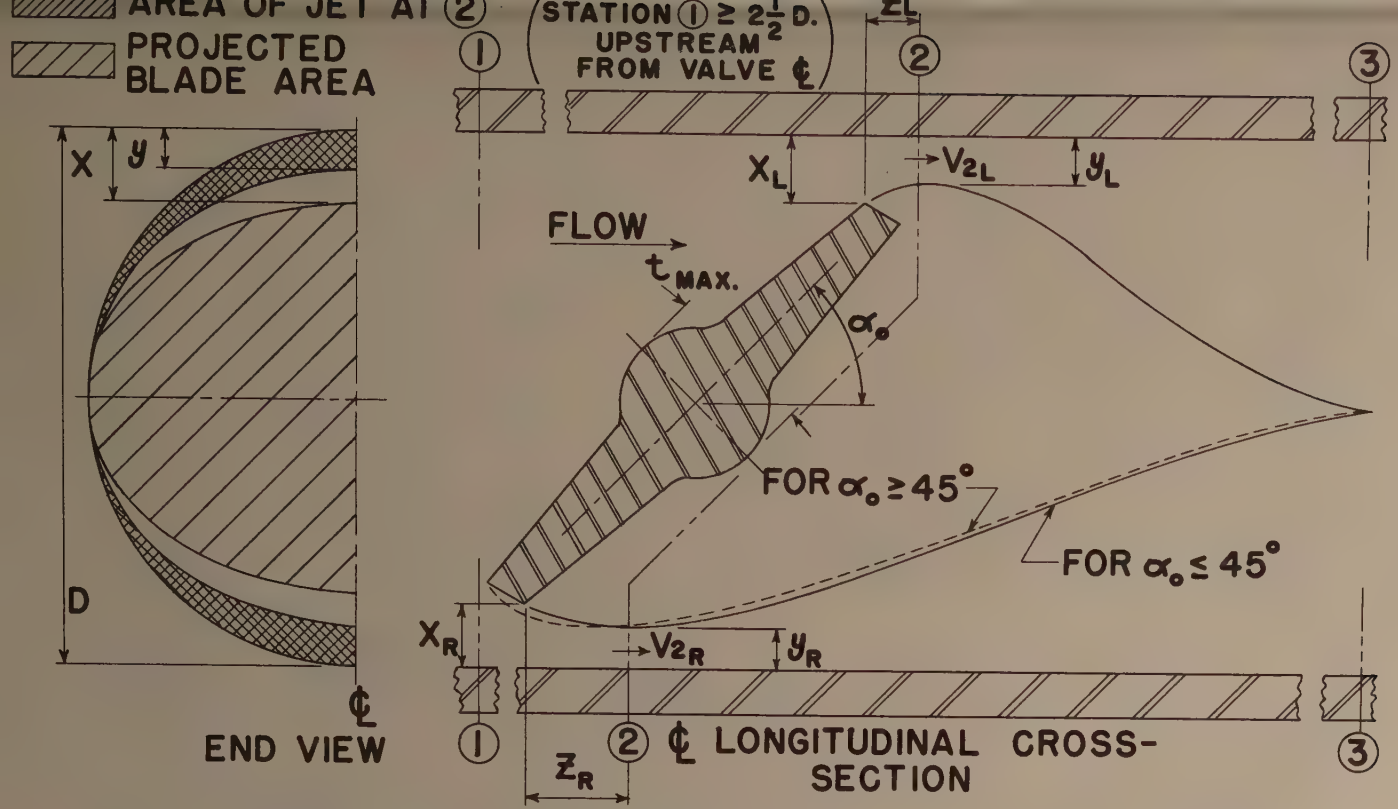

ANALYTICAL FLOW DIAGRAM

FIGURE 1

FIGURE 2

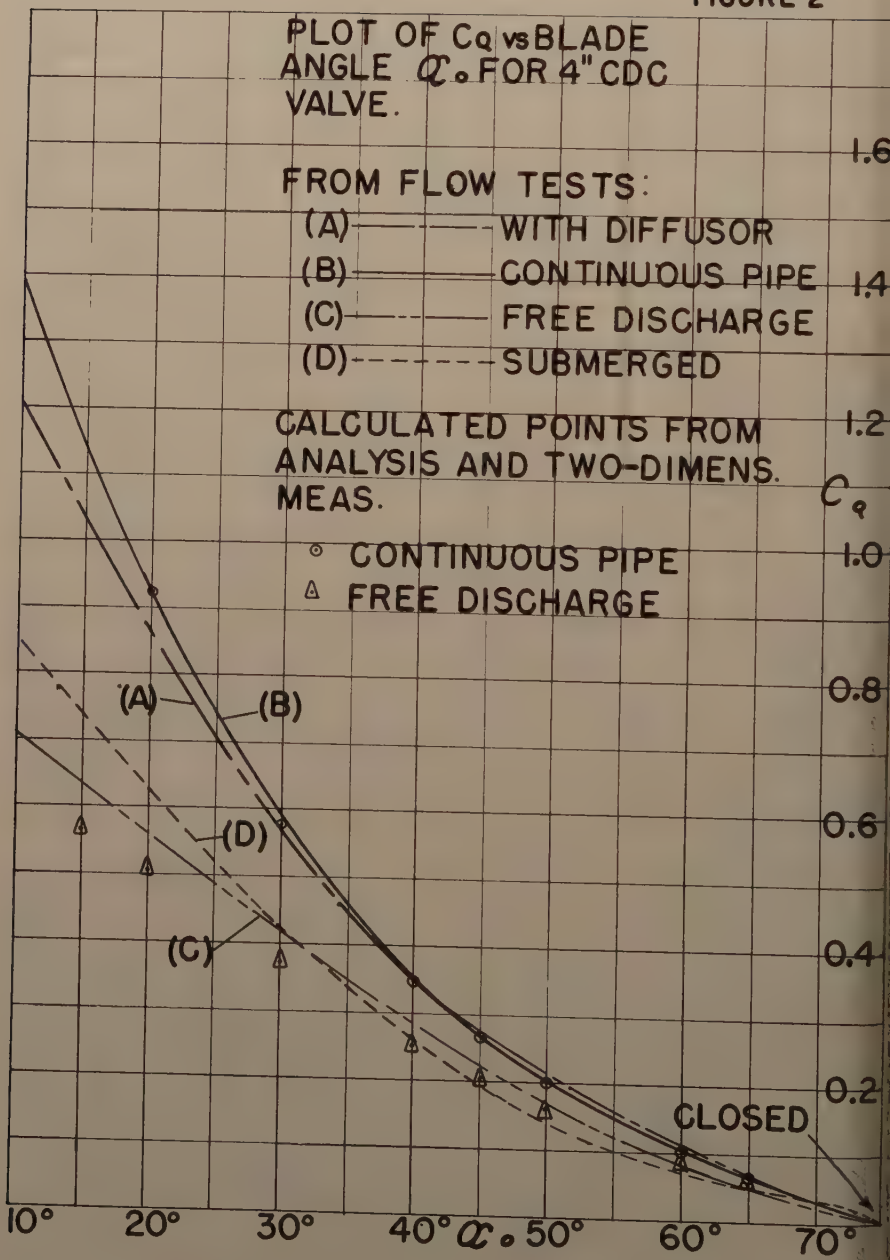
PLOT OF Cq vs BLADE ANGLE α° FOR 4" CDC VALVE.
FROM FLOW TESTS:
(A)——— WITH DIFFUSOR
(B)——— CONTINUOUS PIPE
(C)- - - - FREE DISCHARGE
(D)- - - - - - - SUBMERGED
CALCULATED POINTS FROM ANALYSIS AND TWO-DIMENS. MEAS.
⊙ CONTINUOUS PIPE
△ FREE DISCHARGE
(A)
(B)
(C)
(D)
CLOSED
1.6
1.4
1.2
1.0
0.8
0.6
0.4
0.2
Cq
10°
20°
30°
40°
α°
50°
60°
70°

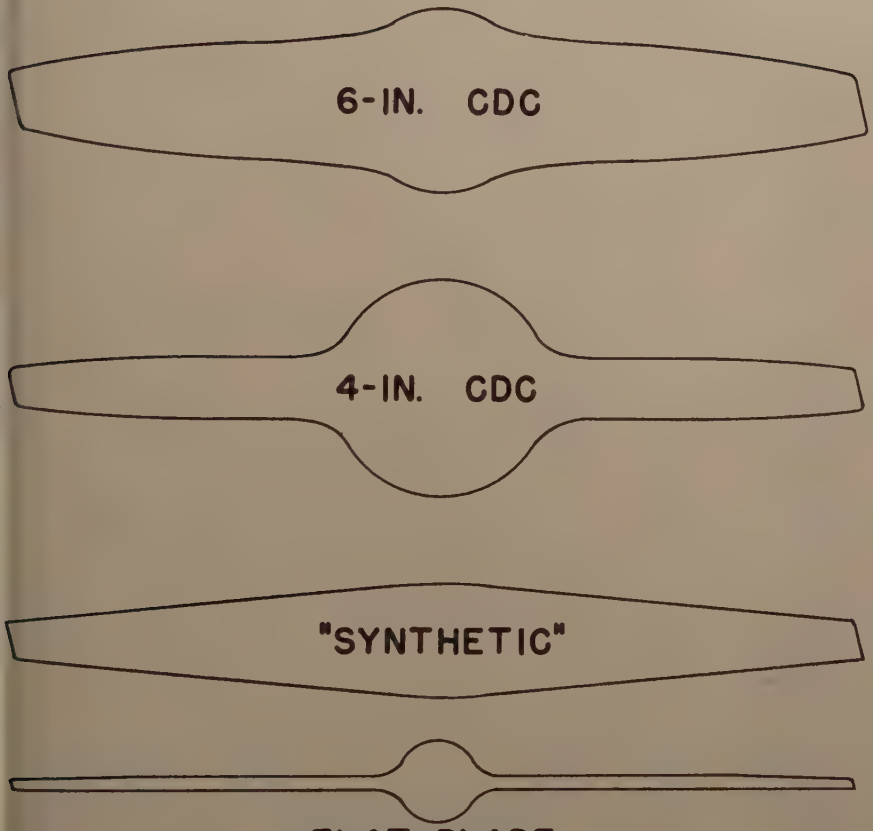

BLADE PROFILES
TWO-DIMENSIONAL STUDY
(REPRESENT PROFILES AT ℄ OF PROTOTYPE)

FIGURE 4

FIGURE 5
LIMITING MINIMUM N_R FOR FREE DISCHARGE FOR C_Q = A CONSTANT - CDC 6" VALVE. (DATA BY J.G. MOSTERT)
CHECKS WITH $N_{R\,MIN.}$ FOR Q_L/Q_R = A CONST.
(TABLE I)
$N_R \times 10^{-5}$
$\left(N_R = \frac{V}{\nu} D\right)$
θ_o
5.0
4.0
3.0
2.0
1.0
0°
10°
20°
30°
40°
50°
60°

FIGURE 6

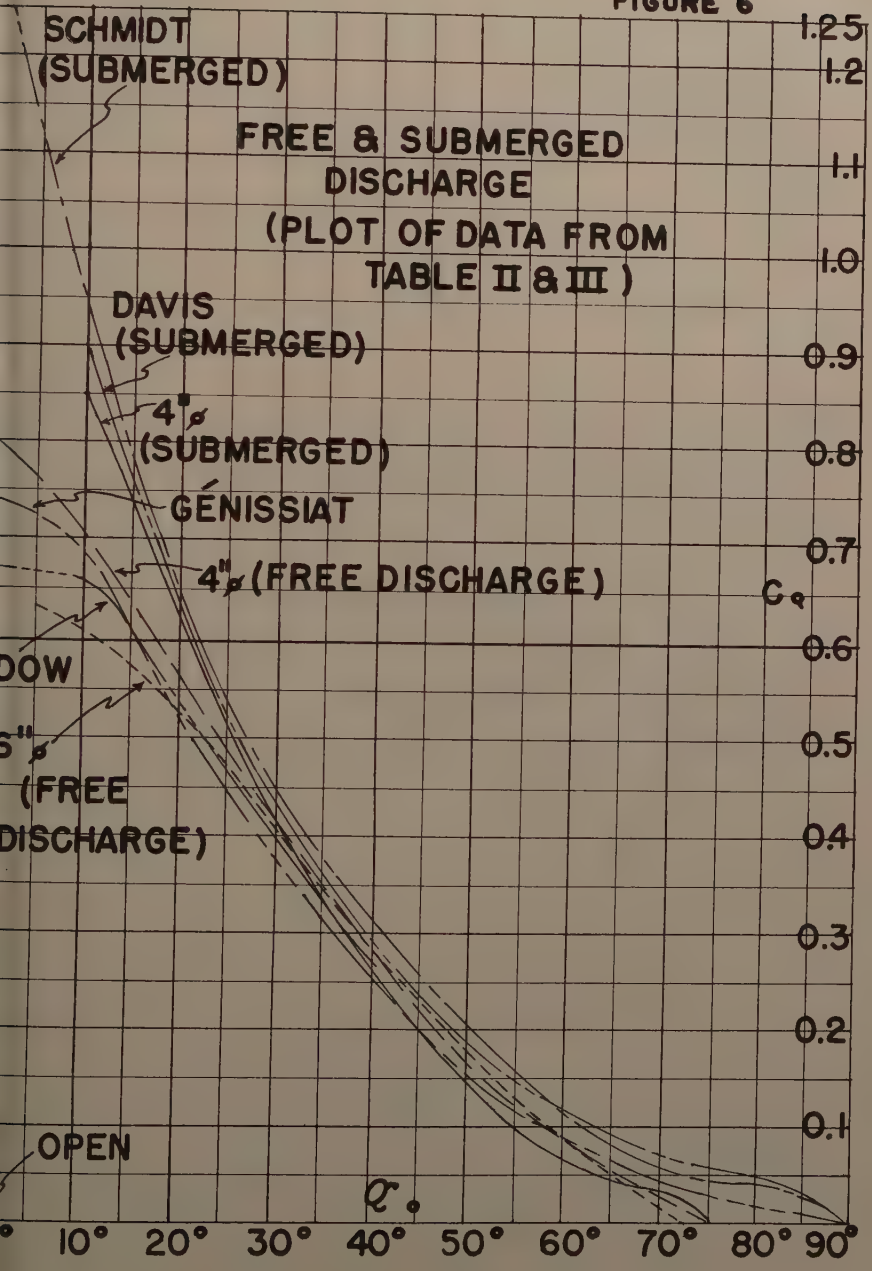
SCHMIDT
(SUBMERGED)
FREE & SUBMERGED
DISCHARGE
(PLOT OF DATA FROM
TABLE II & III)
DAVIS
(SUBMERGED)
4"ø
(SUBMERGED)
GÉNISSIAT
4"ø (FREE DISCHARGE)
DOW
6"ø
(FREE
DISCHARGE)
OPEN
1.25
1.2
1.1
1.0
0.9
0.8
0.7
0.6
0.5
0.4
0.3
0.2
0.1
Cq
θ
10° 20° 30° 40° 50° 60° 70° 80° 90°

FIGURE 7

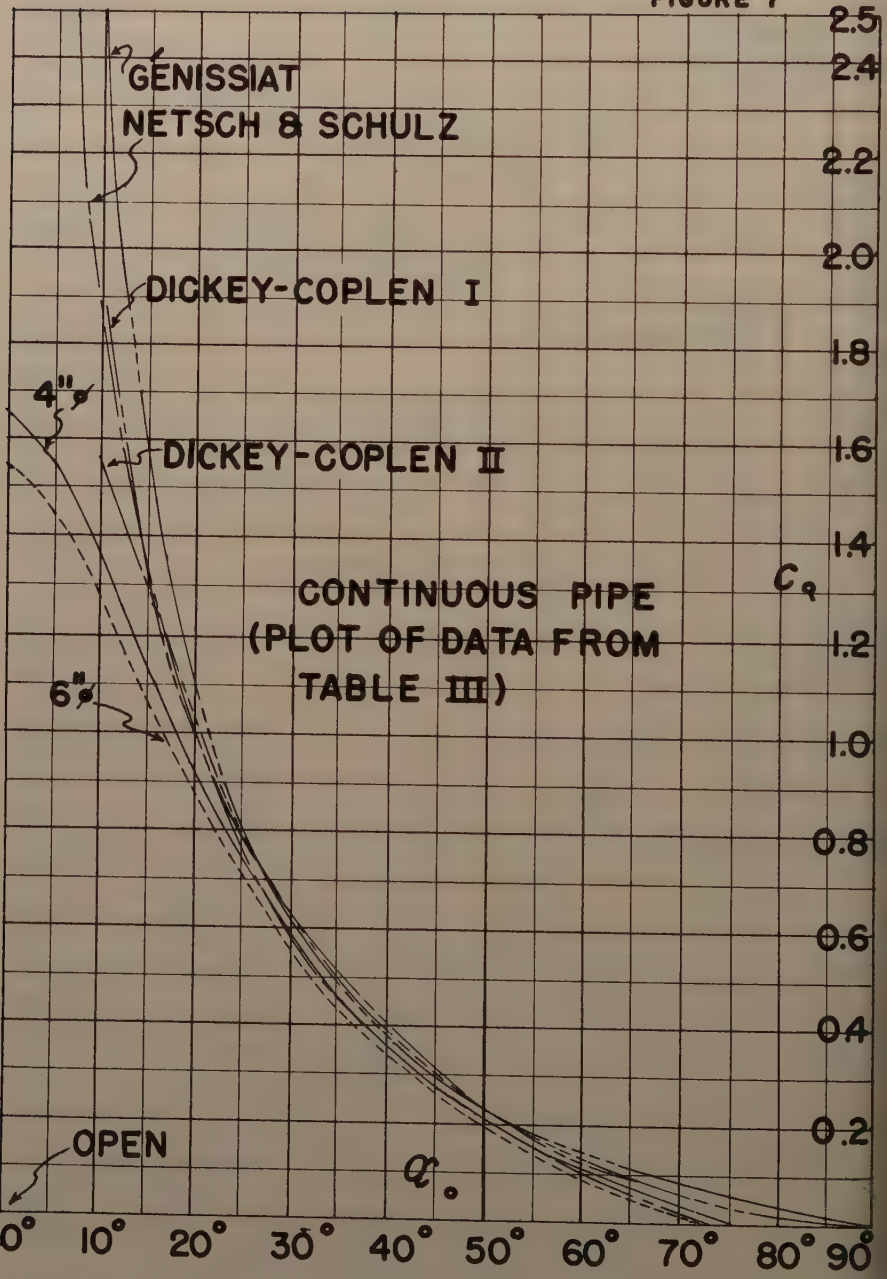
GENISSIAT
NETSCH & SCHULZ
DICKEY-COPLEN I
4"ø
DICKEY-COPLEN II
CONTINUOUS PIPE
(PLOT OF DATA FROM
TABLE III)
6"ø
OPEN
C_q
α°
2.5
2.4
2.2
2.0
1.8
1.6
1.4
1.2
1.0
0.8
0.6
0.4
0.2
0° 10° 20° 30° 40° 50° 60° 70° 80° 90°

Journal of the
HYDRAULICS DIVISION
Proceedings of the American Society of Civil Engineers

MEASUREMENT OF SEDIMENTATION IN TVA RESERVOIRS[a]

E. H. McCain,[1] A.M. ASCE
(Proc. Paper 1277)

INTRODUCTION

Investigations of reservoir sedimentation are of significant importance erever storage reservoirs are an integral part of water conservation and llization projects. The broad objective of any reservoir sediment investi- tion is to provide information upon which to base estimates of the number years that will be required, first, for sufficient sedimentation to occur to erfere with operations, second, for sedimentation to fill the reservoir to elevation where its useful life will be ended and, third, to determine cur- ntly the actual volume of the reservoir for water control operations.

The TVA is presently investigating sedimentation in 30 reservoirs in the lley, comprising a total of 1150 active sediment ranges. The magnitude of se investigations is so great as to warrant special consideration of the ipment used in making the investigations. TVA has developed or assem- d commercial equipment which has materially increased the accuracy of hydrographic investigations as well as the efficiency of the fieldwork, reby, substantially reducing the cost of the investigations.

Equipment

The equipment used consists essentially of the following:

1. Truck and trailer
2. Boat and motors
3. Two-way radios
4. Distance measuring equipment
5. Echo sounding equipment

The equipment is designed to provide complete mobility and permit the re outfit to move readily from a reservoir in one part of an area to that

e: Discussion open until November 1, 1957. Paper 1277 is part of the copyrighted Journal of the Hydraulics Division of the American Society of Civil Engineers, Vol. 83, No. HY 3, June, 1957.
Presented at Knoxville Convention, American Society of Civil Engineers, Knoxville, Tenn., June 8, 1956.
Sedimentation Specialist, Hydr. Data Branch, Tennessee Valley Authority, Knoxville, Tenn.

in another, perhaps several hundred miles distant, in a day's time. Figure 1 shows the truck, trailer, and boat ready for movement. The truck is a 3/4-ton power wagon equipped with four-wheel drive. The four-wheel drive is an important feature in launching the boat into a reservoir and removing it since many reservoirs do not have improved ramps. The truck is also equipped with power brakes for safety and a power winch on the front of the truck that is used to assist with removing the boat from difficult places. The trailer is designed especially for moving boats. It has four wheels, two in tandem, which are mounted with knee-action devices. This permits the bed to be lowered and facilitates the launching and loading of the boat in relatively shallow water. All four wheels are equipped with electric brakes which are operated from the truck cab.

The boat is of wood construction, 20 feet long and approximately 5-1/2 feet wide. It is a flat-bottom boat with a scow bow which provides for stable operation. Its operational weight is approximately 2 tons and it draws about one foot of water. It is powered by 2 Scott-Atwater 33 horsepower outboard motors. The motors are equipped with electric starters and have a forward, neutral, and reverse gear. A unique feature of these motors is the Bail-A-Matic device which provides for automatic bailing of the boat when the motors are operating. When the motors are operating under full power, they will move the boat at a speed of from 12 to 14 miles per hour.

Good communication is very essential for the efficient operation of a sediment investigation party. To provide communication, the TVA party uses 4 two-way FM radio telephones operating on a frequency of 166.825 MC. the truck and the boat have permanently installed General Electric mobile combinations with a carrier power of approximately 8 watts. This provides a range between these two radio telephones of from 10 to 15 miles. A portable radio telephone is used by the instrument man on the bank and one is maintained as a standby. These radio telephones are the Hallicrafters "Littlefone" with an output power of one watt. They have a line-of-sight range of about 5 miles and are powered by self-contained rechargeable wet cell batteries. The total weight of the portable unit is 14 pounds.

Figure 2 is a view of the interior of the boat showing the equipment. The view is from the right stern of the boat looking toward the left bow. The long metal box in the right rear of the boat houses most of the power supply and controls. There are four 6-volt batteries connected to supply 12-volt power for operating the echo recorder, radio, and starting the motor generator. They also supply 6-volt power for starting the outboard motors. In the same box directly to the rear of the batteries is the battery charger. The battery charger operates off of 110-volt AC current from the motor generator and charges the battery with 12-volt DC current. To the rear of the battery charger, are the controls with a control panel at the rear end of the box. The controls are for the radio including a speaker, microphone outlet, and an outlet for a headset, starter controls for the outboard motors, and controls for the battery charger. Directly opposite the battery box on the left side of the boat is the motor generator. The motor generator supplies 750 watts of 110-volt AC power which is used for charging the batteries and operating the 1/2 horsepower 110-volt AC electric motor on the distance measuring device. Between the motor generator and the battery box is the transducer well. The well houses the echo sounding recorder transducer which transmits the sound pressure wave and receives the returning echo. Forward of the transducer well and underneath the operating platform is the fuel supply. The fuel supply

for the outboard motors consists of six 6-gallon cans of gasoline which is sufficient for one-day operation. The gasoline cans are connected by short rubber hoses to copper tubes which run along each side of the boat back to the motors. The fuel supply for the motor generator is a two-gallon can connected directly by copper tubing to the motor generator.

Figure 3 shows the distance measuring device with the motor generator. The measuring device consists of a steel frame on which is mounted a standard automobile wheel, rewind motor, tensiometer, fixed circumference measuring wheel, and the necessary controls. The automobile wheel is used as a drum for 6000 feet of .039-inch diameter music wire. The 1/2 horsepower 110-volt AC rewind motor is mounted on a movable frame and is belt-connected through a jack shaft with the drum. By lifting the motor frame by a lever fastened to the top of the main frame, the drive belt will loosen, thereby giving a clutch between the motor and the drum. The tensiometer consists of a sheave mounted in a sliding bracket with a short rod fastened on one end of the bracket which actuates the plunger in a small pressure cylinder taken from an automobile brake. The pressure in the cylinder is transmitted with fluid through a tube to a pressure gage.

Figure 4 shows the fixed 2-foot circumference measuring wheel which is geared to a Veeder counter which indicates the distance. The opposite end of the Beeder counter shaft is geared to a cam which actuates a microswitch which automatically causes a fix mark on the echo sounder chart at 50-foot intervals of distance along the range. There are two controls for the brake in the automobile wheel drum. The lever near the counter operates the mechanical brake and the wheel near the end of the frame operates the hydraulic brake. In operation the wire on the drum is paid out through the sheave on the tensionmeter and over and around the fixed circumference measuring wheel to the bank. The tension on the music wire, while the boat is moving along the range, is controlled by the brake on the automobile wheel and the distance is recorded automatically on the echo sounder chart or can be read directly on the Veeder counter. The operator has a table fastened to the counter from which he determines the proper tension to maintain on the wire at various distances by observing the pressure gage which is mounted near the counter. When sounding of the range is completed the wire is released from the bank and rewound on the drum at the rate of approximately 600 feet per minute. A foot-operated guide is provided to distribute the wire on the drum as it is being rewound.

The distance device was rated in the field between known distances at 1000-foot intervals up to 6000 feet. It was rated to read correct distance up to 2000 feet by balancing the error due to sag and the stretch due to tension. Because of excessive sag it was necessary to increase the tension for distances between 2000 and 6000 feet, therefore, distances in this range must be corrected from a curve. The accuracy of the equipment has consistently proven to be within one foot up to 2000 feet and within 2 feet from 2000 to 6000 feet. This is well within the limits of accuracy that we must consider.

The echo sounding equipment used is the Bludworth model ES-123 Depth Recorder which is designed especially to record relatively shallow depths of water automatically and with a high degree of accuracy. It is rugged, lightweight and compact, simple in operation, requiring a minimum of maintenance and will stand considerable exposure to the elements. Depths of water from 3 to 180 feet may be permanently recorded in three ranges (0 to 60, 60 to 120, and 120 to 180 feet) at the rate of 300 soundings per minute so that abrupt

changes in depths of water are readily observed with the usual boat speed of about 3 miles per hour. The equipment operates automatically when the power switch is turned on, the only attention required being selection of the depth range, an occasional simple check of the battery voltage, and a check of the motor speed. Total power required is 12 volts DC at 14 amperes, or 168 watts.

Figure 5 is a view of the recorder case showing the operating controls. The controls consist of a volt meter, motor speed indicator, power switch, fix button, range selector, and a gain control.

Figure 6 is an interior view of the echo recorder showing the electronic circuits and chart propulsion mechanism which generate the electrical impulses and receive the reflected pulse, accurately time the interval between the generation of the pulse and the reception of the reflected pulse, translate the interval into units of depth in feet and record the depth permanently on the recorder chart. While the paper moves normally at the rate of 1-1/2 inches per minute, the drive motor speed may be adjusted ±5 percent from normal, to compensate for differences in the temperature and salinity of the water. An adjustable draft lever, which may be locked into position, is provided to compensate for elevation changes in the water surface and also that recordings of depths below the surface or below the bottom of the boat may be made. The outboard transducer housed in the well in the center of the boat contains a transmitting and receiving magnetostriction type unit in a single cast aluminum housing. It is equipped with cords and plugs for connection to the recorder.

Field Investigations

Plate 1 shows the layout of sediment ranges in Douglas Reservoir. This layout is typical for the storage reservoirs in the Valley. The ranges should be located giving consideration to important local tributaries and the drainage area of these tributaries and their probable sediment characteristics. The width of the reservoir should be given consideration. In storage reservoirs subject to considerable drawdown, closer spacing of the ranges within the drawdown reach is desirable as the deposition and movement of sediment throughout this range is greater than in other parts of the reservoir. For example, in Douglas Reservoir which is subject to drawdown, ranges are spaced about two miles apart in the lower and extreme upper ends of the reservoir and 1 to 1-1/2 miles in between.

Prior to the filling of the reservoir the selected ranges are permanently marked at each end and a cross section taken along the range by conventional methods. On some of the main-stream reservoirs which are relatively shallow and have comparatively smooth bottoms, the ranges were marked and the original cross sections were taken by hydrographic methods soon after the reservoir was filled. Utilizing the hydrographic equipment available, this method was more economical in establishing the original cross section where the terrain was not so rugged as on the storage reservoirs. Subsequent investigations on all reservoirs are carried out by hydrographic methods utilizing the equipment described.

The field party required to carry out the sediment investigations consists of 4 men—the party chief who supervises the work and operates the distance measuring device, the echo sounding recorder operator, a transitman who

eeps the boat on a range line, and the motorboat operator. In sounding a ange a light aluminum boat powered by a 16-horsepower motor is used in onjunction with the sounding boat. This boat is for the use of the transitman nd saves numerous trips across the reservoir with the heavier boat. The ransitman goes ahead in the light boat to the range to be sounded and clears nd flags one of the markers. He then meets the sounding boat at the oppo- ite marker. The transitman sets the instrument up over the marker and ights to the marker across the reservoir. An iron pin is then set on the ange line near the water edge and a tape distance taken to it. A distance is aken to the water edge and the wire from the distance measuring device is astened to the iron pin. The echo sounding recorder is started and the boat roceeds along the range line at a speed of approximately 3 miles per hour. 'he transitman, located on the bank where the wire is fastened, keeps the oat on the range line by means of radio communication to the boat operator. 'uring normal weather conditions the boat stays within 2 feet of the range ine. When the boat reaches the opposite bank, the transitman is informed by adio and he releases his end of the wire. As the wire is being rewound on ne drum the transitman is proceeding to the next range where the process is epeated.

The time required to sound a reservoir, such as Douglas where the total ength of reservoir including tributaries is about 80 miles, the number of anges is 51 and the ranges vary in length from a few hundred feet to about 000 feet, is about one week for the field party. In Kentucky Reservoir on the ain stream, where the total number of ranges is less (only 38), the total ength of reservoir is about 230 miles with ranges varying in length up to 0,000, the time required to carry out the investigation is about 3 weeks.

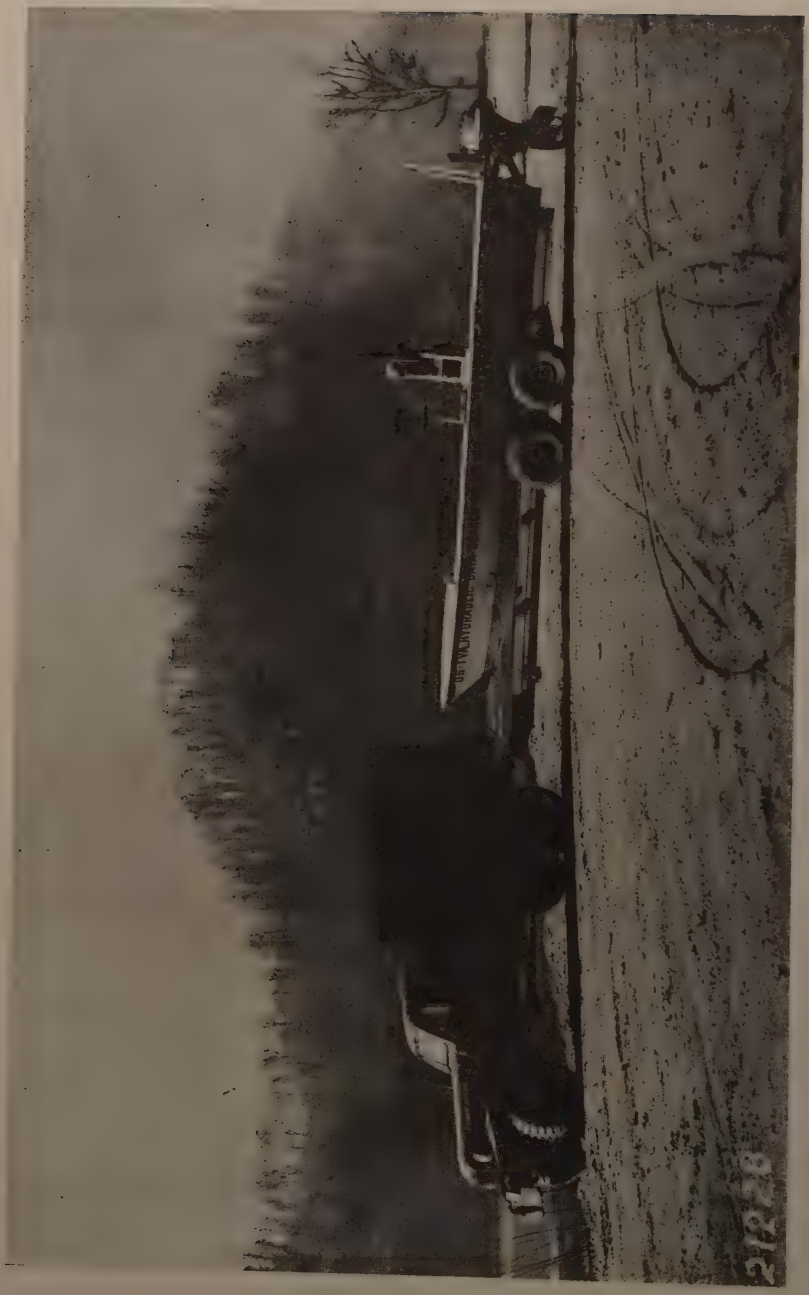

Figure 1.--TRUCK, TRAILER, BOAT, AND MOTORS

Figure 2.--INTERIOR OF BOAT SHOWING EQUIPMENT

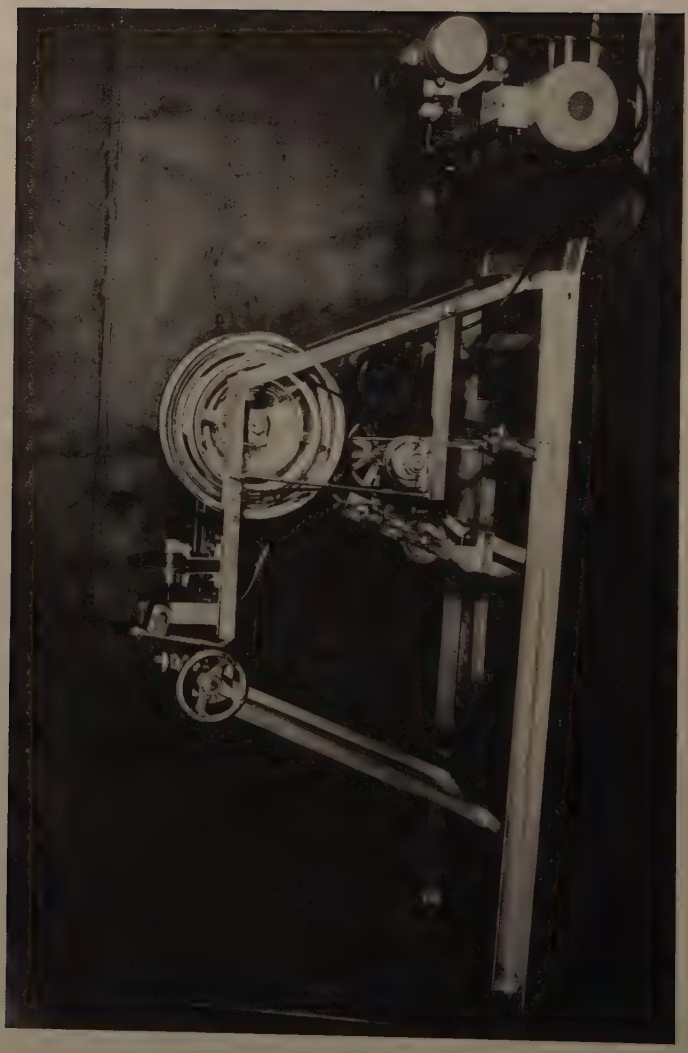

Figure 3.--DISTANCE MEASURING DEVICE WITH MOTOR GENERATOR

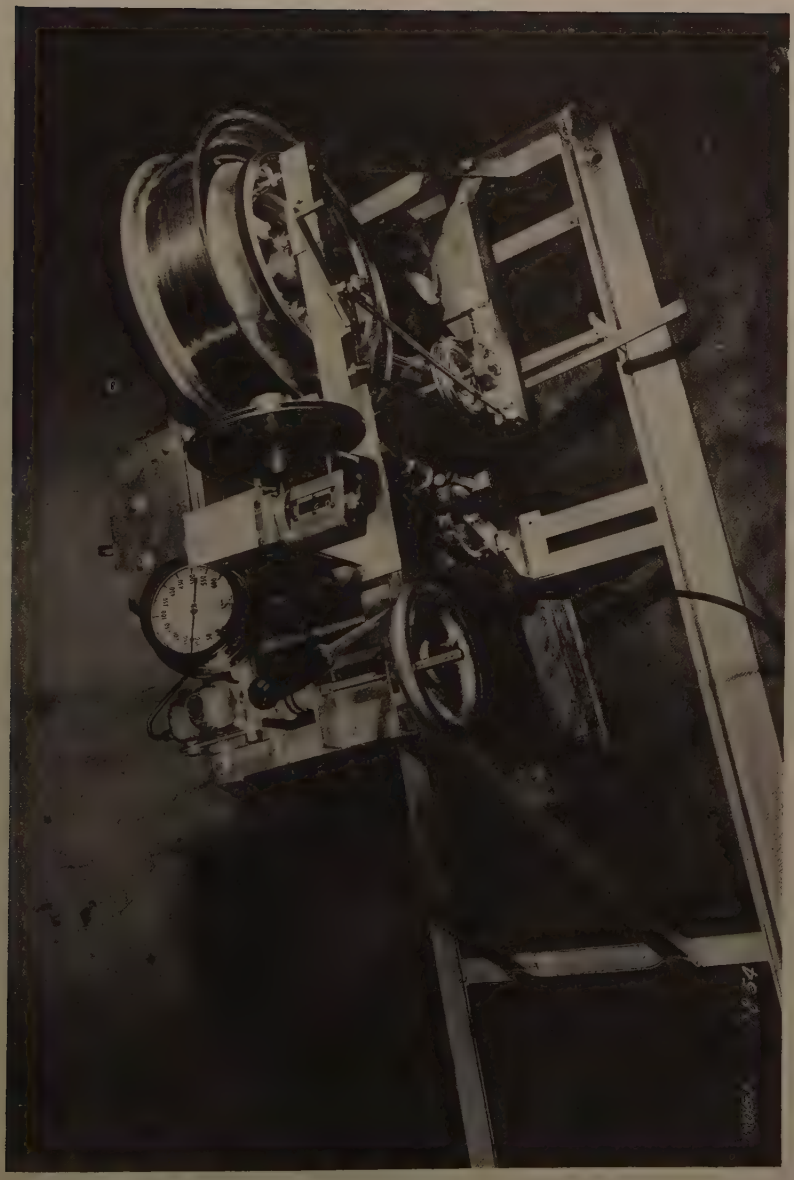

Figure 4.--DISTANCE MEASURING DEVICE SHOWING OPERATING CONTROLS

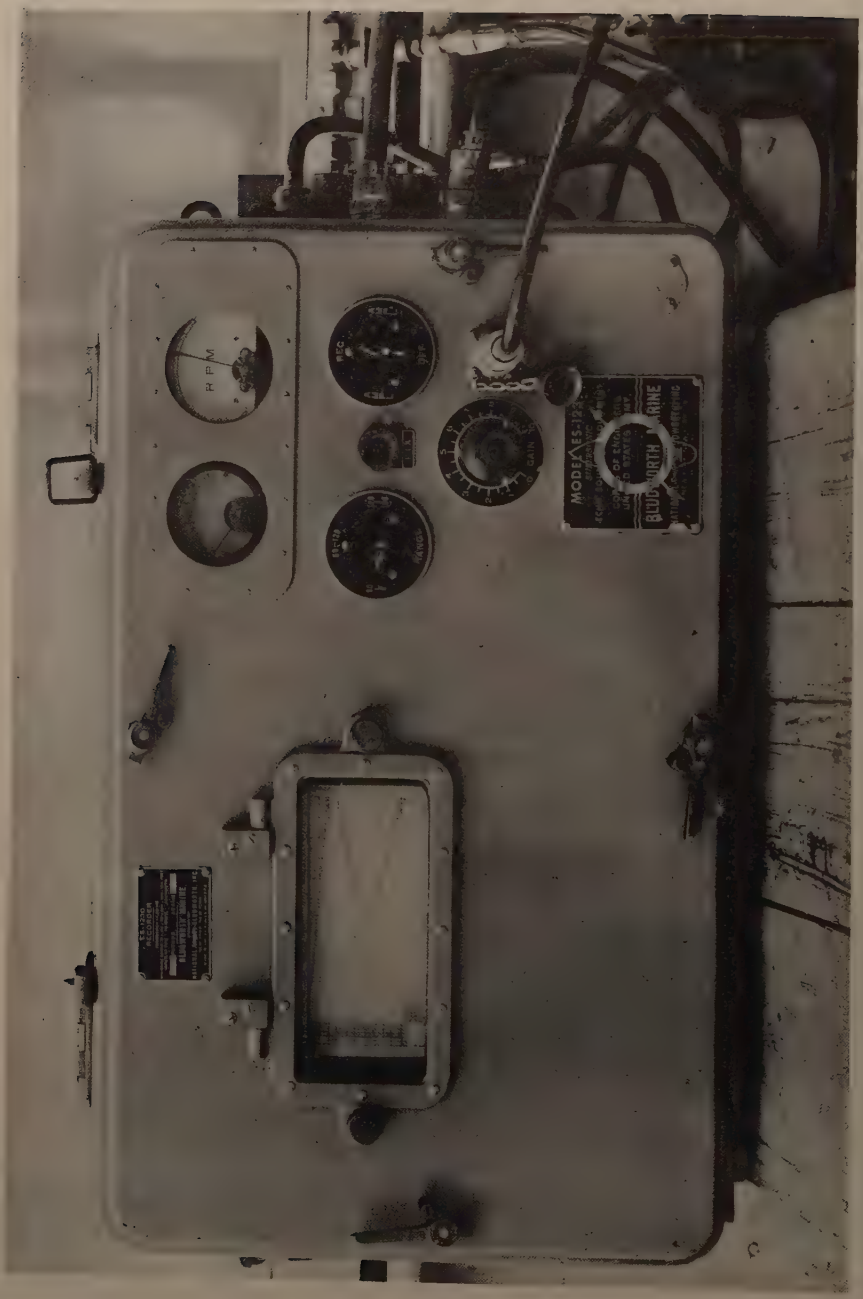

Figure 5.--ECHO SOUNDING RECORDER SHOWING OPERATING CONTROLS

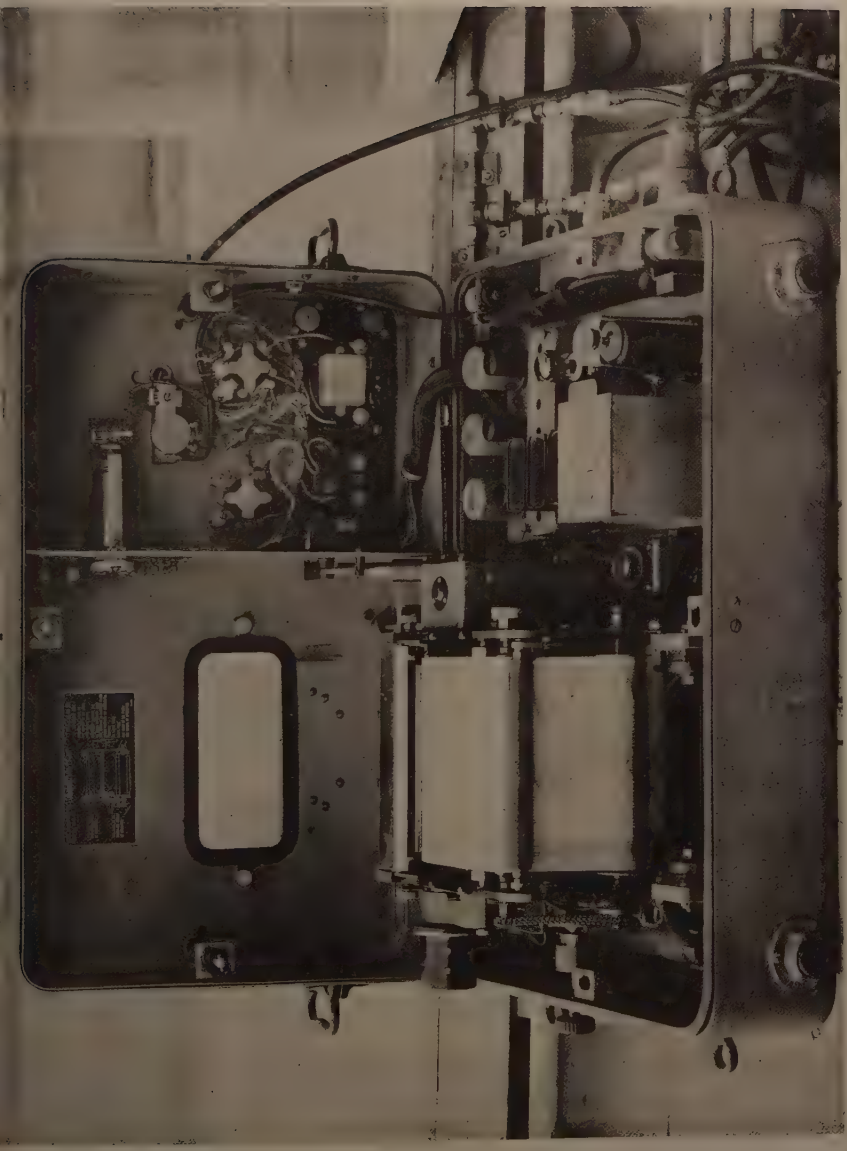

Figure 6.--INTERIOR VIEW OF ECHO SOUNDING RECORDER

PLATE I

DOUGLAS RESERVOIR SEDIMENT RANGES
SCALE IN MILES
0
3
6
JEFFERSON CO
JEFFERSON CITY
New Market
Witt
White Pine
Bybee
Rankin
Clevenger
Chestnut Hill
Dandridge
DAM
N
63
92
70
25
32
55

Paper 1278 HY 3

Journal of the
HYDRAULICS DIVISION
Proceedings of the American Society of Civil Engineers

AUTOMATIC VHF RADIO TELEMETERING OF HYDROLOGIC DATA[1]

James A. Dale[2]
(Proc. Paper 1278)

SYNOPSIS

With the ever-increasing demand for water in this country for power, irrigation, and industrial use, it has become necessary to ensure that existing water-supply facilities are operated as efficiently as possible. The efficient operation of reservoirs deriving their water from natural flow is dependent on a knowledge of the quantity and distribution of water within the drainage area. Although this information can usually be obtained by telephone from observers hired to read a rainfall or stream level gage, it is often desirable to obtain hydrologic data from isolated areas not served by telephone lines. The use of radio as a means of making this information available from these areas naturally suggests itself.

As early as 1937 the Tennessee Valley Authority started work on a radio system to transmit hydrologic data from isolated areas. By 1949 the system consisted of some 20 rain gages and 20 stream gages. Information from these gaging stations was received at nine area offices scattered throughout the Valley. These reports, along with reports received from observers in the area, were tabulated and telephoned to the Forecasting Section in Knoxville daily.

This system had three drawbacks:

1) Operation was not completely automatic.

2) The transmitting frequencies used, which were between 2 and 3 megacycles, were subject to fading and atmospheric disturbances.

3) Because of the rapid advancement in the electronic field, by 1949 the system was obsolete.

Also, the Federal Communications Commission had served notice that at

Note: Discussion open until November 1, 1957. Paper 1278 is part of the copyrighted Journal of the Hydraulics Division of the American Society of Civil Engineers, Vol. 83, No. HY 3, June, 1957.

1. Presented at Knoxville Convention, American Society of Civil Engineers, Knoxville, Tenn., June 8, 1956.
2. Elec. Engr., Hydr. Operations and Tests Section, Hydr. Data Branch, Tennessee Valley Authority, Norris, Tenn.

some future date operation of this type would have to be discontinued on these frequencies.

In 1950 TVA decided to replace the old radio gaging system. Design of a new system was started in 1950 by TVA engineers, and installation was completed in 1955.

System Requirements

The system was designed around the following basic requirements:

1) Location of stream gage and rain gage stations would be essentially the same as in the old system.

2) Receiving stations would be located at seven area offices. Each office would receive only the gaging stations within its area.

3) Each gaging station was to report every two hours and record automatically at the receiving station.

4) Radio frequencies for transmission were to be selected from the 16 frequencies between 169 and 172 megacycles (Mc) allocated by the Federal Communications Commission for the transmission of hydrologic data.

System Layout

The radio frequencies available for use in the system have essentially line-of-sight transmission characteristics, and since gaging station and receiver locations were already established it was necessary to provide relay stations to make possible the reception of gages at the receivers. Tentative relay or repeater station sites were selected with the aid of topographic maps, but final locations were established only after signal strengths between gaging stations, repeater, and receiver were measured with portable and mobile radio equipment. It was found that a total of 13 repeaters would be required, which is approximately one repeater for every three gaging stations. The locations of all stations in the final system are shown on the map in Figure 1.

System Operation

In order to explain the operation of the system, a typical stream gage-repeater-receiver link will be considered. A clock-operated switch at the stream gage initiates the operation of the gaging equipment. An unmodulated carrier from the gage transmitter is transmitted and received at a repeater station, turning on the repeater transmitter. A repeater carrier is transmitted to the receiving location to complete the circuit from the gage. Conversion of stream level at the gaging station into a numerical sequence of events suitable for telemetering is accomplished by a digital converter or keyer. This device translates the river stage into three groups of from 0 to 9 contact closures corresponding to the stage in tens of feet, feet, and tenths of a foot. A fourth group of from 0 to 9 contact operations precedes these three groups and is preset to identify the gaging station. These four groups of contact closures key an audio tone generator, which in turn

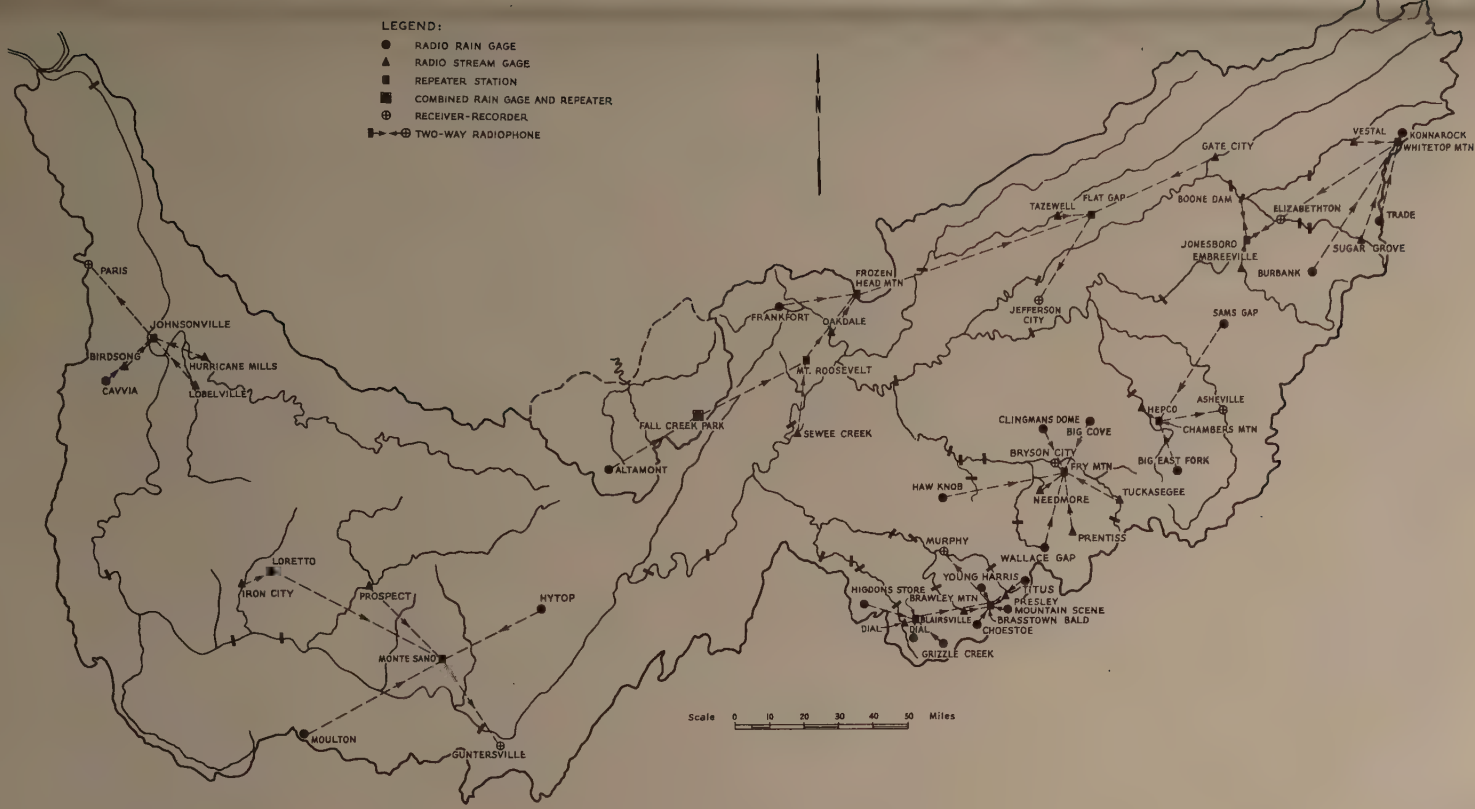

Figure 1.--TVA VERY-HIGH-FREQUENCY RAIN AND STREAM GAGING SYSTEM

frequency-modulates the gage transmitter. This audio tone frequency is designated as frequency A. The digital converter unit also causes a second set of contacts to close between each of the four A tone groups and immediately before and after the first and last groups. These contacts key an audio tone generator on frequency B, which also modulates the transmitter. The audio tone pulses are received at the receiving station via the repeater. After demodulation they pass through frequency-selective filter networks and actuate the A and B tone relays. The A tone relay contacts are connected in turn through a stepping switch to each of four solenoid-operated print wheels in the recorder. The B tone relay contacts actuate the step coil of the stepping switch. Thus it may be seen that the four groups of A tone pulses are each read out in turn by the four print wheels, and the resulting record gives the station number and the stage. Included in the print-out section of the recorder is a date and time stamp which prints opposite the stage recorder.

The chart in Figure 2 shows the time sequence of various operations occurring during one gage transmission. It will be noted that information from the gaging station is sent out twice during one transmission. This is beneficial in verifying the accuracy of the recorded data.

The example illustrated in Figure 2 is station 4 broadcasting a stage of 10.8 feet. At zero time the clock switch initiates equipment operation and the transmitter carrier is turned on. Six seconds later the B tone keyer contacts cause the carrier to be modulated by the B tone. Duration of this modulation is about 1/4 second. At the receiver this modulation pulse causes the B tone relay to operate, which in turn steps the stepping switch in the recorder off the normal "no contact" position to position 1. Immediately after the occurrence of the first B tone pulse the keyer causes a series of four A tone pulses to be transmitted. These are received at the receiver and actuate the A tone relay. The contacts of this relay are connected through the position 1 contacts of the recorder step switch to the solenoid of the first print wheel, and the print wheel is stepped around to position 4. The second B tone impulse is transmitted at 0 + 12 seconds and causes the recorder step switch to move to position 2. The second print wheel is then stepped around to position 1 by the following single A tone pulse. At 0 + 18 seconds the third B tone pulse is transmitted. Following this there are no A tone pulses so the third print wheel is not moved. After the fourth B tone pulse at 0 + 24 seconds a series of eight A pulses steps up the fourth print wheel to position 8. The fifth B tone pulse at 0 + 30 seconds causes the recorder to print and clear. The recording cycle is then repeated, and after the tenth B tone pulse the transmitter is turned off. The resulting printed record is 4108 indicating that station 4 has a stage of 10.8 feet. A typical recorder tape showing the record of ten stations in a two-hour period is illustrated in Figure 3.

Power for Station Operation

With the exception of two rain gages, all stations are served by commercial power. In the event of power failure, emergency power is automatically provided at repeater stations by a gasoline-driven generator having a fuel capacity sufficient for five days of operation. When the repeater is on emergency power a tone is sent out from the repeater at the end of each transmission. This tone operates a relay at the receiver which in turn lights a light on the receiver panel. The light stays on until released manually but

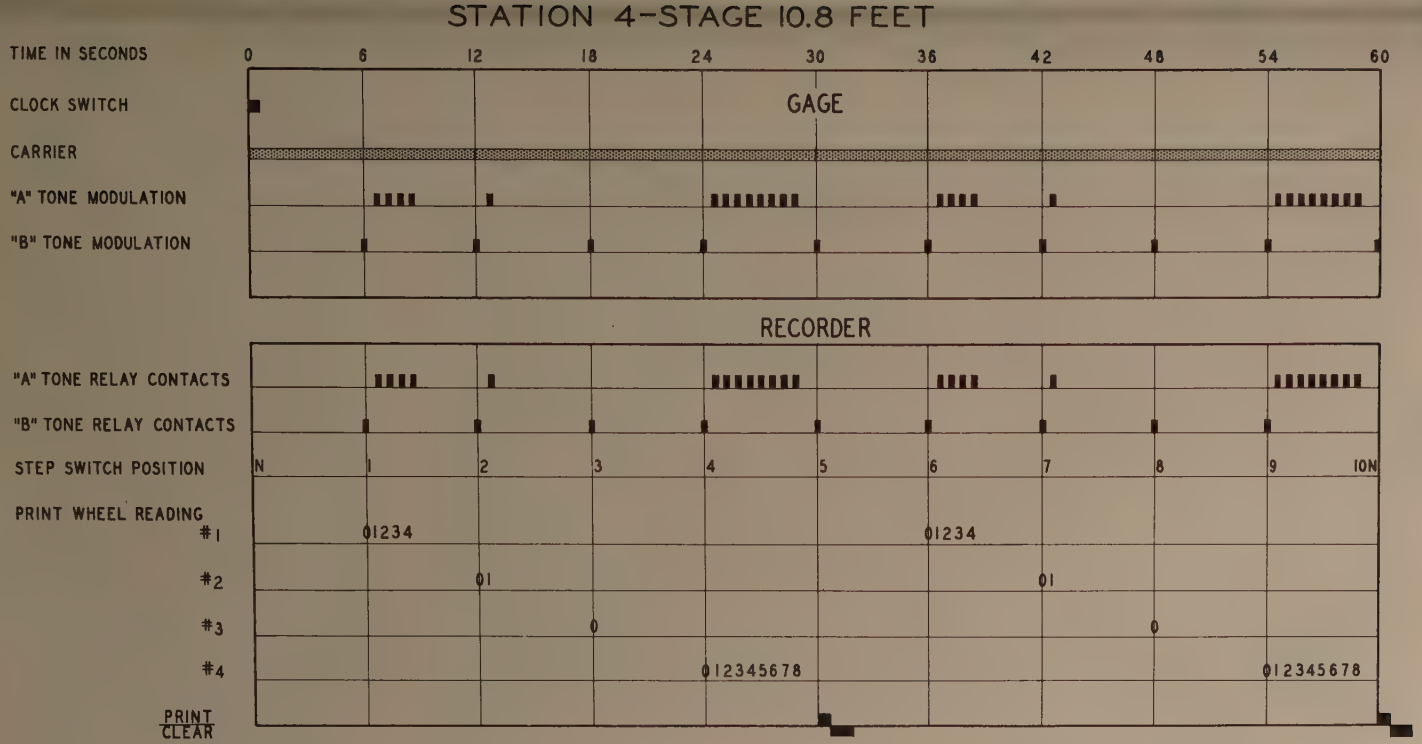

Figure 2.--OPERATIONAL TIME SEQUENCE

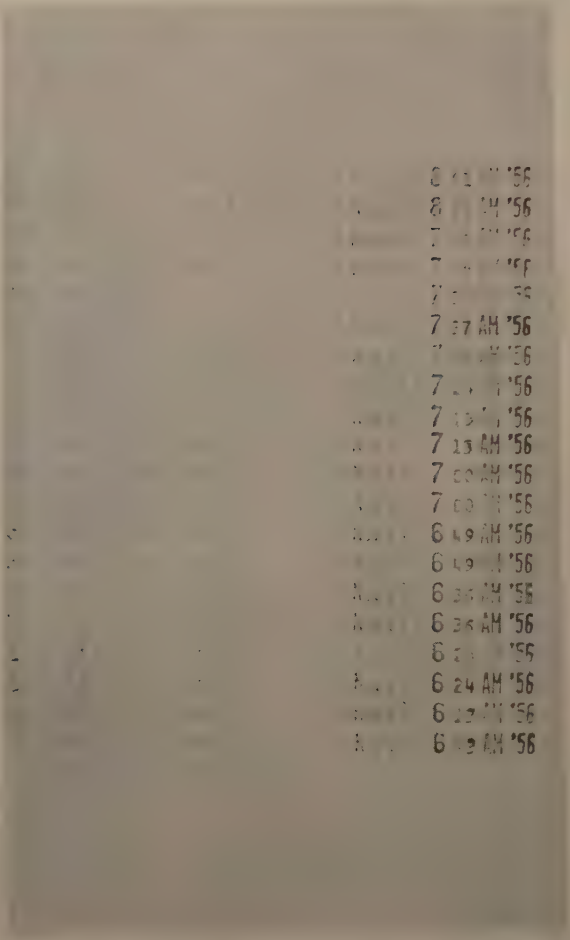

Figure 3.--RECORDER TAPE SHOWING RECORD FOR TEN STATIO

will come on again on the next repeater broadcast if the main power is still off. At gaging stations, ten-day emergency power operation is provided by a 60-ampere-hour battery. Normally a gaging station transmits the required information twice during each broadcast. If the gage is on emergency power the second half of the broadcast appears on the recorder tape as four zeros. No emergency power system is employed at the receiving stations.

Two rain gage stations in the system are in such remote locations that the cost of bringing in commercial power is prohibitive. One of these, Clingmans Dome, is near the middle of the Great Smoky Mountains National Park. The other station, Haw Knob, is in an area populated only by wild boars.

The equipment at these two stations is basically the same as that used at

other stations. Power is provided by two 100-ampere 6-volt heavy-duty truck batteries. These batteries will run the station approximately 25 days. A gasoline-driven generator is provided to charge the batteries. These stations are normally visited every two weeks, and at this time a 3-hour supply of gasoline is added to the generator. The generator is then left running and it will, of course, stop when the fuel supply is exhausted. With additional battery capacity and a longer charging time it should be possible to get at least 60 days of gage operation.

Equipment

In the interest of economy, the system was designed to include standard available components, such as radio transmitters and receivers, when possible. Particular attention was given to the standardization of parts and subassemblies to facilitate servicing and minimize the stock of spare parts required.

Stream Gage

The components of the stream gaging stations are listed below and shown in Figure 4.

1) Keyer or digital converter
2) Clock-operated switches
3) Transmitter assembly
4) Emergency power battery

The keyer was developed at TVA's Hydraulic Laboratory and is manufactured by the Instruments Corporation. Two types are available, one having a range of 00.00 to 99.99 feet and one with a range of 00.0 to 99.9 feet.

The gaging station is turned on once every two hours by a clock-operated switch. Two types of clock switches are used at each gaging station served by commercial power. One is operated by a synchronous electric motor and the other by an electrically wound spring-driven escapement. The more accurate synchronous clock normally operates the station. When a power outage occurs the spring-driven clock is automatically switched in to take over the control function.

The transmitter assembly consists of six panels which are, from top to bottom, identified as follows:

Tone generator panel
Relay panel
Battery charging panel
Power supply
Transmitter
Converter panel

The audio tones are produced by two General Electric tone generators mounted on the tone generator panel. These units are plug-in, making them easily replaceable.

Relays necessary for keyer operation and control functions are located on the relay panel.

The charging panel provides a trickle charge to the emergency power battery.

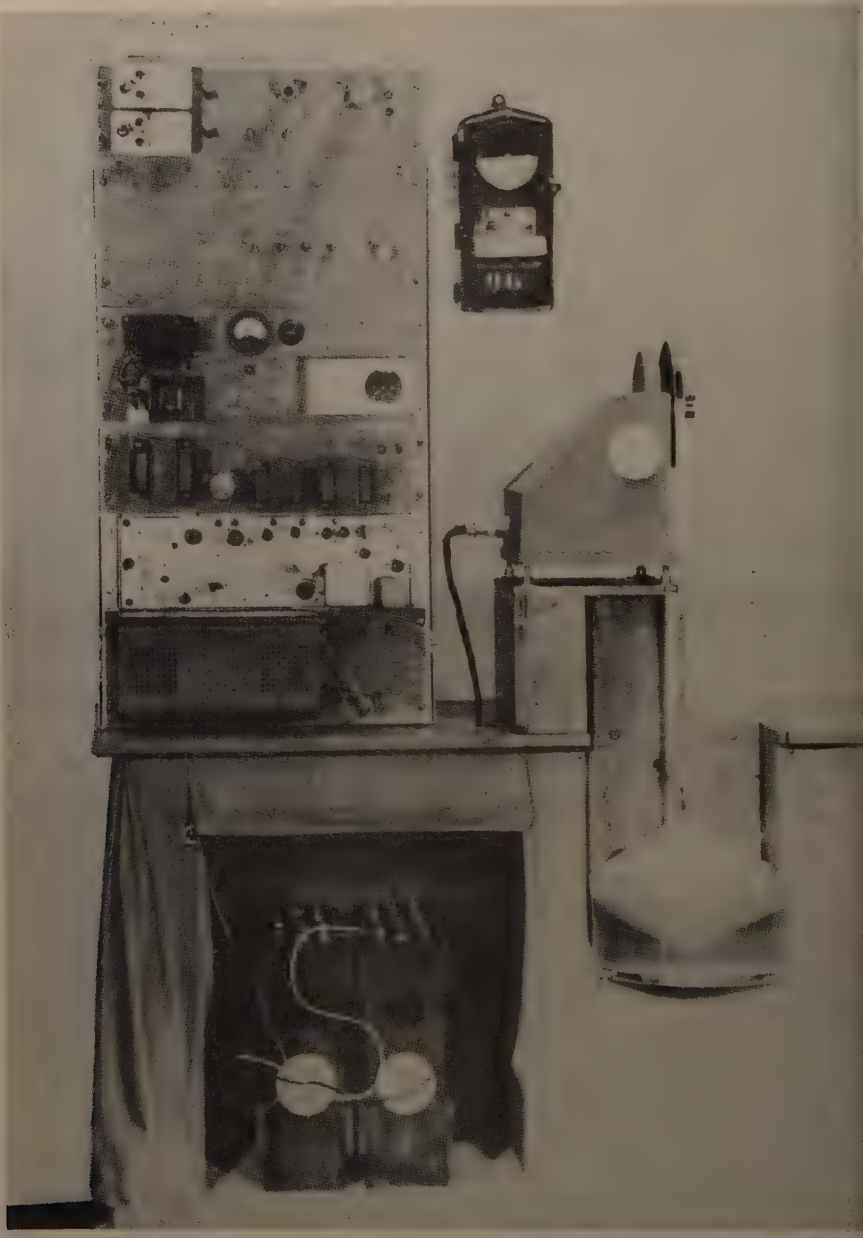

Figure 4.--STREAM GAGE KEYER, TRANSMITTER, CLOCK SWITCH, AND BATTERI

Sample of gaging station equipment as exhibited at Knoxville Conventi of ASCE. Gage well is simulated by a transparent water jar to show t float.

All vacuum tube plate and filament voltages are supplied by the power supply panel.

The radio transmitter is a standard General Electric 6-watt unit.

On the bottom panel is mounted a converter for converting the 12-volt battery power to 115 volts AC. This unit is automatically switched on when the commercial power fails and supplies 115-volt AC to all units.

The emergency power batteries are of the nickel-cadmium type and were chosen because of their ruggedness and ability to stand an overcharge. A typical stream gaging station is shown in Figure 5.

Rain Gage

The rain gage station equipment is identical to that used at the stream gage except for the method used to position the keyer. Rainfall is collected in a standard Instruments Corporation 20-inch capacity weighing type rain gage. The weighing mechanism operates a low-torque potentiometer which in turn positions the keyer through a servo system. The rain gage station broadcasts the catch in the collector to the nearest tenth of an inch. The rain gage collector, keyer, and servo system are shown in Figure 6 and a typical rain gaging station is shown in Figure 7.

Repeater

The repeater consists of a standard General Electric transmitter and receiver, shown in Figure 8. The bottom panel was modified by TVA to include a tone generator for indication of emergency power operation. Accessories at the repeater station include a 400-watt gasoline-driven generator for emergency power, automatic line transfer switch, thermostatically controlled heater and ventilating fan, and voltage regulator. A typical repeater station installation is shown in Figures 9 and 10.

Receiving Station

The receiving station equipment in Figure 11 consists of three units:

1) Receiver
2) Recorder
3) Tone switch unit

The receiver is a standard General Electric unit with no modification. The printing recorder is manufactured by Streeter-Amet and is modified by TVA by the addition of a stepping switch and two relay sub-assemblies. Suitable mounting and auxiliary equipment are provided by TVA.

Antennas

Transmitting antennas used at both repeater and gaging station are of the corner reflector type having a power gain of 5 and a 60-degree beam width. Non-directional ground plane antennas are used on all receivers.

System Versatility

It was mentioned previously that the rain gage collector operated a low-torque potentiometer which in turn positioned the rain gage keyer. Any type

Figure 5.--STREAM GAGING STATION WITH RADIO TRANSMITTER

Panel of transmitter assembly is swung open, showing equipment on b
of panelboard. Antenna is the corner reflector type.

Figure 6.--RAIN GAGE KEYER, COLLECTOR, AND SERVO SYSTEM

e servo system, shown on the exhibition table, replaces the recording chanism in a standard recording gage.

Figure 7.--TYPICAL RADIO RAIN GAGE INSTALLATION

The only necessary connection between the gage and the keyer is electrical through the servo system, so

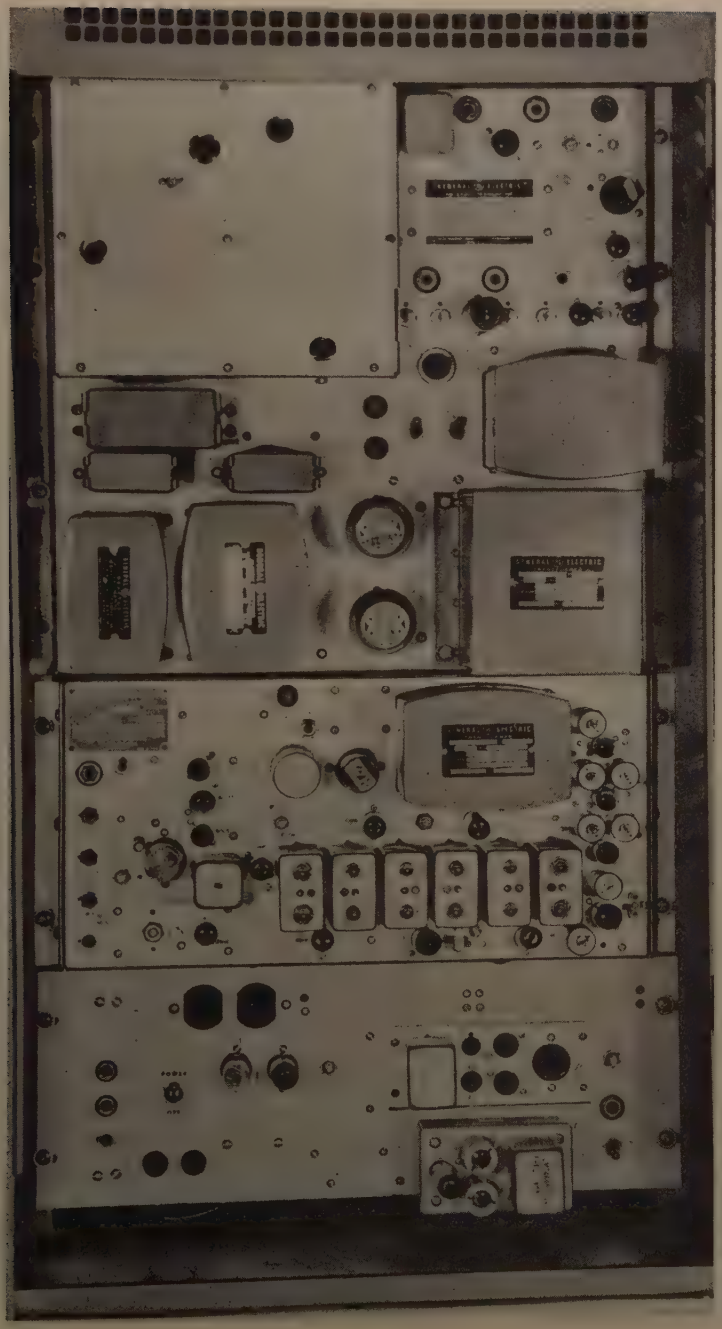

igure 8.--RECEIVING AND TRANSMITTING EQUIPMENT FOR REPEATER

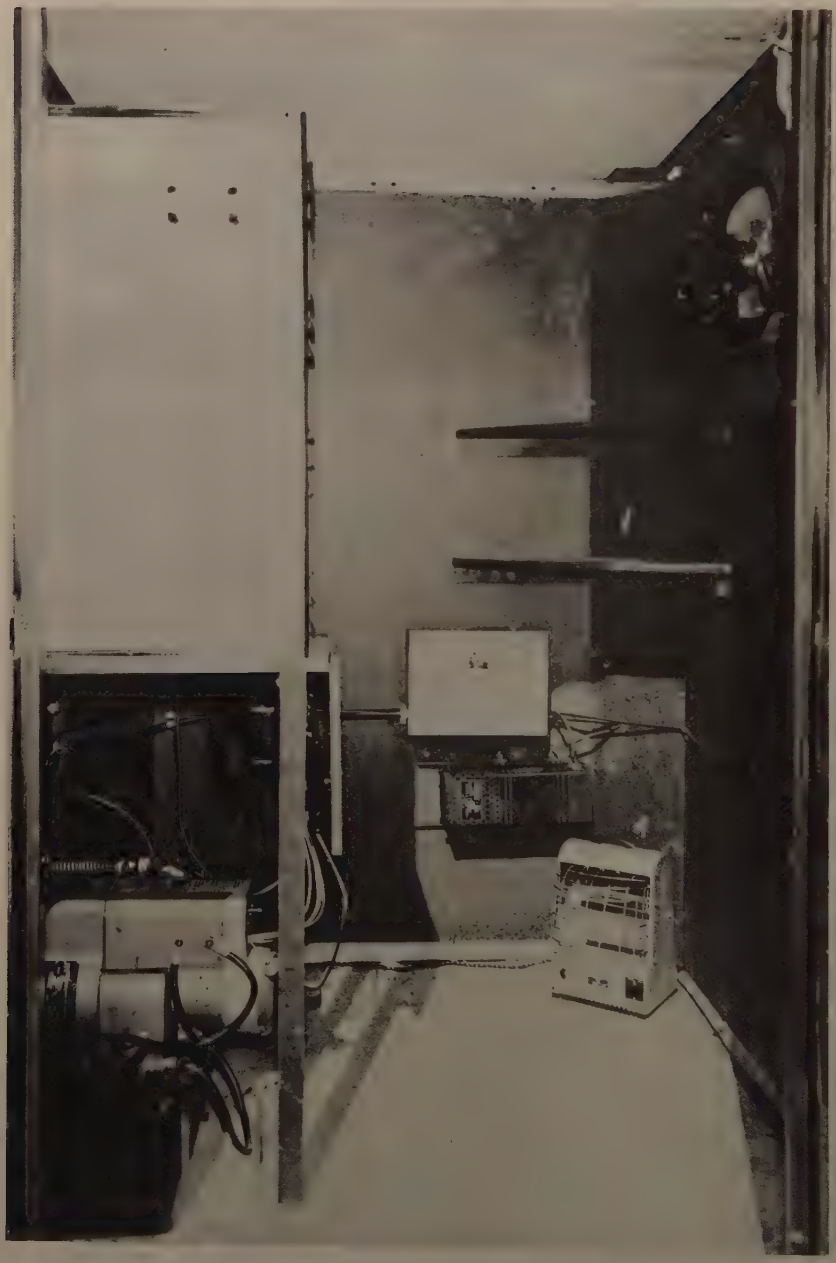

Figure 9.--INTERIOR VIEW OF REPEATER STATION

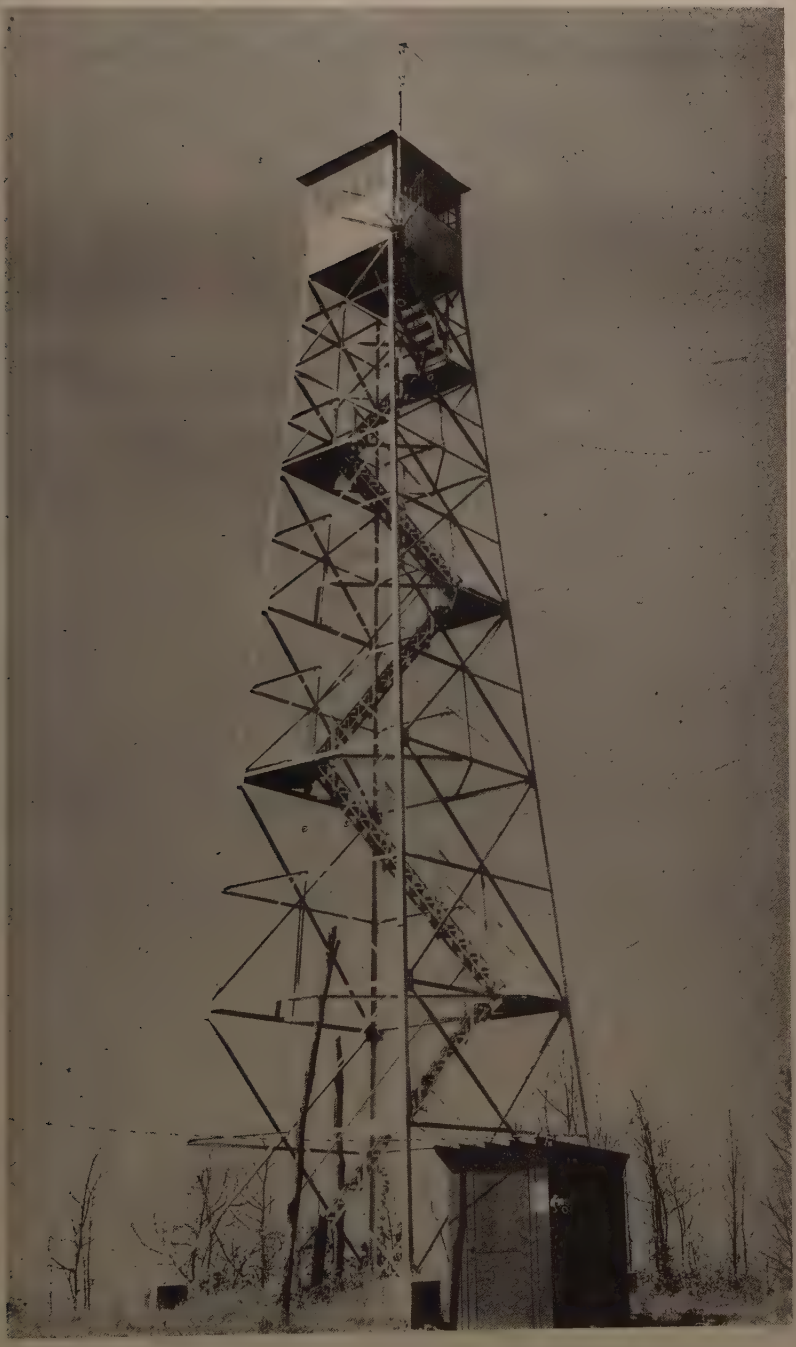

Figure 10.--REPEATER WITH ANTENNAS MOUNTED ON FIRE TOWER

Figure 11.--RECEIVER AND PRINTING RECORDER

of transducer capable of positioning this potentiometer may be used as a sensing element, thus making it possible to transmit other types of information such as pressure, temperature, and relative humidity.

With no modifications to the repeater stations it is also possible to incorporate one or more 2-way radio telephone circuits. For example, by adding a transmitter to the receiver station at Bryson City, 2-way communication could be carried on between Bryson City and cars equipped with standard mobile radio units. The distance of communication is determined by the coverage of the repeater.

System Performance and Cost

Probably the two questions most often asked about the system are: (1) How much did it cost? and (2) How reliable is it?

Our actual equipment cost for the four types of stations is as follows:

Rain Gage	- $2,400
Stream Gage	- $1,800
Repeater	- $2,600
Receiver	- $2,100

All preliminary design costs are included in these figures, as well as costs of construction, assembly, and test. Overhead costs are not included.

Stream gages are installed in the regular stream gage houses so that there is no additional cost for housing. Rain gages include the cost of the equipment house, collector and servo system, which combined result in a higher cost for the rain gage over the stream gage.

As a performance check, a record of monthly reporting efficiencies of all gaging stations is kept. Efficiencies are based on one report every two hours from each station or 12 reports a day. The average system efficiency for February 1956 was 96.0 percent; for March, 96.8 percent; and for April, 97.6 percent.

Journal of the
HIGHWAY DIVISION
Proceedings of the American Society of Civil Engineers

CONTENTS

DISCUSSION
(Proc. Paper 1283)

Note: Paper 1283 is part of the copyrighted Journal of the Hydraulics Division of the American Society of Civil Engineers, Vol. 83, HY 3, June, 1957,

Discussion of
"THE PROBLEM OF RESERVOIR CAPACITY FOR LONG-TERM STORAGE"

by A. Fathy and Aly S. Shukry
(Proc. Paper 1082)

HAROLD EDWIN HURST.[a]—There are two principal problems involved in connection with reservoir capacity for long-term storage. The first is what are the characteristics of natural phenomena such as river-discharges on which the amount of storage for different conditions depends, and what are the relations between them. The second is to devise methods for the regulation of the storage when it has been provided. An answer to the first was given by the writer in a paper to ASCE,(1) while the second was discussed by him in a paper presented to the Institution of Civil Engineers London in March 1956.[7] However a fresh approach to a problem is often valuable. It is unfortunate that the second paper was not available to the authors.

The relations found by the writer are given in equation 2 for random events, and in equations 5, 6 and 8 for some natural phenomena. Eq. 2 was found theoretically and was later verified by W. Feller using a different method.[8] In the case of natural phenomena a mathematical derivation is not at present possible, though some work now in progress may perhaps lead to one. In order therefore to arrive at equation 5 seventy-five phenomena were analysed and for this purpose their observations were divided into 690 sets in which N ranged from 30 to 2000. These were later extended by the addition of the discharges of 21 rivers. The phenomena were divided into classes of similar members, rainfalls, river statistics, varves etc. For any particular class the results from the individual sets of observations were arranged in groups according to values of N. For each group mean values of log R/σ and log N were calculated and plotted against each other. This is shown in Fig. 14 which is fig. 4 of the A.S.C.E. paper(1) which is here reproduced. From this it is clear that the points fall closely on straight lines, which are represented by

$$\log R/\sigma = K \log N/2$$

---

a. Scientific Consultant to the Ministry of Public Works, Egypt; formerly Director- Gen., Physical Dept., Ministry of Public Works, Egypt.

7. Methods of using Long-Term Storage in Reservoirs. Hurst. Proceedings of the Institution of Civil Engineers. London. Part 1. vol. 5. pp. 519-590 September 1956.

8. The asymptotic distribution of the range of sums of independent random variables. Annals of Math. Statistics. Vol. 22. 1951, p. 427.

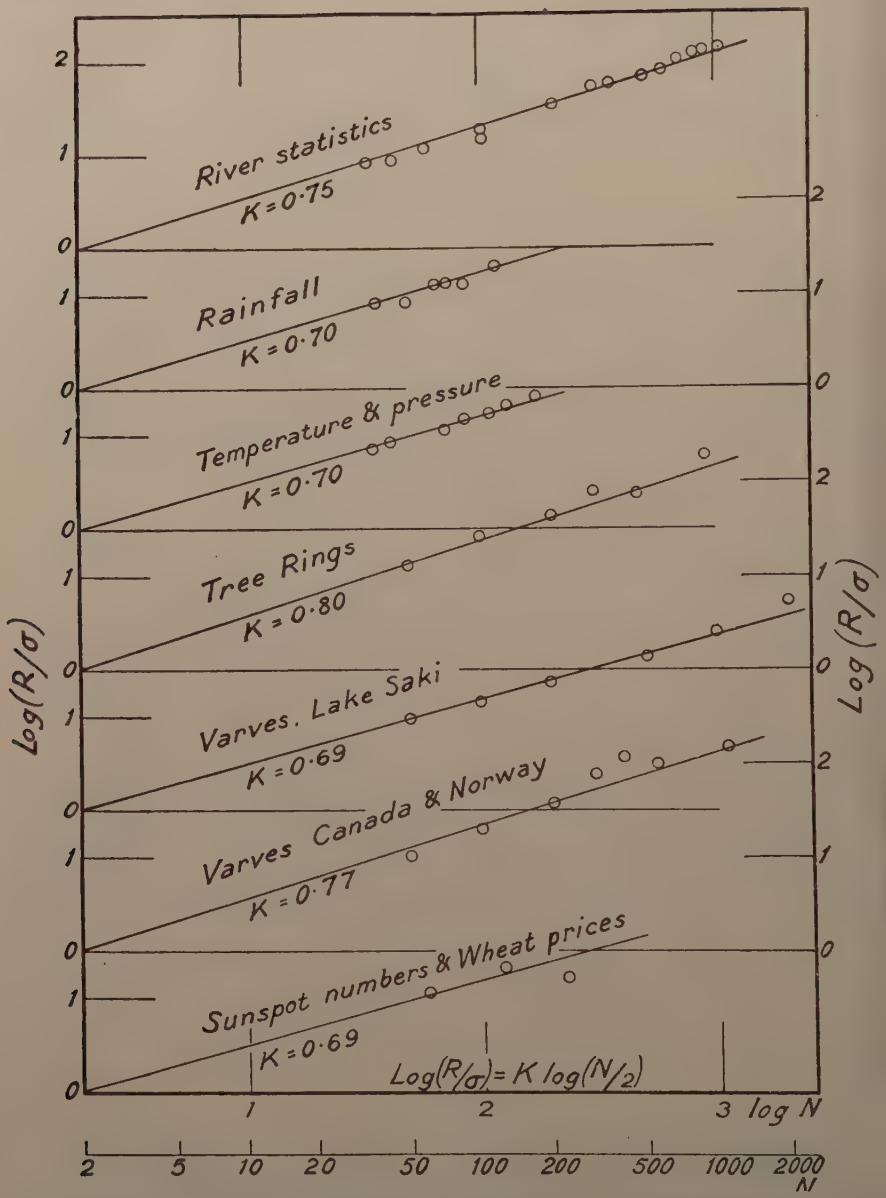

FIG. 4.—RELATION BETWEEN RANGE OF SUMMATION CURVE R, THE STANDARD DEVIATION σ, AND THE YEARS OF RECORD N

Fig. 14

The mean values of K for each of the classes of phenomena varied from 0.69 to 0.80. The 690 individual values of K are normally distributed with a mean value 0.73 and a standard deviation 0.092. The reasons for adopting the simpler formula with one parameter K instead of two are given in the discussion on the paper. The authors object to this on the grounds that "the consistency apparently gained through that extrapolation is the product of the procedure itself and not of any uniformity in the character of the various phenomena examined." However the uniformity is plainly to be seen from fig. 14. It should be pointed out that the dependence of R on N implied in the above equation is a stochastic one, and not, as the authors seem to think it ought to be, a functional one.

The authors' new line of approach is to express R (Equation 10) in terms of M_a a hypothetical absolute mean, N_c the length of the period covered by the range of the mass-curve of the phenomenon considered, which they call the "critical period," and δ_o and δ_c, where δ_o and δ_c are the ratios of the departures from the absolute mean of the mean of the N available observations of the phenomenon and the mean of the N_c observations covering the critical period, to the absolute mean. The introduction of an absolute mean, M_a, which is described as "the most probable value of the mean for any period," but actually does not exist, only serves to obscure the fact that

$$R = N_c (M_o - M_c) \qquad a$$

The authors then proceed to adopt a standard value of 1/2 for N_c/N and propose to take a value of M_o-M_c of 3.5 times the probable error of M_o as a maximum which will not often be exceeded. But M_c is the extreme value of the mean of N_c consecutive observations taken from the sample N, so that M_o-M_c may easily exceed 3.5 times the probable departure of the mean M_o. Substituting these values in equation a we get

$$R = 0{\cdot}5\ N\ 3{\cdot}5\ 0{\cdot}67\ \sigma/\sqrt{N} = 1{\cdot}18\sigma\sqrt{N} \qquad b$$

The coefficient 1.18 is less than the mean 1.25 found for random events. It does not correspond with the 1.66 which results from the complicated operations carried out by the authors. It can be shown however that the standard deviation of R for random events is $0.27\sigma\sqrt{N}$.[8] If this is multiplied by 2.36, as proposed by the authors, we get from equation 2

$$R = 1{\cdot}89\sigma\sqrt{N} \qquad c$$

It must be remembered that this only applies to random events, and that for natural events R increases more rapidly than $\sqrt{N}$ (see fig. 14). The mistake made by the authors is that they fix N_c as 1/2N and then ignore its variation, which is by no means negligible. For example in the case of Aswan discharge, 1870-1956, the critical period started with 1898 and is still continuing.

With regard to the storage S required to meet the maximum deficit when the draft is less than the mean for the period, for which average relations were given by the writer, the authors remark "Thus there are no grounds for

the supposition of a fixed relation between S and R." It is only necessary to look at figures 8 and 9 of (1) which represent mean results from 45 different natural phenomena to see that there are very good grounds in support of a stable mean relation between S and R.

The preceding relates to the statistical description of natural phenomena, and it may be emphasised that there is only one method of investigation, and that is the analysis of a large number of phenomena with records covering long periods. Instead of this the authors make R a function of 4 quantities (equation 10) and then proceed to make hypotheses about all of them and base their conclusions on these.

Incidentally it may be remarked, that the writer's practice of using cumulative sums of departures from the mean (or a base near the mean) is much more convenient than summing the actual observations, since it is less laborious, is largely self checking, and produces a much more compact graph when the cumulative sums are plotted.

As the authors say the decision on the amount of storage to be provided depends on the special conditions of the project, site, water requirements, cost, and, in arid countries, evaporation losses; but other things being equal the larger the storage the better.

Having provided the storage, the very important question of how to use it arises. This has been discussed by the writer in (7) where the method adopted was to experiment with 50 natural phenomena most of them having records covering 100 years or more, taken mainly from river discharges and levels, rainfall, temperature and varves.

The first object was to find a regulation which would make good use of the water and minimise the risk of emptying the reservoir. Nine regulations were tried on the assumption that the first 30 years records were known from which the capacity of the reservoir R was calculated by equation 6. In doing this σ was increased by 10% to allow for the shortness of the known period, and N was taken as 100. The reservoir started half full, and the draft was the mean of the proceding 10 years which was reduced or increased on a sliding scale by a proportion depending on the amount of water in the reservoir. The draft was changed every year. The result of this regulation was that in 14% of the cases a sliding scale depending on the content was needed to prevent the reservoir from emptying, and in only about 10% of the cases would this have made more than a trifling reduction of the draft from the 10 year mean. Similar investigations were made for flood protection.

As the author's paper is not based on the analysis of data relating to a large sample of natural phenomena, but on assumptions which lead to results not in accordance with the known characteristics of natural phenomena, the writer considers it unnecessary to discuss the applications of these results to practical problems.

The following references relate to random variables.

9. E. H. Lloyd and A. A. Anis. "On the range of partial sums of a finite number of independent normal variates." Biometrika, vol. 40, June 1953.

10. A. A. Anis. "The variance of the maximum of partial sums of a finite number of independent normal variates." Biometrika, vol. 42, June 1955.

11. A. A. Anis. "On the moments of the maximum of partial sums of a finite number of independent normal variates." Biometrika.

Discussion of
"FLUID RESISTANCE TO CYLINDERS IN ACCELERATED MOTION"

by S. Russell Keim
(Proc. Paper 1113)

LOUIS W. WOLF.[19]—Mr. Keim has presented useful information on the drag exerted on an immersed object in unsteady motion. There is a regrettable lack of information on this topic and more is certainly needed. Unfortunately, the approach based on a single coefficient cannot be readily extended to other modes of motion. Because the total resistance in unsteady flows has two distinct parts, one due to velocity and the other to acceleration, it seems misleading to combine it into a general coefficient, particularly since valuable information concerning the second part is available.

The unidirectional motion used provides values of the overall resistance for cylinders accelerating with the application of a constant force; this motion is not well suited to the measurement of the components of resistance or the understanding of the mechanism of the formation of the wake. The velocity-dependent drag and acceleration-dependent inertial forces always appear together and can be separated only by application of a knowledge of the variation of the wake or by causing them to vary in such a manner that they can be distinguished. Keulegan and Carpenter[20] and McNown[21] separated the drag and inertial effects for oscillating flows. Because the drag is always in phase with the velocity and the inertial force in phase with the acceleration, the effects were distinguishable. McNown, using Riabouchinsky's model for the wake, has predicted a relationship between C_D and k for flow past a flat plate. Good correlation was achieved between the predicted and experimental values.

A complication in the description of the resistance is the effect of separation and subsequent formation of a wake; the size and shape of the wake affects both the coefficient of virtual mass and the coefficient of drag. In the aforementioned studies of flat plates and cylinders, the coefficient of virtual mass was shown to increase above the classical values with the increasing size of wake. Values of the coefficient of virtual mass of three times the classical value were observed.

Similarly, the pressure behind any object moving in a fluid is dependent upon the wake pattern. For small wakes with a small curvature the pressure is considerably below the ambient whereas for large wakes with relatively large curvature the pressure is higher. Thus the drag coefficient is large for a small wake, and approaches the steady state value for a large wake. Small variations of this pattern occur when eddies are shed. Drag coefficients as large as ten (five times the value for steady flow) have been observed in experiments on flat plates.

---

[19]. Teaching Fellow, Univ. of Michigan, Ann Arbor, Mich.

[20]. Keulegan, G. H., and Carpenter, L. H., Forces on Cylinders and Plates in an Oscillating Fluid. NBS Report 4821, Sept. 1956.

[21]. McNown, J. S., Drag in Unsteady Flow; Proc. 9th Int. Cong. Appl. Mech., Brussels, 1956 (publ. pend.)

The force on any body can be expressed as the sum of the drag $C_D \rho A \frac{v^2}{2}$ and the inertial force ρVka due to the virtual mass of the fluid, C_D being the coefficient of drag and k being the coefficient of virtual mass. Hence, it can be seen that the overall resistance coefficient C, defined by the author, can be written as

$$C = C_D + \frac{\pi}{2} k \left(\frac{da}{v^2}\right)$$

For large accelerations the virtual mass term is dominant, the curves in Figure 4 being asymptotic to a line having a unit slope and an intercept value of $\frac{\pi k}{2}$ for $\frac{da}{v^2} = 1$. For small accelerations the drag term is dominant, with the curves asymptotic to a horizontal line representing the steady state drag. If the coefficients of drag and of virtual mass can be reported separately, a better understanding of the resistance phenomena would be achieved.

Values of k indicated by the asymptotes to Keim's experimental curves are consistently less than the values obtained by Stelson and Mavis[11] for cylinders, and do not vary uniformly with the length to diameter ratio L/d. Stelson and Mavis report virtual mass coefficients of .98, .97, and .90 for L/d ratios of 30, 15, and 5 whereas the author's curves indicate .73, .90, and .50, respectively. A higher rather than a lower value of k would be expected since the formation of a wake increases the virtual mass. Because of the extreme complexity of the problem, limiting values such as these must be carefully assessed.

11. Stelson, J. M. and Mavis, F. T. Virtual Mass and Acceleration in Fluids, Proc. ASCE, Vol. 81, No. 670, 1955.

Discussion of
"FREQUENCY ANALYSES OF STREAMFLOW DATA"

by David K. Todd
(Proc. Paper 1166)

H. ALDEN FOSTER,* M. ASCE.—There has been considerable confusion or many years in the use of the term "frequency" in hydrology. As generally sed, if statistics are arranged so as to show the number of times, or frequency with which, an event happens in a particular way, the arrangement is alled a "frequency distribution." The curve or formula used to describe uch distributions is called a "frequency curve." (Ref. 14, pg. 145). The uthor illustrates such a curve correctly in Fig. 3 where he also shows a cumulative frequency curve," which is the integral of the original frequency urve.

As the frequency curve shows how often a flood of a given magnitude (or etween certain limiting magnitudes) will occur on the average in a 100-year eriod, the cumulative frequency curve shows how often a flood greater (or ess) than a certain magnitude will occur according to the same 100-year ecord. This is also an indication of the "probability" of occurrence of such flood, according to the record; therefor it is proper to refer to the cumulative frequency curve as a "flood-probability curve." This is also in conformance with standard nomenclature in mathematics where the term Probability Integral" is commonly used.

It has become rather common practice in discussing the probability of ccurrence of floods to speak of "flood frequency" as indicating the average me interval between successive occurrences of a flood of a given magnitude,—such as once in 100 years. A better term for this purpose would be recurrence interval" or "return period" of such a flood, and to confine the erm "frequency" to the basic meaning as used by statisticians.

Mr. Todd points out that a number of different mathematical formulas have een proposed for the computation of a theoretical frequency curve to represent a particular set of hydrological data; and that computational procedures ave been developed that make solution of the formulas relatively simple. A ord of caution may be introduced here. Mechanical simplicity of calculation ased on complicated formulas is no guarantee of the precision or reliability the results. Statistical methods can never give precise answers, but only n indication of the probable values that can justifiably be deduced from the ecorded data. The writer pointed this out in 1924 (Ref. 14, pg. 172) by the atement "the theoretical curves should be used only as a guide in the study a given record." The author indicates the fallacy and danger of trying to stimate" a 10,000-year flood from a record of only 20 years duration. reat caution should be used in applying flood-probability analyses to the design of the spillway for a dam, even though the structure is of minor importance. The methods have a proper and useful application, however, in ertain fields, particularly in estimating Average Annual Flood Benefits for a

* Prin. Associate, Parsons, Brinckerhoff, Hall & Macdonald, New York, N. Y.

flood-control project or in trying to determine suitable premiums for flood-insurance policies. (Add ref. 28: H. Alden Foster, 1954; "Flood Insurance," Proc. ASCE, Vol. 80, Sep. No. 483).

The relative advantages of using the "annual flood method" vs. the "basic stage method" or the partial duration series are discussed in Ref. 22; they were also explained by the writer in Ref. 20, pg. 54-57.

The frequency analysis of all flows, involving preparation of a Daily-Flow Duration Curve, is on a somewhat different basis from the use of theoretical frequency curves for determination of flood probabilities. Such a Duration Curve should more properly be considered as a convenient tool for study of the data, just as the hydrograph or mass curve is customarily treated. (Ref 15) Some attempts have been made, however, to plot flow-duration curves b mathematical formulas, notably by Lane and Lei (Ref. 21) who represented the daily-flow duration by the logarithmic-probability curve.

Discussion of
"THE ESTIMATION OF THE FREQUENCY OF RARE FLOODS"

by Benjamin A. Whisler and Charles J. Smith
(Proc. Paper 1200)

GORDON R. WILLIAMS,[1] M. ASCE.—In spite of persistent research over more than 30 years, the problem of estimating the frequency of floods, particularly rare floods, is far from solved and may have to wait for many more decades of records before a reliable answer can be obtained.

The authors' conclusions that the frequency of floods does not follow the mathematical theory of probabilities, appears to be sound from a hydrologic basis alone. It is well known that there are complex cyclical trends affecting flood frequency, beginning with periods as short as a year and extending over several decades or more. Most localities are subject to seasonal trends, thus introducing a short-term rhythmic effect which has little relation to pure chance.

This seasonal effect appears to cause doubts as to the logic in the use of one peak discharge for each month of record. Such data from a dry-season record will introduce many values which are peaks in the river hydrograph but are in no sense flood flows. In fact, the use of monthly peaks causes the method to approach the flow-duration curve in which the discharges compiled are often interdependent and do not represent isolated hydrologic events.

More and more evidence is being obtained that the frequency of rare floods cannot be obtained by extrapolating the well-defined mean curve for frequent floods. This is another conclusion of the paper with which this writer is in accord, but he does have misgivings about the hydrologic soundness of the method by which the conclusion is reached.

There are at least two reasons why there should be two frequency curves, one is meteorologic and the other is hydraulic. The meteorologic reason is that the great storms causing rare floods are possibly different physical phenomenon from the storms causing minor flood rises. For example, rainfall-depth-duration-frequency curves in the West Indies show that the trade-wind showers define one set of depth-duration-frequency curves while the hurricane storms define another set. Rainfall depths from the former curves indicate that the depths from the latter curves are unlikely to occur, even though both curves are defined over a 40 to 50 year period. The hurricane depth-frequency curves have greater slopes when the depths are plotted as ordinates. The floods resulting from these two types of storms also fall into two different frequency distributions. It is entirely possible that rainfall depths from rare storms in the United States define their own frequency curves and that they are not as rare as the extrapolated frequency distribution of lesser storms would indicate.

The hydraulic reason for the different flood frequency relations mentioned above is the effect of channel and valley storage. In the minor flood the channel storage may exert a modifying influence that is essentially proportional to

1. Prof. of Hydr. Eng., Massachusetts Inst. of Technology, Cambridge, Mass.

the flood peak or flood volume. The rare flood, on the other hand, occupies all surcharge storage in swamps and ponds and covers the river valleys from hill to hill. The increment of natural storage per increment of flood volume becomes materially less and the flood rolls on with apparently little modification. It is these effects that have led to man-made encroachments in valleys with later disastrous results when the rare flood takes place.

The use of 24-hour flows may result in unsatisfactory floodpeak estimates in the smaller river basins of less than about 1000 square miles. In even smaller basins of less than 100 square miles the duration of the entire flood hydrograph may be less than 24 hours, and yet an important flash flood peak may have occurred in that interval of time. The 24-hour averages may give an erroneous impression of the range of flood magnitudes with respect to frequency and lead to serious underdesign if hydraulic capacities are to be based on frequency criteria.

Much of the research on flood frequency through the years has attempted to apply precise mathematical laws to a phenomenon which is basically empirical and to a varying degree, cyclical. Furthermore, flood magnitudes are affected by surface conditions in each particular basin, some of which are permanent and some of which seasonal (cyclical) and by storage effects which may vary widely with the degree of basin inundation. Only from a long record can be obtain a reliable discharge-frequency distribution. The true flood producing potentialities of a basin for use in immediate design studies can only be derived from more complex storm studies translated into flood flows by the unit hydrograph method.

PROCEEDINGS PAPERS

The technical papers published in the past year are identified by number below. Technical-division sponsorship is indicated by an abbreviation at the end of each Paper Number, the symbols referring to: Air Transport (AT), City Planning (CP), Construction (CO), Engineering Mechanics (EM), Highway (HW), Hydraulics (HY), Irrigation and Drainage (IR), Pipeline (PL), Power (PO), Sanitary Engineering (SA), Soil Mechanics and Foundations (SM), Structural (ST), Surveying and Mapping (SU), and Waterways and Harbors (WW), divisions. Papers sponsored by the Board of Direction are identified by the symbols (BD). For titles and order coupons, refer to the appropriate issue of "Civil Engineering." Beginning with Volume 82 (January 1956) papers were published in Journals of the various Technical Divisions. To locate papers in the Journals, the symbols after the paper numbers are followed by a numeral designating the issue of a particular Journal in which the paper appeared. For example, Paper 1113 is identified as 1113 (HY6) which indicates that the paper is contained in the sixth issue of the Journal of the Hydraulics Division during 1956.

VOLUME 82 (1956)

JUNE: 990(PO3), 991(PO3), 992(PO3), 993(PO3), 994(PO3), 995(PO3), 996(PO3), 997(PO3), 998 (SA3), 999(SA3), 1000(SA3), 1001(SA3), 1002(SA3), 1003(SA3)[c], 1004(HY3), 1005(HY3), 1006 (HY3), 1007(HY3), 1008 (HY3), 1009 (HY3), 1010 (HY3)[c], 1011 (PO3)[c], 1012 (SA3), 1013 (SA3), 1014(SA3), 1015(HY3), 1016(SA3), 1017(PO3), 1018(PO3).

JULY: 1019(ST4), 1020(ST4), 1021(ST4), 1022(ST4), 1023 (ST4), 1024(ST4)[c], 1025(SM3), 1026 (SM3), 1027(SM3), 1028(SM3)[c], 1029(EM3), 1030(EM3), 1031(EM3), 1032(EM3), 1033(EM3)[c].

AUGUST: 1034(HY4), 1035(HY4), 1036(HY4), 1037(HY4), 1038(HY4), 1039(HY4), 1040(HY4), 1041(HY4)[c], 1042(PO4), 1043(PO4), 1044(PO4), 1045(PO4), 1046(PO4)[c], 1047(SA4), 1048 (SA4)[c], 1049(SA4), 1050(SA4), 1051(SA4), 1052(HY4), 1053(SA4).

SEPTEMBER: 1054(ST5), 1055(ST5), 1056(ST5), 1057(ST5), 1058(ST5), 1059(WW4), 1060(WW4), 1061(WW4), 1062(WW4), 1063(WW4), 1064(SU2), 1065(SU2), 1066(SU2)[c], 1067(ST5)[c], 1068 (WW4)[c], 1069(WW4).

OCTOBER: 1070(EM4), 1071(EM4), 1072(EM4), 1073(EM4), 1074(HW3), 1075(HW3), 1076(HW3), 1077(HY5), 1078(SA5), 1079(SM4), 1080(SM4), 1081(SM4), 1082(HY5), 1083(SA5), 1084(SA5), 1085(SA5), 1086(PO5), 1087(SA5), 1088(SA5), 1089(SA5), 1090(HW3), 1091(EM4)[c], 1092 (HY5)[c], 1093(HW3)[c], 1094(PO5)[c], 1095(SM4)[c].

NOVEMBER: 1096(ST6), 1097(ST6), 1098(ST6), 1099(ST6), 1100(ST6), 1101(ST6), 1102(IR3), 1103 (IR3), 1104(IR3), 1105(IR3), 1106(ST6), 1107(ST6), 1108(ST6), 1109(AT3), 1110(AT3)[c], 1111(IR3)[c]; 1112(ST6)[c].

DECEMBER: 1113(HY6), 1114(HY6), 1115(SA6), 1116(SA6), 1117(SU3), 1118(SU3), 1119(WW5), 1120(WW5), 1121(WW5), 1122(WW5), 1123(WW5), 1124(WW5)[c], 1125(BD1)[c], 1126(SA6), 1127 (SA6), 1128(WW5), 1129(SA6)[c], 1130(PO6)[c], 1131(HY6)[c], 1132(PO6), 1133(PO6), 1134(PO6), 1135(BD1).

VOLUME 83 (1957)

JANUARY: 1136(CP1), 1137(CP1), 1138(EM1), 1139(EM1), 1140(EM1), 1141(EM1), 1142(SM1), 1143(SM1), 1144(SM1), 1145(SM1), 1146(ST1), 1147(ST1), 1148(ST1), 1149(ST1), 1150(ST1), 1151(ST1), 1152(CP1)[c], 1153(HW1), 1154(EM1)[c], 1155(SM1)[c], 1156(ST1)[c], 1157(EM1), 1158 (EM1), 1159(SM1), 1160(SM1), 1161(SM1).

FEBRUARY: 1162(HY1), 1163(HY1), 1164(HY1), 1165(HY1), 1166(HY1), 1167(HY1), 1168(SA1), 1169(SA1), 1170(SA1), 1171(SA1), 1172(SA1), 1173(SA1), 1174(SA1), 1175(SA1), 1176(SA1), 1177(HY1)[c], 1178(SA1), 1179(SA1), 1180(SA1), 1181(SA1), 1182(PO1), 1183(PO1), 1184(PO1), 1185(PO1)[c].

MARCH: 1186(ST2), 1187(ST2), 1188(ST2), 1189(ST2), 1190(ST2), 1191(ST2), 1192(ST2)[c], 1193 (PL1), 1194(PL1), 1195(PL1).

APRIL: 1196(EM2), 1197(HY2), 1198(HY2), 1199(HY2), 1200(HY2), 1201(HY2), 1202(HY2), 1203 (SA2), 1204(SM2), 1205(SM2), 1206(SM2), 1207(SM2), 1208(WW1), 1209(WW1), 1210(WW1), 1211(WW1), 1212(EM2), 1213(EM2), 1214(EM2), 1215(PO2), 1216(PO2), 1217(PO2), 1218 (SA2), 1219(SA2), 1220(SA2), 1221(SA2), 1222(SA2), 1223(SA2), 1224(SA2), 1225(PO)[c], 1226 (WW1)[c], 1227(SA2)[c], 1228(SM2)[c], 1229(EM2)[c], 1230(HY2)[c].

MAY: 1231(ST3), 1232(ST3), 1233(ST3), 1234(ST3), 1235(IR1), 1236(IR1), 1237(WW2), 1238(WW2), 1239(WW2), 1240(WW2), 1241(WW2), 1242(WW2), 1243(WW2), 1244(HW1), 1245(HW1), 1246 (HW1), 1247(HW1), 1248(WW2), 1249(HW1), 1250(HW1), 1251(WW2), 1252(WW2), 1253(IR1), 1254(ST3), 1255(ST3), 1256(HW1), 1257(IR1)[c], 1258(HW1)[c], 1259(ST3)[c].

JUNE: 1260(HY3), 1261(HY3), 1262(HY3), 1263(HY3), 1264(HY3), 1265(HY3), 1266(HY3), 1267 (PO3), 1268(PO3), 1269(SA3), 1270(SA3), 1271(SA3), 1272(SA3), 1273(SA3), 1274(SA3), 1275 (SA3), 1276(SA3), 1277(HY3), 1278(HY3), 1279(PL2), 1280(PL2), 1281(PL2), 1282(SA3), 1283 (HY3)[c], 1284(PO3), 1285(PO3), 1286(PO3), 1287(PO3)[c], 1288(SA3)[c].

---

c. Discussion of several papers, grouped by Divisions.

AMERICAN SOCIETY OF CIVIL ENGINEERS

OFFICERS FOR 1957

PRESIDENT

MASON GRAVES LOCKWOOD

VICE-PRESIDENTS

Term expires October, 1957:
FRANK A. MARSTON
GLENN W. HOLCOMB

Term expires October, 1958:
FRANCIS S. FRIEL
NORMAN R. MOORE

DIRECTORS

Term expires October, 1957:
JEWELL M. GARRELTS
FREDERICK H. PAULSON
GEORGE S. RICHARDSON
DON M. CORBETT
GRAHAM P. WILLOUGHBY
LAWRENCE A. ELSENER

Term expires October, 1958:
JOHN P. RILEY
CAREY H. BROWN
MASON C. PRICHARD
ROBERT H. SHERLOCK
R. ROBINSON ROWE
LOUIS E. RYDELL
CLARENCE L. ECKEL

Term expires October, 1959:
CLINTON D. HANOVER, J
E. LELAND DURKEE
HOWARD F. PECKWORTH
FINLEY B. LAVERTY
WILLIAM J. HEDLEY
RANDLE B. ALEXANDER

PAST-PRESIDENTS

Members of the Board

WILLIAM R. GLIDDEN

ENOCH R. NEEDLE

EXECUTIVE SECRETARY
WILLIAM H. WISELY

TREASURER
CHARLES E. TROUT

ASSISTANT SECRETARY
E. L. CHANDLER

ASSISTANT TREASURER
CARLTON S. PROCTOR

PROCEEDINGS OF THE SOCIETY

HAROLD T. LARSEN
Manager of Technical Publications

PAUL A. PARISI
Editor of Technical Publications

DANIEL GOTTHELF
Asst. Editor of Technical Publications

COMMITTEE ON PUBLICATIONS

JEWELL M. GARRELTS, *Chairman*

HOWARD F. PECKWORTH, *Vice-Chairman*

E. LELAND DURKEE
MASON C. PRICHARD
R. ROBINSON ROWE
LOUIS E. RYDELL